

Adam Mickiewicz University in Poznań

Faculty of Physics

Pickering emulsions formed using ultrasound and electric fields — their characteristics and applications

A dissertation submitted for the degree of Doctor of Philosophy in Physics

by

Rafał Bielas

Supervised by:

Prof. UAM dr hab. Arkadiusz Józefczak

Co-supervised by:

Prof. UAM dr hab. Zbigniew Rozynek



Poznań 2021

Acknowledgments

In the beginning of my thesis, I wish to express my gratitude towards:

- Prof. UAM dr hab. Arkadiusz Józefczak for being a scientific patron and providing a lot of positive support through years of my work on Ph.D. project;
- Prof. UAM dr hab. Zbigniew Rozynek for a guidance, inspiring questions and showing how the scientific synergy could work;
- Prof. UAM dr hab. Tomasz Hornowski for his help and expertise knowledge on the complicated acoustic issues;
- workers and Ph.D. students from the Chair of Acoustics for a friendly atmosphere and an environment for achieving scientific goals;
- all of co-authors of presented publications for fruitful work;
- my family and friends because they believed that I was doing something requisite.

I also thank the Polish National Science Center for its financial support through the research projects within OPUS programs (project no. 2015/19/B/ST3/03055 and no. 2015/17/B/ST7/03566), and within PRELUDIUM program (project no. **2019/35/N/ST5/00402: Formation of Pickering-emulsion-based microcapsules by using magnetic heating and their characterization**).



NATIONAL SCIENCE CENTRE
POLAND

Contents

Abstract	I
Abstract in Polish.....	V
List of publications constituting the dissertation.....	VI
1. Introduction	1
1.1. Particle-stabilized emulsions (Pickering emulsions)	2
1.2. Ultrasonic homogenization	10
1.3. Emulsions under the electric field.....	13
1.4. Propagation of ultrasonic waves in emulsions.....	17
1.5. Magnetic heating of colloidal systems.....	21
1.6. Characteristics of liquids and particles used in experiments.....	26
1.7. Details of experimental techniques	30
2. Overview of the publications constituting the dissertation	38
3. Summary	44
4. Literature used in the introductory part.....	44
5. Publications constituting the dissertation	53
Appendix I: List of other publications	IX
Appendix II: List of significant conference presentations	X
Appendix III: List of awards and distinctions.....	XI
Appendix IV: Other scientific activities	XII

Abstract

Emulsions are mixtures of one liquid dispersed in another liquid and can be found in numerous areas of daily life. These systems are inherently thermodynamically unstable and undergo processes of aging. One of the possibilities to prevent the processes of emulsion aging is to use solid particles that, via the coating of emulsion droplets, can halt the coalescence of droplets and provide emulsion stability. Such emulsions are often called Pickering emulsions. The use of solid particles does not only ensure stability but can also provide intriguing applications of Pickering emulsions, such as the fabrication of colloidal capsules in the pharmacy or food industry or the formation of emulsions responsive to the external stimuli, e.g., magnetic fields.

In the last decades, an obvious scientific interest in Pickering emulsions can be observed. One of the emerging key areas of focus has been on improving the efficiency of formation methods. On the other hand, effort is constantly focused toward finding novel applications of such colloidal systems. When it comes to the efficient formation of Pickering droplets, it is generally challenging to fabricate them in large quantities with a narrow size distribution. The series of publications presented within this Ph.D. thesis begins with the introduction of a novel method for an efficient Pickering emulsion formation process. The proposed approach consisted of two steps, with ultrasonic homogenization and electric fields playing a pivotal role. The use of electric fields did not only lead to a dynamic coalescence of droplets but also prevented the formation of droplet agglomerates. Moreover, it allowed for the formation of Pickering emulsions with a narrow and controllable droplet size distribution.

The process of fabricating Pickering emulsions can be observed by using optical microscopy; however, it is not efficient to use for large quantities of emulsions. This issue also concerned experiments on emulsions prepared using the above-mentioned method. The search for another approach to follow the dynamics of the preparation process and evaluate its stages led to the use of non-destructive ultrasonic measurements. This allowed for following the changes in the fabricated emulsion under electric fields but did not influence the process. The attenuation of an ultrasound travelling through the sample was measured to show the stage of stabilization process *in situ* which has been limited in the

case of optical studies for larger volume of emulsion. What is more, a comparison of the experimental and theoretical results revealed the evident impact of solid particles on the acoustic properties of the emulsion.

Another aim of my Ph.D. project was to determine the differences in the properties of particle-stabilized emulsions during different stages of production. The efficiency of heating under an alternating magnetic field of non-stable emulsions, i.e., prepared only by ultrasonic homogenization was compared with the efficiency of stable emulsion after stabilization under the electric field. The efficiency of the magnetic heating deteriorated after the process under the electric fields. Moreover, the cooling down dynamics after the magnetic heating were also lower when investigating the Pickering emulsions stabilized in electric fields.

The investigated efficiency of magnetic heating seems to be important due to potential applications of Pickering emulsions in, e.g., in magnetic hyperthermia therapy. The process under the alternating magnetic field is dynamic, which raised a reasonable question regarding the eventual induced changes in the structure of the Pickering emulsions. These changes were investigated by following the acoustic properties during and after the application of an alternating magnetic field. For the Pickering emulsions and magnetic dispersions, no significant changes occurred unlike the dispersions of the magnetic and polymer particles. This was because polymer particles exposed to the high-temperature increase melted and formed larger agglomerates. The sintering of temperature-responsive particles under magnetic heating led to the development of a novel potential application of magnetic Pickering droplets, i.e., the formation of colloidal capsules.

The presented studies show the potential of using ultrasound and electric fields to efficiently prepare Pickering emulsions. On the other hand, these studies highlight the interesting aspects of such prepared emulsions, such as heating and cooling rates in magnetic heating experiments and the suitability of using magnetic Pickering droplets as templates for colloidal capsules. Because of this, the results can contribute to the further development of fundamental research on Pickering emulsions, and in the long run, they can aid the practical usage of emulsions in, e.g., hyperthermia treatment or targeted therapy.

My dissertation consists of several parts. In the beginning, a short introduction to relevant literature through a series of published articles is presented. This is preceded by the list of publications and the declarations of their authors. Chapters 1.1–1.7 describe the basic concepts of particle-stabilized emulsions, ultrasonic homogenization, phenomena occurring under the electric field, the theory behind ultrasound measurements in emulsion systems, and heating under the alternating magnetic field, which are the most important scientific topics highlighted in the aforementioned publications. All materials used in the presented experiments are introduced in addition to details on the measurement techniques used. Then, a summary of the papers constituting the thesis is given, showing the connection between the papers and the overall logic behind the presented Ph.D. project. Chapter 3 summarizes the introductory part of the thesis and is followed by the list of references used in the Introduction (Chapter 4). Chapter 5 presents the core of the thesis, i.e., all published papers discussed in the presented dissertation and marked as **[Publication I-VI]**. At the end, appendices featuring my other publications, most prominent conference presentations, awarded distinctions, and scientific activities are presented.

Abstract in Polish

Emulsje to mieszaniny jednej cieczy w drugiej w postaci kropeł, które można spotkać w wielu obszarach naszego codziennego życia. W swej istocie są to układy termodynamiczne niestabilne, ulegające po pewnym czasie procesom starzenia się. Jedną z możliwości przeciwdziałania starzeniu się emulsji jest użycie cząstek stałych, które pokrywając krople emulsji, przeciwdziałają ich łączeniu się i w ten sposób zapewniają stabilność. Takie emulsje nazywa się często emulsjami Pickeringa, a użycie cząstek stałych do pokrycia kropeł zapewnia nie tylko stabilność emulsji, ale może także dostarczać ciekawych zastosowań emulsji takich jak wytwarzanie z nich kapsułek na potrzeby przemysłu farmaceutycznego czy spożywczego, czy podatność na działanie czynników zewnętrznych takich jak pole magnetyczne.

W ostatnich dekadach obserwuje się wyraźne zainteresowanie emulsjami Pickeringa, a jedną z kluczowych kwestii stało się zwiększenie wydajności ich wytwarzania. Z drugiej strony trwają nieustanne prace nad znalezieniem nowych zastosowań takich emulsji. Jeśli chodzi o to pierwsze, okazuje się, że wytwarzanie w dużych ilościach emulsji Pickeringa o wąskim rozkładzie wielkości kropeł nie jest łatwe do osiągnięcia i jest to bez wątpienia ważny problem do rozwiązania. Przedstawiany w niniejszej rozprawie doktorskiej cykl publikacji rozpoczyna się od zaproponowania metody wydajnego takich wytwarzania emulsji. Zaproponowano tutaj dwuetapowy proces, w którym istotną rolę odgrywała ultradźwiękowa homogenizacja i pole elektryczne, którego działanie nie tylko powodowało szybkie łączenie się kropeł, ale także przeciwdziałało łączeniu się tychże kropeł w aglomeraty. Pozwoliło to ostatecznie na uzyskanie emulsji o wąskim i kontrolowanym rozkładzie wielkości kropeł.

Proces wytwarzania emulsji można obserwować za pomocą mikroskopii optycznej. Jednak w taki sposób trudno kontrolować emulsje wytwarzane w dużej ilości. Taki problem również dotyczył eksperymentów związanych z rozwijaniem wspomnianej wyżej metody. Poszukiwanie innego sposobu oceny dynamiki procesu wytwarzania i tego, czy proces jest już zakończony, doprowadziło do zaproponowania nieniszczących badań ultradźwiękowych jako metody, która pozwala na śledzenie produkowanej emulsji, ale sama w sobie nie wpływa na proces powstawania. Zbadano zmianę tłumienia fal ultradźwiękowych

przechodzących przez emulsje stabilizowane w polu elektrycznym, co umożliwiło wyznaczenie etapu stabilizacji emulsji na bieżąco, czego nie dało się uzyskać wprost z badań optycznych. Porównanie wyników eksperymentów ultradźwiękowych z wynikami teoretycznymi pokazało wyraźny wpływ obecności cząstek stałych na własności akustyczne emulsji, co uzasadnia potrzebę dalszych badań ultradźwiękowych nad emulsjami Pickeringa.

Kolejnym etapem mojej pracy było pokazanie różnic we właściwościach emulsji na różnych etapach jej wytwarzania. Porównana została efektywność nagrzewania w zmiennym polu magnetycznym nie w pełni stabilnej emulsji wyjściowej (wytworzonej poprzez ultradźwiękową homogenizację) ze stabilną emulsją docelową (wytworzoną z wykorzystaniem pola elektrycznego). Okazało się, że w magnetycznych emulsjach Pickeringa efektywność nagrzewania magnetycznego pogorszyła się po stabilizacji w polu elektrycznym. Także dynamika chłodzenia po magnetycznym nagrzewaniu była niższa, gdy zbadano emulsje w pełni stabilne w porównaniu z emulsjami wyjściowymi.

Efektywność nagrzewania magnetycznego emulsji Pickeringa może być istotna z punktu widzenia potencjalnych zastosowań np. w terapii hipertermią magnetyczną. Samo nagrzewanie magnetyczne jest procesem dynamicznym, co prowadziło do pytania, czy nie powoduje ono trwałych zmian w strukturze emulsji Pickeringa. Ewentualne zmiany podczas nagrzewania magnetycznego oceniono badając zmiany parametrów akustycznych podczas i po wystawieniu emulsji na działanie zmiennego pola magnetycznego. Dla emulsji Pickeringa, podobnie jak dla cieczy magnetycznych, nie zaobserwowano zmian w stosunku do stanu przed nagrzewaniem. Zmiana była jednak wyraźna dla wystawionych na działanie wysokiej temperatury mieszaniny cząstek magnetycznych i polimerowych. Stało się to dlatego, że cząstki polimerowe stopiły się i stworzyły większe struktury, które pozostawały trwałe także po schłodzeniu do temperatury początkowej. Ten ważny fakt posłużył do wskazania potencjalnego zastosowania kropeł Pickeringa wytwarzanych prezentowaną metodą - tworzenia kapsułek koloidalnych w polu magnetycznym.

Przedstawione w pracy badania z jednej strony pokazują potencjał nowej metody wytwarzania emulsji Pickeringa za pomocą ultradźwięków i pola elektrycznego, a z drugiej wskazują na interesujące aspekty tak przygotowanych emulsji, takie jak efektywność magnetycznego nagrzewania, czy możliwość użycia kropeł Pickeringa jako podstawy do

tworzenia kapsułek koloidalnych. Dzięki temu mogą przyczynić się do dalszego rozwoju badań podstawowych nad emulsjami Pickeringa, ale także w dalszej perspektywie pomóc w praktycznym zastosowaniu emulsji np. w terapii hipertermicznej czy celowanej terapii lekami.

Moja rozprawa doktorska składa się z kilku części. Na początku zostało przedstawione krótkie wprowadzenie do opublikowanych artykułów naukowych. Rozdziały 1.1–1.5 opisują zatem emulsje Pickeringa, zasady działania ultradźwiękowej emulsyfikacji czy zjawiska występujące w emulsjach poddanych działaniu pola elektrycznego. Został także przybliżony sposób propagacji fal ultradźwiękowych w układach takich jak emulsje oraz nagrzewanie pod wpływem zmiennego pola magnetycznego. Użyte materiały i szczegóły techniczne opisywanych w pracach eksperymentów zostały przedstawione w Rozdziałach 1.6–1.7, a rozdział 2 zawiera podsumowanie poszczególnych publikacji wchodzących w skład niniejszej rozprawy. Wstęp do rozprawy kończy krótkie podsumowanie przeprowadzonych badań (Rozdział 3) oraz spis użytej bibliografii (Rozdział 4). Główny rdzeń pracy doktorskiej stanowią opublikowane artykuły naukowe, które zawiera przedstawiono w Rozdziale 5. Zostały one oznaczone w tekście rozprawy jako: **[Publikacje I-VI]**. Końcowe załączniki zawierają listę pozostałych publikacji, których jestem współautorem, ważniejszych wystąpień konferencyjnych, zdobytych wyróżnień i innych aktywności naukowych.

List of publications constituting the dissertation

- I. Efficient formation of oil-in-oil Pickering emulsions with narrow size distributions by using electric fields
Z. Rozynek, **R. Bielas**, A. Józefczak
Soft Matter, 2018, 14, 5140–5149.
IF₂₀₁₈ = 3.399 Ministerial Points₂₀₂₁ = 100 points
- II. Ultrasound control of oil-in-oil Pickering emulsion preparation process
R. Bielas, Z. Rozynek, T. Hornowski, A. Józefczak
Journal of Physics D: Applied Physics, 2020, 53(8): 085301.
IF₂₀₁₉ = 3.169 Ministerial Points₂₀₂₁ = 70 points
- III. The effect of magnetic particles covering the droplets on the heating rate of Pickering emulsions in the AC magnetic field
R. Bielas, T. Hornowski, K. Paulovičová, M. Rajňák, A. Józefczak
Journal of Molecular Liquids, 2020, 320: 114388.
IF₂₀₁₉ = 5.065 Ministerial Points₂₀₂₁ = 100 points
- IV. The effect of particle shell on cooling rates in oil-in-oil magnetic Pickering emulsions
R. Bielas, A. Józefczak
Materials, 2020, 13(21): 4783.
IF₂₀₁₉ = 3.057 Ministerial Points₂₀₂₁ = 140 points
- V. Monitoring of Pickering emulsion stability during magnetic heating using ultrasound measurements
R. Bielas, B. Jameel, A. Józefczak
Measurement, 2021, 178: 109431.
IF₂₀₁₉ = 3.364 Ministerial Points₂₀₂₁ = 200 points
- VI. The potential of magnetic heating for fabricating Pickering-emulsions-based capsules
R. Bielas, D. Surdeko, K. Kaczmarek, A. Józefczak
Colloids and Surfaces B: Biointerfaces, 2020, 192: 111070.
IF₂₀₁₉ = 4.389 Ministerial Points₂₀₂₁ = 100 points

Declarations of authorship contribution

Authorship Statement

I hereby declare that my contribution to the presented publications was as follows:

[1] Z. Rozynek, R. Bielas, A. Józefczak, Efficient formation of oil-in-oil Pickering emulsions with narrow size distributions by using electric fields, *Soft Matter*, 14 (2018) 5140-5149.

My contribution consisted of the primary literature survey, the collection of the part of results and their presentation (Fig. 4 and Fig. 7) as well as the discussion towards finalization of the manuscript.

[2] R. Bielas, Z. Rozynek, T. Hornowski, A. Józefczak, Ultrasound control of oil-in-oil Pickering emulsions preparation, *Journal of Physics D: Applied Physics*, 53 (2019) 085301.

My contribution consisted of the collection of all experimental data, analysis of them and presentation in figures. I also prepared the first version of the manuscript with prof. A. Józefczak.

[3] R. Bielas, T. Hornowski, K. Paulovičová, M. Rajňák, A. Józefczak, The effect of magnetic particles covering the droplets on the heating rate of Pickering emulsions in the AC magnetic field, *Journal of Molecular Liquids*, 320 (2020) 114388.

My contribution consisted of the collection of calorimetric and optical experimental data, the presentation of all data (including these measured in Slovakia) and the preparation of the first version of the manuscript. I also initiated the project and designed the experiments along with prof. A. Józefczak.

[4] R. Bielas, A. Józefczak, The effect of particle shell on cooling rates in oil-in-oil magnetic Pickering emulsions, *Materials*, 13 (2020) 4783.

My contribution consisted of the collection of all experimental data as well as their analysis and presentation. I also prepared the first version of the manuscript.

[5] R. Bielas, B. Jameel, A. Józefczak, Monitoring of Pickering emulsion stability during magnetic heating using ultrasound measurements, *Measurement*, 178 (2021) 109431.

My contribution consisted of the collection of experimental data as well as their analysis and presentation with B. Jameel. I also prepared the first version of the manuscript and designed the experiments along with prof. A. Józefczak.

[6] R. Bielas, D. Surdeko, K. Kaczmarek, A. Józefczak, The potential of magnetic heating for fabricating Pickering-emulsion-based capsules, *Colloids and Surfaces B: Biointerfaces*, 192 (2020) 111070.

My contribution consisted of the collection of experimental data with D. Surdeko as well as their analysis and presentation. I also designed the experiments with prof. A. Józefczak and prepared the first version of the manuscript.

With best regards,

Rafał Bielas

Rafał Bielas

rafal.bielas@amu.edu.pl

May 4, 2021

Co-author Statement

I declare that I am the co-author of the following publications and my contribution to the presented publications was as follows:

[1] Z. Rozynek, R. Bielas, A. Józefczak, Efficient formation of oil-in-oil Pickering emulsions with narrow size distributions by using electric fields, *Soft Matter* 14(24) (2018) 5140-5149.

My participation consisted of participating in the discussion on the obtained results leading to the final version of the manuscript.

[2] R. Bielas, Z. Rozynek, T. Hornowski, A. Józefczak, Ultrasound control of oil-in-oil Pickering emulsions preparation, *Journal of Physics D: Applied Physics* 53(8) (2020) 085301

I and Zbigniew Rozynek designed the ultrasonic measurements. I took part in discussions on the interpretation of the data and the content of the manuscript and I with Rafał Bielas wrote the first version of the manuscript.

[3] R. Bielas, T. Hornowski, K. Paulovičová, M. Rajňák, A. Józefczak, The effect of magnetic particles covering the droplets on the heating rate of Pickering emulsions in the AC magnetic field, *Journal of Molecular Liquids* 320 (2020) 114388.

I with Rafał Bielas developed a concept of experiments and designed them. I also contributed to the finalization of the manuscript.

[4] R. Bielas, A. Józefczak, The Effect of Particle Shell on Cooling Rates in Oil-in-Oil Magnetic Pickering Emulsions, *Materials* 13(21) (2020) 4783.

I and Rafał Bielas initiated the project and designed the experiments. I discussed with co-author the final version of the manuscript.


[5] R. Bielas, B. Jameel, A. Józefczak, Monitoring of Pickering emulsion stability during magnetic heating using ultrasound measurements, *Measurement* 178 (2021) 109431.

My contribution consisted of the initiation of the project and the partial design of the experiments. I also participate in the discussion of the results and finalization process of the manuscript.

[6] R. Bielas, D. Surdeko, K. Kaczmarek, A. Józefczak, The potential of magnetic heating for fabricating Pickering-emulsion-based capsules, *Colloids and Surfaces B: Biointerfaces* 192 (2020) 111070.

I designed the original idea of using an alternating magnetic field to form colloidal capsules. I contributed to the finalization of the manuscript.

With best regards,



Arkadiusz Józefczak
Arkadiusz.jozefczak@amu.edu.pl



Zbigniew Rozynek
Dr. hab. Prof. UAM
zbiroz@amu.edu.pl

June 01, 2021

Co-author statement

To whom it may concern

I hereby declare that I contributed to the following publications:

[1] Z. Rozynek, R. Bielas, A. Józefczak, Efficient formation of oil-in-oil Pickering emulsions with narrow size distributions by using electric fields, *Soft Matter* **14**, 5140–5149 (2018)
by initiating the project, proposing the scientific hypotheses, designing all of the experiments, performing the experiments whose results are presented in Fig. 5, Fig. 6, Fig. S1 and Fig. S2, contributing to data analysis and presentation, writing the first version of the manuscript, and by handling the submission.

[2] R. Bielas, Z. Rozynek, T. Hornowski, A. Józefczak, Ultrasound control of oil-in-oil Pickering emulsions preparation, *Journal of Physics D: Applied Physics* **53**, 085301 (2020)
by co-designing the ultrasonic measurements, taking an active part in discussions on the interpretation of the data, and by participating in writing and discussions towards the finalization of the manuscript together with all authors.

Sincerely yours

Zbigniew Rozynek

15. February 2021

Co-author Statement

I hereby declare that I am co-author of following publication(s):

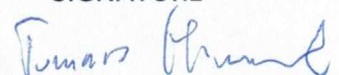
[1] R. Bielas, Z. Rozynek, T. Hornowski, A. Józefczak, Ultrasound control of oil-in-oil Pickering emulsions preparation., *Journal of Physics D: Applied Physics* 53.8 (2019): 085301.

[2] R. Bielas, T. Hornowski, K. Paulovičová, M. Rajňák, A. Józefczak, The effect of magnetic particles covering the droplets on the heating rate of Pickering emulsions in the AC magnetic field., *Journal of Molecular Liquids* 320 (2020): 114388.

My contribution in paper [1] consisted of *performing the theoretical analysis presented in section 3.1 and discussions on the interpretation of the data and the content of the manuscript. In paper [2] my contribution was to work on a final version of the manuscript.*

With best regards,

SIGNATURE



Tomasz Hornowski

hornaku@amu.edu.pl



Institute of Experimental Physics

Slovak Academy of Sciences

Watsonova 47, 040 01 Košice, SLOVAKIA

Tel.: +421-55-7922201, Fax: +421-55-6336292, E-mail: sekr@saske.sk



To whom it may concern

February 01, 2021

Co-author Statement

I hereby declare that I am a co-author of the following publication:

R. Bielas, T. Hornowski, K. Paulovičová, M. Rajňák, A. Józefczak, The effect of magnetic particles covering the droplets on the heating rate of Pickering emulsions in the AC magnetic field., *Journal of Molecular Liquids* 320 (2020): 114388.

My contribution consisted of measurements of magnetic properties of the studied samples.

Sincerely Yours

RNDr. Michal Rajňák, PhD.



Institute of Experimental Physics

Slovak Academy of Sciences

Watsonova 47, 040 01 Košice, SLOVAKIA

Tel.: +421-55-7922201, Fax: +421-55-6336292, E-mail: sekr@saske.sk



February 01, 2021

Co-author Statement

I hereby declare that I am a co-author of the following publication:

R. Bielas, T. Hornowski, K. Paulovičová, M. Rajňák, A. Józefczak, The effect of magnetic particles covering the droplets on the heating rate of Pickering emulsions in the AC magnetic field., *Journal of Molecular Liquids* 320 (2020): 114388.

My contribution consisted of preparation of magnetic particles sterically functionalized with oleic acid.

Sincerely yours


Ing. Katarína Paulovičová, PhD.

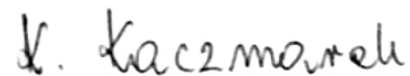
15. February 2021

Co-author Statement

I hereby declare that I contributed to the following publication:

[1] R. Bielas, D. Surdeko, K. Kaczmarek, A. Józefczak, The potential of magnetic heating for fabricating Pickering-emulsion-based capsules., *Colloids and Surfaces B: Biointerfaces* 192 (2020): 111070, by involvement in the data presentation, description and finalization process of the manuscript.

With best regards,



Katarzyna Kaczmarek
katarzyna.kaczmarek@strath.ac.uk

03.05.2021

Co-author Statement

I hereby declare that I am a co-author of the following publication:

1. R. Bielas, D. Surdeko, K. Kaczmarek, and A. Józefczak. The potential of magnetic heating for fabricating Pickering-emulsion-based capsules. *Colloids and Surfaces B: Biointerfaces*, 192:111070, Aug. 2020

My contribution consisted of:

1. performing some of the experiments concerning fabrication of the colloidal capsules described in the article,
2. finalization of the manuscript.

Best regards,

Dawid Surdeko

Dawid Surdeko

d.surdeko@utwente.nl

10. May 2021

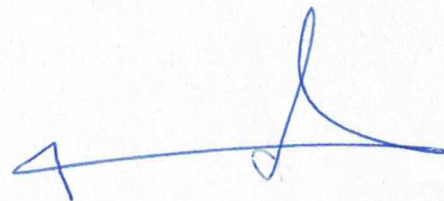
Co-author Statement

I hereby declare that I am co-author of publication:

R. Bielas, B. Jameel, A. Józefczak, Monitoring of Pickering emulsion stability during magnetic heating using ultrasound measurements, *Measurement*, 178 (2021) 109431.

My contribution consisted of the participation in the calorimetric and optical experiments, preparation of the part of Materials and Methods section of the manuscript and preparation of data visualization. I participated also in the discussions towards the final version of the manuscript.

With best regards,



Bassam Jameel

basjam@amu.edu.pl

1. Introduction

Emulsions are omnipresent systems involved in numerous daily activities, ranging from pharmaceuticals, cosmetics, and even the dairy products we consume. However, even a simple experiment mixing water and oil by hand-shaking shows that emulsion systems are inherently fragile. Despite well-grounded approaches to preparing stable emulsions, there is still space for scientific developments to, for instance, make the process more sustainable and eco-friendly. The problems that exist today can be tackled by a synergetic combination of knowledge from different disciplines. In a way, the whole science seems to be based on the synergy between subdisciplines; between the new and old and those near and a far away from each other. In my work, I take advantage of this approach and study Pickering emulsions with the simultaneous use of ultrasound, electric, and magnetic fields.

In the last decade, several research groups have investigated Pickering emulsions. There are interesting reports on using such particle-stabilized emulsions to prepare fruit-filled chocolate candies [1] or gluten-free bread [2] that seem to be both tangible and practical. There are also applications that are not as tangible but just as exciting, such as stimuli-responsive microscale catalysts [3] or microcapsules used in biomedicine [4], which are developed with the contribution of Pickering emulsions. Nevertheless, there is still a need for the development of better routes for producing Pickering emulsions that allow for the emulsions to be produced more rapidly, in larger quantities, and with a more defined droplet size, etc. The process of fabrication (e.g., its dynamics) is often monitored by using optical tools. There is, however, a problem with monitoring this process on industrial scale. Therefore, new ways of monitoring emulsion maturing are needed. Finally, when the emulsion is already prepared, it still needs to be characterized in terms of stimuli-responsiveness, long-term stability or possible destabilization.

The development of scientific fields can be two-fold. On the one hand, an increasing number of novel sorts of particles with unique properties could be proposed as efficient stabilizers of emulsion droplets, opening an fascinating and unending story of science. On the other hand, relatively basic and commonly used particles can be used in new applications. This is the reason why the synergy between relatively narrow disciplines like ultrasound and electrohydrodynamics was used for the efficient formation of Pickering emulsions in this

thesis. Regardless of the chosen strategy, the process of formation must also be characterized and presented as important due to the potential applications.

The presented thesis ties together several aspects that, when considered separately, could be considered quite distinct, such as: the physics of interfaces, the phenomena occurring under the electric field, the efficiency of emulsification procedures, and the propagation of ultrasound in particulate media or magnetic heating. This thesis is based on six scientific papers published in peer-reviewed journals. The main linking point between the articles is the method of emulsion preparation being based on ultrasonic homogenization and the application of electric fields. The main contribution of the presented papers to the above-mentioned fields of knowledge can be summarized as follows:

- A.** A new approach to the fabrication of oil-in-oil Pickering emulsions with a relatively narrow droplet size distribution was developed.
- B.** The usefulness of ultrasound to characterize the process of Pickering emulsion formation was demonstrated.
- C.** The dependency of magnetic heating efficiency on the solidity of the particle shell around the droplets was shown in the case of magnetic Pickering emulsions exposed to alternating magnetic fields.
- D.** A new potential route for the preparation of colloidal capsules via high-temperature increases induced during the magnetic heating of Pickering droplets was demonstrated.

In the next sections (Chapters 1.1–1.5), the presented statements will be rooted in the context of the current state of knowledge. To provide guidance regarding the published papers, some of their technical aspects are also commented on in Chapters 1.7–1.8.

1.1. Particle-stabilized emulsions (Pickering emulsions)

An emulsion is a class of disperse system in which one liquid phase is dispersed in another liquid phase, wherein these liquids are immiscible. During the formation of emulsion droplets (i.e., emulsification), the free energy of the interface changes due to the increase in the total interfacial area and the configurational entropy of the dispersion [5]. As the free energy of the emulsion is higher than that for the system before the emulsification, the (macro)emulsion is inherently thermodynamically unstable and, without stabilization, the emulsion droplets tend

to flocculate and merge (coalesce) over time. There are two approaches that provide stability of the emulsion: (i) lowering the total surface energy by lowering the interfacial tension, as in the case of surfactant-stabilized emulsions, and (ii) forming a mechanical barrier around the droplets to prevent their coalescence. The latter is the basis for particle-stabilized emulsions.

Particle-stabilized emulsions have their origin in the pioneering works of Ramsden [6] and Pickering [7]. In honor of the latter, these emulsions are commonly known as “Pickering emulsions” but, in the literature, one can also encounter other terms referring to such colloidal systems, e.g., “solid-stabilized emulsions”, “particle-laden emulsions” or “armored emulsions”. In Pickering emulsions, the particles adsorb to the droplet surface, forming a layer that prevents merging droplets (coalescence) by providing steric hindrance [8]. In “conventional” emulsions, surfactants adsorb to the interfacial surface and reduce the interfacial tension. At the same time, molecules develop either electrical double layer repulsion or steric repulsion. Pickering emulsions are believed to provide better kinetic stability, as the adsorption of particles at the droplet surface can be irreversible. In the literature, this is usually evidenced through the comparison of the desorption energy (i.e., the energy needed to detach the particle from the droplet surface) with a product of k_B (Boltzmann constant) and the temperature associated with thermal fluctuations.

Using the so-called Young equation, one can characterize the contact angle, θ , based on the respective interfacial tensions at the boundary between the solid, dispersed, and continuous phase, i.e., γ_{s-d} (solid particle-dispersed liquid), γ_{s-c} (solid particle-continuous phase), and γ_{c-d} (continuous phase-dispersed phase), as [9]:

$$\cos \theta = \frac{\gamma_{s-d} - \gamma_{s-c}}{\gamma_{c-d}}. \quad (1.1)$$

In **Figure 1.1**, an arrangement of the particles and the emulsion droplet with different contact angles is presented. This directly shows that the contact angle quantifies the affinity between the particles and the two liquids.

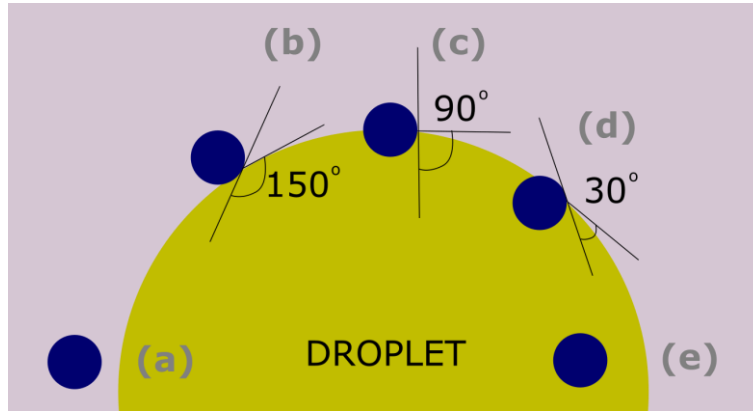


Figure 1.1 The position of solid particles related towards an emulsion droplet for different contact angles. **(a)** The affinity of the particle to the continuous phase is too large and the wettability of the particle by phases of emulsion is nonconformant. **(b)** The contact angle is high and the particle is toward a continuous phase but can still adsorb to the droplet. **(c)** The particle is equally wetted by both phases of emulsion. **(d)** The contact angle is low and the particle is toward a disperse phase. **(e)** The affinity of the particle to a dispersed phase is too large and the wettability of the particle by phases of emulsion is nonconformant.

The energy needed to detach the single particle from the liquid-liquid interface can be written as [9]:

$$\Delta G = \pi r_p^2 \gamma_{c-d} (1 - |\cos \theta|)^2, \quad (1.2)$$

where r_p is the radius of a solid particle. The form of expression, $|\cos \theta|$, indicates that the value of the contact angle governs the way the particle can be detached from the interface. For instance, for $\theta > 90^\circ$, a particle is detached toward a continuous phase rather than to a disperse phase [10]. **Eq. 1.2** is valid provided that the particle size allows for neglecting the gravitational force, which is practically always fulfilled.

For contact angles close to 90 degrees and particle sizes larger than several nanometers, the desorption energy can be several orders of magnitude higher than the Brownian energy, $k_B T$ [11] which is evidence of a strong attachment to the droplet interface. However, it should be noted that the contact angle strongly depends on the chemical properties of the solid particles and a perfect match between the liquids constituting the emulsion phases and stabilizing particles is challenging. In the context of the studies presented within this thesis, the emulsion stability of emulsion will be always associated with a stability against coalescence, i.e., in stable Pickering emulsions, the droplet does not merge after the formation process is finished.

This also means that the droplet size should not increase over a long period of time, although some works have reported a change in the size of emulsion droplets during long experiment durations, which was related to the breaking of droplet agglomerations rather than to coalescence [12].

In the early 2000s, Aveyard *et al.* indicated in their review article [8] that there were only a few reports on Pickering emulsions compared to the plenty of papers concerning surfactant-stabilized emulsions. This was caused by inadequate developments in material sciences in terms of providing a wide class of solid particles that could be used as emulsion stabilizers [11]. Now, in 2021, the situation is entirely different. Pickering emulsions hold promise in regard to applications in numerous fields, including the food industry [13, 14] and cosmetology [15, 16], especially due to the harmful effect of surfactant-stabilized emulsion on skin [17], as well as in pharmacy where Pickering emulsions can act themselves as drug carriers [18] or be precursors for fabricating colloidal capsules [19]. Pickering emulsions and derivative materials have been studied even in the context of the COVID-19 pandemic [20, 21]. Important in the case of Pickering emulsions (and derivatives) orally administered to the human body is the dynamics of digestion differing from those of “conventional” emulsions [22], and this could be an additional reason for using particle-stabilized emulsion systems.

Among the materials used as particle stabilizers, one can find: silica [23, 24], synthetic and natural clays [25-27], graphene oxide [28], polymers [29] and magnetite/maghemite [30, 31] as well as a wide class of bio-originated particles, such as polysaccharides [32], starch [33, 34], and cellulose [35]. This is, thereby, more significant because using sustainable, non-toxic, and eco-friendly particles seems to justify the need for a Pickering emulsion approach to counterbalance conventional surfactant-stabilized systems [36]. Not without significance is what happens after the usage of particles; the end life of particle stabilizers justifies the use of natural organic particles [37]. It is also worth noting that the term “Pickering emulsions” does not include only particle-stabilized systems. This class of colloids is broader and it incorporates emulsions that are not solely stabilized solely with solid particles but with, e.g., gels [38, 39] or proteins [40] as well. For this reason, (non-vegan) mayonnaise is also a kind of Pickering emulsion in which lecithin present in the egg yolk covers the oil droplets [41].

Despite the certain competition between surfactant-stabilized emulsions and Pickering emulsions generated by the sudden renaissance of Ramsden and Pickering concepts as well as the enthusiasm for new perspectives on achieving fast development, there is an open avenue for the combination of surfactants and particles as co-stabilizers. Surface-active agents can alter the wettability of particles and, therefore, improve the stability of emulsion droplets [42] or lead to the formation of switchable Pickering emulsions [43]. Even more recently, the idea of oil-in-dispersion Pickering emulsions was proposed [44] which is also on the frontier of studies on “classic” Pickering emulsions.

When the number of solid particles used as stabilizers is low from the beginning of formation process, the interfacial area cannot be sufficiently covered by particles. In this case, so-called “limited coalescence” occurs [45]. Each coalescence event leads to a progressive reduction of the interfacial area and lasts until the moment when the density of the particle layer around droplet is high enough to halt further coalescence [39]. The main feature of this experimental regime is that the droplet size is governed not by the mean of preparation but by the mass ratio between the dispersed phase and solid phase of emulsion. This relationship between spherical particles and their monolayer-like arrangement at the droplet interface can be described by the following formula [46]:

$$D_d = \frac{2\pi \phi_d}{\sqrt{3} \phi_p} d_p, \quad (1.3)$$

where D_d and d_p are the diameter of the droplets and particles, respectively; ϕ_d and ϕ_p are the volume fractions of the disperse and solid phase, respectively. After basic mathematical transformations, **Eq. 1.3** directly corresponds to the formula presented in **[Publication I-II]** and is derived in the Supplementary Materials to **[Publication I-II]** as well as in other papers [45, 46]. In **Figure 1.2**, such an example of the proportionality between the droplet size and an inverse number of silica nanorods used as stabilizers is shown [47].

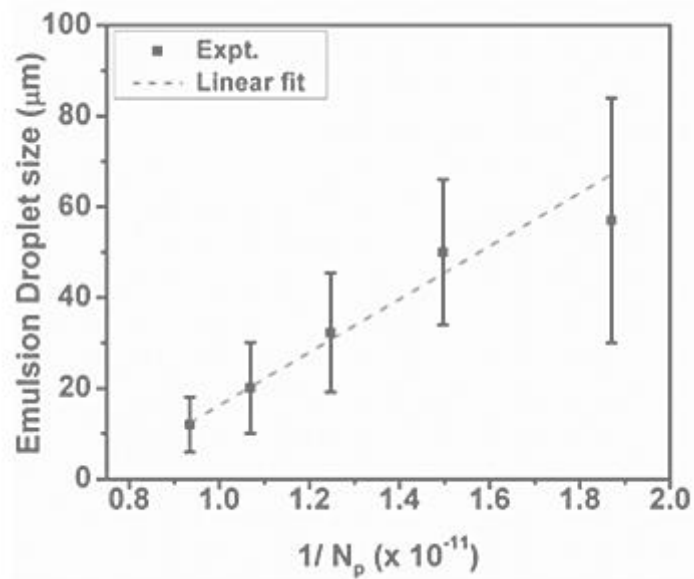


Figure 1.2 The mean droplet size in the function of the inverse number of particles used as stabilizers. The dotted line corresponds to the linear fitting according to the limited coalescence model (Eq. 1.3). The large standard deviations are explained by the shape of the stabilizers that were not spherical. Reproduced with permission from [47]. Copyright (2015) American Chemical Society.

From **Figure 1.2**, one can conclude that the more particles used for stabilizing the emulsion droplets, the smaller the size of droplet. However, even a limited coalescence regime has its limits. For instance, too much particle mass excess over the mass of the dispersed phase can lead to a situation where “free” particles are mainly dispersed in the continuous phase and the droplets are unevenly coated by particles [48]. Although the presence of particles in the continuous phase can be beneficial for emulsion stability [8], it is not economically justified. Some authors have also reported that the full coverage of the droplet surface is not required for preventing coalescence and providing kinetic stability for the emulsion [49].

Already in 1954, Wiley collected existing reports, starting with Pickering original paper, in which the limited coalescence of droplets was described but not necessarily called by name [50]. Wiley indicated that violent mechanical stirring could lead to the formation of droplets with narrow size distributions due to the process of limited coalescence. Additionally, the work of Wiley reproduced above has directly shown directly that the idea of the stabilization of emulsion droplets by particles was indeed known much earlier than the 2000s.

In the literature, oil-in-water or water-in-oil emulsions have mostly been investigated, with oil-in-oil emulsions being remarkably less reported despite their potential use in cosmetics

and pharmaceuticals [51]. Similarly, in the literature, when describing the principles behind Pickering emulsions, the basic ideas, such as the contact angle and particle wettability, are introduced by providing examples of systems containing water. However, non-aqueous Pickering emulsions can be also prepared. Moreover, there are some unique features that make oil-in-oil Pickering emulsions objects of interest. For instance, when the aqueous phase is dispensed, a new type of polymer nanoparticle can be prepared from the Pickering emulsion templates [52], and hydrophilic materials can be efficiently entrapped in the Pickering emulsion droplets [53]. Besides, some model investigations benefit from a lack of water in the tested system, e.g., studies on the electroformation of emulsions. This supports that oil-in-oil emulsions can experience a renaissance in the near future [54], also these stabilized with solid particles.

There exist several methods for fabricating stable Pickering emulsions. Most of them are one-step in nature; however, there are also procedures in which several steps must be taken, e.g., mechanical blending preceded by ultrasonic homogenization or microfluidization [55]. Commonly, a coarse emulsion with large droplets is subsequently dispersed to smaller droplets, as in the case of membrane emulsification techniques. It is worth noting that this is reversed compared to the method of preparation used in the presented thesis. **Table 1.1**, shows a short characterization of the Pickering emulsion formation techniques.

Table 1.1. An overview of the advantages and disadvantages of different Pickering emulsion procedures. The table is partially based on [49].

Method	Simplicity of the system	Duration of process	Narrow size distribution	Formation of small droplets
Microfluidics	no	long	yes	Depends on the parameters
Membrane emulsification	no	long	yes	Depends on the parameters
Mechanical homogenization	yes	short	no	no
Ultrasonic homogenization	yes	short	no	yes
High-pressure homogenization	no	short	no	yes

There exist relatively new approaches to providing precise control over the droplet size namely microfluidics and membrane emulsification, and these are receiving an increasing amount of attention. In microfluidics, Pickering emulsion is prepared droplet-by-droplet via the proper matching between the flow rates, interfacial tensions, and viscosities of phases in corresponding channels of the microfluidic device. This enables the formation of emulsions with very narrow size distributions. When the coefficient of variation (CV) is considered, i.e., the ratio between the standard deviation and the mean droplet diameter commonly used to evaluate droplet size distributions, the microfluidic approach provides emulsions with a CV below 5% [56]. It is worth pointing out that a narrow size distribution is believed to be an important factor in the stabilization of Pickering emulsions as a variation in the size of the droplets can facilitate their coalescence [11]. Another method that provides a quite narrow size distribution of droplets is membrane emulsification. In this technique, the phases of emulsion are pressed through the membrane, and the pore size governs the resulting droplet sizes. In terms of the droplet size distribution, this varies depending on the literature reports. For instance, a CV around 23% was achieved for O/W emulsions stabilized with chitosan-coated alginate particles [57]. However, to achieve CV = 25% in the work of Thompson *et al.* [58], the careful control of oil flux through the membrane must have been applied. Nevertheless, the formation of Pickering emulsions with narrow size distributions is possible using microfluidics and membrane emulsification, although it should be noted that there is an inherent difficulty involved in obtaining high throughput, which narrows the current application possibilities as presented in **Table 1.1**.

In comparison to the methods described above, there are also bulk methods based on different kinds of homogenization routes, i.e., mechanical stirring, ultrasonic homogenization, and high-pressure homogenization, although the latter is rarely used in studies of Pickering emulsions despite its being used in the industry for “conventional emulsions” [49]. In these techniques, shear forces are generated to disperse the inner emulsion phase into small droplets. The process can be quick and result in bulk quantities of emulsions, but the droplet size distribution is difficult to control. For this reason, there is still a need to propose new methods of formation, especially ones that can link the precise prediction of the droplet size and efficient particle usage with the high production rate provided by, e.g., ultrasonic homogenization.

1.2. Ultrasonic homogenization

To disperse a liquid in another liquid and form an emulsion, the subsequent events of droplet break-up must occur. For this purpose, mechanical energy must be provided to the system to generate mechanical shearing that overcomes the Laplace pressure, i.e., a pressure that causes the droplet shape to be dependent on the interfacial tension and droplet radius [59]. The required shearing needed to obtain small droplets can be achieved under a turbulent flow that, according to the so-called Kolmogorov theory, is characterized by the sizes of the induced eddies, i.e., local pressure fluctuations [60]. From the relationship between the possible eddy sizes, one can obtain the formula for the maximum droplet size, D_d , that remains non-fragmented under the turbulences induced by, e.g., mechanical stirring or high-intensity ultrasonic waves:

$$D_d = C \cdot \frac{\gamma_{c-d}^{3/5}}{\epsilon^{2/5} \rho^{1/5}}. \quad (1.4)$$

Eq. 1.4 takes into account the parameters of homogenization, i.e., the energy dissipation rate ϵ (energy dissipated in unit volume per unit time [46]) as well as the parameters of the media, such as the density, ρ , and interfacial tension; C is the constant of the order of unity [59]. Despite the existence of experimental works on the above-mentioned relations, it is still challenging to predict the droplet size after homogenization. This is because of the precise determination of the energy dissipation rate that can vary in the whole volume of the sample. It is also worth noting that, when Pickering emulsions are prepared, the presence of solid particles surely affects the process of homogenization, e.g., the overall density and viscosity increases. However, to the best of my knowledge, such an influence has been not directly investigated in the literature.

Homogenization by using ultrasound is one of the common approaches to fabricating emulsions in bulk quantities, including particle-stabilized emulsions. In principle, there are two mechanisms involved in ultrasonic homogenization. First, larger droplets are formed by the combined action of interfacial waves and so-called Rayleigh-Taylor instability [61]. In the second stage, an acoustic cavitation occurs as a main phenomenon. When the high-intensity acoustic wave travels through the medium, strong pressure fluctuations are generated there. This leads to the formation and collapse of bubbles that generate local turbulence and shear

forces. These contribute to the further fragmentation of the dispersed phase into smaller single droplets. There are experimental works in which the influence of the sonication time and acoustic intensity on the droplet size distribution were investigated, but this was more often for “conventional emulsions” rather than for Pickering emulsions. For instance, in the case of O/W emulsions stabilized with chitosan particles nanoparticles, 5 minutes of sonication with an electric power of 600 W resulted in a droplet size of around 10 μm and quite a wide size distribution [62]. What was interesting, smaller droplets were achieved with lower power and the same sonication time, which was related to the high-temperature increase caused by the ultrasonic homogenization. It should be noted for the record that, in many cases, the exact parameters of sonication are not fully characterized, e.g., by giving only the electric power of the used device, which is an issue raised in the literature [63]. In this work, the emulsions formed via ultrasound homogenization were characterized by the small-angle X-ray scattering (SAXS) method in-line, during the process of preparation. The droplet size decreased significantly with an increasing acoustic intensity. Additionally, the authors directly showed that using homogenization to produce Pickering emulsions leads to a high content (even 60%) of “free” particles floating in the continuous phase [63]. On the other hand, Low *et al.* prepared O/W emulsions stabilized with cellulose nanocrystals with a CV lower than 35%, even when using a traditional ultrasonic homogenizer [64].

As one can see, it is generally difficult to control over the size (and size distribution) of droplets prepared by ultrasonication, as the process of cavitation is dynamic and inherently non-linear. Knowledge regarding the predictable droplet size and distribution is, in turn, crucial from an applicable point of view. In this context, it is important to note that there are theoretical models that can precisely predict the droplet size presented on the basis of the example of cellulose-nanocrystal-stabilized O/W emulsions prepared via sonication [65]. Taking into account the convolution of the effects of dispersed phase and solid phase concentrations as well as the acoustic intensity, it was possible to obtain the dependence between the mean droplet diameter and the sonication duration which depends additionally on input energy density. The exemplary dependence is presented in **Figure 1.3**. It should be noted that the model is valid for situations when the pre-emulsification procedure is involved before the final sonication.

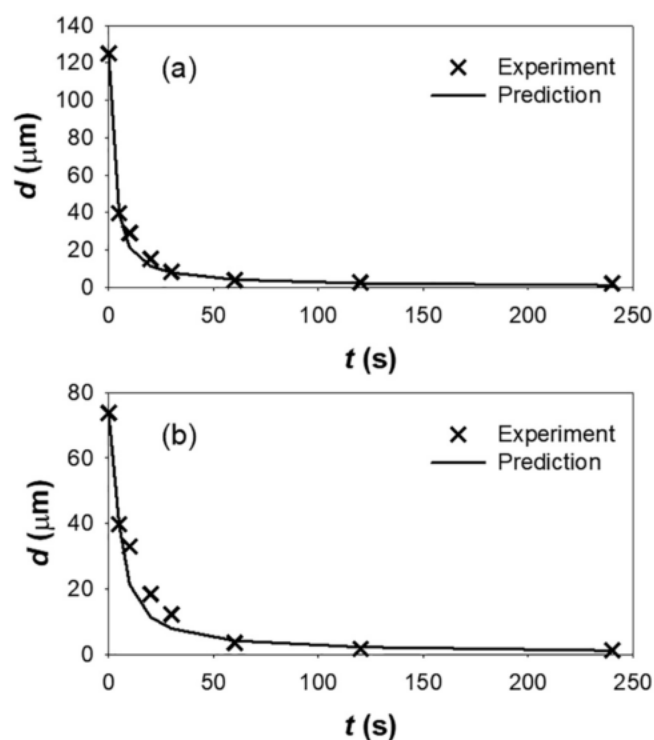


Figure 1.3 An evolution of droplet size as a function of the sonication time. Panel (a) shows the results for high and (b) low potential of droplet break-up. Reproduced from [65].

Using ultrasonic homogenization can be beneficial over other emulsification techniques because it is believed to be less energy-consuming [66] and can result in a significantly smaller droplet size compared to mechanical stirring [67]; however, it seems to depend strongly on the properties of the prepared emulsions, especially the stabilizers used [68].

Emulsions stabilized with particles can be efficiently prepared using ultrasonic homogenization alone. However, when the mass of the particles is much smaller than the mass of the dispersed phase (limited coalescence regime), directly after the bulk methods of fabrication (including ultrasonic homogenization), the droplets cannot be fully coated by the particles. By allowing for the limited coalescence of the uncoated droplets, a dense layer of particles forms. However, such a process can be facilitated by, e.g., using phenomena occurring when a Pickering emulsion with not completely covered droplets is exposed to electric fields.

1.3. Emulsions under the electric field

It is commonly known that two droplets immersed in a liquid medium tend to coalesce to lower the free energy of the system. When these two droplets are additionally subjected to the homogenous direct current (DC) electric field, the process of coalescence is facilitated due to dipolar interactions between the droplets. For weakly conductive liquids (also called “leaky dielectrics”), the presence of an electric potential difference causes the accumulation of free charges at the droplet surface [69]. This allows for the induction of electric dipoles, and the direction of the dipole moment is related to the ratios between the electric permittivity and conductivity of the droplet and that of the surrounding medium; when these are higher for the surrounding medium (for instance, for silicone oil droplets suspended in castor oil), the direction is opposite to that of the electric field [70]. The strength of such interactions between droplets can be expressed as [71]:

$$F_d = -\frac{24\pi\epsilon_c r^6 E^2}{d^4}. \quad (1.5)$$

As can be seen, the attraction of droplets depends on the electric field intensity, E , radius of the droplets, r , electric permittivity of the continuous phase, ϵ_c , and separation between droplets, d . Additionally, the properties of the medium such as the interfacial tension, must also be taken into account in the moment of close vicinity of droplets. When the electrocoalescence of two uncoated droplets was investigated, the time scale of the coalescence event depended on the initial separation between the droplets, the viscosity of the surrounding medium, and the electric field intensity [71]. The presence of solid particles on the droplet surface, as in the case of Pickering droplets, results in retarded coalescence because of the mechanical barrier of the particles. When a number of droplets constituting a dispersed phase are suspended in another liquid (continuous phase), the situation is similar. It is worth noting that the dipolar interactions and resulting electrocoalescence generally should be undesired because of the acceleration of the emulsion aging. However, for limited coalescence regime (Chapter 1.2), electrocoalescence ultimately leads to the stability of the particle shell around the droplets due to “surface-volume gain” after each coalescence event.

The applied voltage does not only cause dipolar interactions of droplets but also induces their deformation. Such a deformation can be described by the so-called Taylor deformation parameter [72]:

$$D = \frac{x_1 - x_p}{x_1 + x_p}, \quad (1.6)$$

where x_1 and x_p relate to the droplet dimension within the direction of the electric field and perpendicular to the electric field, respectively. For a droplet surrounded by dielectric liquid, this deformation can also be theoretically predicted as [69]:

$$D = \frac{9}{16} \frac{\varepsilon_c \varepsilon_0 r E^2}{\gamma_{c-d}} \cdot A. \quad (1.7)$$

The parameter A is a complex relation of the ratios of electric conductivities, electric permittivities (dielectric constants), and viscosities of the disperse and continuous phase. These ratios govern the behavior of a droplet. For instance, for silicone oil droplet immersed in castor oil, the deformation is positive, i.e., the droplet is elongated perpendicularly to the electric field direction, but, for a reverse system parameter, D is negative [69]. It is important to point out that, according to **Eq. 1.7**, the deformation depends on the size of the droplets, and, for the same electric field intensity, smaller droplets are less deformable. As in the case of electric dipolar interactions, the presence of solid particles changes the way the droplet is deformed in the electric field. Considering the particle layer as a two-dimensional suspension, the surface viscosities are increased due to dissipation arising from the particle motion. However, the surface conductivity is not significant for the deformation of droplet [73].

Generally, the change in droplet shape is due to the free electric charges accumulating at the droplet interface under the influence of an applied electric field that induces deforming electrical stresses. Such electric stresses have two components: normal and tangential to the curvature of the droplet. The first is responsible for droplet deformation and the latter induces electrohydrodynamic (EHD) flows. As the tangential component is not balanced by any capillary forces, these EHD flows can freely occur and lead to the shearing of the liquids inside and outside the droplet. For instance, when the particles are located inside the droplet (e.g., during the formation of a single droplet by a mechanical pipette), the EHD flows push them outside the droplet. The flows' direction depends on the electrical conductivities of the droplet and surrounding medium, i.e., when the droplet's electrical conductivity is lower than

that of the surrounding liquid, the flows are from the droplet ends to the center of the droplet [74].

The presence of particles at the droplet surface obviously influences the EHD flows. For non-conductive particles, the induction of EHD flows around the completely covered droplet is retarded [75]. In **Figure 1.4**, the velocity of the EHD flows around the silicone oil droplets stabilized with non-conductive (polystyrene) particles and suspended in castor oil is visualized for different particle coverages by particle image velocimetry (PIV) [75]. As one can see, the increasing coverage by particles reduces the EHD flows. At the same time, the deformation of the droplet is also clearly dependent on the surface coverage.

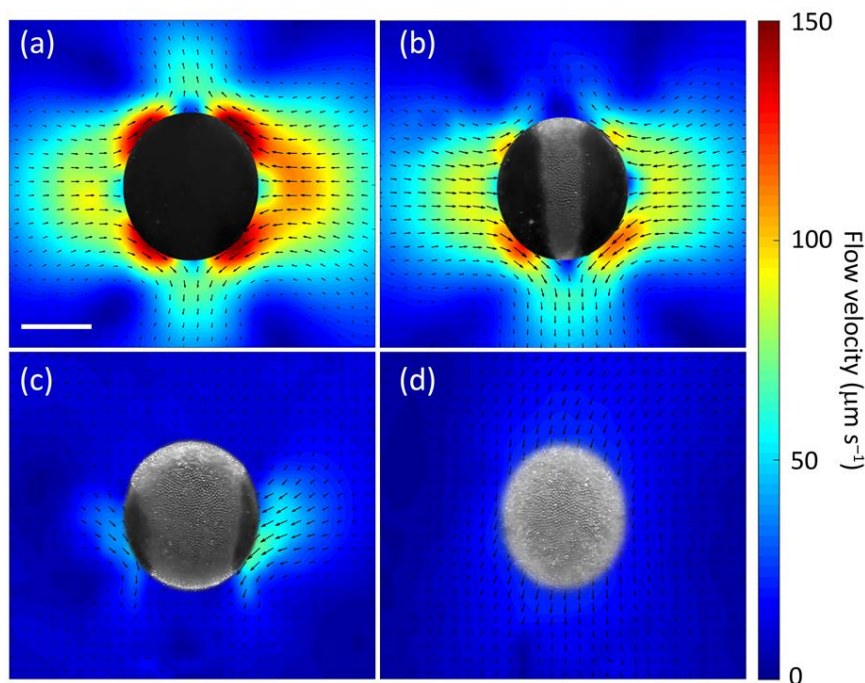


Figure 1.4 The spatial distribution of electrohydrodynamic (EHD) flows around a silicone oil droplet suspended in castor oil covered by polystyrene microparticles. The results in panels (a–d) differs with the increasing coverage of the droplet by particles. Reproduced from [75].

It is beneficial for the formation of the orderly arranged stable particle shell when the EHD flows are directed into the center of the droplet. Then, for the electric properties of the solid particles similar to liquids, the EHD flows push the particles at the surface and arrange them in a densely packed structure [69]. For two droplets partially covered by particles, the electric field can play a dual role. The dipolar interactions make the droplets approach one another, and droplet merging is enabled by the forming of particle free regions on the droplet flanks through EHD liquid flows.

When the intensity of the applied electric field is high, instability occurs, which leads to the electrorotation of the droplets, which is sometimes also referred to as a “Quincke rotation”: based on the German scientist who discovered this phenomenon for particles in the end of 19th century. For a higher electric field intensity, the induced electric dipoles can be misaligned compared to the direction of the electric field, which leads to torque and results in a rotation of the droplet [73]. The electric field intensity needed to cause the electrorotation of the droplets is dependent on the electrical properties of the droplet and surrounding liquid. Also in this case, particle shell affects the droplet behavior. The Quincke rotations are weaker with higher particle coverage, which can be explained by the induced droplet asphericity [73] and by the increased viscous effect that limits the rotation of the droplets in the presence of the particles at the interface [70]. Apart from being an interesting phenomenon, such a rotation of droplets can break droplet chains and agglomerates and, therefore, additionally contribute to the stabilization of the Pickering emulsion. Formation of chains (dipolar interactions) and agglomerates lead potentially to particle bridging, i.e., a situation where two droplets in a chain are stabilized with the same particles. Such a bridge can be removed by altering the wettability of the particles or by inducing shearing at different rates [46]. When the Pickering emulsions are exposed to DC electric fields of different intensities, they experience a variety of shear rates, which leads to the efficient breaking of the agglomerates.

The phenomena occurring in an emulsion under an electric field have been used in numerous studies. For instance, water-in-castor oil emulsions were prepared using DC electric fields [76]. It was shown that the mean size of the droplets decreased with the increasing duration of the emulsification and electric field intensities. More interesting is the process of emulsification being very quick and lasting only several seconds due to very high intensity of the electric field. High-intensity electric fields can be also used to destabilize emulsions, as shown with water-in-oil Pickering emulsions [77]. For petrochemical industry applications, the process of emulsion break-up can lead to the removal of water from the oil with the assistance of solid particles [78] and reversely, the elimination of oil contaminants from water when O/W emulsions are investigated [79].

Oil-in-oil emulsions are remarkably less investigated under an electric field. The use of oil instead of water as a disperse phase can change the behavior of emulsion droplets due to the different relations between the electrical properties of phases. For instance, the electrical

conductivity of distilled water is 5.5×10^6 pS/m and 50 pS/m for castor oil [75, 76]. The mismatch between electrical properties of two oils, e.g., silicone oil and castor oil, is much smaller that brings about the consequences regarding the fundamental research on the behavior of single droplets and oil-in-oil emulsions.

1.4. Propagation of ultrasonic waves in emulsions

As emulsions are ubiquitous colloidal systems needed in many scientific, industrial, and medical fields, robust and efficient methods for their characterization are required. Ultrasound can be used as one of the approaches allowing for the non-destructive and in-line testing of emulsions. This has been utilized *inter alia* to follow the long-term stability of emulsions via the determination of sedimentation or flocculation rates [80, 81] or to evaluate the emulsion structure during process of emulsion formation [82], including the droplet size distributions [83]. Regardless of the exact application, the use of ultrasound to characterize emulsions is based on the link between the properties of a tested medium and its acoustic parameters that can be experimentally measured and theoretically predicted. It is worth explicitly pointing out that, to the best of knowledge, there are only a few studies concerning such ultrasound studies on Pickering emulsions [84-86].

In a real, attenuating medium, the propagation of a plane ultrasonic wave of a given frequency, f , can be described by the complex wave number:

$$k = \frac{2\pi f}{c} + i\alpha. \quad (1.8)$$

In **Eq. 1.8**, c is the speed of the wave propagation (in other words, the speed of the ultrasound or ultrasonic velocity) and α is the attenuation coefficient that describes a decaying wave amplitude with the distance [87]. In homogenous media, i.e., when there are no scatterers as for, e.g., pure oils or homogenous solid materials, an acoustic wave is attenuated due to the viscosity of the medium and the thermal conduction, as is expressed by the well-known Stokes-Kirchhoff equation. Eventually, the relaxation mechanisms relying on the distribution of the energy of macroscopic motions induced by the propagating ultrasound wave to the molecular motions should also be taken into account, e.g., in biological tissues [88]. The speed of the ultrasound, in turn, obeys the so-called Newton-Laplace formula and depends on the density and mechanical properties of the medium. For liquids, these properties are characterized by a bulk elasticity modulus, but, for solid materials, the speed of the ultrasound

additionally depends on shear modulus. It should be noted that, most often, the propagation of the ultrasound is considered to be the propagation of longitudinal waves that can propagate in media characterized by bulk elasticity. In comparison, transverse ultrasonic waves can travel through media characterized by an elasticity of form, which is limited mostly to solids [89].

The situation changes the medium in which the ultrasonic wave is travelling is heterogeneous, i.e., there is more than one phase. Examples include emulsions (liquid-in-liquid), sols (solid-in-liquid), and composites (solid-in-solid). Then, apart from the properties of the phases, such as the viscosity and density, the phenomena occurring at the phase boundaries must also be taken into account. These result from differences in the mechanical and thermal properties between the phases, which contribute to the attenuation of sound and alter the speed of sound. When the compressibility of a particulate (i.e., droplet, particle, etc.) is different from the compressibility of the surrounding medium, its compression and expansion in a response to an ultrasonic wave is different than that of the surrounding liquid. When, in turn, the thermal properties of the phases are different, there would be heat flow between them uncorrelated with the phase of the cyclic pressure changes associated with an incident ultrasonic wave. Last but not least, a density contrast between the phases can take place, which leads to a difference in the inertia between the disperse and continuous phase [90]. Besides, the phases contribute to the absorption due to their intrinsic properties according to “classic absorption”.

It should be noted that the contributions of the mechanisms described above to the attenuation of the ultrasound are generally additive, and overall attenuation of the inhomogeneous medium can be expressed as a simple sum of contributing attenuation coefficients resulting from particular mechanisms [91]:

$$\alpha_{overall} = \alpha_{intrinsic} + \alpha_{scattering} + \alpha_{visco-inertial} + \alpha_{thermal}. \quad (1.9)$$

Over time, theories of different complexities were developed to quantitatively describe the propagation of an ultrasound in complex media. One of the most established theoretical models to date that has sufficiently described the propagation of ultrasound both in dispersions and emulsions is the ECAH theory which combines the works of Epstein and Carhart (1953) and Allegra and Hawley (1972) [92, 93]. This theoretical approach is based on a calculation of wave numbers of incident and scattered waves, while the scattering can be

not only due to the geometry of the objects, e.g., the size of the droplets or particles but foremost due to the differences in the properties of the phases.

When the incident acoustic wave encounters a scatterer such as an emulsion droplet or a particle, this gives a way to the new waves, i.e., the reflected wave, the wave inside the scattering object, and, additionally, visco-inertial and thermal waves in the continuous and dispersed phase [94]. Each of the mentioned waves can be expressed by corresponding wave equations and solved by using spherical Bessel functions and Legendre polynomials. Then, because of the boundary conditions for the inside and outside of the scatterer (e.g., on the droplet surface), one can set six formulas, with the unknown coefficients usually denoted as A_n , B_n , C_n , A'_n , B'_n , and C'_n , respectively corresponding to the wave scattered into the continuous phase, thermal wave and visco-inertial wave, and waves propagating in the inside of the scattering object. This leads to a need to solve a complex matrix. However, it should be noted that only the coefficients A_n are important from the experimental point of view, because only the wave scattered into the continuous phase can be experimentally studied by ultrasonic measurements. The thermal and visco-inertial waves are attenuated completely in a very short distance compared to the size of the objects [93], which excludes the possibility of direct measurement of such waves. However, the contrasts on the phase boundaries still contribute to the solution of the set of equations mentioned above. As the total attenuation of the medium is only dependent on the values of A_n , using the formula for the complex wave number of the composite medium [95], the total attenuation can be derived as [96]:

$$\alpha = -\frac{3\varphi}{2a^3k_c^2} \sum_{n=0}^{\infty} (2n+1)A_n. \quad (1.10)$$

As can be seen, the values of the attenuation coefficients vary with the size of droplets/particles, a , the frequency of ultrasound and the number of scattering objects per volume described by the concentration, φ [91]. The number of coefficients A_n needed for the precise determination of the attenuation coefficient is practically limited, which simplifies the calculations. This is also the case for silicone oil droplets immersed in castor oil where only the thermal properties differ on the phase boundaries and the only thermal waves can be taken into consideration; in the long wavelength limit ($kR \ll 1$), the ultrasonic attenuation is dominated by the zero-order term because the values of A_n decrease very quickly for $n > 2$ [90].

Despite its complexity and the fact that it requires numerical calculations rather than using analytical formulas, the ECAH model is used in numerous works and can be successfully compared with experimental results on emulsions [83, 97]. However, it should be noted that the precision of obtained theoretical results is highly related to computational issues, as the model requires solving complicated matrices. Even though, the model assumes a linear relation between the attenuation coefficient and the concentration of scatterers in the medium. To calculate the attenuation coefficient, the parameters are simply multiplied by the concentration, which is rather an idealistic case. In concentrated emulsions or dispersions, there is multiple scattering, i.e., the interactions of scattered waves with other objects, and this should be taken into consideration [98]. Nevertheless, it is believed that the ECAH theory is valid for low-concentrated systems. Another drawback of using ECAH is the vast amount of data characterizing the properties of the phases that surely influences the results of the modeling but is difficult to collect. This could be especially problematic for non-typical experimental conditions, such as the temperatures higher than room temperature. Importantly, based on reverse analysis, it is possible to obtain a size distribution of the particulates (droplets, particles, bubbles, etc.) according theoretical predictions and experimental results when obtained with a wide-band frequency range [94].

The most important issue in the context of the presented thesis is that the ECAH theory does not consider three-phase systems. This means that Pickering emulsions cannot be efficiently characterized by this model. In fact, in 1990s, Anson and Chivers developed an approach for the modeling of so-called capsulated emulsions [99]. In this approach, droplets with a solid shell around them were considered, and they were modeled by three-phase objects consisting of a core material, shell, and surrounding medium. For each of them separately, the procedure was very similar to the one proposed by ECAH, which complicated the solution of matrices. The Anson and Chivers' model did not seem to lead to extended scientific interest on the ultrasonic testing of "non-conventional emulsions". However, the examples of its usage can be found in the work of Chen [100] and Guedra *et al.* [101]. Analogously, Pickering emulsions could be considered as capsulated emulsions with loose capsule shell and modeled in the future by the mentioned approaches.

When it comes to works that directly relate to ultrasound propagation in Pickering emulsions, Venkataramani *et al.* [86] used a ultrasound spectroscopy device for the determination of the

droplet size distribution in W/O emulsions stabilized with silica particles. The ultrasound was sensitive to changes in the droplet size associated with the slow destabilization of emulsion by droplet coalescence. In another work [85], ultrasonic waves were used to monitor the long-term stability of magnetic Pickering emulsions. The observed changes in the shape of the ultrasonic pulses observed in the following days of the experiment were correlated with changes in the droplet size. ECAH theory predictions, in turn, were shown against experimental results for W/O emulsions stabilized with silica particles [84]. While the experimental and theoretical results were very similar for the suspension of particles, the ECAH theory was not valid for the Pickering emulsions, and other models were used. The same authors employed a reverse analysis of the ultrasonic spectroscopy data for the determination of the size distribution of silica microcapsules [102], which was similar to the works by Anson and Chivers.

As reports on the acoustical properties of magnetic Pickering emulsions are rather rare, some relevant knowledge can be given by studies on magnetic fluids extensively studied by ultrasound [103]. However, to date, in the literature there is no complex report on ultrasonic studies of Pickering emulsions that characterizes such systems while being aware of the limitations of existing theories when described three-phase systems. Pickering emulsions are much more complicated systems compared to, e.g., magnetic fluids which make such direct comparisons impossible. Simultaneously, magnetic colloids, i.e., both magnetic fluids and Pickering emulsions, can be important objects of scientific interests because of their potential for magnetic heating under alternating magnetic fields.

1.5. Magnetic heating of colloidal systems

The magnetic field is one of the stimuli that can be used to induce a specific response in emulsion systems. When magnetic particles reside on the emulsion droplet surface, the application of static (DC) magnetic fields can lead to, for instance, the spatial positioning of the droplets [104] and the controlled separation of the phases [105]. This could be especially applied to improve the efficiency of oil recovery, which is beneficial for combating the effects of climate change. When the applied magnetic field is alternating (AC), e.g., is generated by the alternating current flowing in a magnetic coil, the magnetic particles generate heat that can be used *inter alia* to induce a response of the human body during magnetic hyperthermia

[106] and enhance the permeability of the pores in Pickering emulsion-based colloidal capsules [107]. Temperature increases may also destabilize an emulsion system [108]. It is worth noting that, despite the presented examples, Pickering emulsions are not so thoroughly investigated in the context of magnetic heating as, for instance, magnetic fluids, i.e., suspensions of magnetic particles in liquid. Simultaneously, studies on the magnetic heating of magnetic fluids have been a popular scientific area, specifically focused on magnetic hyperthermia therapeutic applications.

The generation of heat in magnetic colloidal systems occurs due to losses of the magnetic energy in the magnetic particles through relaxation mechanisms, magnetic hysteresis, or the induction of eddy currents. When it comes to magnetic relaxation, it can be modeled by the Linear Response Theory introduced by Rosensweig [109]. The name of the theory refers to the linearity between the intensity of the applied magnetic field, H , and the resulting magnetization, M . If this relationship is fulfilled, the power density dissipated in the volume of the magnetic colloid (e.g. magnetic fluid) can be expressed as:

$$P_{relaxation} = \mu_0 \pi f H^2 \frac{2\pi f \tau}{1+(2\pi f \tau)^2} \chi, \quad (1.11)$$

where μ_0 is the magnetic permittivity of the empty space, f is the frequency of an alternating magnetic field, and χ is an equilibrium magnetic susceptibility. The parameter, τ , is an effective relaxation time, $\tau = \frac{\tau_B + \tau_N}{\tau_B \cdot \tau_N}$, which is dependent on the relaxation times related to the two relaxation mechanisms the magnetic particle can undergo: Brown relaxation (τ_B) and Néel relaxation (τ_N). The alternating magnetic field imposes the aligning of the oscillations of magnetic moment of a particle to the alternating directions of magnetic field. In the Brown mechanism, the magnetic moment oscillates with the whole particle, but, in the case of Néel relaxation, the particle itself remains at rest [110]. The Brown relaxation is dominant with bigger particles compared to the Néel relaxation mechanism. The Brown relaxation time is proportional to the viscosity of the medium surrounding the particle. This means that in highly viscous media, this mechanism can be sufficiently inhibited [111]. **Eq. 1.11** is valid for particles of a monodisperse size. As the magnetic susceptibility and efficient relaxation time differ for different particle sizes, the size distribution function should be introduced to **Eq. 1.11** [112]. Another assumption validating the Linear Response Theory is the size of the particles. When the particle size exceeds the limit for single-domain particles, the application of alternating

magnetic field leads to the movement of the walls between the magnetic domains inside the particle rather than the flipping of the magnetic moment, which is an additional source of energy dissipation [113]. Magnetic domains exist due to the lowering of the system energy. The reorganization and motion of their walls lead to the hysteresis of the magnetization, which is manifested as the loop in the magnetization curve, i.e., the relation between the magnetization and magnetic field [114]. The limiting size when the particle becomes multi-domain differs for different types of magnetic materials. For instance, for iron oxide particles, this size is 160 nm [115], but other authors have indicated that particles consist of nanometric domains already above the size of 100 nm [116]. The generation of eddy currents and, consequently, Joule's heating, in most used magnetic particles (including magnetite/maghemite) is believed to be negligible because of high electrical resistivity of particles and small particle size [114]. It is interesting that Joule heating can be an important factor that limits the practical use of magnetic hyperthermia in clinics [117]. A schematic illustration that summarizes the relaxation and hysteresis mechanisms of magnetic energy losses is presented in **Figure 1.7**.

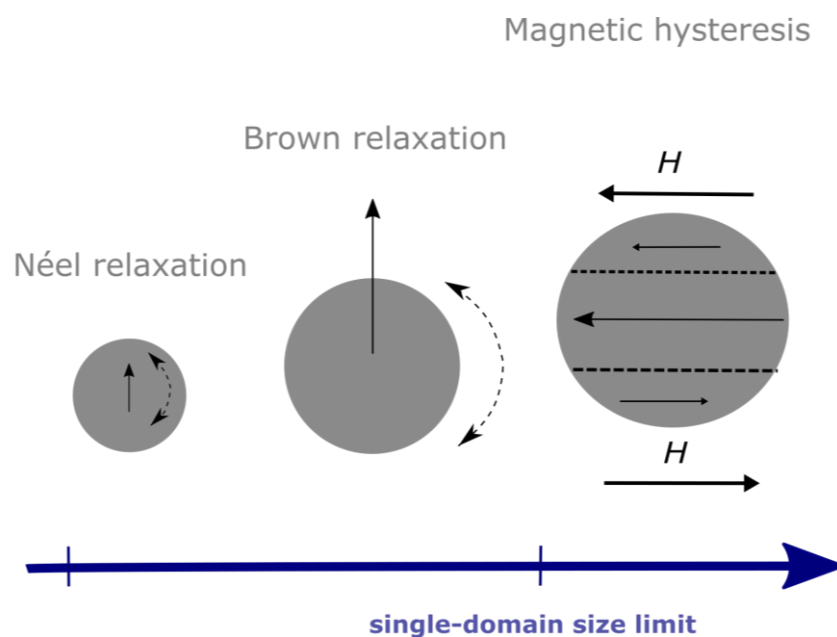


Figure 1.7 A scheme of magnetic hysteresis and Brown and Néel relaxation losses when the magnetic particle is exposed to an alternating magnetic field.

It is believed that the mechanisms of relaxation subside when the magnetic particle size exceeds the limiting value. For larger particles, the relaxation times are very long and can last even years [118]. However, for intermediate-size particles, both magnetic hysteresis and

relaxation mechanisms contribute to the magnetic power dissipation especially for particles with broad size distributions.

From **Eq. 1.11**, it is clear that the magnetic power dissipated into heat in small particles depends on the intensity of the magnetic fields. This dependence is quadratic for relaxation mechanisms, but, in the case of hysteresis losses, the dissipated power is proportional to H^3 [119]. The magnetic power dissipation also depends on the frequency of alternation in the magnetic field. Generally, under the Linear Response Theory, there is a local maximum in the relationship between the power dissipation *versus* the frequency. This is dependent on the particle size, resulting in the need for the optimization of the particle size to obtain the maximum heating performance [120]. The optimization of the heating rate of particles in the function of frequency is also important due to the safety of magnetic hyperthermia therapy and resultant the so-called Hergt-Dutz limit [121] in terms of the possible magnetic field intensity and frequency used in clinics.

Eq. 1.11 is valid for a single particle and the generated heat should increase proportionally with the increasing number of magnetic particles. However, the increasing concentration means that the interparticle distance becomes increasingly smaller with the corresponding formation of agglomerates. As a consequence, the possibility of magnetic interactions between the particles increases. Because of the numerous experimental conditions and the possible differences between them, there is no consensus as to whether magnetic interactions in the particle agglomerates deteriorate [122] or improve [123] the heating efficiency.

To aid the comparison of different magnetic heating experiments, the specific absorption rate (SAR), also referred to as the specific power absorption (SPA) or specific loss power (SLP), is commonly presented,. The exact formula is different in various reports, including:

$$SAR = c_p \cdot \left(\frac{dT}{dt}\right)_{t=0} \text{ or } SAR = \frac{c_p}{m_{magnetic}} \cdot \left(\frac{dT}{dt}\right)_{t=0}. \quad (1.12)$$

In **Eq. 1.12**, c_p relates to the specific heat of the sample. It is commonly calculated as the weighted average of the specific heats of the substrates [124]. In turn, $\frac{dT}{dt}$ is the rate of the temperature increase during the application of the alternating magnetic field. There are different approaches to determine this rate [125, 126], but one of the most common procedure includes the fitting of the experimental temperature elevation curve to the so-

called Box-Lucas equation: $\Delta T(t) = T_{max} \left(1 - e^{-\frac{t}{\tau}}\right)$ [126]. Then, the temperature increase rate is dependent on the derived parameters as: $\frac{dT}{dt} = \frac{T_{max}}{\tau}$ [127]. Sometimes, the mass of the magnetic material $m_{magnetic}$ is also used in the formula to determine SAR. Although it can be beneficial to make the SAR dependent on the mass of the magnetic particles, it also generates an inconsistency in physical units. When the mass of the particles is included in **Eq. 1.12**, the SAR should be expressed in $[W/kg/g_{magnetic}]$. In numerous papers, e.g., [128, 129], the unit for the SAR is simply expressed in $[W/g]$, which is not consistent with units for physical quantities.

Regarding reports on the magnetic heating of Pickering emulsions, there are a few examples. Brugger *et al.* reported the effective magnetic heating of O/W emulsions when magnetite-in-gel nanoparticles were used as stabilizers [130]. Due to the thermosensitivity of the used gel particles, the emulsions could be broken by increasing the temperature. Interestingly, the temperature elevation was lower for the emulsions than for the dispersion of the particles, which was explained by a difference in the heat transfer between samples. A similar difference between emulsions and magnetic fluids was presented in a work featuring the heating of magnetic droplets with an internal structure, so-called endoskeletal droplets [131]. In turn, Kaiser *et al.* used polystyrene-magnetite particles to stabilize emulsions and subsequently destabilize them via temperature increases induced by the alternating magnetic field [132]. Due to the temperature elevation control, it was possible to establish the temperature of switching the stability of emulsion as presented in **Figure 1.8**. Lahiri *et al.* performed extended studies on the heating rate of magnetic Pickering emulsions in terms of the polydispersity, concentration, and viscosity of the surrounding medium [106, 111]. Apart from providing interesting results, these works are important because of their context in magnetic hyperthermia. The important point is that probably due to the process of droplet formation, the authors maintained that the magnetic particles were located inside the emulsion droplets.

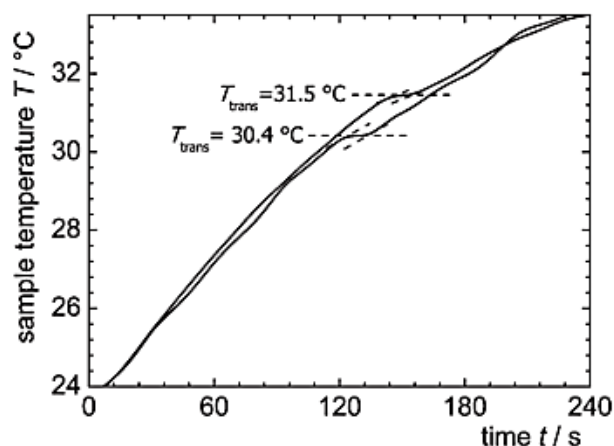


Figure 1.8 The temperature *versus* time observed in the O/W emulsions stabilized with polystyrene-magnetite particles and exposed to the AC magnetic field. The temperature of the transition between the stable and broken emulsion is indicated. Reproduced with permission from [132]. Copyright (2009) American Chemical Society.

In the new review article on magnetic particles confined to liquid interfaces [118], there is no mention about magnetic heating, which confirms the general lack of this topic in such reports. Although magnetic Pickering emulsions are rarely invoked in the context of magnetic heating, the main observations concerning magnetic fluids could be helpful in further discussing the results obtained for Pickering emulsions. The main difference between these colloidal systems seems to be the existence of particles at the interface that can, due to the reduced distance between the particles and the formation of a dense particle shell, negatively affect the heating performance, as was suggested in [\[Publication III-IV\]](#).

1.6. Characteristics of liquids and particles used in experiments

The choice of materials for the emulsions studied in this thesis was, at the beginning, indirectly dictated by a significant amount of experience with experiments on single oil droplets coated by particles and their behavior under electric fields [69, 133]. Besides, the silicone oil–castor oil emulsions due to the matched densities (964 kg/m^3 and 961 kg/m^3 , respectively, measured for $20 \text{ }^\circ\text{C}$, see also: **Figure 1.9**) were more resistant to sedimentation compared to water-based emulsions. Such a stability was important for the further characterization of Pickering emulsions via optical and ultrasonic methods, because enabled the in-line monitoring of the formation process. Moreover, the use of oils opened opportunities for the showing

fundamental processes that occur in Pickering emulsions under electric fields [Publication I]. This was important due to the fact that most studies on the influence of electric fields (e.g., discussed in Chapter 1.3) concern the behavior of single droplets rather than emulsions.

Silicone oil (SO) is a synthetic, polymeric liquid that constitutes silicon–oxygen bonds [134]. For all the experiments described in this thesis, silicone oil was purchased from VWR Chemicals (Rhodosil Oils 47 V 50) and used for the dispersed phase of emulsions. Its kinematic viscosity at room temperature was 50 cSt and its corresponding dynamic viscosity was ~ 0.05 Pa·s. In the pre-eliminary studies of [Publication I] (not published), silicone oils with other viscosities (20, 100, 1000 cSt) were also used to identify the optimal parameters of Pickering emulsions for their efficient formation. However, the change in the silicone oil viscosity did not influence the formation process under the electric field.

Castor oil is a natural oil derived from the tropical plant *Ricinus communis* [135]. Despite its natural origin and inherently inhomogeneous chemical content, its properties are believed to be rather stable, which allows for the comparison of different studies. In the experiments, two types of castor oil were used: purchased from Sigma-Aldrich Co. (no. 83912) [Publication I] and purchased from Merlin Co. (MA-220-1) [Publication II-VI]. During the pre-eliminary studies, the acoustic properties of both castor oils were investigated and no significant difference was observed. This means that the choice of castor oil did not affect the experiments, especially the formation process under the electric field.

To facilitate the process of electrocoalescence, in the experiments presented in [Publication I-III] and [Publication V], the emulsions were heated up to a temperature of 50 °C during the formation process under the electric field. The characteristics of the oils based on the data sheets, literature, and measurements of the density and viscosity at a higher temperature (50 °C) can be found in [Publication II]. For both oils, according to the predictions, the density decreased linearly and the viscosity decreased logarithmically with the temperature as presented in **Figure 1.9**.

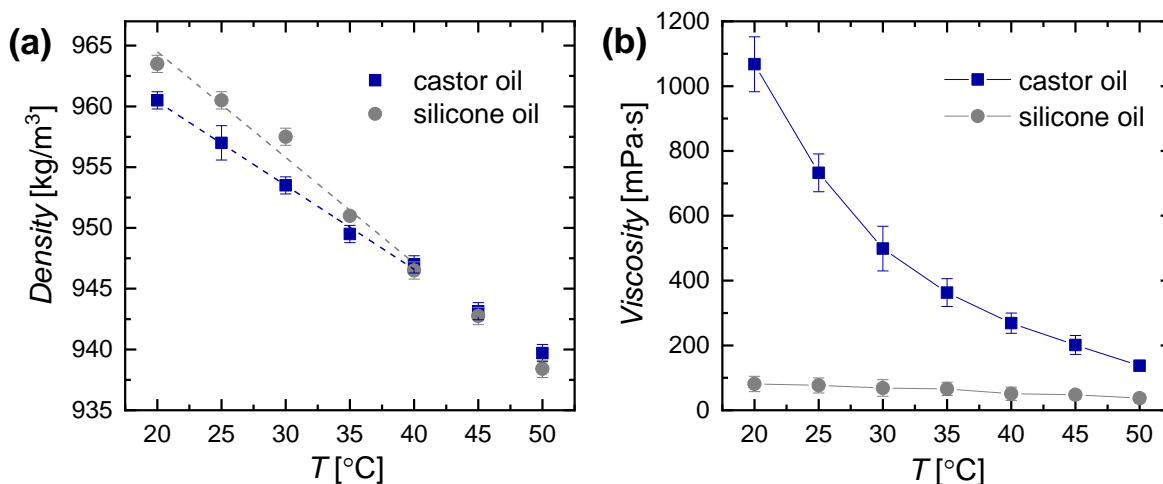


Figure 1.9 (a) Densities and (b) dynamic viscosities of silicone oil and castor oil as a function of temperature. In the case of density measurements, the experimental points at 45 and 50 °C were extrapolated due to the limited temperature range of the density meter.

In the experiments presented in [\[Publication I-II\]](#) and [\[Publication V-VI\]](#), polystyrene (PS) microparticles provided by Microbeads AS (Dynoseeds, TS10 6317, average diameter $\sim 10 \mu\text{m}$, the density of $\sim 1005 \text{ kg/m}^3$) were used. Polystyrene is a commonly used type of plastic obtained via the polymerization of styrene monomers [136]. It is rather low-cost, versatile and resistant to external conditions, which makes this material a good model material for fundamental research. Because of their rather weak affinity to silicone oil droplets suspended in castor oil [137], the polystyrene particles used in [\[Publication I-II\]](#) and [\[Publication VI\]](#) were additionally modified by an acrylate polymer (FluoroPEL™, Cytonix Co.) at the laboratory of the Institute of Physical Chemistry of Polish Academy of Sciences, Warsaw, according to the procedure described in detail in [137]. As shown in [\[Publication VI\]](#), polystyrene can be sintered under a high temperature. In the literature, the temperature of the so-called glass transition, i.e., the temperature when the particles starts melting, is around 105 °C [138]. The sintering of polystyrene (unmodified, average diameter of $40 \sim \mu\text{m}$) was also shown by ultrasonic measurements [\[Publication V\]](#) in which the formation of large sintered structures resulted in a change in the ultrasonic properties.

Magnetic particles were used as stabilizers in the experiments described in [\[Publication III-VI\]](#). They were either purchased from Sigma Aldrich or prepared at the Institute of Experimental Physics of Slovak Academy of Sciences in Košice, Slovakia. The latter were fabricated via a co-precipitation method and additionally coated by oleic acid for

biocompatibility and better stability. At the same time, it was noted that the layer of oleic acid resulted in the worse ability of such particles to be ultrasonically homogenized. In general, pristine, i.e., non-surface-modified, magnetite particles are hydrophilic in nature, but the presence of oleic acid may cause their hydrophobicity [139]. In the case of the experiments presented within this thesis, all magnetic particles turned out to cover the silicone oil–castor oil interface, but those modified with oleic acid exhibited worse performance **[Publication III]**.

Regardless of the origin of the magnetic particles, their magnetic properties were characterized in the Institute of Experimental Physics of Slovak Academy of Sciences in Košice, Slovakia. They consisted of iron oxide, which is usually believed to be a mixture of magnetite and hematite [140]. The fact that the magnetic particles were not of one single chemical substance probably caused the small differences between the saturation magnetization of the particles of different sizes **[Publication III]**. The primary scientific interest in such particles is nowadays driven by their potential biomedical application, namely magnetic hyperthermia therapy. The capability of iron oxide particles to be a source of heat under alternating (AC) magnetic fields is also the reason why these were used in the presented thesis.

Generally, the main focus should be on ensuring the stabilization of the magnetic particles, especially when using them for medical applications. In the literature [110], one can find the formula for the critical size of particle agglomerates:

$$d = \sqrt{\frac{6 k_B T}{\pi \Delta \rho g h}}, \quad (1.13)$$

where $\Delta \rho$ is the difference in the densities between the particles and surrounding medium, g is the gravitational acceleration, and h is the height of the sample. Nevertheless, in the case of the presented works, the magnetic particles were mostly stabilizers of the Pickering emulsions **[Publication III-V]** or single Pickering droplets **[Publication VI]**. This means that the stabilization of the particles was rather not crucial when compared with, e.g., magnetic fluid hyperthermia experiments. However, sedimentation of the particles was noted with the optical microscopy imaging of large single Pickering droplets. The difference in density between the magnetic particles ($\sim 5000 \text{ kg/m}^3$ [115]) and castor oil ($\sim 960 \text{ kg/m}^3$) was much larger than with the polystyrene particles which caused the quick sedimentation of magnetite-covered droplets and hampered the microscopy measurements. The same was the case for the sedimentation in the dispersion of the magnetite particles in castor oil, which was used as

either the comparable medium for investigating the acoustic properties of heated Pickering emulsions [Publication V] or as a “heating bath” for the formation of capsules from single Pickering droplets [Publication VI].

To compare the performance of the polystyrene particles as stabilizers and show the versatility of the developed method for Pickering emulsion formation under an electric field, other types of soft polymeric microparticles were also utilized, as presented in Supplementary Materials of [Publication I]. The following was purchased from Cospheric Co.: dyed polyethylene (PE) particles (with a size of $\sim 20\ \mu\text{m}$ and $\sim 50\ \mu\text{m}$) and silica particles (with a size of $\sim 8\ \mu\text{m}$). Besides, the potential of sintering of the soft PS particles was contrasted with that of the PE particles (with a size of $\sim 30\ \mu\text{m}$) [Publication VI].

In the presented experiments, the samples differed in terms of the content of the particles and silicone oil (dispersed phase). In all cases, the mass concentration of silicone oil was related to the castor oil, e.g., “10% of silicone oil” meant that the mass concentration of the silicone droplets in relation to that of the castor oil was 10%. The concentration of the particles was usually given as mass ratios between the particles and silicone oil, primarily to investigate the limited coalescence regime (Eq. 1.3). The exception was the dispersion of the magnetic particles used in [Publication V-VI]. In this case, the actual mass of the particles dispersed in castor oil (magnetic fluid) was important to be noted.

1.7. Details of experimental techniques

1.7.1. Preparation of Pickering emulsions

Across all experiments, the procedure of fabricating stable Pickering emulsions was the same and consisted of two steps: (i) ultrasonic homogenization that led to the formation of pre-emulsion and (ii) the exposition of pre-emulsion into DC electric fields.

In the first step, all substances, i.e., both the stabilizing particles and oils, were mixed together using an ultrasonic homogenizer (Sonoplus HD 300, Bandelin), which worked at the frequency of 18 kHz and emitted an ultrasonic wave of an intensity of $\sim 17\ \text{W}/\text{cm}^2$. The acoustic intensity was determined using the calorimetric method described *inter alia* in [141]. Briefly, the probe of the homogenizer was placed inside the sample cell, which was filled with distilled water of a known weight and specific heat. The temperature increase rate during the sonication was

obtained and used to determine the acoustic power input throughout its duration. Considering the area of the probe's tip, the intensity was calculated as the ratio of the acoustic power and this area. The acoustic intensity was the same in each presented experiment. The sonication was brief (30 seconds in [Publication I-II] and 60-120 seconds in [Publication III]), but this was a sufficient amount of time for the formation of small droplets merely coated with solid particles. The indirect evidence of such a poor coverage in all the experiments was that the droplet sizes increased significantly under the electric field. When the limited coalescence regime is fulfilled, such unstable emulsion droplets (referred to here as pre-emulsions) undergo a process of coalescence because of the insufficiently dense particle layer acting as a mechanical barrier. According to Eq. 1.3, the size of the droplets depends on the ratio between the mass of the dispersed phase and the mass of the solid particles. In the experiments, such different mass ratios were used depending on the particular experimental protocol. After pre-eliminatory tests with a mechanical rotor-stator homogenizing device (not published), ultrasonic homogenization was chosen, mainly because of the presence of air bubbles produced in the pre-emulsion by the rotor-stator device and the amount of particles sticking to its tip.

In the second step, the homogenized emulsion (i.e., pre-emulsion) was exposed to the DC electric field. If possible, the same sample cell was used for both homogenization and stabilization under electric fields, as in the case of [Publication II]. Inside the sample cell, two plane copper electrodes were placed and attached to the internal side of the measurement cell walls. They were connected to a power supply, signal generator, and high-voltage amplifier. In [Publication I-II], respectively, the used devices were: DF 1730SL (NDN Co.), SDG1025, (Sigilent Technologies Co.), and 10HVA24-BP1 (HVP Co.); however, in the experiments described in [Publication III-VI], a DC-to-DC high voltage amplifier (UltraVolt1AA12-P4, Advanced Energy Inc.) was used. Besides, the generated electric signal was of a negligible frequency (i.e., practically a DC electric field was used), and the electric field intensity inside the sample cell was from 200 V/mm to 600 V/mm. A higher electric field intensity (600 V/mm) was used cyclically for a short period of time to induce electrorotations (Quincke rotations) to break the droplet chains and provide a Pickering emulsion homogeneously distributed in the measurement cell. This was crucial *inter alia* for an efficient characterization by both the optical and ultrasonic methods.

1.7.2. Characterization by optical studies

In the described experiments, the emulsion samples were placed in different types of measurement cells. The precision of the optical microscopy imaging required a relatively short optical path and the transparency of the cell's walls. Therefore, the sample cells used in [\[Publication I\]](#) were made of glass, and their size was 30 mm × 18 mm × 1.3 mm, with the camera directed along the shortest dimension. A comparison of the sample cells of different dimensions is presented of Supplementary Materials to [\[Publication II\]](#). The results provided direct evidence of the noticeable worse quality of the optical imaging data obtained with a longer optical path. This small glass cuvette was also used in other publications in cases when the emulsions were characterized by optical imaging.

The experimental setup for the optical imaging consisted of a digital camera (UI-3590CP-C-HQ, IDS) equipped with a zoom lens system with a high magnification (MVL12X3Z, Thorlabs). Additionally, a light source was required for a better image quality recorded on the PC. Some of the images presented in the discussed articles were acquired in the post-analysis of the recorded videos. Because of the inherent high magnification of the optical system, to determine the droplet size distribution after the process of formation [\[Publication I\]](#), the images were taken using diverging lens. This enabled the identification of a large number of droplets within a single image.

The above-mentioned droplet size distribution was calculated based on a randomly chosen part of the picture. The ImageJ software, which is a common tool for the analysis of microscopy imaging data [142], did not bring about satisfactory results, as the Pickering emulsions presented in the obtained images had the tendency to form chains and the software did not properly distinguish single droplets from each other nor particles from the these droplets. The size of the droplets was therefore simply determined via calculation of the droplet sizes in pixels and a comparison of this value to the length of the scale bar. Overall, this turned out to be a simple but robust method. The analysis of the results, including the procedure of fitting to the semi-logarithmic distribution curve, was performed in OriginLAB 2019. It is worth noting that OriginLAB software was used to analyze the raw data and visualize it for all the presented experiments, including the optical, ultrasonic, and calorimetric studies.

In the case of magnetic Pickering emulsions, the optical evaluation of the emulsion appearance was impeded due to the poor transparency of the system with magnetite-stabilized droplets. To obtain the images of the single droplets and evaluate the particle shell around them, a multiple dilution of the system with pure castor oil was required. It is worth noting that the structure of the emulsion, e.g., droplet agglomerates, was surely affected by the dilution, and the obtained images could only roughly reflect the factual structure. It is important to note that, as in the emulsions images in **[Publication III-VI]**, the size of the emulsion droplets seems to not be governed by **Eq. 1.3** despite the use of the same formation process as usual.

In **[Publication II]**, the optical imaging was supplemented by ultrasonic techniques that allowed for following the process of formation under the electric field in-line even for thicker sample cells (larger volume of emulsion).

1.7.3. Characterization by ultrasonic studies

As indicated in Chapter 1.4, an analysis of the ultrasonic waves propagating through the medium can be used for characterizing the medium's properties. In the presented works **[Publication II]** and **[Publication V]**, piezoelectric ultrasonic transducers were used for this purpose. To generate an ultrasound, piezoelectric crystals in the transducer must be driven by an electric signal, which was achieved using the OPBOX 2.1 (Optel Co.) ultrasonic system connected to a PC by a USB port. An unipolar spike pulse (with an amplitude of 360 V, fall time of 20 ns, and pulse repetition frequency of 0.9 kHz) was generated by the transducer and after the propagation through the sample cell was detected and recorded with a sampling frequency of 100 MHz. The software allowed for the export of raw data as ultrasonic A-scans and the subsequent analysis of recorded ultrasonic pulses.

In opposition to optical imaging studies, in the case of analyzing an ultrasound wave, the measurement cell cannot be too small. This was due to the fact that for too a short distance between the ultrasonic transmitter and receiver, the ultrasonic pulses were poorly distinguishable from each other. Additionally, the multiple reflections of the ultrasound inside the glass cells' walls contributed to the overall shape of the signal. This is why the sample cells used for the ultrasound studies in **[Publication II]** were made from polystyrene, and their dimensions were 45 mm × 10 mm × 10 mm. Standardized cuvettes used for

spectrophotometry were chosen. Due to the large difference in the acoustic impedance inside and outside of the sample's walls, the walls were covered by a thin layer of coupling agent, as commonly used in ultrasonography for acoustic impedance matching. Then, a pair of transducers was attached to the outside of the walls. A different experimental system was used for the studies in **[Publication V]**. In this case, one piezoelectric transducer acted as both a transmitter and receiver. The acoustic wave travelled through the tested medium and came back after the reflection of the planar bottom side of the sample cell. Another difference was that sample cell was made of glass and the acoustic signal propagated from the top to down of the measurement cell. The reason for this was two-fold. First, the high temperature increase during the magnetic heating prevented the use of temperature-responsive polystyrene as the material. Additionally, the sample cell must have been large enough to enable the immersion of the transducer. All measurements were performed at a fixed distance between the transducer and the bottom of the sample cell, and this distance was determined from the calculation of the speed of the ultrasound in distilled water at the given temperature.

In both described publications, the relative acoustics parameters were determined, i.e., the change in the attenuation coefficient and the change in the speed of the ultrasound (sound velocity). The reason for this was that both formation under an electric field and heating under the alternating magnetic field are dynamic processes, and the change occurring (or not) during them was important and interesting to be characterized. In **[Publication II]**, the change in the ultrasonic attenuation was related to the beginning value, i.e., to the properties of pre-emulsion freshly prepared via ultrasonic homogenization measured in the temperature of ~50 °C. Also, the theoretical predictions for the oil-in-oil emulsion with bare droplets were presented as “excessive attenuation”. This means that only the contribution of the droplets as scatterers was taken into account without an intrinsic attenuation caused by the properties of the oils. In **[Publication V]**, the speed of the ultrasound and attenuation coefficient were related to the values before magnetic heating.

The change in the attenuation coefficient measured experimentally was expressed by:

$$\Delta\alpha = \frac{20}{l} \log_{10} \frac{A_2}{A_1}. \quad (1.14)$$

In the **Eq. 1.14**, l relates to the distance acoustic wave travelled through the sample cell; in the case of the transmission mode **[Publication II]**, it was the distance between two

transducers, and, in the case of the pulse-echo mode **[Publication V]**, it was the double distance between the transducer and the bottom of a sample cell. Generally, the attenuation coefficient is related to the ratio between the ultrasonic pulse amplitude observed at different distances of propagation (different positions of the transducer). When only a change in the attenuation coefficient for the given fixed distance is investigated, the ratio of amplitudes observed for different times can be calculated. It should be noted that the form of **Eq. 1.14** was not completely the same in both presented papers. In **[Publication II]**, it was intended to follow the decreasing amplitude of the ultrasonic pulse during the electric field application (A_2) in relation to the amplitude measured just before the electric field was turned on (A_1). To show the stability of the emulsion during the magnetic heating in **[Publication V]**, the amplitude of the ultrasonic signal observed just before the AC magnetic field was applied (A_2) was related to the amplitudes measured every second after magnetic heating (A_1).

The change in the speed of the ultrasound in **[Publication V]** was expressed by the simple formula:

$$\Delta c = c_0 - c_n . \quad (1.15)$$

The speed of ultrasound c_0 was calculated as the ratio of the distance acoustic wave travelling through the sample cell l and the time of propagation through the sample just before the AC magnetic field application was initiated. Analogically, c_n was calculated using the same distance and time of flight measured every second after magnetic heating. In the case of **[Publication V]**, the technical problem was the fast heating of the transducer chassis when it was immersed in the tested medium during the application of the alternating magnetic field. To overcome this, the ultrasonic pulse was measured before the magnetic heating and then just after the magnetic field was turned off.

In both **[Publication II]** and **[Publication V]**, most of the results were presented for a single (central) frequency of the generated signal, which is generally a feature of any given transducer. However, useful information that characterizes the tested system can be derived when the acoustic parameters are expressed in a frequency domain. Such results are presented in the Supplementary Materials of **[Publication V]**. The attenuation coefficient was calculated based on Fast Fourier Transform of ultrasound pulses recorded in a tested medium (in this case, the dispersion of magnetite and polystyrene particles in castor oil) and a reference medium (distilled water). Generally, to calculate the absolute value of the

attenuation coefficient, the attenuation coefficient of the reference medium should be included in the equation. As the ultrasound attenuation of water is very low [143], it was neglected in the presented case. It should also be stressed here that the analysis of the attenuation coefficient and phase velocity in the function of frequency is powerful only when the transducers generate a signal with a wide range of frequencies, but this was not the case in the presented experiment. The spectra of the pulses were quite narrow due to the long pulse length, as the testing signal consisted of several periods of a wave.

1.7.4. Magnetic properties of particles and emulsions

The heating rate of the medium under AC magnetic fields depends on numerous factors, as discussed in Chapter 1.5. It is commonly known that a magnetization of material, i.e., the density of the magnetic moments inside it, also influences its heating performance; weaker magnetic properties of the material should result in worse magnetic heating. This is why the characterization of magnetic particles (in the form of powders) was performed in addition to the pre-emulsions and emulsions stabilized with them. The magnetization curves, i.e., the relations between the magnetization and magnetic field, were determined using a vibrating-sample magnetometer (VSM) device at the Institute of Experimental Physics of Slovak Academy of Sciences in Košice, Slovakia. In this technique, the magnetic moment information is obtained from using Faraday's law of magnetic induction [144]. When the magnetized sample vibrates in the magnetic field, the voltage can be induced in the surrounding induction coils, which is proportional *inter alia* to the magnetization. The magnetization curves are presented in [Publication III]. Its abbreviated version was also presented in [Publication V].

1.7.5. Calorimetric measurements

To generate the alternating magnetic field in the experiments described in [Publication III-VI], an induction heating system (EASYHEAT, Ambrell Co.) was used. Different magnetic field intensities (from 5.2 kA/m to 16.2 kA/m) were induced inside the induction coil with dimensions of 57 mm × 49 mm by changing the amplitude of the current in the coil. The values of the magnetic field intensities given in the presented articles were calculated based on the well-known Biot-Savart law [145]. In the experiments, both the time of heating [Publication III] as well as the temperature above which the system automatically turned off [Publication IV-V] could manipulate the magnetic field. The magnetic coil was internally cooled down,

which diminished the effect of the induction heating of the coil on the temperature elevation in the tested samples.

A thermometer with an optical fiber sensor (FLUOTEMP, Photon Control Inc.) was used in the presented studies to measure the temperature increase inside the sample cells under the AC magnetic field. Compared to other thermometry techniques, such as using a thermocouple, in the case of the optical fiber sensor, the magnetic field with a high intensity did not influence the results. The sensor was placed in the middle of a sample always at the same height. This was important, as the results of magnetic heating measurements can be affected by the different positions of the temperature sensor [126]. For experiments described in **[Publication V]**, the cuvette filled with the emulsion had to be larger regarding the dimensions of the ultrasonic transducer. The presence of the transducer prevented the placement of the temperature sensor directly in the middle of the sample. Therefore, the sensor was located in a fixed position in the middle of sample height (as in the other experiments) but close to the cuvette wall to not affect the ultrasound generated by the immersed transducer. The provided by the manufacturer range of temperature was from $-10\text{ }^{\circ}\text{C}$ to $80\text{ }^{\circ}\text{C}$; however, for the extremely high temperatures observed in **[Publication VI]**, the optical sensor was not sufficient to follow the temperature increase. This was overcome by using a simple thermovision camera (VT02, Fluke Co.) and reproducing the temperature from the images.

2. Overview of the publications constituting the dissertation

The previous chapters introduced the topic of Pickering emulsions and the use of ultrasound and electric fields for their preparation; these briefly characterized the propagation of ultrasonic waves in disperse media and the process of magnetic heating. Moreover, the materials and methods used in the papers constituting this thesis were provided. These issues needed to be given to justify the title of the thesis and show how **[Publication I-VI]** are linked to each other. Below, the merits of each publication from **[Publication I-VI]** are presented.

[Publication I]:

In many reports, ultrasonic devices with different acoustic intensities and times of working have been used alone to produce Pickering emulsions with a satisfactory droplet size and coverage of the droplets by particles. In this publication, a novel approach to efficiently fabricate oil-in-oil Pickering emulsions was proposed. It involved the ultrasonic homogenization of oils and particles and the subsequent application of an electric field. The several mechanisms occurring in emulsions under the electric fields, i.e., dipolar interactions between droplets, their electro-coalescence, Quincke rotations and the induction of electrohydrodynamic (EHD) flows (also discussed in the Introduction in Chapter 1.3), were shown to efficiently form droplets covered by particles in bulk quantities. The optical microscopy imaging revealed that the process of formation required using the above-mentioned mechanisms to prepare Pickering emulsions in relatively short period of time (several minutes). The distribution of the stable emulsion droplets measured via optical imaging has proven to be narrow in comparison to other techniques allowing for the formation of emulsions in bulk quantities, such as membrane emulsification or mechanical stirring. At the same time, the mean droplet size followed the well-known relation between the mass of a solid and disperse phase for a limited coalescence regime.

To summarize:

- Ultrasound and electric fields can be used to form stable oil-in-oil Pickering emulsions with narrow size distributions.
- Via the dipolar interactions, electrohydrodynamic flows, and electrorotations observed in the emulsion under the electric fields, the output emulsion droplets were sufficiently

coated by particles, and the agglomerates of droplets could be relatively easily broken by the electric field of the high intensity.

- The method of formation is characterized by a high throughput compared to other methods such as microfluidics.

[Publication II]:

The process of the fabrication of the Pickering emulsion, as described in **[Publication I]**, was monitored to provide quantitative information regarding the final droplet size and the coverage of the droplets by solid particles. As long as thin sample cells were used (i.e., with a short optical path), the optical microscopy technique was convenient. However, when using thicker cuvettes (e.g., for yielding higher production rates of Pickering emulsions), a large number of scattering objects in the light path prevented meaningful optical observations. Therefore, in the search for a better approach to monitoring the growth of Pickering emulsions, a simple and low-cost technique was proposed that enabled the *in situ* and real-time sampling of emulsions. In the method, non-destructive ultrasound was utilized to characterize the emulsion in different stages of the formation process without the need for stopping the process. Although ultrasound methods are used in the industry for quality control and provide insight into the structure of colloidal systems, surprisingly, until now, there have been only a few reports about using ultrasound to characterize emulsions stabilized solely with solid particles. Here, the ultrasound method was used strictly to follow the process of formation introduced in **[Publication I]**, but general observations regarding the characteristics of the Pickering emulsions gathered via the ultrasound were also drawn. When compared with the optical microscopy imaging data, the change in the ultrasonic attenuation coefficient was sensitive to the droplet size. This was in accordance with predictions because the processes affecting the propagation of the acoustic wave in the emulsion are dependent on the size of the scatterers. Theoretical predictions based on Epstein-Carhart-Allegra-Hawley's (ECAH) theory for silicone oil droplets suspended in castor oil revealed that, when the size of droplets is within the range 10–300 μm , the attenuation coefficient should increase monotonically. This enabled following the process of emulsion formation under an electric field due to two aspects: (i) in the process of formation, the size of the droplets increases along with the coverage of interfaces by particles; (ii) the size of the droplets when polystyrene particles of 10 μm as stabilizers was in the range 10–300 μm . The change in the ultrasonic attenuation

coefficient exhibited “saturation”, i.e., the attenuation stopped increasing after several minutes of electric field application that was correlated with the stabilization of the Pickering droplet shells. Additionally, this paper showed the discrepancy between optical data, experimental data for the ultrasonic attenuation coefficient, and theoretical predictions based on ECAH theory. Such a discrepancy highlights that, for Pickering emulsions, existing ultrasonic theories for particulate systems are not valid. This also means that, to obtain a droplet size distribution of Pickering emulsion based on ultrasonic studies, there is a need for the development of more a sophisticated theoretical model.

To summarize:

- The change in the ultrasonic attenuation coefficient was correlated with the stabilization process of the Pickering emulsions under the electric field.
- This change was not constant and the observation of its halting could be used for establishing the time when the particle shell around the droplets is sufficient and halts the further coalescence of droplets.

[Publication III]:

The method of formation by using ultrasound and electric fields was clearly sufficient for the oil-in-oil Pickering emulsions. However, the combination of two separate steps in the method also opened the unique possibility to characterize the properties of the emulsions in two different stages: (i) for pre-emulsions (coarse emulsions) with insufficient coverage by particles, and (ii) for stable Pickering emulsions. The resistance of emulsion droplets to the coalescence events was evidence of a final stability after the application of DC electric fields. From earlier studies on magnetic hyperthermia in agar phantom, it was clear that magnetic heating is influenced by the surrounding medium, i.e., the internal structure of agar tissue-mimicking phantoms inhibited the Brown relaxation process in magnetic particles. It was hypothesized that a similar effect can occur when the magnetic particles reside in the droplet interface and are densely-packed. In fact, the studies on magnetic heating in Pickering emulsions stabilized with magnetite particles showed the difference between pre-emulsions and stable emulsions, which was repeatable for different concentrations of magnetic particles and different magnetic field intensities. The difference still existed for different particle sizes and regardless of the surface functionalization of particles, which eliminated the inhibition of

Brown relaxation as the main reason of a change in heating performance. In the study, the term: “spherical cluster” was proposed to describe the Pickering droplet sufficiently coated by a dense layer of magnetic particles. In such geometry, strong interactions between particles can occur, and the heat transfer from the inside of droplet can be halted when the droplet is armored by a solid particle shell.

To summarize:

- The heating rates of the Pickering pre-emulsions and emulsions under the AC magnetic field were different for different sizes and concentrations of stabilizing magnetic particles as well as for different the magnetic field intensities.
- Regardless of the content of the studied medium and magnetic field parameters, temperature increases were smaller for stable emulsions compared to pre-emulsions.
- A hypothesis regarding the influence of the particle shell around the droplet on magnetic interactions and the restrained heat transfer from the magnetic Pickering droplets was proposed.

[Publication IV]:

In the case of studies on magnetic heating, cooling rate analysis is not as common as the presentation of heating rates. Also in my studies, in the beginning, the investigation was focused only on the heating process. However, to evaluate the hypothesis of the heat transfer being affected by the stable particle shell around the Pickering droplets, the investigation of what happens after heating was important. The differences in cooling rates between the pre-emulsions and stable emulsions were less significant than in terms of the process of heating. However, it was shown that the cooling rates were lower for the emulsions stabilized in the electric field regardless of the intensity of the magnetic field and concentration of the particles used in the experiments. It is worth noting that all samples were thermostated under the same temperature (20 °C). The process of cooling down was sometimes surprisingly long, which may suggest that heat transfer in stable Pickering emulsions is not only slower but also sustained. Unfortunately, the clear evaluation of the temperature in the vicinity of the droplet interface on the nanoscale is still challenging and, for performed calorimetric studies under non-adiabatic conditions, it is impossible.

To summarize:

- The temperature decrease after the application of an AC magnetic field was less dynamic in emulsions than in pre-emulsions.
- When a magnetic field with a lower intensity was used for magnetic heating, the process of cooling was also less dynamic.

[Publication V]:

During the studies on magnetic heating of Pickering emulsion, there was a repeatable pivotal question: Does the process of magnetic heating alter the properties of emulsions? Because of the fragile structure of emulsions and their poor optical transparency, evaluation via optical microscopy imaging was impossible. To investigate the stability of Pickering emulsions in-line, the ultrasound technique was proposed. As in the case of **[Publication II]**, the change in the acoustic properties, i.e., the ultrasonic attenuation coefficient and speed of ultrasound, were studied. The hypothesis was that potential structural changes of the emulsion when exposed to the AC magnetic field should be reflected in the ultrasonic properties. The change in the acoustic properties was therefore correlated with the temperature change during heating and cooling. The emulsion results were compared with the magnetic fluid results and the oil dispersions of the magnetic and soft (polystyrene) particles. When the temperature returned to room value, the acoustic parameters were also comparable with those before the magnetic heating of the emulsions and magnetic fluids. However, this was not the case for the magnetite-polystyrene dispersions in castor oil. Under a high temperature, the polystyrene particles sintered, and the structure of the medium was irreversibly changed.

To summarize:

- The changes in the speed of the ultrasound and ultrasonic attenuation coefficient were used to follow the changes in the emulsions, magnetic fluids, and dispersions of magnetic and soft particles under the influence of the AC magnetic field.
- As the ultrasonic properties are dependent on the temperature, these changes were correlated with the temperature evolution.
- After cooling down to the initial temperature, the acoustic properties returned to the initial values, which provided evidence that there was no permanent structural change during magnetic heating.

- The formation of polystyrene-magnetite agglomerates and sintered polystyrene particles was detected via ultrasound and proved the potential of magnetic heating in sintering soft particles.

[Publication VI]:

The alternating magnetic field was shown to induce a high-temperature increase in oil-in-oil Pickering emulsions stabilized with magnetic particles. When the temperature increase is sufficiently high, particles susceptible to the temperature elevation can be sintered (e.g., polystyrene particles). In this work, Pickering emulsions were stabilized both with magnetic and polystyrene particles to investigate the potential of the magnetic heating of Pickering droplets in the formation of capsules, i.e., the droplets with rigid shells. Two approaches were proposed: (i) the exposition of Pickering droplets covered simultaneously with two types of particles to an AC magnetic field and (ii) the exposition of single droplets covered by soft particles and immersed in a castor oil-based magnetic fluid to magnetic heating. In the case of the second experimental protocol, the rigidity of the shell was evaluated by electric field stress according to **Eq. 1.6**.

To summarize:

- The use of ultrasound and electric fields led to the formation of Pickering droplets stabilized with both magnetic and polystyrene particles.
- Pickering droplets stabilized with soft particles can be transformed into colloidal capsules due to the sintering of the particles under high-temperature increases induced by magnetic particles exposed to the AC magnetic field.
- This work is also important as there are few reports using mixed particles as stabilizers in Pickering emulsions, and using emulsions with multicomponent particle shell has been indicated as the potential future direction of development in this field [146].

3. Summary

This Ph.D. dissertation, i.e., the presented introduction and the papers constituting the core of the thesis, indicates that particle-stabilized emulsions can be formed using ultrasound and electric fields and that the characterization of such systems brings about an original and novel contribution to the field of ultrasonic testing and magnetic heating.

It is clear that not all issues were fully addressed in this thesis. The outcomes of the presented papers are expected to be further studied in future investigations regarding the optimization of colloidal capsule formation under AC magnetic fields and their efficient characterization by non-destructive testing. Moreover, this Ph.D. project lacked the development of a consistent numerical model from which the Pickering droplet size distribution can be determined based on ultrasound studies. Nevertheless, I believe that this work has already paved the way for further ultrasonic studies, which is valuable, as ultrasonic studies on Pickering emulsions have not yet attracted much scientific interest despite the presented potential of ultrasound-based techniques in characterizing particle-stabilized colloidal systems.

The presented thesis has provided promising results regarding a novel method for preparing Pickering emulsions and suggests the existence of interesting processes on the edge of Pickering emulsions and magnetic hyperthermia experiments that have not been investigated in the past. Therefore, I believe that the presented works can contribute to the development of the field concerning novel colloidal systems.

4. Literature used in the introductory part

1. Skelhon, T. S.; Grossiord, N.; Morgan, A. R.; Bon, S. A. F., Quiescent water-in-oil Pickering emulsions as a route toward healthier fruit juice infused chocolate confectionary. *Journal of Materials Chemistry* **2012**, *22*, (36), 19289-19295.
2. Yano, H.; Fukui, A.; Kajiwara, K.; Kobayashi, I.; Yoza, K.-i.; Satake, A.; Villeneuve, M., Development of gluten-free rice bread: Pickering stabilization as a possible batter-swelling mechanism. *LWT - Food Science and Technology* **2017**, *79*, 632-639.
3. Li, Z.; Shi, Y.; Zhu, A.; Zhao, Y.; Wang, H.; Binks, B. P.; Wang, J., Light-Responsive, Reversible Emulsification and Demulsification of Oil-in-Water Pickering Emulsions for Catalysis. *Angewandte Chemie International Edition* **2021**, *60*, (8), 3928–3933.
4. Pang, Y.; Sun, Y.; Luo, Y.; Zhou, M.; Qiu, X.; Yi, C.; Lou, H., Preparation of novel all-lignin microcapsules via interfacial cross-linking of pickering emulsion. *Industrial Crops and Products* **2021**, *167*, 113468.
5. Tadros, T. F., Emulsion Science and Technology: A General Introduction. In *Emulsion Science and Technology*, 2009; pp 1–56.

6. Ramsden, W., Separation of solids in the surface-layers of solutions and 'suspensions'(observations on surface-membranes, bubbles, emulsions, and mechanical coagulation).—Preliminary account. *Proceedings of the royal Society of London* **1904**, 72, (477-486), 156–164.
7. Pickering, S. U., Cxcvi.—emulsions. *Journal of the Chemical Society, Transactions* **1907**, 91, 2001–2021.
8. Aveyard, R.; Binks, B. P.; Clint, J. H., Emulsions stabilised solely by colloidal particles. *Advances in Colloid and Interface Science* **2003**, 100, 503–546.
9. Binks, B. P.; Horozov, T. S., *Colloidal particles at liquid interfaces*. Cambridge University Press: 2006.
10. Denkov, N. D.; Ivanov, I. B.; Kralchevsky, P. A.; Wasan, D. T., A possible mechanism of stabilization of emulsions by solid particles. *Journal of Colloid and Interface Science* **1992**, 150, (2), 589–593.
11. Wu, J.; Ma, G.-H., Recent Studies of Pickering Emulsions: Particles Make the Difference. *Small* **2016**, 12, (34), 4633–4648.
12. Marefati, A.; Rayner, M., Starch granule stabilized Pickering emulsions: an 8-year stability study. *Journal of the Science of Food and Agriculture* **2020**, 100, (6), 2807–2811.
13. Xiao, J.; Li, Y.; Huang, Q., Recent advances on food-grade particles stabilized Pickering emulsions: Fabrication, characterization and research trends. *Trends in Food Science & Technology* **2016**, 55, 48–60.
14. Wang, W.; Du, G.; Li, C.; Zhang, H.; Long, Y.; Ni, Y., Preparation of cellulose nanocrystals from asparagus (*Asparagus officinalis* L.) and their applications to palm oil/water Pickering emulsion. *Carbohydrate Polymers* **2016**, 151, 1–8.
15. Wu, F.; Deng, J.; Hu, L.; Zhang, Z.; Jiang, H.; Li, Y.; Yi, Z.; Ngai, T., Investigation of the stability in Pickering emulsions preparation with commercial cosmetic ingredients. *Colloids and Surfaces A: Physicochemical and Engineering Aspects* **2020**, 602, 125082.
16. Marto, J.; Ascenso, A.; Gonçalves, L. M.; Gouveia, L. F.; Manteigas, P.; Pinto, P.; Oliveira, E.; Almeida, A. J.; Ribeiro, H. M., Melatonin-based pickering emulsion for skin's photoprotection. *Drug Delivery* **2016**, 23, (5), 1594–1607.
17. Lémery, E.; Briançon, S.; Chevalier, Y.; Bordes, C.; Oddos, T.; Gohier, A.; Bolzinger, M.-A., Skin toxicity of surfactants: Structure/toxicity relationships. *Colloids and Surfaces A: Physicochemical and Engineering Aspects* **2015**, 469, 166–179.
18. Shah, B. R.; Li, Y.; Jin, W.; An, Y.; He, L.; Li, Z.; Xu, W.; Li, B., Preparation and optimization of Pickering emulsion stabilized by chitosan-tripolyphosphate nanoparticles for curcumin encapsulation. *Food Hydrocolloids* **2016**, 52, 369–377.
19. Baillot, M.; Bentaleb, A.; Laurichesse, E.; Schmitt, V.; Backov, R., Triggering the Mechanical Release of Mineralized Pickering Emulsion-Based Capsules. *Langmuir* **2016**, 32, (16), 3880–3889.
20. Peng, S.; Cao, F.; Xia, Y.; Gao, X.-D.; Dai, L.; Yan, J.; Ma, G., Particulate Alum via Pickering Emulsion for an Enhanced COVID-19 Vaccine Adjuvant. *Advanced Materials* **2020**, 32, (40), 2004210.
21. Roy, P. K.; Binks, B. P.; Fujii, S.; Shoval, S.; Bormashenko, E., Composite Liquid Marbles as a Macroscopic Model System Representing Shedding of Enveloped Viruses. *The Journal of Physical Chemistry Letters* **2020**, 11, (11), 4279–4285.
22. Sarkar, A.; Zhang, S.; Holmes, M.; Ettelaie, R., Colloidal aspects of digestion of Pickering emulsions: Experiments and theoretical models of lipid digestion kinetics. *Advances in Colloid and Interface Science* **2019**, 263, 195–211.
23. Frelichowska, J.; Bolzinger, M.-A.; Chevalier, Y., Pickering emulsions with bare silica. *Colloids and Surfaces A: Physicochemical and Engineering Aspects* **2009**, 343, (1), 70–74.
24. Ridet, L.; Bolzinger, M.-A.; Gilon-Delepine, N.; Dugas, P.-Y.; Chevalier, Y., Pickering emulsions stabilized by charged nanoparticles. *Soft Matter* **2016**, 12, (36), 7564–7576.

25. Yu, L.; Li, S.; Stubbs, L. P.; Lau, H. C., Rheological investigation of clay-stabilized oil-in-water Pickering emulsions for potential reservoir applications. *Journal of Petroleum Science and Engineering* **2021**, 204, 108722.
26. Brunier, B. I. m.; Sheibat-Othman, N.; Chniguir, M.; Chevalier, Y.; Bourgeat-Lami, E., Investigation of four different Laponite clays as stabilizers in Pickering emulsion polymerization. *Langmuir* **2016**, 32, (24), 6046–6057.
27. Li, Y.; Zhao, R.; Hu, F.; Lu, P.; Ji, D.; Luo, Q.; Li, G.; Yu, D.; Wang, H.; Song, Z.; Li, S.; Liu, W., Laponite/lauric arginate stabilized AKD Pickering emulsions with shell-tunable hydrolytic resistance for use in sizing paper. *Applied Clay Science* **2021**, 206, 106085.
28. Luo, Q.; Wang, Y.; Yoo, E.; Wei, P.; Pentzer, E., Ionic liquid-containing pickering emulsions stabilized by graphene oxide-based surfactants. *Langmuir* **2018**, 34, (34), 10114–10122.
29. Li, W.; Suzuki, T.; Minami, H., The interface adsorption behavior in a Pickering emulsion stabilized by cylindrical polystyrene particles. *Journal of colloid and interface science* **2019**, 552, 230–235.
30. Xie, C.-Y.; Meng, S.-X.; Xue, L.-H.; Bai, R.-X.; Yang, X.; Wang, Y.; Qiu, Z.-P.; Binks, B. P.; Guo, T.; Meng, T., Light and magnetic dual-responsive Pickering emulsion micro-reactors. *Langmuir* **2017**, 33, (49), 14139–14148.
31. Raju, R. R.; Liebig, F.; Klemke, B.; Koetz, J., pH-responsive magnetic Pickering Janus emulsions. *Colloid and Polymer Science* **2018**, 296, (6), 1039–1046.
32. Cui, F.; Zhao, S.; Guan, X.; McClements, D. J.; Liu, X.; Liu, F.; Ngai, T., Polysaccharide-based Pickering Emulsions: Formation, Stabilization and Applications. *Food Hydrocolloids* **2021**, 106812.
33. Zhu, F., Starch based Pickering emulsions: Fabrication, properties, and applications. *Trends in Food Science & Technology* **2019**, 85, 129–137.
34. Saari, H.; Rayner, M.; Wahlgren, M., Effects of starch granules differing in size and morphology from different botanical sources and their mixtures on the characteristics of Pickering emulsions. *Food Hydrocolloids* **2019**, 89, 844–855.
35. Zhai, X.; Lin, D.; Liu, D.; Yang, X., Emulsions stabilized by nanofibers from bacterial cellulose: New potential food-grade Pickering emulsions. *Food Research International* **2018**, 103, 12–20.
36. Sarkar, A.; Dickinson, E., Sustainable food-grade Pickering emulsions stabilized by plant-based particles. *Current Opinion in Colloid & Interface Science* **2020**, 49, 69–81.
37. Dupont, H.; Maingret, V.; Schmitt, V.; Héroguez, V., New Insights into the Formulation and Polymerization of Pickering Emulsions Stabilized by Natural Organic Particles. *Macromolecules* **2021**.
38. Tan, H.; Sun, G.; Lin, W.; Mu, C.; Ngai, T., Gelatin particle-stabilized high internal phase emulsions as nutraceutical containers. *ACS applied materials & interfaces* **2014**, 6, (16), 13977–13984.
39. Destribats, M.; Rouvet, M.; Gehin-Delval, C.; Schmitt, C.; Binks, B. P., Emulsions stabilised by whey protein microgel particles: towards food-grade Pickering emulsions. *Soft Matter* **2014**, 10, (36), 6941-6954.
40. McClements, D. J., Protein-stabilized emulsions. *Current opinion in colloid & interface science* **2004**, 9, (5), 305–313.
41. Pawlik, A.; Kurukji, D.; Norton, I.; Spyropoulos, F., Food-grade Pickering emulsions stabilised with solid lipid particles. *Food & Function* **2016**, 7, (6), 2712–2721.
42. Kruglyakov, P.; Nushtayeva, A.; Vilkova, N., Experimental investigation of capillary pressure influence on breaking of emulsions stabilized by solid particles. *Journal of colloid and interface science* **2004**, 276, (2), 465–474.
43. Zhu, Y.; Jiang, J.; Liu, K.; Cui, Z.; Binks, B. P., Switchable Pickering Emulsions Stabilized by Silica Nanoparticles Hydrophobized in Situ with a Conventional Cationic Surfactant. *Langmuir* **2015**, 31, (11), 3301–3307.

44. Xu, M.; Zhang, W.; Jiang, J.; Pei, X.; Zhu, H.; Cui, Z.; Binks, B. P., Transition between a Pickering Emulsion and an Oil-in-Dispersion Emulsion Costabilized by Alumina Nanoparticles and a Cationic Surfactant. *Langmuir* **2020**, *36*, (51), 15543–15551.
45. Arditty, S.; Whitby, C. P.; Binks, B. P.; Schmitt, V.; Leal-Calderon, F., Some general features of limited coalescence in solid-stabilized emulsions. *The European Physical Journal E* **2003**, *11*, (3), 273–281.
46. French, D. J.; Taylor, P.; Fowler, J.; Clegg, P. S., Making and breaking bridges in a Pickering emulsion. *Journal of Colloid and Interface Science* **2015**, *441*, 30–38.
47. Daware, S. V.; Basavaraj, M. G., Emulsions Stabilized by Silica Rods via Arrested Demixing. *Langmuir* **2015**, *31*, (24), 6649–6654.
48. Levine, S.; Bowen, B. D.; Partridge, S. J., Stabilization of emulsions by fine particles I. Partitioning of particles between continuous phase and oil/water interface. *Colloids and surfaces* **1989**, *38*, (2), 325–343.
49. Albert, C.; Beladjine, M.; Tsapis, N.; Fattal, E.; Agnely, F.; Huang, N., Pickering emulsions: Preparation processes, key parameters governing their properties and potential for pharmaceutical applications. *Journal of Controlled Release* **2019**, *309*, 302–332.
50. Wiley, R. M., Limited coalescence of oil droplets in coarse oil-in-water emulsions. *Journal of Colloid Science* **1954**, *9*, (5), 427–437.
51. Binks, B. P.; Tyowua, A. T., Oil-in-oil emulsions stabilised solely by solid particles. *Soft Matter* **2016**, *12*, (3), 876–887.
52. Klapper, M.; Nenov, S.; Haschick, R.; Müller, K.; Müllen, K., Oil-in-Oil Emulsions: A Unique Tool for the Formation of Polymer Nanoparticles. *Accounts of Chemical Research* **2008**, *41*, (9), 1190–1201.
53. Lu, X.; Katz, J. S.; Schmitt, A. K.; Moore, J. S., A Robust Oil-in-Oil Emulsion for the Nonaqueous Encapsulation of Hydrophilic Payloads. *Journal of the American Chemical Society* **2018**, *140*, (10), 3619–3625.
54. Zia, A.; Pentzer, E.; Thickett, S.; Kempe, K., Advances and Opportunities of Oil-in-Oil Emulsions. *ACS Applied Materials & Interfaces* **2020**, *12*, (35), 38845–38861.
55. Jafari, S. M.; He, Y.; Bhandari, B., Production of sub-micron emulsions by ultrasound and microfluidization techniques. *Journal of Food Engineering* **2007**, *82*, (4), 478–488.
56. Priest, C.; Reid, M. D.; Whitby, C. P., Formation and stability of nanoparticle-stabilised oil-in-water emulsions in a microfluidic chip. *Journal of Colloid and Interface Science* **2011**, *363*, (1), 301–306.
57. Nan, F.; Wu, J.; Qi, F.; Fan, Q.; Ma, G.; Ngai, T., Preparation of uniform-sized colloidosomes based on chitosan-coated alginate particles and its application for oral insulin delivery. *Journal of Materials Chemistry B* **2014**, *2*, (42), 7403–7409.
58. Thompson, K.; Armes, S.; York, D., Preparation of pickering emulsions and colloidosomes with relatively narrow size distributions by stirred cell membrane emulsification. *Langmuir* **2011**, *27*, (6), 2357–2363.
59. Walstra, P., Principles of emulsion formation. *Chemical Engineering Science* **1993**, *48*, (2), 333–349.
60. Whitby, C. P.; Parthipan, R., Influence of particle concentration on multiple droplet formation in Pickering emulsions. *Journal of colloid and interface science* **2019**, *554*, 315–323.
61. Sivakumar, M.; Tang, S. Y.; Tan, K. W., Cavitation technology – A greener processing technique for the generation of pharmaceutical nanoemulsions. *Ultrasonics Sonochemistry* **2014**, *21*, (6), 2069–2083.
62. Costa, A. L. R.; Gomes, A.; Cunha, R. L., One-step ultrasound producing O/W emulsions stabilized by chitosan particles. *Food Research International* **2018**, *107*, 717–725.
63. Lee, Y.-T.; Li, D. S.; Ilavsky, J.; Kuzmenko, I.; Jeng, G.-S.; O'Donnell, M.; Pozzo, L. D., Ultrasound-based formation of nano-Pickering emulsions investigated via in-situ SAXS. *Journal of Colloid and Interface Science* **2019**, *536*, 281–290.

64. Low, L. E.; Wong, S. K.; Tang, S. Y.; Chew, C. L.; De Silva, H. A.; Lee, J. M. V.; Hoo, C. H.; Kenrick, K., Production of highly uniform Pickering emulsions by novel high-intensity ultrasonic tubular reactor (HUTR). *Ultrasonics Sonochemistry* **2019**, *54*, 121–128.
65. Siva, S. P.; Kow, K.-W.; Chan, C.-H.; Tang, S. Y.; Ho, Y. K., Prediction of droplet sizes for oil-in-water emulsion systems assisted by ultrasound cavitation: Transient scaling law based on dynamic breakup potential. *Ultrasonics Sonochemistry* **2019**, *55*, 348–358.
66. Chandrapala, J.; Oliver, C.; Kentish, S.; Ashokkumar, M., Ultrasonics in food processing. *Ultrasonics Sonochemistry* **2012**, *19*, (5), 975–983.
67. Taha, A.; Hu, T.; Zhang, Z.; Bakry, A. M.; Khalifa, I.; Pan, S.; Hu, H., Effect of different oils and ultrasound emulsification conditions on the physicochemical properties of emulsions stabilized by soy protein isolate. *Ultrasonics Sonochemistry* **2018**, *49*, 283–293.
68. Taha, A.; Ahmed, E.; Ismaiel, A.; Ashokkumar, M.; Xu, X.; Pan, S.; Hu, H., Ultrasonic emulsification: An overview on the preparation of different emulsifiers-stabilized emulsions. *Trends in Food Science & Technology* **2020**, *105*, 363–377.
69. Rozynek, Z.; Castberg, R.; Kalicka, A.; Jankowski, P.; Garstecki, P., Electric field manipulation of particles in leaky dielectric liquids. *Arch. Mech* **2015**, *67*, (5), 385–399.
70. Rozynek, Z.; Banaszak, J.; Mikkelsen, A.; Khobaib, K.; Magdziarz, A., Electrorotation of particle-coated droplets: from fundamentals to applications. *Soft Matter* **2021**.
71. Mhatre, S.; Deshmukh, S.; Thaokar, R. M., Electrocoalescence of a drop pair. *Physics of Fluids* **2015**, *27*, (9), 092106.
72. Abbasi, M. S.; Song, R.; Cho, S.; Lee, J., Electro-Hydrodynamics of Emulsion Droplets: Physical Insights to Applications. *Micromachines* **2020**, *11*, (10), 942.
73. Ouriemi, M.; Vlahovska, P. M., Electrohydrodynamic Deformation and Rotation of a Particle-Coated Drop. *Langmuir* **2015**, *31*, (23), 6298–6305.
74. Dommersnes, P.; Rozynek, Z.; Mikkelsen, A.; Castberg, R.; Kjerstad, K.; Hersvik, K.; Otto Fossum, J., Active structuring of colloidal armour on liquid drops. *Nature Communications* **2013**, *4*, (1), 2066.
75. Mikkelsen, A.; Khobaib, K.; Eriksen, F. K.; Måløy, K. J.; Rozynek, Z., Particle-covered drops in electric fields: drop deformation and surface particle organization. *Soft Matter* **2018**, *14*, (26), 5442–5451.
76. Karyappa, R. B.; Naik, A. V.; Thaokar, R. M., Electroemulsification in a Uniform Electric Field. *Langmuir* **2016**, *32*, (1), 46–54.
77. Hwang, K.; Singh, P.; Aubry, N., Destabilization of Pickering emulsions using external electric fields. *Electrophoresis* **2010**, *31*, (5), 850-859.
78. Kwon, W.-T.; Park, K.; Han, S. D.; Yoon, S. M.; Kim, J. Y.; Bae, W.; Rhee, Y. W., Investigation of water separation from water-in-oil emulsion using electric field. *Journal of Industrial and Engineering Chemistry* **2010**, *16*, (5), 684–687.
79. Xie, G.; Luo, J.; Liu, S.; Guo, D.; Zhang, C., Electric-fields-enhanced destabilization of oil-in-water emulsions flowing through a confined wedgelike gap. *Journal of Applied Physics* **2010**, *108*, (6), 064314.
80. Chanamai, R.; Herrmann, N.; McClements, D. J., Probing Flocculation Structure by Ultrasonic Spectroscopy, Viscometry, and Creaming Measurements. *Langmuir* **2000**, *16*, (14), 5884–5891.
81. Nelson, P. V.; Povey, M. J. W.; Wang, Y., An ultrasound velocity and attenuation scanner for viewing the temporal evolution of a dispersed phase in fluids. *Review of Scientific Instruments* **2001**, *72*, (11), 4234–4241.
82. Su, Q.; Tan, C.; Dong, F., Measurement of Oil–Water Two-Phase Flow Phase Fraction With Ultrasound Attenuation. *IEEE Sensors Journal* **2018**, *18*, (3), 1150-1159.
83. Dong, T.; Norisuye, T.; Nakanishi, H.; Tran-Cong-Miyata, Q., Particle size distribution analysis of oil-in-water emulsions using static and dynamic ultrasound scattering techniques. *Ultrasonics* **2020**, *108*, 106117.
84. Tran, T. N.; Nakanishi, H.; Norisuye, T.; Tran-Cong-Miyata, Q., Ultrasound Scattering Studies on Pickering Emulsion. *Proceedings of Symposium on Ultrasonic Electronics* **2016**, *37*.

85. Józefczak, A.; Wlazło, R., Ultrasonic studies of emulsion stability in the presence of magnetic nanoparticles. *Advances in Condensed Matter Physics* **2015**, 2015.
86. Venkataramani, D.; Smay, J.; Aichele, C., Transient stability of surfactant and solid stabilized water-in-oil emulsions. *Colloids and Surfaces A: Physicochemical and Engineering Aspects* **2016**, 490, 84–90.
87. Treeby, B. E.; Cox, B. T.; Zhang, E. Z.; Patch, S. K.; Beard, P. C., Measurement of broadband temperature-dependent ultrasonic attenuation and dispersion using photoacoustics. *IEEE transactions on ultrasonics, ferroelectrics, and frequency control* **2009**, 56, (8), 1666–1676.
88. Vilensky, G.; ter Haar, G.; Saffari, N., A model of acoustic absorption in fluids based on a continuous distribution of relaxation times. *Wave Motion* **2012**, 49, (1), 93–108.
89. Gallego-Juárez, J. A., Basic Principles of Ultrasound. In *Ultrasound in Food Processing*, 2017; pp 1–26.
90. Challis, R.; Povey, M.; Mather, M.; Holmes, A., Ultrasound techniques for characterizing colloidal dispersions. *Reports on progress in physics* **2005**, 68, (7), 1541.
91. McClements, D. J., Principles of Ultrasonic Droplet Size Determination in Emulsions. *Langmuir* **1996**, 12, (14), 3454–3461.
92. Epstein, P. S.; Carhart, R. R., The absorption of sound in suspensions and emulsions. I. Water fog in air. *The Journal of the Acoustical Society of America* **1953**, 25, (3), 553–565.
93. Allegra, J. R.; Hawley, S. A., Attenuation of Sound in Suspensions and Emulsions: Theory and Experiments. *The Journal of the Acoustical Society of America* **1972**, 51, (5B), 1545–1564.
94. McClements, D. J.; Povey, M. J. W., Scattering of ultrasound by emulsions. *Journal of Physics D: Applied Physics* **1989**, 22, (1), 38–47.
95. Challis, R.; Tebbutt, J.; Holmes, A., Equivalence between three scattering formulations for ultrasonic wave propagation in particulate mixtures. *Journal of Physics D: Applied Physics* **1998**, 31, (24), 3481.
96. Dukhin, A. S.; Goetz, P. J., *Characterization of liquids, dispersions, emulsions, and porous materials using ultrasound*. Elsevier: 2017.
97. Hipp, A. K.; Storti, G.; Morbidelli, M., Acoustic Characterization of Concentrated Suspensions and Emulsions. 2. Experimental Validation. *Langmuir* **2002**, 18, (2), 405–412.
98. Forrester, D. M.; Pinfield, V. J., The absorption of ultrasound in emulsions: computational modelling of thermal effects. *Scientific Reports* **2018**, 8, (1), 12486.
99. Anson, L. W.; Chivers, R. C., Ultrasonic scattering from spherical shells including viscous and thermal effects. *The Journal of the Acoustical Society of America* **1993**, 93, (4), 1687–1699.
100. Chen, Y., Ultrasonic wave propagation in concentrated emulsions and encapsulated emulsions. *SCIENCE AND ENGINEERING* **2007**, 500, 7.
101. Guédra, M.; Valier-Brasier, T.; Conoir, J.-M.; Coulouvrat, F.; Astafyeva, K.; Thomas, J.-L., Influence of shell compressibility on the ultrasonic properties of polydispersed suspensions of nanometric encapsulated droplets. *The Journal of the Acoustical Society of America* **2014**, 135, (3), 1044–1055.
102. Tran, T. N.; Shibata, D.; Norisuye, T.; Nakanishi, H.; Tran-Cong-Miyata, Q., Determination of particle size distribution and elastic properties of silica microcapsules by ultrasound spectroscopy. *Japanese Journal of Applied Physics* **2016**, 55, (7S1), 07KC01.
103. Patel, J. K.; Parekh, K., Effect of carrier and particle concentration on ultrasound properties of magnetic nanofluids. *Ultrasonics* **2015**, 55, 26–32.
104. Tham, F. K.; Ng, W. M.; Leong, S. S.; Yeap, S. P.; Low, S. C.; Lee, H. L.; Lim, J., Magnetophoresis of Magnetic Pickering Emulsions Under Low Field Gradient: Macroscopic and Microscopic Motion. *Langmuir* **2021**, 37, (5), 1811–1822.
105. Lin, Z.; Zhang, Z.; Li, Y.; Deng, Y., Magnetic nano-Fe₃O₄ stabilized Pickering emulsion liquid membrane for selective extraction and separation. *Chemical Engineering Journal* **2016**, 288, 305–311.

106. Lahiri, B.; Ranoo, S.; Zaibudeen, A.; Philip, J., Magnetic hyperthermia in magnetic nanoemulsions: Effects of polydispersity, particle concentration and medium viscosity. *Journal of Magnetism and Magnetic Materials* **2017**, 441, 310–327.
107. Qiu, D.; An, X., Controllable release from magnetoliposomes by magnetic stimulation and thermal stimulation. *Colloids and Surfaces B: Biointerfaces* **2013**, 104, 326–329.
108. Low, L. E.; Tey, B. T.; Ong, B. H.; Tang, S. Y., Unravelling pH-responsive behaviour of Fe₃O₄@CNCs-stabilized Pickering emulsions under the influence of magnetic field. *Polymer* **2018**, 141, 93–101.
109. Rosensweig, R. E., Heating magnetic fluid with alternating magnetic field. *Journal of magnetism and magnetic materials* **2002**, 252, 370–374.
110. Dutz, S.; Hergt, R., Magnetic particle hyperthermia—a promising tumour therapy? *Nanotechnology* **2014**, 25, (45), 452001.
111. Lahiri, B. B.; Ranoo, S.; Philip, J., Effect of orientational ordering of magnetic nanoemulsions immobilized in agar gel on magnetic hyperthermia. *Journal of Magnetism and Magnetic Materials* **2018**, 451, 254–268.
112. Rosales, S.; Casillas, N.; Topete, A.; Cervantes, O.; González, G.; Paz, J.; Cano, M., Evaluating physical changes of iron oxide nanoparticles due to surface modification with oleic acid. *Chinese Physics B* **2020**, 29, (10), 100502.
113. Pilati, V.; Gomide, G.; Gomes, R. C.; Goya, G. F.; Depeyrot, J., Colloidal Stability and Concentration Effects on Nanoparticle Heat Delivery for Magnetic Fluid Hyperthermia. *Langmuir* **2021**, 37, (3), 1129–1140.
114. Dennis, C. L.; Ivkov, R., Physics of heat generation using magnetic nanoparticles for hyperthermia. *International Journal of Hyperthermia* **2013**, 29, (8), 715–729.
115. Estelrich, J.; Escribano, E.; Queralt, J.; Busquets, M. A., Iron Oxide Nanoparticles for Magnetically-Guided and Magnetically-Responsive Drug Delivery. *International Journal of Molecular Sciences* **2015**, 16, (4), 8070–8101.
116. Krishnan, K. M.; Pakhomov, A. B.; Bao, Y.; Blomqvist, P.; Chun, Y.; Gonzales, M.; Griffin, K.; Ji, X.; Roberts, B. K., Nanomagnetism and spin electronics: materials, microstructure and novel properties. *Journal of materials science* **2006**, 41, (3), 793–815.
117. Stigliano, R. V.; Shubitidze, F.; Petryk, J. D.; Shoshiashvili, L.; Petryk, A. A.; Hoopes, P. J., Mitigation of eddy current heating during magnetic nanoparticle hyperthermia therapy. *International Journal of Hyperthermia* **2016**, 32, (7), 735–748.
118. Martínez-Pedrero, F., Static and dynamic behavior of magnetic particles at fluid interfaces. *Advances in Colloid and Interface Science* **2020**, 284, 102233.
119. Kachniarz, M.; Szewczyk, R., Study on the Rayleigh Hysteresis Model and its Applicability in Modeling Magnetic Hysteresis Phenomenon in Ferromagnetic Materials. *Acta Physica Polonica, A* **2017**, 131, (5).
120. Mehdaoui, B.; Meffre, A.; Carrey, J.; Lachaize, S.; Lacroix, L.-M.; Gougeon, M.; Chaudret, B.; Respaud, M., Optimal Size of Nanoparticles for Magnetic Hyperthermia: A Combined Theoretical and Experimental Study. *Advanced Functional Materials* **2011**, 21, (23), 4573–4581.
121. Gresits, I.; Thuróczy, G.; Sági, O.; Kollarics, S.; Csósz, G.; Márkus, B.; Nemes, N.; Hernández, M. G.; Simon, F., Non-exponential magnetic relaxation in magnetic nanoparticles for hyperthermia. *Journal of Magnetism and Magnetic Materials* **2021**, 526, 167682.
122. Fu, R.; Yan, Y.; Roberts, C.; Liu, Z.; Chen, Y., The role of dipole interactions in hyperthermia heating colloidal clusters of densely-packed superparamagnetic nanoparticles. *Scientific reports* **2018**, 8, (1), 1–10.
123. Sakellari, D.; Brintakis, K.; Kostopoulou, A.; Myrovali, E.; Simeonidis, K.; Lappas, A.; Angelakeris, M., Ferrimagnetic nanocrystal assemblies as versatile magnetic particle hyperthermia mediators. *Materials Science and Engineering: C* **2016**, 58, 187–193.
124. Vinogradov, A., Physicochemical and acoustic properties of water-based magnetic colloid. *Colloid Journal* **2004**, 66, (1), 29–37.

125. Lahiri, B.; Ranoo, S.; Philip, J., Uncertainties in the estimation of specific absorption rate during radiofrequency alternating magnetic field induced non-adiabatic heating of ferrofluids. *Journal of Physics D: Applied Physics* **2017**, 50, (45), 455005.
126. Wildeboer, R.; Southern, P.; Pankhurst, Q., On the reliable measurement of specific absorption rates and intrinsic loss parameters in magnetic hyperthermia materials. *Journal of Physics D: Applied Physics* **2014**, 47, (49), 495003.
127. Engelmann, U. M.; Seifert, J.; Mues, B.; Roitsch, S.; Ménager, C.; Schmidt, A. M.; Slabu, I., Heating efficiency of magnetic nanoparticles decreases with gradual immobilization in hydrogels. *Journal of Magnetism and Magnetic Materials* **2019**, 471, 486-494.
128. Patil, R. M.; Thorat, N. D.; Shete, P. B.; Otari, S. V.; Tiwale, B. M.; Pawar, S. H., In vitro hyperthermia with improved colloidal stability and enhanced SAR of magnetic core/shell nanostructures. *Materials Science and Engineering: C* **2016**, 59, 702–709.
129. Lanier, O. L.; Korotych, O. I.; Monsalve, A. G.; Wable, D.; Savliwala, S.; Grooms, N. W. F.; Nacea, C.; Tuitt, O. R.; Dobson, J., Evaluation of magnetic nanoparticles for magnetic fluid hyperthermia. *International Journal of Hyperthermia* **2019**, 36, (1), 686-700.
130. Brugger, B.; Richtering, W., Magnetic, Thermosensitive Microgels as Stimuli-Responsive Emulsifiers Allowing for Remote Control of Separability and Stability of Oil in Water-Emulsions. *Advanced Materials* **2007**, 19, (19), 2973–2978.
131. Prilezky, T. A.; Furst, E. M., Magnetite nanoparticles program the assembly, response, and reconfiguration of structured emulsions. *Soft matter* **2019**, 15, (7), 1529–1538.
132. Kaiser, A.; Liu, T.; Richtering, W.; Schmidt, A. M., Magnetic capsules and Pickering emulsions stabilized by core– shell particles. *Langmuir* **2009**, 25, (13), 7335–7341.
133. Rozynek, Z.; Dommersnes, P.; Mikkelsen, A.; Michels, L.; Fossum, J. O., Electrohydrodynamic controlled assembly and fracturing of thin colloidal particle films confined at drop interfaces. *The European Physical Journal Special Topics* **2014**, 223, (9), 1859–1867.
134. Russo, A.; Morescalchi, F.; Donati, S.; Gambicorti, E.; Azzolini, C.; Costagliola, C.; Semeraro, F., Heavy and standard silicone oil: intraocular inflammation. *International ophthalmology* **2018**, 38, (2), 855–867.
135. Mutlu, H.; Meier, M. A., Castor oil as a renewable resource for the chemical industry. *European Journal of Lipid Science and Technology* **2010**, 112, (1), 10–30.
136. Loos, C.; Syrovets, T.; Musyanovych, A.; Mailänder, V.; Landfester, K.; Nienhaus, G. U.; Simmet, T., Functionalized polystyrene nanoparticles as a platform for studying bio–nano interactions. *Beilstein journal of nanotechnology* **2014**, 5, (1), 2403–2412.
137. Rozynek, Z.; Kaczmarek-Klinowska, M.; Magdziarz, A., Assembly and rearrangement of particles confined at a surface of a droplet, and intruder motion in electro-shaken particle films. *Materials* **2016**, 9, (8), 679.
138. Kang, E.; Graczykowski, B.; Jonas, U.; Christie, D.; Gray, L. A. G.; Cangialosi, D.; Priestley, R. D.; Fytas, G., Shell Architecture Strongly Influences the Glass Transition, Surface Mobility, and Elasticity of Polymer Core-Shell Nanoparticles. *Macromolecules* **2019**, 52, (14), 5399–5406.
139. Lobato, N. C. C.; Mansur, M. B.; Ferreira, A. d. M., Characterization and Chemical Stability of Hydrophilic and Hydrophobic Magnetic Nanoparticles. *Materials Research* **2017**, 20, 736–746.
140. Kaczmarek, K.; Hornowski, T.; Kubovčíková, M.; Timko, M.; Koralewski, M.; Józefczak, A., Heating Induced by Therapeutic Ultrasound in the Presence of Magnetic Nanoparticles. *ACS Applied Materials & Interfaces* **2018**, 10, (14), 11554–11564.
141. Mason, T. J.; Lorimer, J. P.; Bates, D. M., Quantifying sonochemistry: Casting some light on a 'black art'. *Ultrasonics* **1992**, 30, (1), 40-42.
142. Schneider, C. A.; Rasband, W. S.; Eliceiri, K. W., NIH Image to ImageJ: 25 years of image analysis. *Nature Methods* **2012**, 9, (7), 671–675.
143. Smith, M. C.; Beyer, R. T., Ultrasonic absorption in water in the temperature range 0–80 C. *The Journal of the Acoustical Society of America* **1948**, 20, (5), 608–610.

144. Adeyeye, A. O.; Shimon, G., Chapter 1 - Growth and Characterization of Magnetic Thin Film and Nanostructures. In *Handbook of Surface Science*, Camley, R. E.; Celinski, Z.; Stamps, R. L., Eds. North-Holland: 2015; Vol. 5, pp 1–41.
145. Skumiel, A.; Kertmen, A.; Nowaczyk, G., Investigation of the magnetic hyperthermia effect in an aqueous dispersion of colloidosomal nanoparticle clusters. *Journal of Molecular Liquids* **2019**, 283, 91–95.
146. Harman, C. L. G.; Patel, M. A.; Guldin, S.; Davies, G.-L., Recent developments in Pickering emulsions for biomedical applications. *Current Opinion in Colloid & Interface Science* **2019**, 39, 173–189.

5. Publications constituting the dissertation

[Publication I]

Efficient formation of oil-in-oil Pickering emulsions with narrow size distributions by using electric fields

Z. Rozynek, R. Bielas, A. Józefczak

Soft Matter, 2018, 14, 5140-5149



Cite this: *Soft Matter*, 2018, 14, 5140

Efficient formation of oil-in-oil Pickering emulsions with narrow size distributions by using electric fields†

Z. Rozynek, * R. Bielas  and A. Józefczak 

Droplets covered by adsorbed particles are used in a wide range of research studies and applications, including stabilising emulsions used in the food or cosmetic industries, and fabricating new materials, such as microcapsules or multi-cavity structures. Pickering emulsions are commonly prepared by bulk emulsification techniques, for instance, by ultrasonic homogenisation or mechanical stirring, by membrane emulsification, or with the use of microfluidics. The latter two methods typically allow for more precise control of the droplet size distribution, whereas the bulk techniques guarantee high throughput. Here we propose a new bulk approach to fabricating Pickering emulsions by utilising electric fields. We prepare oil-in-oil emulsions stabilised by microparticles and control the mean size of the Pickering droplets. In our approach we take advantage of total surface area reduction of emulsion droplets by electrocoalescence. This leads to an increase in particle coverage, and eventually to formation of densely packed particle shells on Pickering droplets. First, we prepare an unstable pre-emulsion with droplets having small sizes and low particle coverages, from which the final Pickering emulsion is formed *via* consecutive coalescence events speeded up by application of electric fields. We monitor the development of the emulsions with optical microscopy imaging. The results demonstrate that the utilisation of electric fields goes beyond the mere role of enhancing coalescence; it plays an important role in surface particle manipulation and droplet rotation that further promote formation of stable particle-covered drops.

Received 30th March 2018,
Accepted 27th May 2018

DOI: 10.1039/c8sm00671g

rsc.li/soft-matter-journal

1 Introduction

Pickering emulsions have received great research interest in recent years because they have generated and hold promise for a variety of practical applications in fields such as medicine,¹ the food industry,² the oil industry,³ and biofuel processing.⁴ Pickering emulsions can also be used in material engineering, *e.g.* for fabricating granular or colloidal capsules^{5,6} or multicavity structures.⁷ Moreover, particle-covered droplets (Pickering droplets) possess physical characteristics that make them useful as model systems, for example, for studying particle-layer buckling on curved interfaces⁸ or the mechanics,⁹ electrorotation, and collective motion of deformable shells.¹⁰

Particle-stabilised emulsions can replace conventional emulsions stabilised with surfactants, particularly in areas where surfactants should be avoided, *e.g.* in home and personal care products that cause skin and eye irritation,¹¹ or where surfactants may cause serious environmental pollution.¹² Lately, research on Pickering

emulsions has gained momentum and led to academic results that have paved the way for research commercialisation. Yet, to achieve higher performance within both academic and industrial contexts, further understanding of Pickering emulsions is required. This includes advancing techniques for more efficient formation of Pickering emulsions.

There are different approaches to fabricating Pickering emulsions. Bulk emulsification techniques are most commonly used, and these include mechanical stirring^{13–15} or shaking¹⁶ and ultrasonic homogenisation.^{17–19} When it comes to fabrication efficiency, bulk emulsification methods are superior to microfluidics²⁰ or membrane emulsification.²¹ However, the latter two approaches typically allow for more precise control of droplet size.²²

Here, we propose a new bulk approach to fabricating Pickering emulsions by electric fields that are primarily used to promote attraction of droplets. However, the application of electric fields here goes beyond the mere role of enhancing coalescence. Two electric field-induced physical mechanisms, namely electrohydrodynamic (EHD) flows and Quincke rotation, are important for surface particle manipulation facilitating easier coalescence of droplets partially covered by particles. The above-mentioned phenomena also ensure that the fabricated Pickering droplets possess shells comprising very densely packed particles

Institute of Acoustics, Faculty of Physics, Adam Mickiewicz University, Umultowska 85, 61-614 Poznań, Poland. E-mail: zbiroz@amu.edu.pl

† Electronic supplementary information (ESI) available: Three supplementary movies. See DOI: 10.1039/c8sm00671g

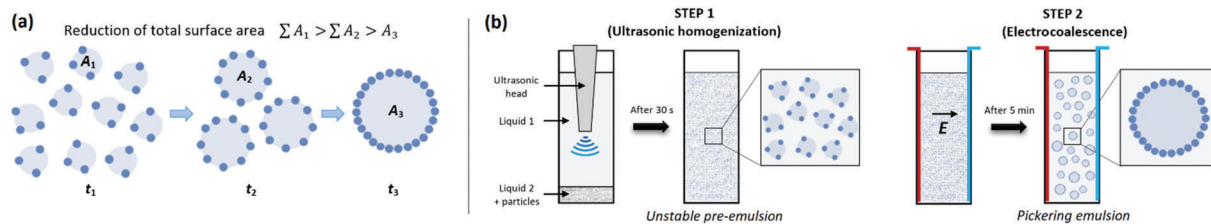


Fig. 1 (a) Formation of a Pickering droplet *via* subsequent coalescence of several small drops. We exploit the reduction of total surface area through coalescence to increase particle coverage, ultimately leading to formation of a stable Pickering droplet. (b) A schematic illustration of the Pickering emulsion fabrication process. In the first step, an initial emulsion is formed by ultrasonic homogenisation. Such an emulsion of very small droplets is unstable because solid particles do not cover the entire drop surface (see the enlarged image on the left). In the second step, an electric field is used for coalescing droplets. It typically takes several minutes to form a Pickering emulsion consisting of drops densely covered by particles (see the enlarged image on the right).

and prevent formation of droplet agglomerates or particle-bridged droplets.^{23,24} In this approach, we take advantage of the total surface area reduction of coalescing drops. It is well known that coalescence of two drops of similar size reduces the available surface area by approximately 20%. Thus, coalescence of droplets partially covered with particles results in an increase of surface particle coverage, which may eventually lead to formation of a stable particle-covered drop, as illustrated in Fig. 1a. In order to form an unstable pre-emulsion, we use ultrasonic homogenisation. Then, in the main step of the Pickering emulsion fabrication, electric fields are used, as schematically illustrated in Fig. 1b.

With respect to fabrication, stabilisation, and manipulation of non-Pickering emulsions by electric fields, there are many research studies in which different electrostatic and electrokinetic phenomena are utilised. Electro-spraying is used for emulsion drop formation in different dispersing phases,²⁵ electric field-induced drop breakup has applications in fine emulsification,²⁶ high-intensity electric fields may prevent droplet coalescence,²⁷ and dielectrophoresis or electrophoresis are used for phase separation.²⁸

The literature on Pickering emulsions subjected to electric fields mainly includes studies related to their destabilisation and manipulation, *e.g.* studies on electric field-induced structural changes of Pickering drops²⁹ or electric field-driven droplet consolidation for production of porous materials.³⁰ A plethora of research results are available on individual Pickering droplets, or Pickering droplet pairs, subjected to external electric fields. These cover studies on arrested coalescence,^{31,32} deformation,^{33,34,76} breakup,³⁵ rotation,³⁶ or the mechanics^{37,38} of Pickering drops. Electric fields can also be used to form individual Pickering droplets by utilising electrohydrodynamic flows, and electrostatic interactions.^{39,40}

Here, we use electric fields to fabricate Pickering emulsion drops in bulk quantities. The primary purpose of applying external electric fields is to promote attraction of droplets, enabling coalescence. In principle, emulsion drop coalescence may occur spontaneously without the assistance of electric fields, for example, through droplet collisions caused by liquid convection or Brownian diffusion.⁴¹ However, the process of a droplet growing, for instance, from tens to hundreds of micrometres, may last several hours or days, depending on parameters such as the viscosity of the continuous phase, interfacial tension, or droplet concentration (for more details, see ref. 42–44).

Electric fields may greatly enhance the coalescence of emulsion droplets.^{45–48} As we demonstrate in the Results section, the Pickering fabrication process can be speeded up by two orders of magnitude with the assistance of electric fields. The application of electric fields here goes beyond the mere role of enhancing coalescence. Two electric field-induced physical mechanisms, namely electrohydrodynamic (EHD) flows and Quincke rotation, are important for surface particle manipulation allowing particle-laden drops to coalesce.

Below we will briefly discuss the physical phenomena involved in the system studied here. All of the physical phenomena are schematically presented in Fig. 2.

1.1. Electrohydrodynamic flows

When a silicone oil drop is immersed in castor oil and subjected to a direct current (DC) electric field, free charges accumulate at the drop interface so that the drop acquires a dipole moment. Because the values of the silicone oil droplet's electrical conductivity and dielectric constant are smaller than those of the surrounding castor oil, the droplet's dipole moment is in the opposite direction to the electric field. This leads to drop compression along the electric field direction and to the induction of EHD flows directed from the drop electric poles to the drop electric equator (for more details, see the ESI† materials). As long as the electric field strength is weak (typically $< 300 \text{ V mm}^{-1}$) the induced EHD flows can be used to convect surface particles away from the drop's electric poles, as presented in Fig. 2a, facilitating coalescence.

1.2. Dipolar interactions

Droplet dipolar interactions together with EHD flows may contribute to droplet attraction. After an external electric field is applied to a silicone oil drop suspended in castor oil, the droplet acquires a dipole moment. For droplets aligned along the electric field direction, the dipolar interaction is always attractive, as shown in Fig. 2b, which greatly aids drop coalescence. Theoretical simulations show that the droplets' dipole-dipole interactions dominate at short separation distances, whereas EHD interactions may dominate at greater drop separation distances.⁴⁹

Because the dipolar interaction decays rapidly with the droplet separation distance, the attractive interaction is effective only when the polarized drops are at close distances. Therefore, for low concentrations of silicone oil, the electrocoalescence dynamics

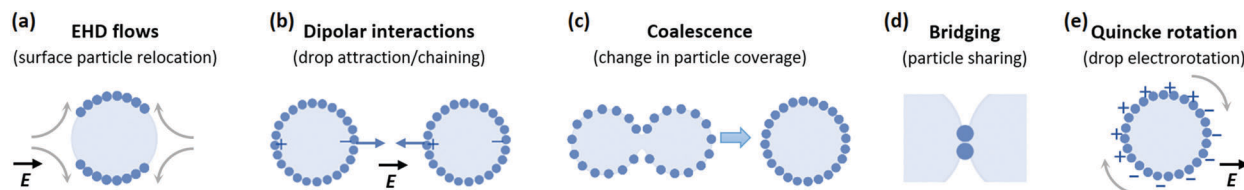


Fig. 2 Sketches illustrating the physical phenomena present in the experiments: (a) electric field-induced liquid flows (EHD flows) move surface particles away from the droplet's electric poles, (b) the droplets' dipole–dipole interactions aid coalescence by attracting the droplets to one to another, (c) coalescence leads to the decrease of drop surface area and the increase of surface particle coverage, (d) droplets of emulsion can be bridged by particle bridging—an undesirable effect that may lead to the formation of droplet clusters, (e) Quincke rotation of a particle-covered drop due to the electric torque present when the charge distribution on a drop surface is imbalanced. The electric field is in the horizontal direction, as indicated by the black arrow.

will be very low. In fact, for dilute emulsions, there exists an electric field threshold below which electrocoalescence occurs only to a limited extent.⁵⁰ This is not the case here, as we use a silicone oil concentration of $\sim 10\%$, and the coalescence dynamics is high.

The properties of the droplet interface can be altered by the presence of impurities retarding the rate of coalescence. In addition, particle bridging (different droplets sharing the same particles) can occur. Then, the dipolar interactions may lead to drop chaining, *i.e.* particle-covered droplets aligning along the electric field direction. We tackle this problem by inducing liquid shearing, as will be described later in the text.

1.3. Coalescence

When droplets are brought into close proximity (*e.g.* by mechanical liquid shearing, gravity, or electric fields as is the case here) they may coalesce, leading to the increase of surface particle coverage, as presented in Fig. 2c. As long as the electric poles of the drops are particle-free, the mechanism for merging two particle-laden droplets is the same as for pure droplets. The presence of particles on the drop surface may affect the surface tension; yet, in our system, the change is marginal⁹ and we neglect this effect. For droplets with greater particle coverage, the coalescence can be impeded due to the presence of particles at the electric pole regions, making a physical barrier between droplets. In addition, surface particles may affect the capillary pressure and rheological properties of the thin film of castor oil, making it more difficult for droplets to coalesce.⁵¹ As already mentioned, in this work we use electric fields to facilitate coalescence through EHD flows that aid to convect particles away from electric poles. Besides electric field strength and frequency, there are other parameters that influence the electrocoalescence rate, and these include surface tension and the viscosity of the dispersing phase. For experimental and theoretical study results on electro-coalescence of leaky dielectric fluids, such as the silicone and castor oils used here, we refer the reader to these articles.^{49,52,53} Another note on the droplet coalescence is that when the surface particle coverage of two original drops (to be coalesced) is sufficiently large, the drop merging can lead to formation of arrested structures (arrested coalescence) that may acquire aspherical shapes.^{54,55}

1.4. Particle bridging

Droplets in emulsions can be bridged by particles, *i.e.* one or more particles are shared by two droplets as illustrated in Fig. 2d.

This effect is often undesirable, as it may lead to the formation of droplet clusters or large agglomerations, and to enhancement of creaming rates. Particle bridging is sensitive to the particles' three-phase contact angle, and will likely occur at intermediate contact angles between 30° and 70° due to the surface particles having a slight preference for the continuous phase. Particle bridges can be broken by shearing at low rates (for more details, see ref. 23 and 24). We use strong electric fields to induce convective flows in the cell and local liquid turbulences through droplet electro-rotation to gently shear the emulsion droplets.

1.5. Quincke rotation

In strong DC electric fields, pure silicone oil droplets suspended in castor oil undergo electrorotation. Addition of surface particles may decrease the value of the critical electric field for the onset of Quincke rotation. Silicone oil droplets partly or completely covered by non-conductive microparticles begin to Quincke rotate at electric field strengths below 600 V mm^{-1} . Such electrorotation of a droplet is a particular form of the aforementioned EHD flows, and is driven by electric forces acting on free charges built up on the surface of a droplet (for more details, see ref. 56 and 57). Here, we use the Quincke instability to induce shearing for breaking both particle bridges and droplet chains. A sketch illustrating Quincke rotation of a Pickering droplet is shown in Fig. 2e.

2 Materials and methods

2.1. Experimental set-up

A schematic illustration of the set-up used for electrocoalescing drops to form Pickering emulsions and for monitoring this process is shown in Fig. 3. The set-up consisted of a sample cell placed on a mechanical XYZ translation stage, a signal generator (SDG1025, Sigilent), a high-voltage bipolar amplifier (10HVA24-BP1, HVP), a CMOS camera (UI-3590CP-C-HQ, IDS) mounted on a high-magnification zoom lens system (MVL12X3Z, Thorlabs), an LED light source, and a computer for collecting images and recording videos. The sample cell was made of glass, size $30 \text{ mm} \times 18 \text{ mm} \times 1.3 \text{ mm}$, and two copper plates constituting electrodes were placed inside the cell. In the experiment, we used two electric field strengths, namely 200 V mm^{-1} and 600 V mm^{-1} . The weaker electric field was used to assist coalescence of droplets, while stronger fields were primarily used to break

droplet aggregations (or prevent their formation) and to further promote droplet coalescence.

2.2. Oils and particles

In our experiments, we used silicone oil (6678.1000, Rhodorsil Oils 47, density $\sim 0.96 \text{ g cm}^{-3}$ at 25°C , and viscosity $\sim 50 \text{ mPa s}$ at 25°C) as a dispersed phase, and castor oil (83912, Sigma-Aldrich, density $\sim 0.96 \text{ g cm}^{-3}$ at 25°C , and viscosity $\sim 700 \text{ mPa s}$ at 25°C) as a dispersing phase. Different particle materials were used to make silicone oil Pickering droplets, and these include: green-dyed and red-dyed polyethylene (PE) particles (with size $\sim 20 \mu\text{m}$ and $\sim 50 \mu\text{m}$, respectively, and density $\sim 0.98 \text{ g cm}^{-3}$, purchased from Cospheric, USA); silica particles (with size $\sim 8 \mu\text{m}$ and density $\sim 1.8 \text{ g cm}^{-3}$, purchased from Cospheric, USA), and polystyrene particles (PS, Dynoseeds TS10 6317, with size $\sim 10 \mu\text{m}$ and density $\sim 1.05 \text{ g cm}^{-3}$, purchased from Microbeads AS, Norway). The pristine PS particles were surface modified (as described in ref. 58) to change the three-phase contact angle and increase their affinity towards silicone oil.

2.3. Preparation of the pre-emulsion

To form a pre-emulsion, from which the final Pickering emulsion is made, we used an ultrasonic homogeniser (Bandelin Sonopuls HD 3100 equipped with a KE 76 probe, working at a frequency of 20 kHz). First, a dispersion of particles in silicone oil was formed using the homogeniser for 5 s. The ultrasonic wave intensity (estimated using the calorimetric method⁵⁹) amounted to $\sim 17 \text{ W cm}^{-2}$. Then we added castor oil and formed a pre-emulsion by homogenising the three-phase sample for 30 s. The droplet size distribution and droplet mean diameter of a pre-emulsion were evaluated using optical microscopy, and the results are shown in Fig. 7b, together with the results obtained for the fabricated Pickering emulsions. As presented in the figure, the droplet size distributions were fitted with log-normal functions. However, for calculating the coefficient of variation (CV) we used Gaussian functions (not plotted) that fit the data reasonably well, *i.e.* the mean values of droplet sizes obtained by fitting the experimental results with the Gaussian function were similar to those obtained by fitting the data with the log-normal function. We decided to do that for the convenient comparison of our data with those reported in the literature, *i.e.* the size distribution of droplets in an emulsion is often presented as a CV value.

The mean diameter (D) for the pre-emulsion was $7.4 \mu\text{m}$, the standard deviation (σ) was $5.2 \mu\text{m}$, and the CV was $\sim 70\%$, calculated as $\text{CV}\% = (\sigma/D) \times 100$.

3 Results

3.1. Emulsion evolution

All the emulsions in this study are oil-in-oil emulsions (with or without particles) prepared using silicone oil as the dispersed phase and castor oil as the continuous phase. Initially, we conducted experiments on coalescence of particle-free emulsion droplets without and with the presence of an electric field (Fig. 4a and b, respectively). This is to demonstrate the significance of electric field activity on the evolution dynamics of the emulsions. In the experiment shown in Fig. 4b, we used a direct current (DC) electric field of 200 V mm^{-1} (the electric field was strong enough to facilitate rapid droplet attraction leading to coalescence but weak enough to avoid droplet breakup).

One minute after the electric field application, it was already possible to resolve droplets in the image, *i.e.* droplets electrocoalesce and grow quickly to sizes a few times larger than the mean droplet size of the pre-emulsion emulsion. As electrocoalescence progresses, the mean droplet size increases. The small, densely dispersed droplets coalesced into several large drops, and after 20 min, the emulsion had almost phase separated. We observed that phase separation of the emulsion through electrocoalescence is >100 times faster than without the electric field (there is practically no change in Fig. 2a). In Fig. 4c and d we present the evolution of emulsions made with PS particles (size $\sim 10 \mu\text{m}$) and subjected to a DC electric field. First, we performed experiments in which we applied an electric field of 200 V mm^{-1} . Maintaining the same electric field strength throughout the experiment resulted in formation of unwanted droplet clusters (see Fig. 4c).

Such clustering may occur when droplets are bridged by microparticles preventing droplets from coalescing further (this effect will be investigated in the next section). To minimize droplet clustering and enable droplets to coalesce and eventually form a Pickering emulsion, we induced liquid shearing by applying strong electric fields. Note that the shearing process is only effective for a short time (several seconds). For that reason, we designed an experiment (see Fig. 4d) in which we alternate the electric field strength between 200 V mm^{-1} and 600 V mm^{-1} every 15 seconds. Though the pre-emulsions were similar to the experiment presented in Fig. 4c, the results after applying $200\text{--}600 \text{ V mm}^{-1}$ were different compared to the emulsion subjected to a 200 V mm^{-1} electric field. Only the application of weak and strong electric fields in an alternating fashion leads to the formation of a stable Pickering emulsion.

Fig. 5a presents a magnified optical microscopy image of the emulsion subjected to electric fields ($200\text{--}600 \text{ V mm}^{-1}$) for 30 minutes. No droplet clustering is observed in the image, *i.e.* the particle-covered droplets are separated from one another. A majority of the Pickering droplets have spherical or slightly aspherical shapes. Turning off the electric field does not induce

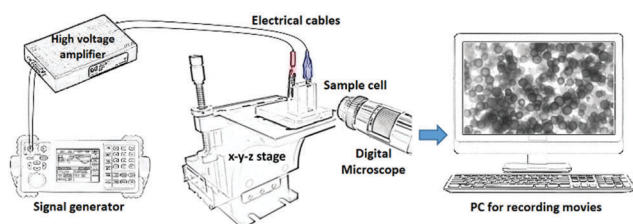


Fig. 3 A schematic illustration of the experimental set-up, consisting of a sample cell placed on a mechanical XYZ translation stage, a digital microscope for viewing in the direction perpendicular to the electric field direction, a signal generator and a voltage amplifier for generating high-voltage signals, and a computer for recording videos.

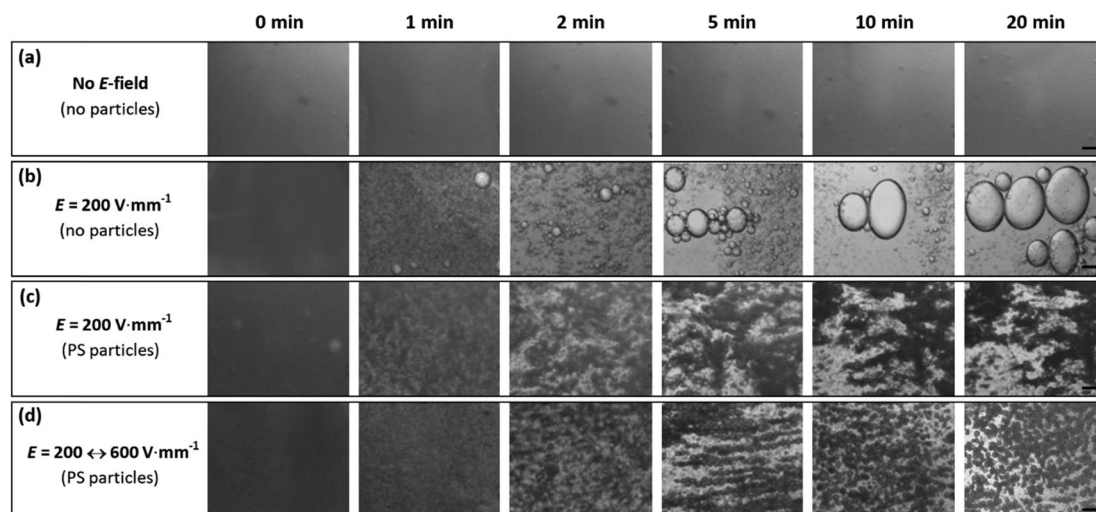


Fig. 4 Optical microscopy images showing the evolution of emulsions of silicone oil in castor oil (a and b) without and (c and d) with PS particles (size $\sim 10 \mu\text{m}$). All the emulsions were prepared at a 1 : 10 ratio of silicone oil to castor oil by weight. In the experiments with particles, the particle to silicone oil ratio was 1 : 4 by weight. (a) When no electric field is present, there are no observable changes (within the 20 min experiment) in the emulsion without particles, and de-emulsification takes approximately 100 times longer than when (b) an electric field of 200 V mm^{-1} is applied. (c) Application of an electric field of 200 V mm^{-1} to an emulsion with PS particles results in formation of undesirable droplet clusters. (d) Application of weak (200 V mm^{-1}) and strong (600 V mm^{-1}) electric fields in an alternating fashion (every 15 seconds) leads to formation of a stable Pickering emulsion. Strong electric fields are used to gently shear the emulsion droplets, which aids droplet coalescence and prevents clustering. All images were captured at the same microscope magnification, and the scale bar is $500 \mu\text{m}$. The external DC electric field was in the horizontal direction. In all the experiments, the sample cell was kept at $\sim 50 \text{ }^\circ\text{C}$.

observable particle movement within the particle shell of such droplets because the surface particles are arranged in a jammed, nearly hexagonal structure as shown in Fig. 5b. Among the entire population of droplets, some droplets with an oval shape are preserved after switching off the electric field. Arrested coalescence occurs when the particle coverage of the two original droplets (from which the oval-shaped Pickering droplet is formed) is sufficiently high before coalescence. In such a non-spherical Pickering droplet, the particles form a rigid film that resists the Laplace pressure gradient, which attempts to drive the coalesced droplet towards a spherical shape. We also observed several droplets that were partially

covered with particles. Examples of an oval-shaped Pickering droplet and a droplet partially covered by particles are presented in Fig. S1 (ESI[†]).

3.2. Electric field phenomena in play

Droplets of the initial emulsion (just after homogenising) have, on average, low particle coverage at their surfaces, which is favourable for coalescence. As the Pickering emulsion is being formed, the particle coverage increases, impeding droplet merging. However, partially particle-covered droplets (even with high particle coverage) may still coalesce, provided the regions near their contact are particle-free. In our silicone oil in castor oil emulsion, the presence of weak ($< 300 \text{ V mm}^{-1}$) electric fields may induce local (near a droplet) EHD liquid flows.

These flows aid to convect particles away from a droplet's electrical poles. Therefore, when two droplets with particle-free electric poles are electrostatically attracted to one another, they may easily coalesce. In Fig. 6a, we demonstrate EHD flow-assisted particle convection on droplet surfaces enabling two droplets to merge into a Pickering droplet (see also Movie S1, ESI[†]). The figure shows two partially particle-covered silicone oil droplets in castor oil. Initially, before applying the electric field, the PS particles (size $\sim 10 \mu\text{m}$) were distributed randomly on the droplet surfaces. Application of a direct current electric field of 200 V mm^{-1} (in the horizontal direction) induces EHD flows from the droplet electric poles towards the droplet electric equator (see the curved arrows in Fig. 6a). The flows convect PS particles away from the droplets' electric poles. Driven by both the attractive EHD and the electrostatic forces, the two droplets approach one another and eventually coalesce, forming

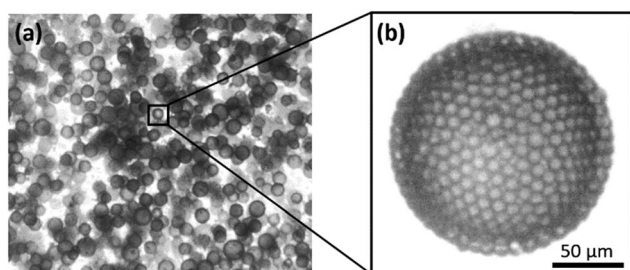


Fig. 5 (a) An optical microscopy image of a Pickering emulsion after the application of an electric field ($200\text{--}600 \text{ V mm}^{-1}$) for 30 min. The silicone oil to castor oil ratio was 1 : 10 by weight, and the PS particle (size $\sim 10 \mu\text{m}$) to silicone oil ratio was 1 : 4 by weight. The particle-covered droplets are separated from one another, *i.e.* no droplet clustering is observed. (b) The majority of the Pickering droplets have spherical or slightly aspherical shapes, and the surface particles are arranged in a jammed, nearly hexagonal structure.

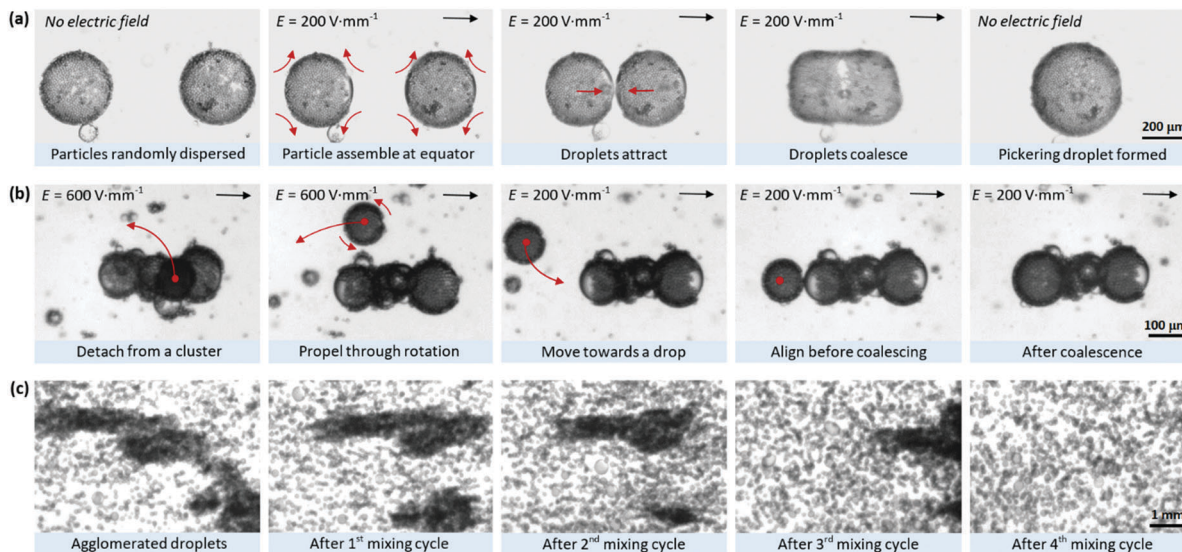


Fig. 6 (a) Droplet coalescence through EHD and ES interactions. The surface particles, initially randomly dispersed on the droplets' surfaces (with no electric field), are convected away from the droplets' electric poles by EHD flows (induced by a DC electric field of 200 V mm^{-1}). The two droplets attract one another through both the EHD and electrostatic forces. Finally, the droplets coalesce, resulting in formation of a Pickering droplet with densely packed surface particles (PS, sized $\sim 10 \text{ }\mu\text{m}$). (b) A droplet that is part of a disintegrating cluster propels away from it through electric field-induced rotation at $E = 600 \text{ V mm}^{-1}$. Lowering the electric field strength to 200 V mm^{-1} enables droplet translation (through both the EHD and electrostatic forces) towards another droplet partially covered by particles. Finally, the two droplets coalesce. (c) Breaking of droplet agglomerates through liquid shearing. An electric field of 600 V mm^{-1} was used for 15 seconds to locally (through electrorotation) and globally (through electric field-induced convective flows in an entire cell) shear the emulsion. This resulted in breaking the droplet agglomerates down to individual droplets.

a Pickering droplet with a densely packed particle shell (right-most panel in Fig. 6a).

The two droplets presented in Fig. 6a have no close neighbours, so the EHD flows are strong enough to move particles. The EHD flows are reduced on the surface of a droplet in a crowded emulsion. This is because when two (or more) droplets are “in contact” (*i.e.* separated only by a thin layer of castor oil), a dipole moment is formed on two sides of the agglomerated structure rather than on each individual droplet. For example, if three droplets are in contact and aligned along the electric field direction, there will be no (or significantly reduced) flow around the middle droplet. In addition, in crowded emulsions, droplets are very densely populated, their locations are constrained, and their motions are significantly impeded, as is the motion of the dispersing phase. Thus, reducing the concentration of the dispersed phase prevents such a situation. We experimentally observed that emulsions with silicone oil concentrations below 30% are preferable. Droplets can be locally crowded even in low-concentration emulsions. In addition, they can be bridged by particles, and form large agglomerations. To tackle these problems, we simply increased the electric field strength (typically to 600 V mm^{-1}) for several seconds to shear the liquid. In such strong electric fields, Quincke electrorotation of individual droplets and small aggregated structures can be induced. Electrorotating objects shear the emulsion locally, which helps to damage particle bridges between droplets and re-position droplets. The subsequent application of a low-intensity electric field (*e.g.* 200 V mm^{-1}) leads to dipolar alignment and coalescence of droplets that before were either misaligned or particle bridged.

In Fig. 6b we show a possible route for droplet disintegration from a cluster to allow merging with another available droplet. A droplet, partially covered with particles, is initially attached to a small droplet cluster. Application of a high electric field of 600 V mm^{-1} causes the droplet to disintegrate from the cluster and propel away through electrorotation. The droplet stops rotating after we lower the electric field to 200 V mm^{-1} . Then, the attractive dipolar forces and EHD flows bring the droplet towards another droplet available for coalescence. After a short time, two droplets coalesce (see also Movie S2, ESI†). In Fig. 6c, we demonstrate breaking of large droplet agglomerates through liquid shearing. In each “mixing” cycle we used a DC electric field of 600 V mm^{-1} for 15 seconds to locally (through electrorotation) and globally (through electric field-induced convective flows in an entire cell) shear the emulsion. This resulted in breaking the droplet agglomerates down to individual droplets, and eventually led to formation of a stable Pickering emulsion (see also Movie S3, ESI†).

3.3. Size of Pickering droplets

The following formula can be helpful when designing a Pickering emulsion with specific droplet sizes (for the formula derivation see ESI†; also see ref. 60 and 61).

$$r_d = 3.6 \frac{\rho_p \cdot m_d}{\rho_d \cdot m_p} \cdot r_p \quad (1)$$

r_d , m_d , ρ_d – radius, mass and density of a desired Pickering droplet. r_p , m_p , ρ_p – radius, mass and density of particles covering the droplet.

In this formula, we assume that the surface particles are spherical and densely packed within the monolayered particle shell (particle coverage 0.9), and that the three-phase contact angle is 90° . In order to fully cover either $80\ \mu\text{m}$, $160\ \mu\text{m}$ or $240\ \mu\text{m}$ size silicone oil droplets with $10\ \mu\text{m}$ size PS particles, we calculated (assuming that $\rho_p/\rho_d = 1$) the particle to silicone oil ratios to be 1:2, 1:4, and 1:8, respectively. We then designed an experiment to verify whether the Pickering droplet size can be tuned by choosing an adequate particle concentration.

In Fig. 7a we present optical microscope images of Pickering emulsions at different particle to silicone oil mass ratios, namely 1:2, 1:4, and 1:8. The emulsions were formed by applying a DC electric field ($200\text{--}600\ \text{V}\ \text{mm}^{-1}$) for 30 minutes. The silicone oil to castor oil ratio was 1:10 by weight.

We visually inspected the three emulsions and found that the majority ($>90\%$) of droplets were densely covered by particles and were spherical or slightly aspherical. As in the previous experiment presented in Fig. 4d and 5, we found several oval-shaped droplets, and some droplets partially covered by particles. To quantitatively present the distribution of droplet size, we measured 200 droplets in each emulsion using an optical microscope and plotted diameter histograms, shown in Fig. 7b. The data were fitted with log-normal functions. However, as discussed in the Preparation of the pre-emulsion section, to obtain the values of both the mean diameter and the coefficient of variance of the three corresponding emulsions, we used Gaussian functions (not plotted here). For the Pickering emulsions with particle to silicone oil mass ratios 1:2, 1:4, and 1:8, the mean diameters are $78\ \mu\text{m}$, $154\ \mu\text{m}$, and $263\ \mu\text{m}$, respectively. These values are consistent with the theoretical values calculated above.

The homogeniser-prepared emulsions typically comprise droplets with different particle concentrations (because of the stochastic nature of the process of homogenisation). Also, using other methods of preparation leads to this result; for example, in microfluidic systems, the particle concentration is found to be Poisson distributed.⁶² For this reason, the droplets fully covered by particles (formed through a stochastic process of electrocoalescence) in the stable Pickering emulsion are polydispersed in size. As presented in the histogram in Fig. 7b, the initial emulsion also contains droplets of different sizes. However, as long as the particle concentration in each droplet is the same, differences in drop sizes should not affect

the size polydispersity of the Pickering droplets. To fabricate a Pickering emulsion with monodispersed Pickering droplets, it is therefore essential to prepare an initial emulsion with droplets of identical particle concentration. Unfortunately, this is practically very challenging. For this reason, the size distribution function of Pickering droplets in our experiments has a finite width. The CV values (and σ) are 20.5%, 18.2%, and 17.5% (and 16, 28, and $46\ \mu\text{m}$), for the Pickering emulsions with particle to silicone oil mass ratios 1:2, 1:4, and 1:8, respectively. These are relatively low CV values compared with other bulk emulsification methods (we will elaborate on that in the next section) and are more than three times lower than the CV values of the initial emulsion.

4 Discussion and conclusions

In this paper, we present an approach to efficient fabrication of oil-in-oil Pickering emulsions by employing electric fields. The route is straightforward, robust, and can be used to produce Pickering droplets with narrow size distributions that are lower than those achieved typically by bulk methods such as ultrasonic or mechanical homogenisation,^{19,63} and comparable to membrane emulsification methods.^{64,65} There exist methods for producing Pickering droplets with narrower droplet size distributions than those presented here. However, in those methods Pickering emulsions are typically formed *via* more complex processes, and/or require preparation of pre-emulsions with very narrow size distributions of droplets, and/or are very time consuming.^{66,67} For example micrometer-sized Pickering droplets produced with the use of a microfluidic device by Subramaniam *et al.*⁶⁷ were of a similar size (CV below 10%), but were produced with a frequency of $\sim 0.2\ \text{Hz}$. To produce a few hundreds of mL would require several years.

The limited coalescence approach utilized in this work was used by other researchers for fabrication of Pickering droplets (also in very concentrated emulsions),^{68–72} and it allowed them to design Pickering emulsions with desirable average droplet sizes. As in the other research contributions, in this work, we also observed that the average droplet diameter was inversely proportional to the number of solid particles. Interestingly, the CV values of the Pickering emulsions were at least two times

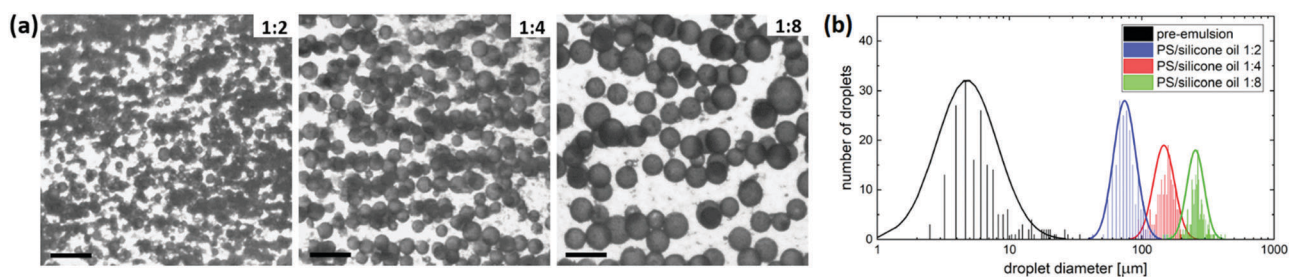


Fig. 7 (a) Optical microscope images of Pickering emulsions at different particle to silicone oil mass ratios by weight (1:2, 1:4, 1:8), and (b) the corresponding histograms with size distributions. The Pickering droplet populations have log-normal distributions. The silicone oil to castor oil ratio was 1:10 by weight. An electric field ($200\text{--}600\ \text{V}\ \text{mm}^{-1}$) was applied for 30 minutes. In all the experiments, the sample cell was maintained at $\sim 50\ ^\circ\text{C}$. All images were captured at the same microscope magnification, and the scale bars are $500\ \mu\text{m}$.

lower than those of the initial emulsion. At this point, we cannot provide any explicit information on the narrow droplet size distributions. We observed that the values of the CV decreased as the limited coalescence progressed. Zou *et al.*⁷³ studied the evolution of the droplet size distribution during coalescence induced by mechanical shearing. They found that a bimodal size distribution of the initial emulsion disappeared during the early stage of the coalescence leading to narrower droplet size distribution, and that in all the performed experiments the final distribution of the Pickering droplets was Gaussian, as is the case in our work.

As was demonstrated here, a sensible usage of electric fields (*e.g.* alternating the electric field strength) led to formation of Pickering droplets that were well dispersed in the continuous phase (not agglomerated), and the droplets' shells were composed of densely packed particles. We produced Pickering droplets using various materials, and the method enabled formation of Pickering droplets in a wide range of sizes without needing any modification of the experimental set-up, as is the case for microfluidic or membrane emulsification approaches, where microfluidic chips or membranes have to be redesigned. Any type of microparticle material can be used provided that the particles bind strongly to the droplets' interfaces and that their electrical conductivity values are approximately the same order of magnitude or smaller than those of the liquids. In our experiments we used polystyrene, polyethylene, and silica particles (see Fig. S2, ESI[†]). A subtle point is that if oils and particles are chosen so that there is a large density difference between oils or between oils and particles, the dispersed phase may sediment. However, this problem can be tackled, for example, by introducing convective flows from the bottom of the sample cell.

One of the strategies for producing Pickering emulsions involves adsorption of particles initially located in the dispersing phase, after droplet formation. In such a scheme, to form a Pickering emulsion quickly, the particle concentration in the dispersing phase has to be much greater than theoretically required for the formation of stable Pickering droplets. In many studies, the utilization of particles was inefficient, *e.g.* most particles (even up to $\sim 90\%$) did not contribute to the formation of Pickering droplets but instead resided in the continuous phase.^{21,68} Unless desired (*e.g.* sometimes excess solid particles are used for emulsion thickening),⁷⁴ this is not very beneficial economically. In this respect, our method is superior. It allows for very efficient consumption of particles, *i.e.* most of them, if not all, can be utilised for Pickering droplet fabrication.

In our studies, we used silicone oil as a dispersed phase and castor oil as the continuous phase. We also tested the reverse configuration. However, when the system was reversed (*i.e.* castor oil droplets were formed in silicone oil) and subjected to electric fields, the castor oil droplets stretched, and the EHD flows went from the droplets' electric equators towards their electric poles. Covering the droplets' poles impeded their coalescence. In addition, we faced some technical difficulties, *i.e.* castor oil droplets wetted both the walls of a sample cell and the electrodes. Generally, the castor oil in silicone oil Pickering

emulsion can be fabricated. For a review of the stabilisation of silicone-in-vegetable oils and vegetable-in-silicone oils emulsions, we refer the reader to the article by Binks and Tyowua.⁷⁵

The method presented here can be further optimised by adequately choosing the parameters: the electric field strength, the periods at which the electric field is at higher or lower voltage, or the electric field frequency. Here are two examples: (i) we observed that at electric field strengths higher than 600 V mm^{-1} , it takes less time to break large aggregates down. However, strong electric fields should be avoided when Pickering emulsions with large Pickering droplets are of concern. This is because large droplets may easily break up in high electric fields, reversing the coalescence and slowing down the Pickering emulsion fabrication; and (ii) when particles with small permanent charges are to be used for Pickering droplets, it is helpful to change the electric field polarity from time to time to avoid droplet electrophoretic migration towards one of the electrodes. We also note that reducing the viscosity of oils, particularly the dispersing liquid (*e.g.* by replacing castor oil with corn oil, or by increasing the temperature), speeds up the formation of a Pickering emulsion. One final note on the fabrication process is that the EHD convective organization of particles at droplets' interfaces not only promotes coalescence but also ensures that particles in the shell are well packed.

We foresee that this convenient and easily scalable route for fabricating Pickering emulsions will facilitate a foundation for many applications in which Pickering droplets with narrow size distribution need to be produced in large quantities. We also expect many derivative methods to be developed soon. It would be interesting to follow the dynamics of Pickering emulsion formation. In our ongoing research we employ non-invasive ultrasonic methods and optical microscopy, and the preliminary data indicate that ultrasound can be easily and cheaply used to monitor Pickering emulsion development.

Author contributions

Z. R. initiated the project and designed all of the experiments. R. B. and Z. R. performed all experiments, and contributed to data analysis and presentation. Z. R. wrote the first version of the manuscript. All authors took part in discussions towards the finalization of the manuscript.

Conflicts of interest

There are no conflicts of interest to declare.

Acknowledgements

Z. R. acknowledges financial support of the Polish National Science Centre through OPUS programme (grant number 2015/19/B/ST3/03055). R. B. and A. J. were supported by Polish National Science Centre through OPUS programme (2015/17/B/ST7/03566). The authors wish to thank Marta Obrepalska for experimental help during the initial phase of the project.

We wish to thank Dr A. Magdziarz, the owner of the company CADENAS in Poland, for research suggestions, for her constructive feedback and assistance in collecting data.

References

- M. H. Asfour, H. Elmotasem, D. M. Mostafa and A. A. A. Salama, *Int. J. Pharm.*, 2017, **534**, 325–338.
- E. Dickinson, *Curr. Opin. Colloid Interface Sci.*, 2010, **15**, 40–49.
- B. Peng, L. Zhang, J. Luo, P. Wang, B. Ding, M. Zeng and Z. Cheng, *RSC Adv.*, 2017, **7**, 32246–32254.
- S. Drexler, J. Faria, M. P. Ruiz, J. H. Harwell and D. E. Resasco, *Energy Fuels*, 2012, **26**, 2231–2241.
- Z. Rozynek and A. Józefczak, *Eur. Phys. J.: Spec. Top.*, 2016, **225**, 741–756.
- T. Bollhorst, K. Rezwan and M. Maas, *Chem. Soc. Rev.*, 2017, **46**, 2091–2126.
- V. O. Ikem, A. Menner, T. S. Horozov and A. Bismarck, *Adv. Mater.*, 2010, **22**, 3588–3592.
- F. Sicard and A. Striolo, *Nanoscale*, 2017, **9**, 8567–8572.
- A. Mikkelsen, P. Dommersnes, Z. Rozynek, A. Gholamipour-Shirazi, M. d. S. Carvalho and J. O. Fossum, *Materials*, 2017, **10**, 436.
- P. Dommersnes, A. Mikkelsen and J. O. Fossum, *Eur. Phys. J.: Spec. Top.*, 2016, **225**, 699–706.
- J. Marto, A. Ascenso, S. Simoes, A. J. Almeida and H. M. Ribeiro, *Expert Opin. Drug Delivery*, 2016, **13**, 1093–1107.
- T. Cserhati, E. Forgacs and G. Oros, *Environ. Int.*, 2002, **28**, 337–348.
- B. Duncan, R. F. Landis, H. A. Jerri, V. Normand, D. Benczédi, L. Ouali and V. M. Rotello, *Small*, 2015, **11**, 1302–1309.
- K. Yamanaka, S. Nishino, K. Naoe and M. Imai, *Colloids Surf., A*, 2013, **436**, 18–25.
- J. Frelichowska, M.-A. Bolzinger and Y. Chevalier, *J. Colloid Interface Sci.*, 2010, **351**, 348–356.
- S. Melle, M. Lask and G. G. Fuller, *Langmuir*, 2005, **21**, 2158–2162.
- B. P. Binks and D. Yin, *Soft Matter*, 2016, **12**, 6858–6867.
- C. Wen, Q. Yuan, H. Liang and F. Vriesekoop, *Carbohydr. Polym.*, 2014, **112**, 695–700.
- A. Kaiser, T. Liu, W. Richtering and A. M. Schmidt, *Langmuir*, 2009, **25**, 7335–7341.
- Q. Y. Xu, M. Nakajima and B. P. Binks, *Colloids Surf., A*, 2005, **262**, 94–100.
- K. L. Thompson, S. P. Armes and D. W. York, *Langmuir*, 2011, **27**, 2357–2363.
- C. Priest, M. D. Reid and C. P. Whitby, *J. Colloid Interface Sci.*, 2011, **363**, 301–306.
- D. J. French, A. T. Brown, A. B. Schofield, J. Fowler, P. Taylor and P. S. Clegg, *Sci. Rep.*, 2016, **6**, 31401.
- D. J. French, P. Taylor, J. Fowler and P. S. Clegg, *J. Colloid Interface Sci.*, 2015, **441**, 30–38.
- A. Jaworek, *J. Microencapsulation*, 2008, **25**, 443–468.
- R. B. Karyappa, A. V. Naik and R. M. Thaokar, *Langmuir*, 2016, **32**, 46–54.
- W. D. Ristenpart, J. C. Bird, A. Belmonte, F. Dollar and H. A. Stone, *Nature*, 2009, **461**, 377–380.
- W. T. Kwon, K. Park, S. D. Han, S. M. Yoon, J. Y. Kim, W. Bae and Y. W. Rhee, *J. Ind. Eng. Chem.*, 2010, **16**, 684–687.
- K. Hwang, P. Singh and N. Aubry, *Electrophoresis*, 2010, **31**, 850–859.
- B. Neirinck, J. Fransaer, O. Van der Biest and J. Vleugels, *Adv. Eng. Mater.*, 2007, **9**, 57–59.
- G. Chen, P. Tan, S. Chen, J. Huang, W. Wen and L. Xu, *Phys. Rev. Lett.*, 2013, **110**, 064502.
- A. B. Pawar, M. Caggioni, R. Ergun, R. W. Hartel and P. T. Spicer, *Soft Matter*, 2011, **7**, 7710–7716.
- R. B. Karyappa, S. D. Deshmukh and R. M. Thaokar, *Phys. Fluids*, 2014, **26**, 122108.
- M. Ouriemi and P. M. Vlahovska, *J. Fluid Mech.*, 2014, **751**, 106–120.
- E. G. Kim, K. Stratford, P. S. Clegg and M. E. Cates, *Phys. Rev. E: Stat., Nonlinear, Soft Matter Phys.*, 2012, **85**, 020403.
- M. Ouriemi and P. M. Vlahovska, *Langmuir*, 2015, **31**, 6298–6305.
- A. Mikkelsen, P. Dommersnes and J. O. Fossum, *Rev. Cubana Fis.*, 2016, **33**, 47–49.
- M. M. Cui, T. Emrick and T. P. Russell, *Science*, 2013, **342**, 460–463.
- Z. Rozynek, R. Castberg, A. Kalicka, P. Jankowski and P. Garstecki, *Arch. Mech.*, 2015, **67**, 385–399.
- Z. Rozynek, A. Mikkelsen, P. Dommersnes and J. O. Fossum, *Nat. Commun.*, 2014, **5**, 3945.
- D. S. Martula, R. T. Bonnecaze and D. R. Lloyd, *Int. J. Multiphase Flow*, 2003, **29**, 1265–1282.
- D. A. Beysens, *Phys. A*, 1997, **239**, 329–339.
- H. Tanaka, *Phys. Rev. Lett.*, 1994, **72**, 1702–1705.
- B. Deminiere, A. Colin, F. L. Calderon and J. Bibette, in *Modern Aspects of Emulsion Science*, The Royal Society of Chemistry, 1998, pp. 261–291, DOI: 10.1039/9781847551474-00261.
- A. I. Abubakar and J. O. Bello, *Sep. Sci. Technol.*, 1991, **26**, 1329–1340.
- T. J. Williams and A. G. Bailey, *IEEE Trans. Ind. Appl.*, 1986, **IA-22**, 536–541.
- S. E. Taylor, *Colloids Surf.*, 1988, **29**, 29–51.
- C. D. Gatti, C. A. Hall and R. L. Halm, EP0841362B1, 2003.
- J. C. Baygents, N. J. Rivette and H. A. Stone, *J. Fluid Mech.*, 1998, **368**, 359–375.
- V. Vivacqua, S. Mhatre, M. Ghadiri, A. M. Abdullah, A. Hassanpour, M. J. Al-Marri, B. Azzopardi, B. Hewakandamby and B. Kermani, *Chem. Eng. Res. Des.*, 2015, **104**, 658–668.
- H. Fan and A. Striolo, *Soft Matter*, 2012, **8**, 9533–9538.
- K. Aida, Y. H. Na, T. Nagaya and H. Orihara, *Phys. Rev. E: Stat., Nonlinear, Soft Matter Phys.*, 2010, **82**, 031805.
- Y. Lin, P. Skjetne and A. Carlson, *Int. J. Multiphase Flow*, 2012, **45**, 1–11.
- G. Chen, P. Tan, S. Y. Chen, J. P. Huang, W. J. Wen and L. Xu, *Phys. Rev. Lett.*, 2013, **110**, 064502.
- Z. Liu, X. Fu, B. P. Binks and H. C. Shum, *Soft Matter*, 2017, **13**, 119–124.
- P. F. Salipante and P. M. Vlahovska, *Phys. Fluids*, 2010, **22**, 112110.

- 57 D. Das and D. Saintillan, *J. Fluid Mech.*, 2017, **829**, 127–152.
- 58 Z. Rozynek, M. Kaczmarek-Klinowska and A. Magdziarz, *Materials*, 2016, **9**, 679.
- 59 T. J. Mason, J. P. Lorimer and D. M. Bates, *Ultrasonics*, 1992, **30**, 40–42.
- 60 M. Destribats, S. Gineste, E. Laurichesse, H. Tanner, F. Leal-Calderon, V. Heroguez and V. Schmitt, *Langmuir*, 2014, **30**, 9313–9326.
- 61 R. M. Wiley, *J. Colloid Sci.*, 1954, **9**, 427–437.
- 62 C. H. Chen, D. A. Saville and I. A. Aksay, *Appl. Phys. Lett.*, 2006, **88**, 154104.
- 63 G. Zhang and C. Wang, *Materials*, 2016, **9**, 572.
- 64 M. S. Manga and D. W. York, *Langmuir*, 2017, **33**, 9050–9056.
- 65 Q. Yuan, O. J. Cayre, M. Manga, R. A. Williams and S. Biggs, *Soft Matter*, 2010, **6**, 1580–1588.
- 66 J. Giermanska-Kahn, V. Schmitt, B. P. Binks and F. Leal-Calderon, *Langmuir*, 2002, **18**, 2515–2518.
- 67 A. B. Subramaniam, M. Abkarian and H. A. Stone, *Nat. Mater.*, 2005, **4**, 553–556.
- 68 S. Arditty, C. P. Whitby, B. P. Binks, V. Schmitt and F. Leal-Calderon, *Eur. Phys. J. E: Soft Matter Biol. Phys.*, 2003, **11**, 273–281.
- 69 C. P. Whitby, L. Lotte and C. Lang, *Soft Matter*, 2012, **8**, 7784–7789.
- 70 J. W. J. de Folter, E. M. Hutter, S. I. R. Castillo, K. E. Klop, A. P. Philipse and W. K. Kegel, *Langmuir*, 2014, **30**, 955–964.
- 71 M. Destribats, M. Rouvet, C. Gehin-Delval, C. Schmitt and B. P. Binks, *Soft Matter*, 2014, **10**, 6941–6954.
- 72 B. P. Binks and C. P. Whitby, *Langmuir*, 2004, **20**, 1130–1137.
- 73 Z. Zou, Z. Sun and L. An, *Chin. J. Polym. Sci.*, 2014, **32**, 255–267.
- 74 S. Abend and G. Lagaly, *Clay Miner.*, 2001, **36**, 557–570.
- 75 B. P. Binks and A. T. Tyowua, *Soft Matter*, 2016, **12**, 876–887.
- 76 A. Mikkelsen, K. Khobaib, F. K. Eriksen, K. J. Måløy and Z. Rozynek, *Soft Matter*, 2018, DOI: 10.1039/c8sm00915e.

Electronic Supplementary Material for

Efficient formation of oil-in-oil Pickering emulsions with narrow size distributions by using electric fields

Z. Rozynek,^{†*} R. Bielas,[†] A. Józefczak

Institute of Acoustics, Faculty of Physics, Adam Mickiewicz University, Poznań, Poland

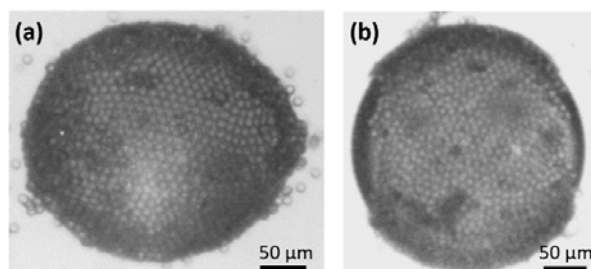


Fig. S1 Optical microscopy images of silicone oil droplets with PS particles (size of $\sim 10 \mu\text{m}$), formed in castor oil. **(a)** Droplets with an oval shape can be typically found at the end of the Pickering emulsion fabrication, as the arrested coalescence occasionally occurs. **(b)** An example of a partially particle-covered droplet. Several such droplets were identified in the image at the end of the Pickering emulsion fabrication described in **Fig. 4d**.

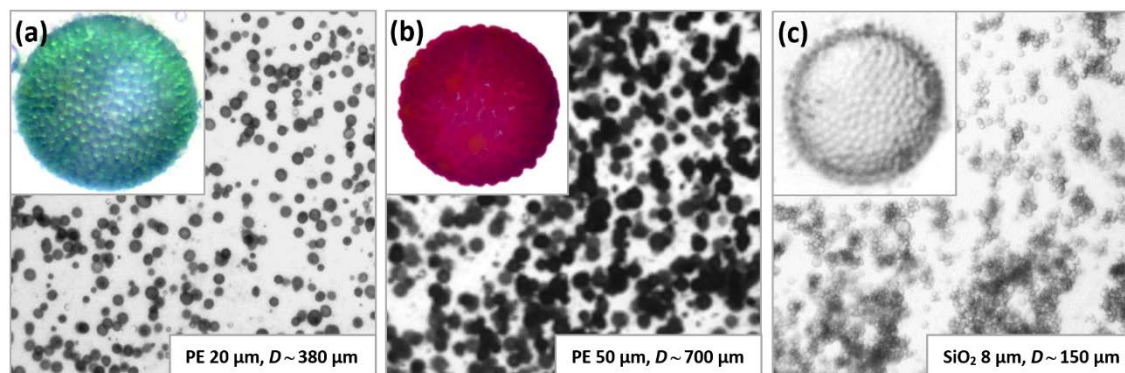


Fig. S2 Optical microscopy images of a Pickering emulsion after the application of an electric field ($200 \leftrightarrow 600 \text{ V/mm}$) for 10 min. The silicone oil to castor oil ratio was **(a)** 1:20 **(b)** 1:5, and **(c)** 1:10 by weight, and the following particles were used: **(a)** polyethylene (PE, sized $\sim 20 \mu\text{m}$), **(b)** polyethylene (PE, sized $\sim 50 \mu\text{m}$), and **(c)** silica (SiO₂, sized $\sim 8 \mu\text{m}$). The particle-covered droplets are separated from one another, i.e. no droplet clustering is observed when PE particles are used. Droplets with silica particles tend to agglomerate. This is because the three-phase contact angle is greater than that in the case of PE particles—compare the enlarged images.

Behaviour of silicone oil droplet in electric fields:

When a silicone oil droplet formed in castor oil is subjected to a DC (or slowly changing AC) electric field, free charges (ionic impurities) in the oils accumulate at the drop interface, inducing a dipole moment. Because the electrical conductivity and dielectric constant of a silicone oil droplet are smaller than those of the surrounding castor oil, the droplet's dipole moment is in the opposite direction of the electric field. The action of the applied electric field on the free charges at the silicone oil droplet yields electric stresses that deform such droplet to obtain an oblate geometry. More specifically, at the electric poles of the drop (surface areas closest to the electrodes), electric stress has only a normal component that is balanced by capillary forces and the pressure difference across the drop interface. There are no free charges at the electric equator of the droplet, and thus there is no electric stress at this area of the droplet. Everywhere else at the droplet interface, electric stress has two components: normal and tangential to that interface. As a result of normal electric stress, the droplet is compressed along the electric field direction, obtaining (within a second) an oblate shape. Tangential electric stress induces electrohydrodynamic (EHD) flows at the droplet interface that shear the liquids inside and outside the droplet. In general, the direction of these EHD flows depends on the free charge distribution at the drop interface. In the case of a silicone oil drop suspended in castor oil, the EHD flows at the drop surface are directed from the drop poles to the drop equator (for more details, see¹). As long as the electric field strength is weak (typically $< 200 \text{ V mm}^{-1}$), the induced EHD liquid flows can be used to convect and eventually assemble surface particles, as we discuss later in this section. At strong DC electric fields, weakly-conductive drops may undergo electrorotation²⁻⁴ or break apart.⁵ The accumulation of free charges at the interface of a drop requires finite time. For the drop system studied here, the time for free charges to build up at the drop interface (the Maxwell-Wagner relaxation time)¹ was $\sim 1 \text{ s}$. Therefore, when applying alternating current (AC) electric fields with sufficiently high frequencies (above 1 Hz), the electric field changes direction so quickly preventing free charges accumulation at the drop interface.

Calculation of Pickering droplet size (also see ⁶⁻⁸):

We wish to calculate the concentration of particles measured by mass (m %) that needs to be used to occupy entire surface of a droplet of a specific radius.

$$\frac{m_p}{m_d} = \frac{\rho_p \cdot V_p \cdot N_p}{\rho_d \cdot V_d \cdot N_d}, \text{ here } N_d = 1 \text{ thus } \frac{m_p}{m_d} = \frac{\rho_p \cdot r_p^3}{\rho_d \cdot r_d^3} N_p \quad (1)$$

We need to find number of particles, N_p .

The area of a droplet with radius r_d is: $A_D = 4 \cdot \pi \cdot r_d^2$ and should be equal to the area occupied by N_p circles (projection of spherical particles with radius r_p on a two-dimensional surface of a droplet) divided by the packing density factor ϕ .

$$A_D = N_p \cdot \pi \cdot r_p^2 \cdot \frac{1}{\phi} \quad (2)$$

Packing density of circles on a sphere is generally a function of number of the circles. For an infinite number of circles, the packing density approaches 0.906, *i.e.*, achieve the same optimal packing density as for circles forming hexagonal pattern on a 2D plane. Since we assume here that $R_d \gg r_p$, the packing density ϕ can be assigned as approximately 0.9.

Thus

$$N_p = \frac{4 \cdot r_d^2}{r_p^2} \phi \quad (3)$$

and

$$\frac{m_p}{m_d} = \frac{\rho_p \cdot r_p^3 \cdot 4 \cdot r_d^2}{\rho_d \cdot r_d^3 \cdot r_p^2} \phi = 4 \cdot \phi \frac{\rho_p \cdot r_p}{\rho_d \cdot r_d} \quad (4)$$

Finally

$$r_d = 3.6 \frac{\rho_p \cdot m_d}{\rho_d \cdot m_p} \cdot r_p \quad (5)$$

For example, $r_d = 400 \text{ }\mu\text{m}$ if $\frac{m_p}{m_d} [\%] = 12 \%$, $\rho_p = 0.3 \text{ g/cm}^3$; $\rho_d = 0.9 \text{ g/cm}^3$; $r_p = 40 \text{ }\mu\text{m}$;

1. G. Taylor, *Proc. R. Soc. Lond. A*, 1966, **291**, 159-166.
2. P. F. Salipante and P. M. Vlahovska, *Phys. Fluids*, 2010, **22**, 112110.
3. D. Das and D. Saintillan, *J. Fluid Mech.*, 2017, **829**, 127-152.
4. P. Dommersnes, A. Mikkelsen and J. O. Fossum, *Eur. Phys. J.-Spec. Top.*, 2016, **225**, 699-706.
5. Rahul B. Karyappa, Shivraj D. Deshmukh and Rochish M. Thakkar, *J. Fluid Mech.*, 2014, **754**, 550-589.
6. M. Destribats, S. Gineste, E. Laurichesse, H. Tanner, F. Leal-Calderon, V. Heroguez and V. Schmitt, *Langmuir*, 2014, **30**, 9313-9326.
7. R. M. Wiley, *Journal of Colloid Science*, 1954, **9**, 427-437.
8. M. Destribats, M. Rouvet, C. Gehin-Delval, C. Schmitt and B. P. Binks, *Soft Matter*, 2014, **10**, 6941-6954.



Cite this: *Soft Matter*, 2019, 15, 1692

DOI: 10.1039/c9sm90016k

rsc.li/soft-matter-journal

Correction: Efficient formation of oil-in-oil Pickering emulsions with narrow size distributions by using electric fields

Z. Rozynek, * R. Bielas  and A. Józefczak 

Correction for 'Efficient formation of oil-in-oil Pickering emulsions with narrow size distributions by using electric fields' by Z. Rozynek *et al.*, *Soft Matter*, 2018, **14**, 5140–5149.

In this paper, in the first paragraph on page 7, the sentence “In order to fully cover either 80 μm , 160 μm or 240 μm size silicone oil droplets with 10 μm size PS particles, we calculated (assuming that $\rho_p/\rho_d = 1$) the particle to silicone oil ratios to be 1 : 2, 1 : 4 and 1 : 8 respectively” is incorrect. This sentence should instead read “In order to fully cover either 80 μm , 160 μm or 320 μm size silicone oil droplets with 10 μm size PS particles, we calculated (assuming that $\rho_p/\rho_d = 1.1$) the particle to silicone oil ratios to be 1 : 2, 1 : 4 and 1 : 8 respectively.”

The Royal Society of Chemistry apologises for these errors and any consequent inconvenience to authors and readers.



[Publication II]

Ultrasound control of oil-in-oil Pickering emulsion preparation
process

R. Bielas, Z. Rozynek, T. Hornowski, A. Józefczak

Journal of Physics D: Applied Physics, 2020, 53(8): 085301.

Ultrasound control of oil-in-oil Pickering emulsions preparation

Rafał Bielas¹, Zbigniew Rozynek¹, Tomasz Hornowski¹
and Arkadiusz Józefczak¹

Institute of Acoustics, Faculty of Physics, Adam Mickiewicz University in Poznań, Uniwersytetu
Poznańskiego 2, 61-614 Poznań, Poland

E-mail: aras@amu.edu.pl

Received 16 April 2019, revised 12 November 2019

Accepted for publication 18 November 2019


Published 12 December 2019



Abstract

Particle-stabilised emulsions are of interest to many scientists in both academia and industry as they hold promise for numerous applications. There is a lot of research effort put into developing new methods for their fabrication. Often, different experimental techniques are used for monitoring the process of the emulsion formation. However, the control of the emulsion fabrication and its real-time characterisation is generally challenging. In this work, we propose a convenient method to control fabrication of Pickering emulsions using ultrasound. The benefit of acoustical measurements compared to other techniques is their ability to test the medium in a non-destructive way, without requiring special sample preparation (e.g. dilution like in the case of DLS or NMR) nor a usage of thin sample cells (e.g. in the case of optical microscopy). Here, ultrasonic measurements are able to follow droplets growth during the emulsion development using the limited coalescence approach. We found that ultrasonic attenuation increased with the droplet size within the time frame of droplet stabilisation. Following these changes in ultrasonic attenuation enabled the study of macroscopic behaviour—for example, estimation of a time when droplets achieve their final size and become fully covered by solid particles. These results are compared with the results obtained from the optical measurements. We also make an attempt to theoretically describe ultrasound propagation in particle-stabilised emulsions by comparing our experimental results with the scattering theory ECAH for emulsions.

Keywords: Pickering emulsions, particle-stabilized emulsions, ultrasonic attenuation, limited coalescence, electric field, ultrasound

 Supplementary material for this article is available [online](#)

(Some figures may appear in colour only in the online journal)

1. Introduction

Pickering emulsion, an emulsion stabilised by solid particles accumulated at the surface of droplets, has been extensively studied over the last decades. This is because such emulsions have generated and hold promise for many practical applications [1–7]. Much of the research on Pickering emulsions concerns describing the mechanisms involved in their stabilisation, the effects of the characteristics of particles on

their physicochemical properties, and developing methods for Pickering emulsion characterisation and fabrication [8–10]. This research contributes to the area of emulsion formation, which is here achieved by electro-coalescing emulsion droplets while simultaneously controlling the emulsion maturing using ultrasound.

There are many different routes for the fabrication of Pickering emulsions [11–17]. Yet, scientists are constantly developing new methods for more efficient formation of such emulsions. Recently, we proposed a new bulk approach, in which we used electric fields to quickly form stable oil-in-oil

¹ Author to whom any correspondence should be addressed.

emulsions with narrow-size distribution of particle-covered droplets [18]. We presented qualitatively the development of Pickering emulsions through optical microscopy imaging. The optical microscopy technique was convenient when we used thin sample cells (i.e. with a short optical path). However, when we used thicker cuvettes (e.g. for yielding higher production rates of Pickering emulsions), a large number of scattering objects in the light path prevented meaningful optical observations, and we struggled with monitoring the fabrication process. When searching for a solution, we realised that the monitoring of emulsion preparation, for example, by detecting changes in droplet size, is generally challenging, and the development of a simple and cheap technique that would enable in-situ and real-time sampling of emulsions is vital.

Besides the conventional optical microscopy, different techniques and tools have been used for emulsion droplet sizing, such as small-angle x-rays or neutron scattering (SAXS/SANS) [19–23], nuclear magnetic resonance (NMR) [24–28], a Coulter counter [29–31], a particle video microscope (PVM) [32–34], focused beam reflectance measurement (FBRM) [35, 36], and dynamic light scattering (DLS) [37–40]. Yet, each of the methods has one or (commonly) more of the following disadvantages: it is costly, time-consuming, slow, requires specific sample preparation before measurements (e.g. diluting droplet concentrations below 1%), requires usage of a specifically designed sample cell, is not readily available, or is unsuitable for sampling different kinds of emulsions. In addition, it is advantageous that the technique for observing the growth of Pickering emulsion does not impose any adaptation of sample cells, allows non-invasive sample measurements (e.g. no measuring probes should be placed inside measured samples), and is easy to adopt and operate.

Ultrasound-based methods can be considered here, as these are robust and easy to implement, and offer cheap and very reliable measurements. Typically, acoustic spectroscopy is employed for in-situ emulsion characterisation [41–43]. Venkataramani *et al* [44] and Tran *et al* [45] elucidated the use of acoustic spectroscopy to characterise emulsion stabilisation and destabilisation mechanisms in particle-stabilised water-in-oil emulsions. In general, acoustic spectroscopy is a powerful technique, as it provides very accurate information when experimental data are properly fitted to theoretical models. However, the commercially available spectroscopes use a variable gap method for acoustic particle/droplet sizing. Thus, collecting an acoustic spectrum usually takes several minutes. In addition, the transducers are typically immersed in liquid, which typically demands placing the sample in the special chamber to provide accurate data.

Here, we propose a route to overcome the abovementioned limitations, making it possible to easily monitor development of Pickering emulsions *in situ* with ultrasound with satisfying precision. We use two transducers placed outside the sample cell that work in a transmission mode at a single ultrasound frequency (5 MHz). Single-frequency ultrasound has been used by several groups to characterise dispersions and emulsions [46–50], but little literature exists about its use for monitoring the growth of Pickering emulsions and studies of emulsion droplet coalescence. There are many reports

presenting the use of ultrasound attenuation measurements for characterising surfactant-stabilised emulsions [51, 52]. Yet, there are very few works describing ultrasonic propagation in particle-stabilised emulsions despite a significant difference in their structure in comparison to surfactant-stabilised emulsions. The research results presented here aim to fill out the knowledge gap in this research area.

In our work, ultrasound exhibits a dual role. High-energy acoustic waves are used to form pre-emulsion in the process of ultrasonic homogenisation. Low-energy ultrasound is convenient for following the evolution of emulsion systems under electric fields. During the formation, changes in ultrasonic attenuation are measured and correlated with the average size of the coalescing emulsion droplets. The emulsion is also examined visually by optical microscopy. Similar optical observations were performed in our previous research [18], where the emphasis was placed on revealing physical mechanisms that led to emulsion stabilisation in the electric field for the limited coalescence regime.

2. Materials and methods

2.1. Materials

Oil-in-oil Pickering emulsions were prepared using silicone oil (Rhodorsil oils 47 V 50) for the dispersed phase, castor oil (MERLIN, MA-220-1) for the continuous phase, and polystyrene (PS) particles (Dynoseeds, TS10 6317, Microbeads AS, Norway) with average size $\sim 10 \mu\text{m}$ as stabilisers. Polystyrene particles were surface modified using the procedure described in detail in [53]. The surface modification was done to increase particles binding energy at the silicone oil-castor oil interface so that moderate liquid shearing would not cause detachment of the interfacial particles. Because the experiments on developing Pickering emulsions were carried out at 50°C , we experimentally determined the viscosity and density values of both oils at that temperature using a Brookfield DV-II+ viscometer and Anton Paar DMA 38 density meter. We also measured the speed of sound in the castor oil and silicone oil using an OPTTEL pulse-echo system. Table 1 presents all measured values, together with other parameters provided by the manufacturers or found in the literature. These values are later used for calculating the ultrasound attenuation coefficient (see section 3.1).

2.2. Ultrasonication and electric-field-assisted formation of Pickering emulsions

Pickering emulsions were prepared according to the procedure described in [18]. Unstable pre-emulsions—systems with droplets of small size and low particle coverage—were made first; from these, we formed the final stable Pickering emulsions via consecutive electro-coalescence events. We prepared nine pre-emulsions with three different mass concentrations of silicone oil to castor oil (5%, 10% and 15%), and three different mass ratios of PS particles to silicone oil (1:2, 1:4 and 1:8). To form each pre-emulsion, we made a dispersion of PS particles in silicone oil. Subsequently, castor oil was added

Table 1. List of physical parameters of oils (at 50 °C) and the pristine PS particles (at 25 °C).

Parameter and units	Silicone oil	Castor oil	PS particles
Density ($\text{kg} \cdot \text{m}^{-3}$)	948 (measured)	925 (measured)	1043 [58]
Dynamic viscosity ($\text{Pa} \cdot \text{s}$)	0.04 (measured)	0.13 (measured)	—
Speed of sound ($\text{m} \cdot \text{s}^{-1}$)	906 (measured)	1376 (measured)	2320 [59]
Thermal conductivity ($\text{W} \cdot \text{m}^{-1} \cdot \text{K}^{-1}$)	0.15 [54]	4.73 [56]	0.1 [60]
Thermal expansion ($\times 10^{-4} \text{K}^{-1}$)	9.5 (data sheet)	7.7 [57]	0.7 [60]
Specific heat ($\text{J} \cdot \text{kg}^{-1} \cdot \text{K}^{-1}$)	1460 [55]	1800 (data sheet)	1300 [61]
Electrical conductivity ($\text{pS} \cdot \text{m}^{-1}$)	5.0 (data sheet)	60.0 (data sheet)	0.1 (data sheet)

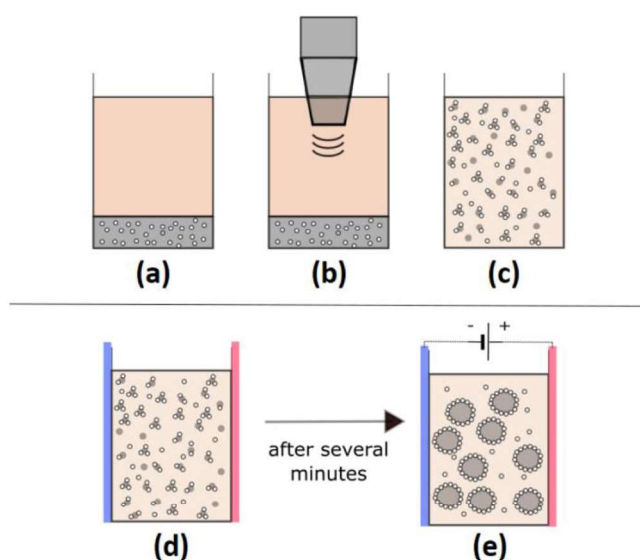


Figure 1. A schematic illustration of the fabrication of a Pickering emulsion. (a)–(c) In the first step, an initial emulsion is formed by ultrasonic homogenisation. The particle concentrations on the droplets' surfaces are too low to prevent coalescence. (d) and (e) In the second step, an electric field is used to coalesce droplets and increase coverage by particles. Typically, process of final stabilisation of Pickering emulsion takes several minutes.

to that dispersion (see figure 1(a)). Next, the substrates were mixed together using an ultrasonic homogeniser (Bandelin Sonopuls HD 3100 with KE 76 probe and a working frequency of 20 kHz) for 30 s, as illustrated in figure 1(b). Using the calorimetric method [62], we estimated the intensity of acoustic waves to be $\sim 17 \text{ W cm}^{-2}$. The homogenisation resulted in an unstable pre-emulsion with small droplets ($\sim 10 \mu\text{m}$) that were either particle-free or partially covered by particles (see figure 1(c)). Then, we applied electric fields (for 20 min) to form a Pickering emulsion (see figures 1(d) and (e)). Electric fields were used for more than enhancing coalescence; they also played an important role in surface particle manipulation and droplet rotation that further promoted the formation of stable particle-covered drops (as described in detail in our previous work [18]).

2.3. Experimental setup

Figure 2 shows a schematic illustration of the setup used for electro-coalescing droplets to form Pickering emulsions and for monitoring this process. The setup consisted of a

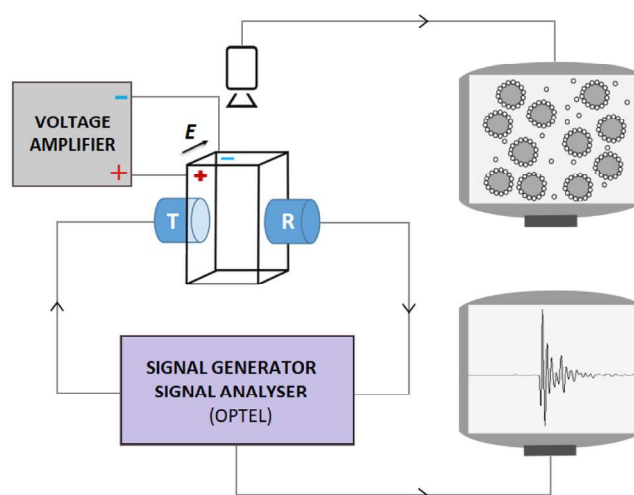


Figure 2. A scheme of experimental setup for ultrasound control of Pickering emulsion formation process. It consisted of a sample cell with two copper electrodes, a voltage amplifier for generating high-voltage signals, a digital microscope, an ultrasonic measurement system with a transmitter and a receiver, and a computer for saving and displaying optical microscopy images and data from the ultrasonic experiment.

sample cell placed on a mechanical XYZ translation stage, a signal generator (SDG1025, Siglent), a high-voltage bipolar amplifier (10HVA24-BP1, HVP), a digital microscope (AM7115MZTL, Dino-Lite) for either top or side viewings, an ultrasonic measuring system, and a computer for collecting images and recording videos. We used two sample cells with the following heights, widths and thicknesses: $30 \text{ mm} \times 18 \text{ mm} \times 1.3 \text{ mm}$ and $45 \text{ mm} \times 10 \text{ mm} \times 10 \text{ mm}$. The height and width of the cells did not affect the optical measurements. However, their thickness was important for the optical observations (see figure S1). We used the thicker sample cell in all experiments except those presented in figures 6(a) and S1(a). Two copper plate-shaped electrodes were placed inside the sample cell and connected to the voltage amplifier. In the experiment, we alternated between two electric field strengths: $200 \text{ V} \cdot \text{mm}^{-1}$ and $600 \text{ V} \cdot \text{mm}^{-1}$ were applied for 30 s and 5 s, respectively. As a result, it was possible to prevent droplet aggregation because of electrorotation occurring under higher electric field strength. It also prevented particle bridges formation, which is a common problem when Pickering emulsions are prepared. During the experiments, a temperature of $50 \text{ }^\circ\text{C} \pm 5 \text{ }^\circ\text{C}$ was kept inside the cell.

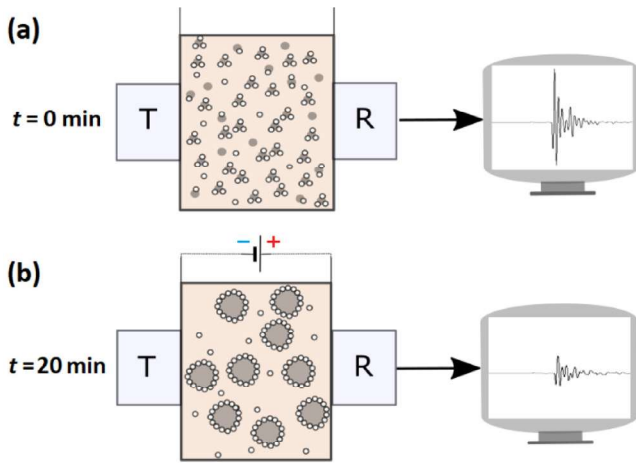


Figure 3. A scheme of the acoustic measurements. (a) Before applying an electric field, an ultrasonic wave propagates through the pre-emulsion with small energy loss. (b) During the experiment under the electric field, emulsion droplets coalesce, affecting the magnitude of the ultrasonic attenuation.

The ultrasonic measurement system consisted of two piezoelectric transducers (OPTEL, operating at a frequency of 5 MHz and a diameter of 10 mm). The unipolar spike pulse (with an amplitude of 360 V, fall time 20 ns and pulse repetition frequency 0.9 kHz) was generated by the transmitter (T) and, after travelling through the sample, was detected by the receiver (R) and recorded with the sampling frequency 100 MHz. The two transducers were driven by a pulser/receiver ultrasonic testing device (OPTEL, OPBOX 2.1) connected to PC. Amplitudes of signals possible to obtain during measurements were small enough to not affect the structure of a tested system. Because of high acoustic frequency, high viscosity of the oils and small acoustic pressure, thermal and mechanical effects of ultrasound did not occur and did not influence the studied medium.

2.4. Ultrasonic measurements

As presented in figure 2, we attached a pair of piezoelectric transducers (a transmitter and a receiver) to the walls of the sample cell through a thin layer of gel to ensure good acoustic impedance matching. We used the transmission method of measurement, i.e. an ultrasound wave was emitted by one transducer and received by another after travelling through the sample cell filled with an emulsion. Measurements were performed at different times both before and during the application of the electric field (0, 1, 2, 5, 10, 15 and 20 min). Figure 3 presents a scheme of the acoustic measurement. Before applying an electric field, an ultrasonic wave propagated through the pre-emulsion with small energy loss (figure 3(a)). When an electric field was applied, the average size of emulsion droplets increased and the shape of the pulse of the ultrasonic wave changed (see figure 3(b)). The change of the magnitude of the ultrasonic attenuation is calculated using the following expression:

$$\Delta\alpha = \frac{20}{l} \log \frac{A_t}{A_0}, \quad (1)$$

where l is the path the wave travels from the initial location to the receiver (here, it equals the width of the sample cell), A_t is the amplitude of the ultrasonic impulse measured at time t and A_0 is the amplitude of the ultrasonic pulse measured before applying the electric field.

3. Results and discussions

3.1. Theoretical analysis

For the experiments presented in the current work, ultrasound was used to monitor the variations in droplet diameters via ultrasonic attenuation coefficient. The mechanisms of sound attenuation in colloids include the viscous mechanism related to the shear dissipative waves generated by the particulate (droplet, particle or bubble) oscillating in the acoustic field; the thermal mechanism related to the heat flow between the material phases owing to the temperature gradient generated near the surface of the particulate; and the scattering mechanism, in which a part of the acoustic wave is redirected and does not reach the detector. Other mechanisms of attenuation such as absorption in pure components are treated as background. If the particulate radius R is small in comparison with wavelength λ (long wavelength limit, $kR \ll 1$, where $k = 2\pi/\lambda$ is the wavenumber), the viscous and thermal absorption mechanisms contribute mainly to the ultrasound attenuation; otherwise, scattering dominates. A well-known theory describing the propagation of sound in particulate media is ECAH [63, 64], which predicts the ultrasound attenuation that behaves according to the formula

$$\alpha = -\frac{3\phi}{2k^2R^3} \sum_{n=0}^{\infty} (2n+1) \operatorname{Re} A_n, \quad (2)$$

where ϕ is the concentration of the scatterers (droplets, particles). The coefficients A_n represent the amplitude of the compression wave field diffracted by a suspended scatterers. The first in the series, coefficient A_0 (zero-order term), describes the energy losses due to the thermal mechanism; the second, A_1 (first-order term), describes the energy losses due to the viscosity mechanism. In the long wavelength limit, when the densities of the phases do not differ greatly (emulsions), the ultrasonic attenuation is dominated by zero-order term. But when the density ratio of the particulate and continuous phase exceeds 2 (suspensions), the first-order term tends to dominate, and zero-order term can be neglected. At higher values of kR , more and more coefficients A_n have to be taken into account to obtain complex diffracted field patterns of the scattered wave.

The problem of using ECAH theory here lies in the transformation of our system, i.e. during the transition from simple emulsion (silicone oil droplets in castor oil) to droplets encapsulated by polystyrene particles. The ECAH theory is usually applied to stable systems where the physical parameters are constant in time. However, in our system, because of the adsorption of polystyrene particles onto the interface between silicone oil droplets and castor oil, the physical parameters of the scatterers (silicone oil droplets encapsulated by polystyrene particles) change their values continuously. This is

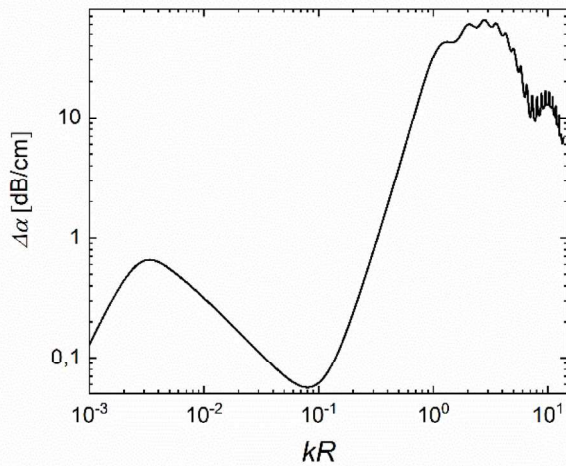


Figure 4. Theoretical dependence of the excess ultrasonic attenuation on mean diameter in the emulsion of 10% concentration of silicone oil droplets in castor oil. The first maximum corresponds to thermal losses, while the second corresponds to the ultrasound scattering. The calculations were carried out for 5 MHz ultrasound.

one reason for the changing of ultrasound attenuation with time—the effect that is difficult to quantify. The other reason for changing ultrasound attenuation in our system is the evolution of the droplet size due to electro-coalescence, and this mechanism of ultrasound attenuation can be predicted by ECAH theory. Because of that, we decided to compare the experimental results with the theoretical predictions based on ECAH theory for the simple emulsion of silicone oil-castor oil, assuming the growth of the droplet size but omitting the effect of adsorption of polystyrene particles onto the interface. To determine the ultrasound attenuation coefficient, we measured the mean size of droplets at different times. The temporal evolution of droplet size in the theoretical model was then described by the average droplet diameter taken from microscopy imaging data for 10% mass concentration of silicone oil to castor oil at selected times.

Figure 4 presents the calculated dependence of ultrasonic attenuation coefficient on the kR . The first maximum relates to the thermal losses on the interfacial border, while the second relates to the scattering of the ultrasound wave. In our experiments, the size of droplets is in the range of 10 μm –300 μm , which corresponds to the kR values of 0.1–3.5 when 5 MHz frequency ultrasound is used. According to the calculations presented in figure 4, the ultrasound scattering is the main contributor to the ultrasound attenuation.

Figure 5 presents the theoretical dependence of ultrasonic attenuation change on the droplet diameter in a simplified system of silicone oil-castor oil emulsion. It can be seen that the coefficient of attenuation is very sensitive to the change in droplet size from 100 μm to 300 μm at the 5 MHz frequency of the ultrasound.

In the next sections, the performed calculations presented above for predicting the attenuation of ultrasound in oil-in-oil emulsions will be discussed and compared with optical and acoustical experimental data.

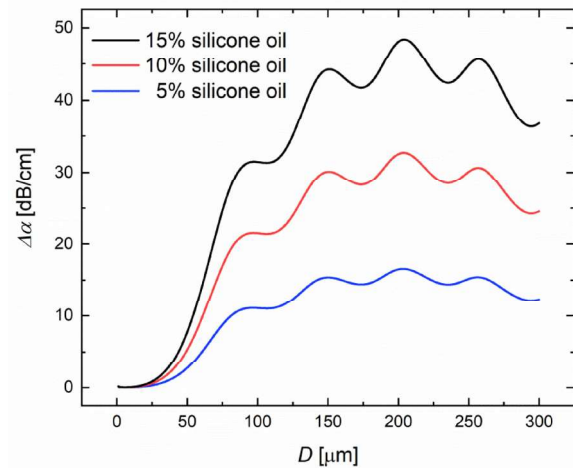


Figure 5. The theoretical dependence of ultrasonic attenuation change versus droplet diameter for the silicone oil-castor oil emulsion and for the three different concentrations of silicone oil. The frequency of ultrasound was 5 MHz.

3.2. Optical microscopy imaging and measurements by ultrasound

As long as the optical path for a light passing through a sample cell is short (typically up to a few mm), it is possible to use optical microscopy imaging to monitor the Pickering emulsion formation and to characterise the size of emulsion droplets [17, 18, 65]. Here, at first, we used a sample cell with a thickness of 1.3 mm that enabled optical microscopy observations of the emulsion maturing through electro-coalescence. An emulsion with 15% silicone oil and a 1:4 PS particles-to-silicone (PS:SO) mass ratio was subjected to DC electric fields for 20 min. One minute after the electric field application, it was already possible to recognise droplets in the image, but hard to precisely resolve their sizes and particle shell structures. The droplets electro-coalesced and grew quickly to sizes a few times larger than the mean droplet size of the pre-emulsion. As the electro-coalescence progressed, the mean droplet size increased and the droplets' concentration decreased. The small, densely dispersed droplets coalesced into several large drops with increased particle coverage; after several minutes, a stable Pickering emulsion was formed. Figure 6(a) presents optical microscopy images qualitatively showing the evolution of the emulsion. We analysed optical microscopy images and estimated the average diameters of droplets at different times (see table in figure 6(a)). However, quantification was challenging and accurate image analysis could be done only towards the end of the process, i.e. when the droplets were large and their concentration was reduced, enabling their characterisation by optical imaging.

In our second experiment, we used a thicker sample cell (10 mm) and performed an experiment using the same pre-emulsion and experimental procedures. Because of the strong light scattering in the thick sample cell, it was impossible to accurately estimate the sizes of droplets through optical microscopy. Figure S1 presents the images taken during the

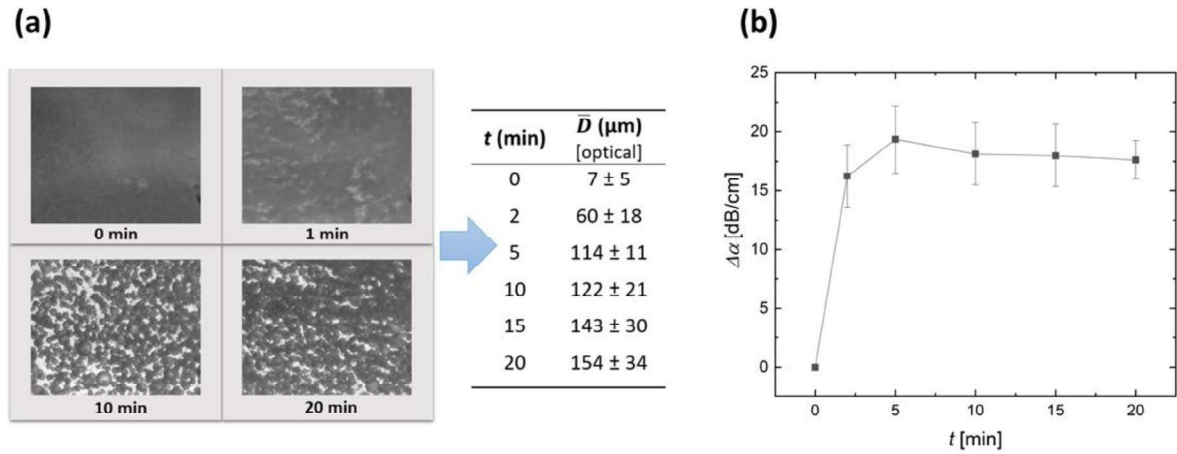


Figure 6. (a) Optical data collected from microscopy imaging showing the temporal change in emulsion appearance under electric field (for 15% silicone oil and 1:4 PS:SO mass ratio). The emulsion was studied in the sample cell with a thickness of 1.3 mm. The mean values of emulsion droplet size were estimated through analysis of optical microscopy images and are presented in the table. (b) Changes of the magnitude of ultrasonic attenuation plotted against time (15% silicone oil and 1:4 PS:SO mass ratio).

experiment. However, we estimated the mean droplet size of the Pickering emulsion at the end of the experiment. We greatly reduced the number of light scatterers by diluting the emulsion with clean castor oil. The final mean size of Pickering droplets was similar to that of the Pickering emulsion formed in the thin sample cell. We expected the fabrication paths of the Pickering emulsion to be the same for sample cells with different thicknesses and the results strengthen our hypothesis.

During the experiment, we also collected data from the ultrasonic system, i.e. we monitored the amplitude of the transmitted ultrasound pulse. Then, we calculated the change of the magnitude of the ultrasonic attenuation coefficient using equation (1). The results are plotted in figure 6(b), where each black square data point is connected by a line.

The non-numeric data in figure 6(a) seem to reflect the data presented in figure 6(b) very well. According to the optical data, significant increase in droplet size is visible in the first minutes after electric field was turned on. Also, the ultrasonic results confirm this observation. From theoretical ultrasonic attenuation data presented in figure 5, the change in size of emulsion droplets in the first 2 min of measurement was around $60 \mu\text{m}$. It is almost the same value as in the inset table shown in figure 6(a). Over the subsequent minutes of stabilisation in electric field, the droplet size estimated from the theoretical attenuation data does not correspond that well to the optical data. This discrepancy can be explained by the presence of dense shell of polystyrene particles surrounding the droplets. Therefore, with time, the formed Pickering emulsion resembles ‘pure’ emulsion less and less, which was modelled in our theoretical calculations.

Nevertheless, we propose using ultrasound for monitoring emulsion formation, particularly when optical microscopy measurements become difficult either due to light scattering or the small size of emulsion droplets. Indeed, we found that for the emulsion systems studied here, it is impractical to use optical microscopy techniques for sample cells with thicknesses above 2 mm (see also figure S1 in supplementary

materials (stacks.iop.org/JPhysD/53/085301/mmedia)). The next section presents ultrasound data from the experiments carried out in a sample cell with a thickness of 10 mm, and discusses the influence of both the PS particle and silicone oil concentrations on the dynamics of Pickering emulsion formation.

3.3. Influence of particle and silicone oil concentrations on magnitudes of the attenuation coefficient

The limited coalescence approach utilised in this work allows designing Pickering emulsions with desirable average droplet sizes [66, 67]. It can be calculated through the equation:

$$D_d = 3.6 \cdot D_p \cdot \frac{\rho_p}{\rho_d} \cdot \frac{m_d}{m_p}. \quad (3)$$

In this equation, the subscripts ‘d’ and ‘p’ denote droplet and particle, respectively; D , ρ , and m are diameter, density and mass, respectively. A derivation of similar formulas can be found in [68, 69]. In order to calculate the amount of particles needed to densely cover $80 \mu\text{m}$, $160 \mu\text{m}$ or $320 \mu\text{m}$ silicone oil droplets with $10 \mu\text{m}$ PS particles, we assume that the particles are spherical and the three-phase contact angle is 90° . For density ratio $\rho_p/\rho_d = 1.1$, we estimated the particle-to-silicone oil mass ratios to be approximately 1:2, 1:4 and 1:8, respectively [18].

We prepared three pre-emulsions with these mass ratios, all with the same concentration of silicone oil in relation to castor oil (15%). We monitored the process of Pickering emulsion formation using ultrasound. Figure 7 presents the changes in the magnitude of the attenuation coefficients as the electro-coalescence progressed, leading to the formation of a stable emulsion. Schematic illustrations of final droplet sizes were placed for each of the PS:SO ratios. We fitted the data points to the following function:

$$\Delta\alpha = \Delta\alpha_{\max} - \exp(B - \tau \cdot t), \quad (4)$$

which gives estimates of the characteristic time of emulsion development through parameter τ . This function describes the

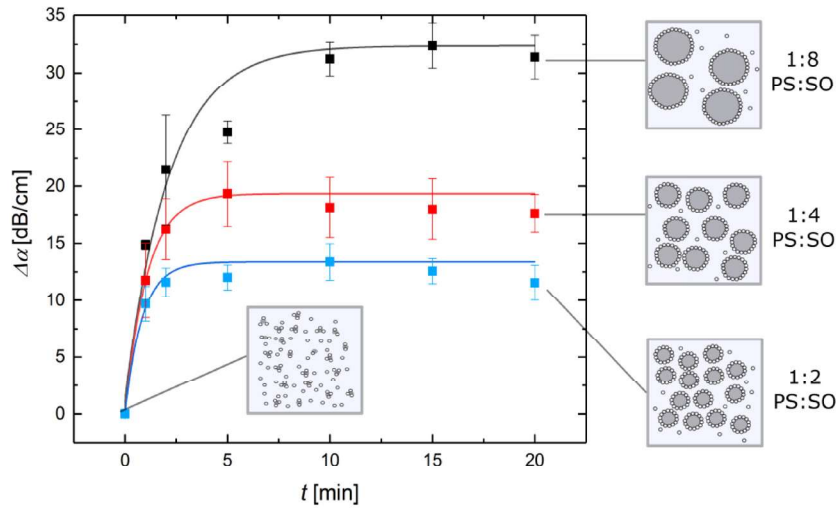


Figure 7. Changes in the ultrasonic attenuation coefficient plotted against time for three emulsions with different PS:SO mass ratios. Solid lines correspond to the data fitted with equation (4). The concentration of silicone oil was 15%.

data well, especially specific saturation point, as long as the measured mean size of emulsion droplet is between $\sim 10 \mu\text{m}$ and $\sim 300 \mu\text{m}$, i.e. for larger droplets the attenuation coefficient falls, rendering equation (4) inappropriate for fitting (see the theoretical results in figure 4 for $kR \geq 5$).

As expected, the magnitude of changes of the ultrasonic attenuation coefficient was the largest for the sample with the smallest concentration of particles ($\Delta\alpha > 30 \text{ dB}\cdot\text{cm}^{-1}$). This is because large emulsion droplets formed, contributing to stronger ultrasound wave attenuation, in accordance with the model presented in figure 4. The mean droplet sizes of the final Pickering emulsion were estimated (through the analysis of optical images) to be $106 \pm 23 \mu\text{m}$, $154 \pm 34 \mu\text{m}$, and $273 \pm 38 \mu\text{m}$ for emulsions with mass ratios of 1:2, 1:4 and 1:8, respectively. These values coincide well with those predicted theoretically using equation (3). The fitting curves provided us with rough estimates of the times needed to develop nearly completed Pickering emulsions. We estimated these times (values at an arbitrarily chosen reference value of 99% of α_{max}) to be $\sim 3 \text{ min}$, $\sim 5 \text{ min}$ and $\sim 10 \text{ min}$ for emulsions with mass ratios of 1:2, 1:4 and 1:8, respectively.

The propagation of ultrasound waves is sensitive to differences in droplet dimensions, which are reflected in changes in the ultrasound attenuation coefficient. Figure 8 presents the results of experiments carried out on emulsions with three different concentrations of silicone oil in relation to castor oil: 5%, 10% and 15%. We fitted the data points to the function in equation (4). The magnitude of changes of the ultrasonic attenuation was the largest for emulsions with the highest concentration in the dispersed phase. This is because there are more inhomogeneous zones in the medium contributing to acoustic energy dissipation.

3.4. Dynamics of Pickering stabilisation process

In our previous work [18], we conducted experiments on the coalescence of emulsion droplets with and without an electric field. We observed that the electro-coalescence of droplets can

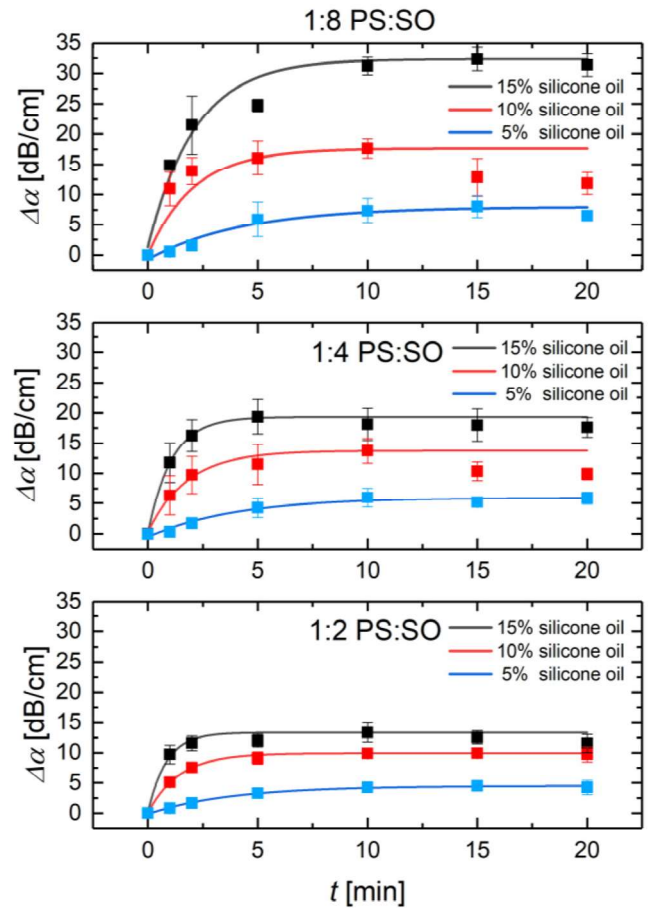


Figure 8. Changes in the ultrasonic attenuation coefficient as a function of time for emulsions with silicone oil concentrations of 5%, 10% and 15%. Solid lines correspond to the data fitted with equation (4).

be sped up by two orders of magnitude with the assistance of electric fields. We also observed the dynamic of a change in emulsion macrostructure. The bar chart in figure 9 graphically depicts the close correlation between parameter τ (obtained

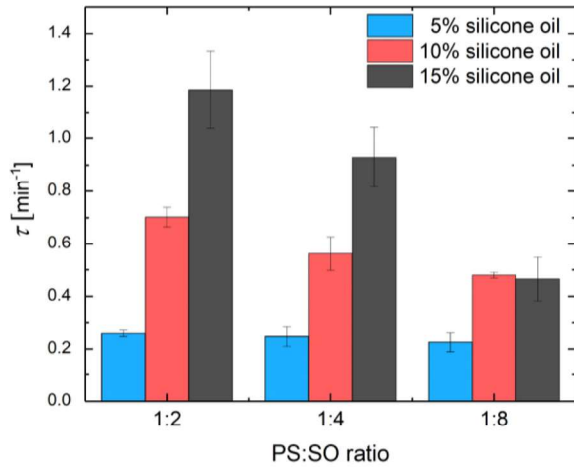


Figure 9. Parameter τ expressing the rate of change in ultrasonic attenuation for different concentrations of silicone oil and PS:SO mass ratios. The parameter was taken from fitting the experimental data (points from figure 8) to the function: $\Delta\alpha = \Delta\alpha_{\max} - \exp(B - \tau \cdot t)$.

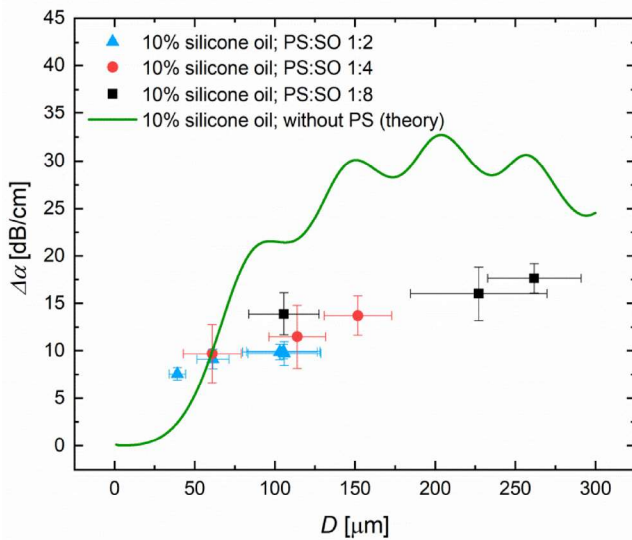


Figure 10. The comparison of the experimental results with the theoretical prediction for the ultrasound attenuation in 10% emulsion of the silicone oil droplets in castor oil. The theoretical line was calculated for 5 MHz ultrasound.

by fitting the data in figure 8 to equation (4) and the concentrations of silicone oil and PS particles.

As the concentration of emulsion droplets increases, the average distance between droplets decreases. The attractive electrostatic force between two droplets scales as s^{-4} , where s is the separation distance between the droplets. This implies that electro-coalescence should occur at a faster rate for emulsions with higher droplet concentrations. Indeed, the fastest growth (expressed by the highest value of τ) was found for emulsions with the highest concentration in the dispersed phase (black bars). As discussed above, particle concentration determines the size of Pickering droplets. Emulsions with the highest particle concentrations had the smallest Pickering droplets. Such emulsions should be formed faster than emulsions with lower particle concentrations, as the number of

coalescence events is smaller. This is what we observed experimentally, i.e. the emulsions with the highest particle concentrations evolved into Pickering emulsions at the fastest rate consistently for different concentrations of silicone oil.

Figure 10 shows the comparison of the experimental results with the theoretical prediction for the ultrasound attenuation in 10% emulsion of the silicone oil droplets in castor oil. It can be seen that the theory predicts, at least qualitatively, the evolution of the droplets size on the basis of the coefficient of ultrasonic attenuation. Certainly, the agreement could be better if the encapsulation of the droplets by the shell of polystyrene particles was taken into account. If the thermo-physical properties of the shell were similar to those of the continuous phase, the change in ultrasonic attenuation would be small, but the silicone oil and polystyrene particles differ in their thermal properties, especially in the coefficient of thermal expansion (see table 1), so the change can be expected to be bigger. On the other hand, obtained differences in theoretical and experimental data may indicate the importance of presence of particle shell around droplets in ultrasonic attenuation measurements.

The size range presented in figure 10 has been explored by many researchers studying either particle- or surfactant-stabilised emulsions [70–74]. Emulsions with droplet sizes we formed in our experiment are also often used in industrial applications [75–78]. Previously reported results concerned characterisation of already prepared emulsions by using acoustic spectroscopy and corresponding scattering theory ECAH for droplet sizes of tens of micrometres [44, 45]. It is worth mentioning that the sensitivity of monitoring the droplet sizes by the ultrasonic attenuation is not limited to region of $kR 10^{-1}$. The growth of attenuation in the region of thermal losses ($10^{-3} \leq kR \leq 10^{-2}$)—see the first maximum plotted in figure 4—can be utilised to monitor the evolution of the small droplets of hundreds nm in size using the same single ultrasound frequency of 5 MHz. In principle, it is possible to study emulsions with other droplet sizes by using ultrasound with different frequencies. Because the intrinsic absorption of emulsion phases is strongly dependent on frequency [79], the model curve (in figure 4) shifts along the droplet size axis.

4. Conclusion

In summary, we have presented the use of ultrasonic measurements as a convenient route for non-destructive studying of the formation of oil-in-oil Pickering emulsions stabilised by microparticles. By tracking the changes of the ultrasonic attenuation coefficient, we were able to characterise the dynamics of the evolution of emulsions. We showed experimentally that ultrasound was particularly useful for studying emulsion droplets when the change in droplets' size induced by electro-coalescence occurred in the range between several μm and a few hundred μm . This change was significantly more dynamic both for higher concentration of silicone oil droplets and higher amounts of particles used to stabilise the system, which was also depicted by quantitative parameter τ . It can roughly indicate the moment of bulk stabilisation of

emulsion by particles, which is not possible utilising solely the optical measurements.

Finally, we note that the magnitude of ultrasound attenuation calculated using the ECAH theory generally exceeds the value from the experiment. That is because the theory does not account for the presence of particle shell around emulsion droplets. There exist theories that include the third phase and allow more accurate calculations of the ultrasound attenuation [80], though such calculations are non-trivial. Our work demonstrates that there is a need for developing models that would enable non-complex calculations and, at the same time, provide a satisfactory consistency between theory and experiment for such three-phase systems of Pickering emulsions.

Acknowledgments

A J acknowledges financial support of the Polish National Science Centre through the OPUS programme (Grant No. 2015/17/B/ST7/03566). Z R was supported by the Polish National Science Centre through the OPUS programme (Grant No. 2015/19/B/ST3/03055) and the Polish-U.S. Fulbright Commission through the Fulbright scholarship. The authors wish to thank Dr A Mikkelsen for valuable discussions.

Declaration of conflicts

There are no conflicts of interest to declare.

Author contributions

Z R designed the method of emulsion preparation in electric fields; A J and Z R designed the ultrasonic measurements. R B performed the experiments as well as analysed and presented the data. T H performed the theoretical analysis presented in section 3.1. R B and A J wrote the first version of the manuscript. All authors took part in discussions on the interpretation of the data and the content of the manuscript.

ORCID iDs

Rafał Bielas  <https://orcid.org/0000-0001-6260-6444>
 Zbigniew Rozynek  <https://orcid.org/0000-0002-0785-7088>
 Tomasz Hornowski  <https://orcid.org/0000-0001-9767-6928>
 Arkadiusz Józefczak  <https://orcid.org/0000-0001-7722-7025>

References

- [1] Ikem V O, Menner A, Horozov T S and Bismarck A 2010 Highly permeable macroporous polymers synthesized from pickering medium and high internal phase emulsion templates *Adv. Mater.* **22** 3588–92
- [2] Dickinson E 2010 Food emulsions and foams: Stabilization by particles *Curr. Opin. Colloid Interface* **15** 40–9
- [3] Drexler S, Faria J, Ruiz M P, Harwell J H and Resasco D E 2012 Amphiphilic nanohybrid catalysts for reactions at the water/oil interface in subsurface reservoirs *Energy Fuels* **26** 2231–41
- [4] Rozynek Z and Józefczak A 2016 Patchy colloidosomes—an emerging class of structures *Eur. Phys. J.* **225** 741–56
- [5] Peng B, Zhang L, Luo J, Wang P, Ding B, Zeng M and Cheng Z 2017 A review of nanomaterials for nanofluid enhanced oil recovery *RSC Adv.* **7** 32246–54
- [6] Asfour M H, Elmotasem H, Mostafa D M and Salama A A A 2017 Chitosan based Pickering emulsion as a promising approach for topical application of rutin in a solubilized form intended for wound healing: *in vitro* and *in vivo* study *Int. J. Pharmaceut.* **534** 325–38
- [7] Bollhorst T, Rezwan K and Maas M 2017 Colloidal capsules: nano- and microcapsules with colloidal particle shells *Chem. Soc. Rev.* **46** 2091–126
- [8] Wu J and Ma G-H 2016 Recent studies of pickering emulsions: particles make the difference *Small* **12** 4633–48
- [9] Binks B P and Tyowua A T 2016 Oil-in-oil emulsions stabilised solely by solid particles *Soft Matter* **12** 876–87
- [10] Yang Y, Fang Z, Chen X, Zhang W, Xie Y, Chen Y, Liu Z and Yuan W 2017 An overview of pickering emulsions: solid-particle materials, classification, morphology, and applications *Frontiers Pharmacol.* **8** 287
- [11] Melle S, Lask M and Fuller G G 2005 Pickering emulsions with controllable stability *Langmuir* **21** 2158–62
- [12] Xu Q Y, Nakajima M and Binks B P 2005 Preparation of particle-stabilized oil-in-water emulsions with the microchannel emulsification method *Colloids Surf. A* **262** 94–100
- [13] Kaiser A, Liu T, Richtering W and Schmidt A M 2009 Magnetic capsules and pickering emulsions stabilized by core-shell particles *Langmuir* **25** 7335–41
- [14] Thompson K L, Armes S P and York D W 2011 Preparation of Pickering emulsions and colloidosomes with relatively narrow size distributions by stirred cell membrane emulsification *Langmuir* **27** 2357–63
- [15] Yamanaka K, Nishino S, Naoe K and Imai M 2013 Preparation of highly uniform Pickering emulsions by mercaptopcarboxylated gold nanoparticles *Colloids Surf. A* **436** 18–25
- [16] Wen C, Yuan Q, Liang H and Vriesekoop F 2014 Preparation and stabilization of d-limonene Pickering emulsions by cellulose nanocrystals *Carbohydr. Polym.* **112** 695–700
- [17] Binks B P and Yin D 2016 Pickering emulsions stabilized by hydrophilic nanoparticles: *in situ* surface modification by oil *Soft Matter* **12** 6858–67
- [18] Rozynek Z, Bielas R and Józefczak A 2018 Efficient formation of oil-in-oil Pickering emulsions with narrow size distributions by using electric fields *Soft Matter* **14** 5140–9
- [19] Radiman S, Fountain L E, Toprakcioglu C, de Vallera A and Chieux P 1990 In SANS study of polymer-containing microemulsions *Trends in Colloid and Interface Science IV* ed M Zulauf et al (Darmstadt: Steinkopff) pp 54–9
- [20] Goddeeris C, Cuppo F, Reynaers H, Bouwman W G and Van den Mooter G 2006 Light scattering measurements on microemulsions: estimation of droplet sizes *Int. J. Pharmaceut.* **312** 187–95
- [21] Kataoka H, Ueda T, Ichimei D, Miyakubo K, Eguchi T, Takeichi N and Kageyama H 2007 Evaluation of nanometer-scale droplets in a ternary o/w microemulsion using SAXS and ¹²⁹Xe NMR *Chem. Phys. Lett.* **441** 109–14
- [22] Wang L, Tabor R, Eastoe J, Li X, Heenan R K and Dong J 2009 Formation and stability of nanoemulsions with mixed ionic–nonionic surfactants *Phys. Chem. Chem. Phys.* **11** 9772–8
- [23] Lee Y-T, Li D S, Ilavsky J, Kuzmenko I, Jeng G-S, O'Donnell M and Pozzo L D 2019 Ultrasound-based

- formation of nano-Pickering emulsions investigated via in-situ SAXS *J. Colloid Interface Sci.* **536** 281–90
- [24] Denkova P S, Tcholakova S, Denkov N D, Danov K D, Campbell B, Shawl C and Kim D 2004 Evaluation of the precision of drop-size determination in oil/water emulsions by low-resolution NMR spectroscopy *Langmuir* **20** 11402–13
- [25] Lingwood I A, Chandrasekera T C, Kolz J, Fridjonsson E O and Johns M L 2012 Emulsion droplet sizing using low-field NMR with chemical shift resolution and the block gradient pulse method *J. Magn. Reson.* **214** 281–8
- [26] Pawlik A, Kurukji D, Norton I and Spyropoulos F 2016 Food-grade Pickering emulsions stabilised with solid lipid particles *Food Funct.* **7** 2712–21
- [27] Gestranus M, Stenius P, Kontturi E, Sjöblom J and Tammelin T 2017 Phase behaviour and droplet size of oil-in-water Pickering emulsions stabilised with plant-derived nanocellulosic materials *Colloids Surf. A* **519** 60–70
- [28] Ling N N A, Haber A, May E F, Fridjonsson E O and Johns M L 2017 By-line NMR emulsion droplet sizing *Chem. Eng. Sci.* **160** 362–9
- [29] Sprow F B 1967 Distribution of drop sizes produced in turbulent liquid-liquid dispersion *Chem. Eng. Sci.* **22** 435–42
- [30] Dickinson E, Galazka V B and Anderson D M 1991 Emulsifying behaviour of gum arabic. Part 1: effect of the nature of the oil phase on the emulsion droplet-size distribution *Carbohydr. Polym.* **14** 373–83
- [31] Das K P and Kinsella J E 1993 Droplet size and coalescence stability of whey protein stabilized milkfat peanut oil emulsions *J. Food Sci.* **58** 439–44
- [32] Boxall J A, Koh C A, Sloan E D, Sum A K and Wu D T 2010 Measurement and calibration of droplet size distributions in water-in-oil emulsions by particle video microscope and a focused beam reflectance method *Ind. Eng. Chem. Res.* **49** 1412–8
- [33] Pauchard V and Roy T 2014 Blockage of coalescence of water droplets in asphaltene solutions: a jamming perspective *Colloids Surf. A* **443** 410–7
- [34] Patil A V, Sole Marti X, Tetlie P and Johansen S T 2017 Development of an advanced imaging technique for dynamic emulsion stability *Chem. Eng. J.* **322** 90–101
- [35] Greaves D, Boxall J, Mulligan J, Montesi A, Creek J, Sloan E D and Koh C A 2008 Measuring the particle size of a known distribution using the focused beam reflectance measurement technique *Chem. Eng. Sci.* **63** 5410–9
- [36] Schümann H, Khatibi M, Tutkun M, Pettersen B H, Yang Z and Nydal O J 2015 Droplet size measurements in oil-water dispersions: a comparison study using FBRM and PVM *J. Dispers. Sci. Technol.* **36** 1432–43
- [37] Sacanna S, Kegel W K and Philipse A P 2007 Thermodynamically stable Pickering emulsions *Phys. Rev. Lett.* **98** 158301
- [38] Leong T S H, Wooster T J, Kentish S E and Ashokkumar M 2009 Minimising oil droplet size using ultrasonic emulsification *Ultrason. Sonochem.* **16** 721–7
- [39] Sihler S, Schrade A, Cao Z H and Ziener U 2015 Inverse Pickering emulsions with droplet sizes below 500 nm *Langmuir* **31** 10392–401
- [40] Gupta A, Eral H B, Hatton T A and Doyle P S 2016 Controlling and predicting droplet size of nanoemulsions: scaling relations with experimental validation *Soft Matter* **12** 1452–8
- [41] Chanamai R, Herrmann N and McClements D J 1998 Ultrasonic spectroscopy study of flocculation and shear-induced floc disruption in oil-in-water emulsions *J. Colloid Interface Sci.* **204** 268–76
- [42] Canselier J P and Oumeddour R 2010 Optimization of oil-in-water emulsion stability: experimental design, multiple light scattering, and acoustic attenuation spectroscopy AU—Bendjaballah, Malek *J. Dispers. Sci. Technol.* **31** 1260–72
- [43] Dukhin A S and Goetz P J 2017 Applications for emulsions and other soft particles *Characterization of Liquids, Dispersions, Emulsions, and Porous Materials Using Ultrasound* 3rd edn (New York: Elsevier) pp 393–428
- [44] Venkataramani D, Smay J E and Aichele C P 2016 Transient stability of surfactant and solid stabilized water-in-oil emulsions *Colloids Surf. A* **490** 84–90
- [45] Tran T N, Nakanishi H, Norisuye T and Tran-Cong-Miyata Q 2016 Ultrasound scattering studies on pickering emulsion *Proc. of Symp. on Ultrasonic Electronics* p 37 (<http://use-jp.org/proceedings/USE16/pdf/2P1-7.pdf>)
- [46] Nelson P V, Povey M J W and Wang Y 2001 An ultrasound velocity and attenuation scanner for viewing the temporal evolution of a dispersed phase in fluids *Rev. Sci. Instrum.* **72** 4234–41
- [47] Pawelzyk P, Toledo M L and Willenbacher N 2013 Ultrasonic in-line monitoring of styrene miniemulsion polymerization *Chem. Eng. J.* **219** 303–10
- [48] Józefczak A and Wlazło R 2015 Ultrasonic studies of emulsion stability in the presence of magnetic nanoparticles *Adv. Condens. Matter Phys.* **2015** 9
- [49] Silva L, Bibiano D, Figueiredo M and Costa-Félix R 2015 *Effects of the Concentration of Emulsion of Oil-in-Water on the Propagation Velocity and Attenuation* (Bristol: IOP Publishing) p 012005
- [50] Su Q, Tan C and Dong F 2018 Measurement of oil-water two-phase flow phase fraction with ultrasound attenuation *IEEE Sens. J.* **18** 1150–9
- [51] McClements D J 1991 Ultrasonic characterisation of emulsions and suspensions *Adv. Colloid Interface Sci.* **37** 33–72
- [52] McClements D J 2007 Critical review of techniques and methodologies for characterization of emulsion stability *Crit. Rev. Food Sci. Nutr.* **47** 611–49
- [53] Rozynek Z, Kaczmarek-Klinowska M and Magdziarz A 2016 Assembly and rearrangement of particles confined at a surface of a droplet, and intruder motion in electro-shaken particle films *Materials* **9** 679
- [54] Jamieson D T and Irving J B 1976 Thermal conductivity of silicone oils of the polymethylphenyl siloxane type *Thermal Conductivity 14* ed P G Klemens and T K Chu (Boston, MA: Springer) pp 279–86
- [55] Povey M J W and Holmes M J 2017 Ultrasonic particle sizing in emulsions *Ultrasound in Food Processing* (New York: Wiley)
- [56] Stallard J M 1966 *Some Thermodynamic Properties of Castor Oil Versus Temperature and Pressure* (Whithe Oak, MD: Naval Ordnance Lab)
- [57] Patel V R, Dumancas G G, Kasi Viswanath L C, Maples R and Subong B J J 2016 Castor oil: properties, uses, and optimization of processing parameters in commercial production *Lipid Insights* **9** 1–12
- [58] Patnode W and Scheiber W 1939 The density, thermal expansion, vapor pressure, and refractive index of styrene, and the density and thermal expansion of polystyrene *J. Am. Chem. Soc.* **61** 3449–51
- [59] Selfridge A R 1985 Approximate material properties in isotropic materials *IEEE Trans. Son. Ultrason.* **32** 381–94
- [60] Wypych G 2012 PS polystyrene *Handbook of Polymers* ed G Wypych (Oxford: Elsevier) pp 541–7
- [61] Gaur U and Wunderlich B 1982 Heat capacity and other thermodynamic properties of linear macromolecules. V. Polystyrene *J. Phys. Chem. Ref. Data* **11** 313–25
- [62] Mason T J, Lorimer J P and Bates D M 1992 Quantifying sonochemistry: casting some light on a ‘black art’ *Ultrasonics* **30** 40–2

- [63] Epstein P S and Carhart R R 1953 The absorption of sound in suspensions and emulsions. I. Water fog in air *J. Acoust. Soc. Am.* **25** 553–65
- [64] Allegra J R and Hawley S A 1972 Attenuation of sound in suspensions and emulsions: theory and experiments *J. Acoust. Soc. Am.* **51** 1545–64
- [65] Destribats M, Rouvet M, Gehin-Delval C, Schmitt C and Binks B P 2014 Emulsions stabilised by whey protein microgel particles: towards food-grade Pickering emulsions *Soft Matter* **10** 6941–54
- [66] Arditty S, Whitby C P, Binks B P, Schmitt V and Leal-Calderon F 2003 Some general features of limited coalescence in solid-stabilized emulsions *Eur. Phys. J. E* **11** 273–81
- [67] Binks B P and Whitby C P 2004 Silica particle-stabilized emulsions of silicone oil and water: aspects of emulsification *Langmuir* **20** 1130–7
- [68] Wiley R M 1954 Limited coalescence of oil droplets in coarse oil-in-water emulsions *J. Colloid Sci.* **9** 427–37
- [69] Destribats M, Gineste S, Laurichesse E, Tanner H, Leal-Calderon F, Heroguez V and Schmitt V 2014 Pickering emulsions: what are the main parameters determining the emulsion type and interfacial properties? *Langmuir* **30** 9313–26
- [70] Richter A, Voigt T and Ripperger S 2007 Ultrasonic attenuation spectroscopy of emulsions with droplet sizes greater than 10 μm *J. Colloid Interface Sci.* **315** 482–92
- [71] Whitby C P, Lotte L and Lang C 2012 Structure of concentrated oil-in-water Pickering emulsions *Soft Matter* **8** 7784–9
- [72] Manga M S and York D W 2017 Production of concentrated pickering emulsions with narrow size distributions using stirred cell membrane emulsification *Langmuir* **33** 9050–6
- [73] French D J, Brown A T, Schofield A B, Fowler J, Taylor P and Clegg P S 2016 The secret life of Pickering emulsions: particle exchange revealed using two colours of particle *Sci. Rep.* **6** 31401
- [74] Wang L J, Yin S W, Wu L Y, Qi J R, Guo J and Yang X Q 2016 Fabrication and characterization of Pickering emulsions and oil gels stabilized by highly charged zein/chitosan complex particles (ZCCPs) *Food Chem.* **213** 462–9
- [75] Marefati A, Rayner M, Timgren A, Dejmek P and Sjöo M 2013 Freezing and freeze-drying of Pickering emulsions stabilized by starch granules *Colloids Surf. A* **436** 512–20
- [76] Xiao J, Li Y and Huang Q 2016 Recent advances on food-grade particles stabilized Pickering emulsions: fabrication, characterization and research trends *Trends Food Sci. Technol.* **55** 48–60
- [77] Yano H, Fukui A, Kajiwara K, Kobayashi I, Yoza K-I, Satake A and Villeneuve M 2017 Development of gluten-free rice bread: Pickering stabilization as a possible batter-swelling mechanism *LWT—Food Sci. Technol.* **79** 632–9
- [78] Dejmek P, Timgren A, Sjöo M and Rayner M 2018 New particle stabilized emulsions and foams EP 2651243 B1, 2011/12/15 (<https://patents.google.com/patent/EP2651243A4/en>)
- [79] Challis R E, Povey M J W, Mather M L and Holmes A K 2005 Ultrasound techniques for characterizing colloidal dispersions *Rep. Prog. Phys.* **68** 1541
- [80] Anson L W and Chivers R C 1993 Ultrasonic scattering from spherical shells including viscous and thermal effects *J. Acoust. Soc. Am.* **93** 1687–99

Ultrasound control of oil-in-oil Pickering emulsions preparation

Rafał Bielas, Zbigniew Rozynek, Tomasz Hornowski, Arkadiusz Józefczak*

*Institute of Acoustics, Faculty of Physics, Adam Mickiewicz University in Poznań, Uniwersytetu Poznańskiego 2,
61-614 Poznań, Poland*

**Corresponding author: aras@amu.edu.pl*

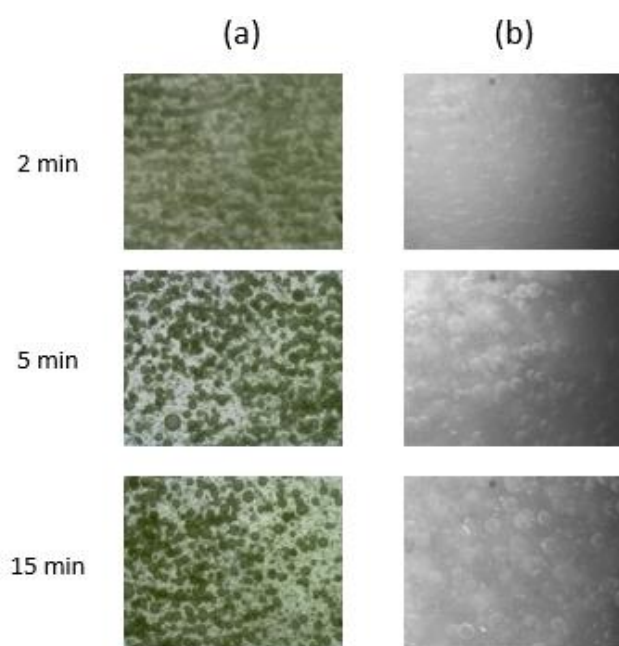


Figure S1. Comparison of the appearance of Pickering emulsion droplets created in **(a)** thin (1.3 mm) and **(b)** thick (10 mm) sample cells. When the thicker sample cell was used, a large number of scattering objects in the light path prevented meaningful optical observations. Emulsion concentration was 10%, mass ratio between polystyrene particles and silicone oil was 1:4.

[Publication III]

The effect of magnetic particles covering the droplets on the heating rate of Pickering emulsions in the AC magnetic field

R. Bielas, T. Hornowski, K. Paulovičová, M. Rajňák, A. Józefczak

Journal of Molecular Liquids, 2020, 320: 114388.



The effect of magnetic particles covering the droplets on the heating rate of Pickering emulsions in the AC magnetic field

Rafał Bielas^a, Tomasz Hornowski^a, Katarína Paulovičová^b, Michal Rajňák^{b,c}, Arkadiusz Józefczak^{a,*}

^a Chair of Acoustics, Faculty of Physics, Adam Mickiewicz University in Poznań, Uniwersytetu Poznańskiego 2, 61-614 Poznań, Poland

^b Institute of Experimental Physics, Slovak Academy of Sciences, Watsonova 47, Košice 040 01, Slovakia

^c Faculty of Electrical Engineering and Informatics, Technical University of Košice, Letná 9, 04200 Košice, Slovakia

ARTICLE INFO

Article history:

Received 28 July 2020

Received in revised form 17 September 2020

Accepted 20 September 2020

Available online 23 September 2020

Keywords:

Magnetic heating

Alternating magnetic field

Pickering emulsions

Magnetic particles

Emulsion stability

Coalescence

ABSTRACT

Emulsions stabilized with magnetic particles have been reported as useful for numerous applications, including thermal medical therapies where they can be used as heating materials. It is well-known that magnetic particles placed in the alternating magnetic field can act as heating agents. The generation of thermal energy is owing to magnetic energy dissipation caused by Néel and Brown relaxation, and hysteresis loss. These mechanisms depend on the properties of the applied magnetic field and the characterization of magnetic particles used as well. But, when residing on droplet surfaces e.g. as stabilizers in Pickering emulsions, magnetic particles somehow can be found trapped and their movement can be limited. Also, the change in Pickering droplet sizes and the increasing solidity of particle shell, e.g. through the coalescence events of droplets, can influence how magnetic energy is dissipated in such multi-phase system.

In our work, we investigate the efficiency of magnetic heating of oil-in-oil emulsions stabilized with magnetite particles of various sizes. The results indicate that the temperature rise in such systems varied for different concentrations of particles used, but also for the different macroscopic appearance of emulsions, i.e. coarse emulsions, not fully-covered by particles and final emulsions with stable droplets demonstrated different heating efficiency when placed in the alternating magnetic field. The emulsion droplets with different particle coverage were obtained either by using only ultrasonic homogenization or using ultrasound and a subsequent coalescence under the electric field. The presented study can help in the development of applications of magnetite-stabilized droplets in heating, e.g. when magnetic Pickering droplets are used as thermal agents in hyperthermia treatment or as templates for colloidal capsules.

© 2020 The Authors. Published by Elsevier B.V. This is an open access article under the CC BY license (<http://creativecommons.org/licenses/by/4.0/>).

1. Introduction

Particle-stabilized emulsions (Pickering emulsions) have been reported as very useful in various applications during last decades. The constant and progressive development of material engineering science allowed to produce particles of different sizes and shapes that can be used as stabilizers in colloidal systems [1–3] what extends significantly the possibilities of further applications, among others, in targeted drug delivery systems [4] and water decontamination procedures [5,6]. Especially, emulsions stabilized with magnetic materials are considered a good candidates for such applications because of their potential responsiveness to the external magnetic field.

Magnetic Pickering droplets were also reported to be used in applications where a crucial requirement is an efficient heating. The use of small objects possessing magnetic properties enables inducing a temperature elevation locally when the alternating magnetic field is

applied. For example, such non-contact heating methods were proposed for precise local heating of small liquid volumes using magnetite-silica particles [7]. Such droplet system heated magnetically overcomes a problem of other similar systems – a direct contact between elements. Additionally, magnetism of particles was used both for heat generation and for further droplet manipulation. As it was shown, such local, the non-contact-generation of heat could be useful, e.g. for enhancing PCR (polymerase chain reaction) protocol [8]. The use of magnetic materials placed in the alternating magnetic field is favorable comparing to other methods of non-contact local heating such as using laser light [9]. The penetration depth is not limited in case of magnetic heating. In the literature, there are some examples of evaluating heating efficiency of Pickering emulsions stabilized with magnetic particles. In work of Kaiser et al. [10] the magnetic heatability of magnetite-polystyrene particles was observed and obtained temperature increase was utilized to cyclic stabilizing and destabilizing emulsion system. Lahiri et al. in their papers [11,12] produced effectively nano-emulsions with magnetite particles and evaluated the influence of various parameters on the magnetic heating efficiency. They also

* Corresponding author.

E-mail address: aras@amu.edu.pl (A. Józefczak).

suggested that magnetic nano-emulsions could be used as agents in magnetic hyperthermia. However, it is worth pointing out that they described a system with magnetic nanoparticles residing inside emulsion droplets that introduced the additional issues such as limited convection from the droplet inside.

The capability of magnetic materials exposed to the alternating magnetic field to induce a local temperature increase results from a magnetic energy dissipation. Namely, Néel and Brown relaxation phenomena, and hysteresis losses are responsible for energy loss under high-frequency AC magnetic field [13–15]. The mechanisms of relaxation are believed to be dominating in small particles. For magnetite and maghemite particles the boundary may be even up to 160–170 nm [16]. Rosensweig expressed the heat generated in a given volume of the sample (P_R) due to relaxation mechanisms as [15]:

$$P_R = \mu_0 \pi f H_0^2 \frac{2\pi f \tau}{1 + (2\pi f \tau)^2} \chi_0 \quad (1)$$

where μ_0 is a magnetic permeability of free space, f is a frequency of the AC magnetic field, H_0 is a magnitude of magnetic field, χ_0 is an equilibrium magnetic susceptibility. τ is the effective relaxation time: $\tau = \frac{\tau_B + \tau_N}{\tau_B \tau_N}$. τ_B and τ_N are characteristic relaxation times corresponding for Brown and Néel relaxation mechanism.

Bigger particles exhibit additional energy dissipation due to the movements of domain walls that leads to the magnetic hysteresis in the system [13]. The more significant hysteresis loop, the more magnetic energy is transformed into a heat [14]:

$$P_H = \mu_0 f \oint H_0 dM \quad (2)$$

where the above integer describes the area of hysteresis loop (M – magnetization of the sample). The dependence obeys the third power law of H according to the prediction by Lord Rayleigh and numerous of experiments [17,18]:

$$P_H = \frac{4}{3} \mu_0 f \alpha_R H_0^3 \quad (3)$$

where α_R is a so-called Rayleigh coefficient.

Therefore, one can see that calorimetric effect under the AC magnetic field depends on the one hand on properties of magnetic materials used, and on the other, on properties of the applied magnetic field. The proper settings of parameters may cause an efficient heating as it is in case of magnetic fluid hyperthermia [19], and in case of colloidal capsules where cargo can be released due to the sufficiently high temperature induced by the AC magnetic field [20]. Recently, the potential of using magnetically induced temperature rise for colloidal capsules formation was also shown [21].

Pickering emulsions are believed to be more stable than surfactant-stabilized emulsions [22,23]. The stability is a key requirement for produced emulsion and it is often understood as a prevention against aging processes (mainly, emulsion droplets coalescence and their flocculation). The presence of solid particle shell around Pickering droplet constitutes a mechanical barrier what ensures effectively this prevention. In this study, we will show that solid particle shell influences not only the stability of emulsions against coalescence but also has an impact on heating rate of emulsions stabilized with magnetite particles and placed in the alternating magnetic field. For this purpose, we used coarse oil-in-oil emulsions stabilized with magnetite nano- and microparticles formed by ultrasound and compared them with those stabilized subsequently under the electric field.

2. Materials and methods

2.1. Materials

In the experiments, we used a silicone oil (Rhodorsil, 47 V 50, viscosity of 50 mPa·s, electric permittivity of 5) and castor oil (MERLIN, MA 220–1, viscosity of 700 mPa·s, electric permittivity of 2.5) as an inner and outer phase of the oil-in-oil emulsions, respectively. We stabilized the emulsions with different pristine magnetite particles (**MPs**): smaller (**nMPs**, 50–100 nm in size, density of about 4800–5100 kg·m⁻³) and bigger (**μMPs**, <5 μm in size, density of about 4800–5100 kg·m⁻³) purchased from Sigma-Aldrich Co., and with magnetite nanoparticles produced by the co-precipitation method and functionalized with oleic acid (**OA-MPs**, the size of about 10 nm). All particles used in the experiment were in the form of powder.

2.2. Preparation of magnetite particles functionalized with oleic acid

To obtain the functionalized magnetic nanoparticles we used the bottom-up approach. The nanoparticles with inverse spinel structure were synthesized by the co-precipitation method using an aqueous solutions of starting materials (FeSO₄·7H₂O and FeCl₃·6H₂O) and precipitating agent (NH₄OH). Ferrous and ferric ions were precipitated in alkaline solution with an excess ammonium hydroxide in stoichiometric ratio 1:2. The nucleation and growth of the spherical magnetite nanoparticles were carried out at 80–82 °C. During synthesis, the reaction mixture was continuously stirred with a mechanical stirrer (IKA) at 5000 RPM for 1 h. The precipitations of magnetic nanoparticles were performed in the presence of oleic acid to prevent both agglomeration and/or oxidation of the nanoparticles. After completion of the chemical reaction, the resultant black precipitate (containing sterically functionalized magnetite nanoparticles) was separated by a permanent magnet and then the nanoparticles were washed with deionized water and acetone. This procedure was repeated five times, and nanoparticles without impurities were dried at 100 °C in an oven for 2 h.

2.3. Characterization of magnetic particles by using VSM

The magnetization curves were measured at $T = 298$ K using a vibrating sample magnetometer (VSM) installed on a cryogen-free superconducting magnet from Cryogenic Ltd. Fig. 1 presents the room temperature magnetization curves of powders consisting of different magnetic particles. The saturation magnetization is close to bulk magnetite for multi-domain particles. The value of saturation magnetization is below bulk magnetite for single superparamagnetic particles because of iron oxidation [24]. The contribution of maghemite lowers the value of the effective bulk magnetization. As an inset picture, we included measurements of magnetization curves for small values of magnetic field for **nMPs** and **μMPs**. They show the magnetic hysteresis in both types of magnetic particles.

2.4. Preparation of the samples of pre- and final emulsions

In the first step, magnetic particles in a form of powder were dispersed in silicone oil by vigorous shaking. Such dispersion was subsequently mixed with castor oil using ultrasound that provided a primary homogeneity of the mixture. We used the ultrasonic homogenizer (Sonoplus HD 300, Bandelin, acoustic intensity estimated as 17 W·cm⁻², working frequency of 18 kHz) to produce coarse emulsions what we termed pre-emulsions. The samples differed with magnetite particles to silicone oil mass ratios (1:2, 1:4, or 1:10) and with a concentration of silicone oil in relation to castor oil (5, 10, or 15% w/w). Due to an acoustic cavitation under the high-intensity ultrasonic field, small silicone oil droplets were produced. The sonication lasted 60 s when pristine magnetic particles were used as stabilizers and 120 s for functionalized nanoparticles as we noticed that the mixtures with

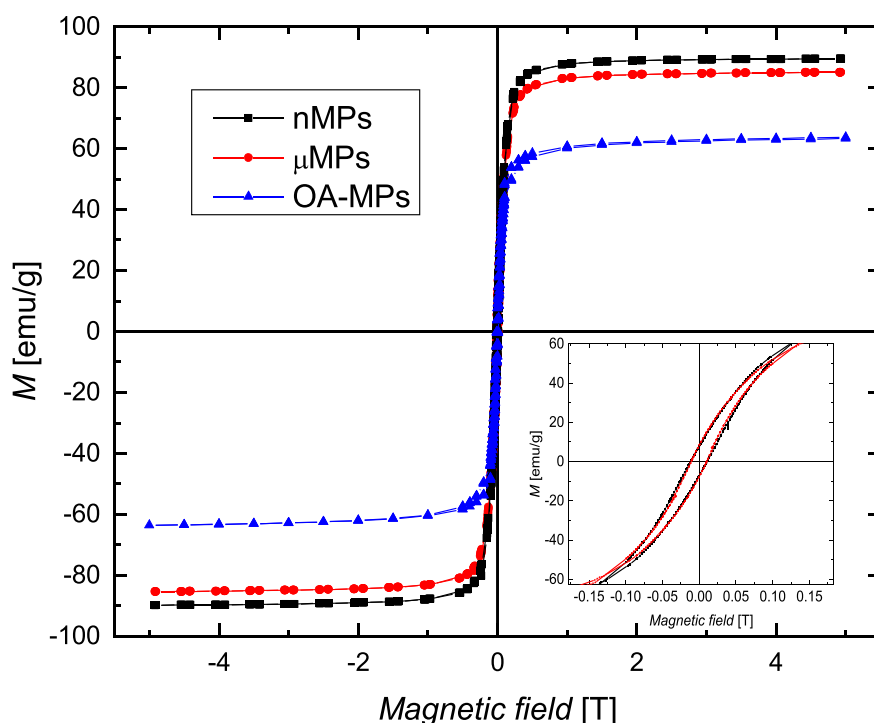


Fig. 1. Magnetization curves of magnetic powders consisting of different magnetic particles. The measurements were performed for the temperature of 298 K. The inset picture presents hysteresis loops established for **nMPs** and **μMPs** for small magnetic fields.

functionalized magnetic nanoparticles did not undergo emulsification easily. The use of an acoustic homogenization alone did not lead to the high enough coverage of droplets by particles to prevent further coalescence of droplets. Such a system was not completely stable [25,26]. So, the ultrasonic homogenization was followed by the stabilization under the electric field. The use of the electric field allowed us to obtain droplets with higher coverage by particles as the silicone oil droplets coalesced simply because of droplet-droplet dipolar interactions and electrohydrodynamic flows, as in case of previous work where non-magnetic soft particles were used as stabilizers [25]. The process of electro-coalescence stopped when the particle shell around droplets was sufficiently solid to prevent further coalescence events. The system after several minutes under the electric field became more stable as compared to the situation after ultrasonic homogenization. Consequently, the further comparison of magnetic heating efficiency between merely stable and more stable system was possible to perform. It is worth noting that electrohydrodynamic flows facilitate the process of merging droplets by changing the structure of particle coating around the droplets, i.e. the particles are being packed in the vicinity of the center of a droplet, whereas the droplet's flanks remain uncoated which generally promotes the coalescence [25,27].

The process of structuring the particles on the droplet surface can be compared with the aggregation of particles under the electric field reported in studies on ferrofluids as there is the same responsible phenomenon. However, in the process of the formation of stable magnetic Pickering emulsions, we did not observe the patterns presented in [28]. For our three-phase system with specific electrical permittivity of each component, in the magnetic particles, more charges are produced on the inside of the particle-castor oil interface and the net electric dipole across the magnetic particle is parallel to the applied electric field. However, on the silicone oil-castor oil interface, more charges are produced on the outside and the net dipole moment is pointed against the direction of the electric field. Thus, the magnetic particles can form the chains as a result of the dipole-dipole interaction. However, collision with the oppositely polarized silicone oil droplet may result in joining of the silicone oil droplet to the chain of magnetic

particles. This assumption would require a numerical simulation in the future.

After ultrasonic homogenization, the glass measurement cell (30 mm × 18 mm × 0.3 mm) was filled with a sample of pre-emulsion and the copper electrodes were placed on its sides. The electrodes were connected to DC-to-DC high voltage amplifier (UltraVolt 1AA12-P4, Advanced Energy Co.). The electric field intensity was from 200 to 600 V/mm. The process of stable Pickering emulsions formation in the electric field was monitored using a CMOS camera (UI-3590CP-C-HQ, IDS) connected to PC. However, because of the poor transparency of magnetite-stabilized systems, the direct optical observations were possible only after a dilution of the samples. That is why we did not observe pre-emulsions. To facilitate the dynamics of electrocoalescence (due to lower viscosity of both emulsion phases), the temperature within the sample was maintained as ~50 °C. The appearance of emulsions, i.e. the systems that underwent the electro-coalescence, is presented in Fig. 2.

Based on the presented images, droplet size distributions were calculated. For emulsions with **nMPs** mean diameter, $\langle D \rangle = 47.38 \mu\text{m}$, standard deviation, $\sigma = 19.56 \mu\text{m}$, for these stabilized with **OA-MPs** $\langle D \rangle = 79.97 \mu\text{m}$, standard deviation, $\sigma = 31.12 \mu\text{m}$, and for systems with **μMPs** ($\langle D \rangle = 85.93 \mu\text{m}$, standard deviation, $\sigma = 20.41 \mu\text{m}$). The small difference in size between droplets coated by **OA-MPs** and **μMPs** stems probably from the significantly weaker attachment of **OA-MPs** particles to the oil-oil interface. Even though, in general, using smaller particles should lead to smaller droplets, small particles coated by oleic acid led to the formation of quite large droplets. Also, droplets stabilized with **OA-MPs** seemed to tend to agglomeration, although oleic acid is used to prevent agglomerations of particles. It should be noted that surface modification altered properties of the particles, including colloidal electric charge. Additionally, the surfactant layer changes the wettability of particles, and, as a result, **OA-MPs** possibly penetrate less the inner phase of the emulsion (silicone oil droplets). It means that a bigger surface area is exposed to direct contact with other particle surfaces what makes the chain-like structures stronger.

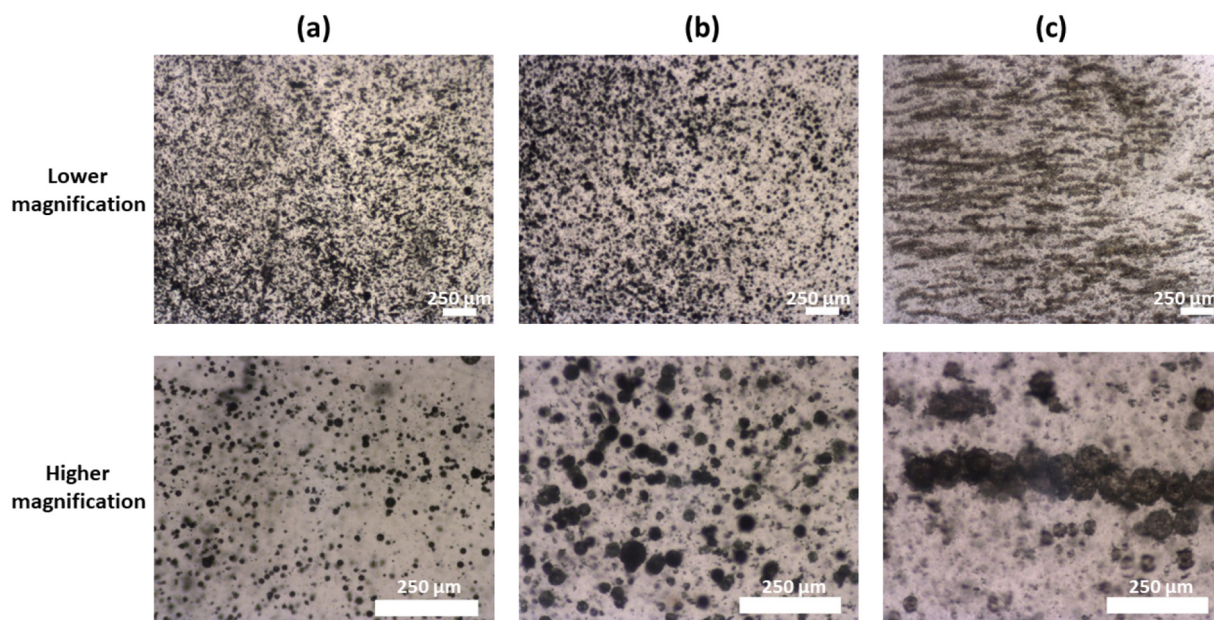


Fig. 2. Emulsions stabilized with different types of magnetic particles: (a) magnetic nanoparticles, **nMPs**, (b) magnetic microparticles, **μMPs**, and (c) prepared magnetic nanoparticles with oleic acid coating, **OA-MPs**. The pictures were taken by optical microscopy imaging after stabilization under the electric field and a proper dilution. The initial magnetic particles – silicone oil mass ratio was 1:4 and the concentration of silicone oil in relation to castor oil was 10% w/w. The scale bars represent 250 μm .

2.5. Magnetic characterization of the samples of pre- and final emulsions

The magnetization curves for pre-emulsions and emulsions after an application of the electric field were measured at $T = 298\text{ K}$ using the same vibrating sample magnetometer (VSM) as in Section 2.3. The samples varied with the type of magnetite particles used. The magnetic particles – silicone oil mass ratio was 1:4 and the concentration of silicone oil in relation to castor oil was 10% w/w. The results are presented in Fig. 3.

The magnetization occurred to be different for different types of particles what corresponds well to the results in Fig. 1. For the systems with smallest particles (**OA-MPs**) practically zero hysteresis can be observed. However, the differences are also clear between samples with pre-emulsions and emulsions stabilized under the electric field. For **OA-MPs**, this difference is the most significant that can arise from the fact that in **OA-MPs** the ‘pure’ mechanism of magnetic relaxation exists. This mechanism can be influenced by the attachment of particles into the interface more strongly than for **nMPs**, where also magnetic hysteresis can play a role. Hysteresis should not be dependent on the potential inhibition of oscillations of a particle in the alternating magnetic field.

2.6. Calorimetric measurements in the alternating magnetic field

To measure the calorimetric effect of the application of the alternating magnetic field in magnetite-stabilized emulsions we used a commercially available induction heating system (EASYHEAT, Ambrell Co.). In our experiments, the frequency of the field was 356 kHz and the intensity was from 5.2 kA/m to 16.2 kA/m. We used a temperature sensor system (FLUOTEMP, Photon Control Inc.) with an optic fiber temperature probe, model FTP-NY2, to measure how the temperature in sample cell increased in time of 30 s as a result of magnetic energy dissipation. The optical fiber was placed centrally in the sample cell that was located in the water-cooled induction coil and thermally insulated. Therefore, one can assume that temperature rise from the coil was negligible. The schematic illustration of the experiment is presented in Fig. 4.

3. Results and discussion

3.1. Magnetic heating measurements of Pickering emulsions stabilized with MPs of different sizes

The effect of different-size magnetite particles on the heating efficiency of Pickering emulsions was evaluated by preparing a series of samples in which continuous phase and dispersed phase with magnetite particles of different **MPs** fractions were used. The results are presented in Fig. 5 and Fig. 6.

In Figs. 5 and 6 there are depicted significant differences in heating for coarse and final emulsions, i.e. for emulsions prepared only by using ultrasound versus emulsions additionally placed in the electric field. For all of measurements, the systems exposed to the electric field prior to the magnetic field exhibited weaker heating efficiency; the temperature increase for emulsions are lower than for pre-emulsions.

Besides, one can see that in the pre-emulsions and emulsions stabilized with bigger particles (**μMPs**) the temperature increase was higher comparing to the emulsions stabilized with smaller magnetic particles (**nMPs**). Also, the amount of magnetic particles influenced heating efficiency. In both Figs. 5 and 6, for each measurement, the maximum temperature elevation within the sample was achieved for the highest magnetic particles to silicone oil mass ratios that correspond to the amount of particles used to stabilize silicone droplets. In the same way, the higher concentration of silicone oil (inner phase) in relation to castor oil (outer phase of the emulsion) caused the higher temperature increase during the measurements. In the systems with high concentration of silicone oil, more droplets covered by magnetic particles resided in the sample and acted as sources of heat.

We also tested systems stabilized with magnetite nanoparticles functionalized additionally with oleic acid (**OA-MPs**) to compare them with emulsions and pre-emulsions stabilized with particles without coating. We measured the temperature increase within 30 s under the alternating magnetic field for one, chosen magnetic particles to silicone oil mass ratio, 1:4, and three different concentrations of silicone oil in relation to outer phase (castor oil). The results are presented in Fig. 7.

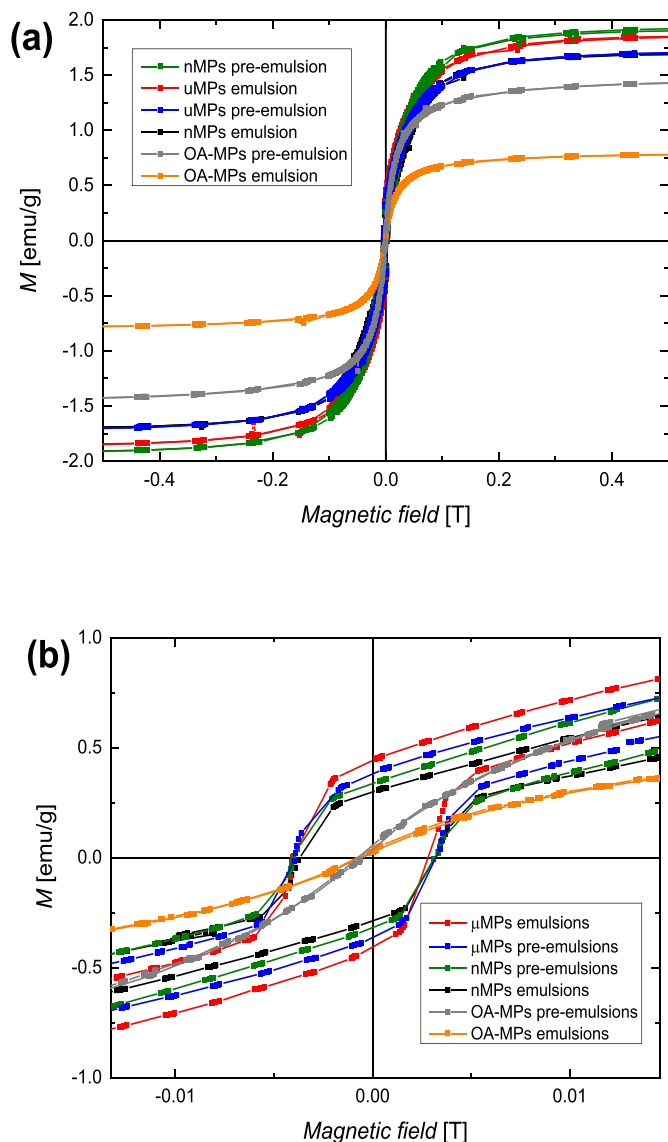


Fig. 3. (a) Magnetization curves of pre-emulsions and emulsions with different magnetic particles. The measurements were performed for the temperature of 298 K. (b) Hysteresis loops established for the samples in the low magnetic field.

As for magnetic particles without any modification, the heating efficiency was dependent on the concentration of silicone oil in relation to the outer phase of the emulsion (castor oil) in the tested system. More dense emulsions contained more magnetic material what means that there were more sources of the heat. What is more important, for those smaller particles, coated with oleic acid, the influence of additional stabilization of the emulsion under the electric field was also proven. For each concentration of silicone oil, the temperature increased faster and more dynamic for pre-emulsions comparing to stable ones. It is worth pointing out that the final temperature elevations presented in Fig. 7 were considerably lower than for emulsions and pre-emulsions stabilized with other particles (i.e. **nMPs** and **μMPs**). It was mainly because of smaller size of a magnetic core in **OA-MPs**. However, the particle coating alone can be responsible for worse heating performance because the additional layer around particle can increase relaxation time and, therefore, lower the efficiency of magnetic energy loss in nanoparticles [29]. On the other hand, the studies show that additional coating can be helpful in enhancing heating efficiency [30]. It should be noted that in literature the influence of particle coating on the heating rate in magnetic heating was rather not evaluated for Pickering emulsions.

For comparing different types of stabilizers, the results from calorimetric measurements for 1:4 magnetic particles to silicone oil (**MPs: SO**) mass ratio were resumed in Table 1. This presents maximum temperature increase in pre-emulsions and emulsions after 30 s in the alternating magnetic field (AMF).

According to results presented above, one can see that the temperature increase within the sample depended on the stability of particle shell around emulsion droplets and the size of magnetic particles used as stabilizers. We want now to elucidate and discuss the reasons for such results.

There are a number of scientific papers that have commented on magnetic particle size as a factor influencing the efficiency of magnetic heating, mostly regarding the magnetic fluids. As it was mentioned in Introduction section, it is well-established that in small magnetite particles the magnetic relaxation is responsible for heating under the alternating magnetic field. Both Néel and Brown relaxation times depend on a size of magnetic particles (magnetic or hydrodynamic) that causes that the magnetic energy loss is also sensitive to the differences in size of magnetic particles. The results from Fig. 5 were taken for non-modified magnetite particles with sizes of 50–100 nm (**nMPs**) that should be regarded mostly as single-domain particles [16]. From those results, one can also see that in pre-emulsions and emulsions stabilized with **nMPs** the temperature elevation is higher for the increasing concentration of the samples.

The model presented by Rosensweig [15] explains the influence of relaxation mechanisms on heating efficiency of magnetic particles (see, Eq. (1)). However, this model is limited to non-interacting particles. The real magnetic colloids are in general concentrated and the possibility of interactions between particles must be taken into account when determining heating efficiency for those systems [31]. To evaluate the impact of interactions on the heating efficiency, magnetic fluids with different concentrations were studied. But, it is difficult to draw definite conclusions because of aforementioned dependence of relaxation times on size of particles. In general, for systems where Brown relaxation was dominating a higher concentration led to an increase in heating efficiency. The opposite results were shown for smaller particles [31] (i.e. where Néel mechanisms of relaxation dominated). So, it could be said that for each sample exists an optimum concentration for achieving maximum performance of magnetic heating [32]. Lahiri et al. repeated this suggestion when analyzed heating in magnetic nano-emulsions [12]. In our experiment, there is a significant increase in heating efficiency for higher concentrations regardless of a size of magnetite particles. So, existing in our pre-emulsions and emulsions interactions between particles facilitate magnetic heating, at least for values of magnetic field frequency we used (356 kHz). It can be related to the relatively low mass concentration of particles in relation to the mass of the whole emulsion what is in the range of 0.5–6.1% depending upon the sample. For higher amount of magnetic material the maximum would appear provided that magnetic interactions between particles residing at the droplet interface also are distance-dependent.

Above-mentioned facts do not explain the apparent difference in heating between pre-emulsions and stable emulsions. The same particles were used with the same concentration for both systems but the outcome of measurements was clearly different. We propose two potential explanation for this. Firstly, the dominating relaxation mechanism in samples stabilized with **OA-MPs** and **nMPs** is Brown mechanism. It depends on viscosity of the surrounding medium and, as it was shown, its inhibition drastically deteriorates the heating efficiency in magnetic fluids [33] and in magnetic nano-emulsions as well [11]. In our case, magnetic nanoparticles resided at the same time in both viscous media (i.e. partially in the inner and the outer phase of emulsions) that can lead to their immobilization against the changes of magnetic field directions. After the stabilization in the electric field, particles are more densely packed at the interface that, in our opinion, makes the oscillations of particles harder comparing to the pre-emulsions. The particles are arranged there in a less compact way.

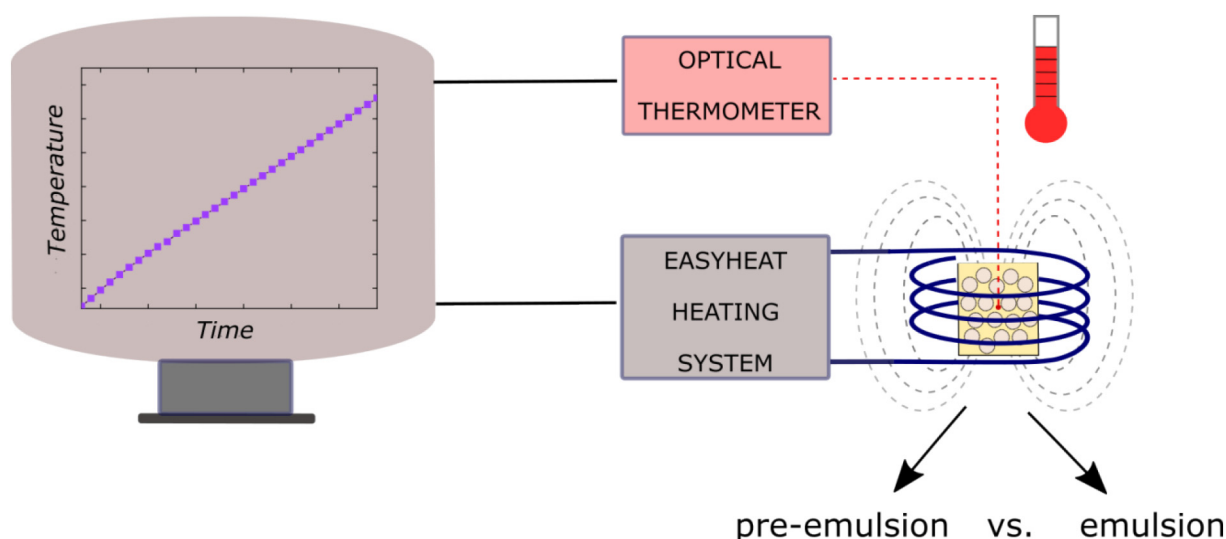


Fig. 4. A scheme of the magnetic heating measurements. Measurement cells before (pre-emulsions) and after (emulsions) the stabilization in the electric field were placed in the magnetic coil. The temperature rise due to the magnetic heating was recorded in the function of time by using optical sensor placed in the middle of the cell.

Secondly and more importantly, there is a significant difference between pre-emulsions and emulsions when it comes to heat transfer between the inside and outside Pickering droplets. For stable emulsions, particle shell around droplet is solid. It may cause very efficient heating of magnetic particles towards the inside of droplet. Because of solidity of particle shell, the heat transfer into outer phase of emulsion is impeded as the very local temperature of the particle shell is much more higher. Droplets in our system underwent the process of electro-coalescence

and the change in solidity of particle shell went parallel to an increase of droplet size. It also could influence the heat transfer as there are less droplets dispersed in the carrier medium but more silicone oil is entrapped within the particle shells. It is worth pointing out that in our calorimetric measurements the thermometer is placed in the outer phase. What is interesting, for colloidal systems stabilized both with magnetite and soft particles (polystyrene), such differences between pre-emulsions and emulsions were not significant [21].

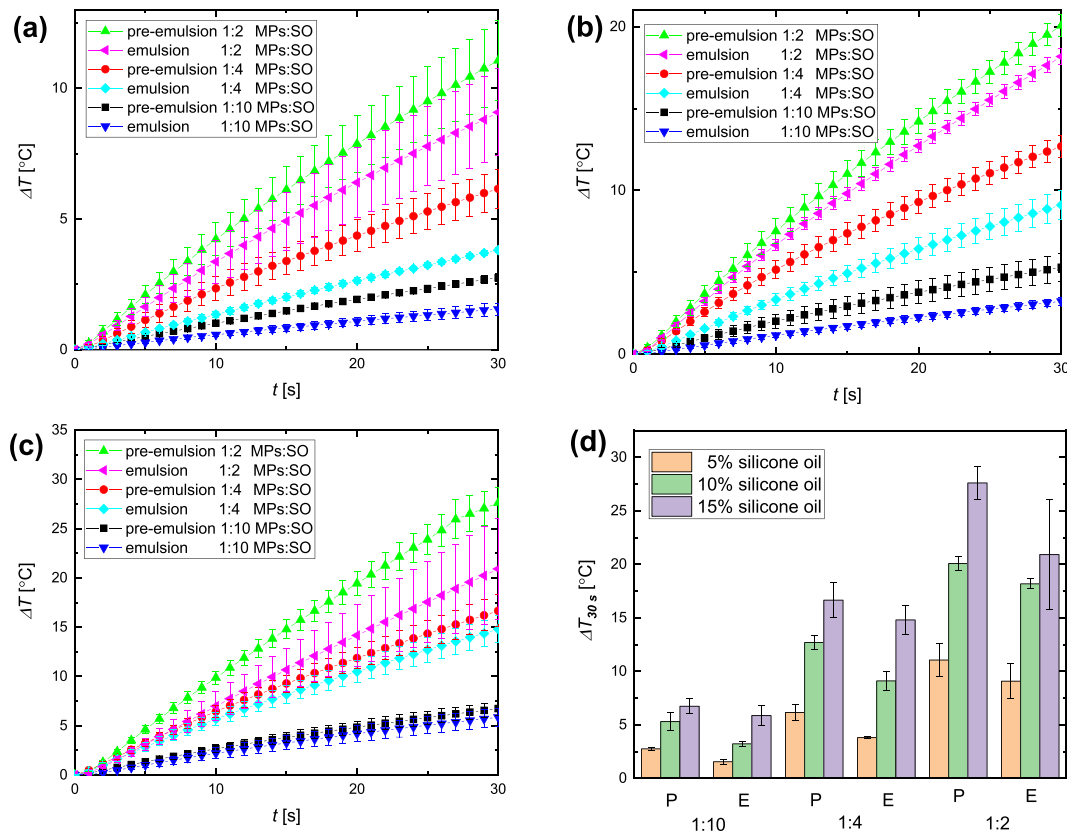


Fig. 5. Temperature increase vs. time recorded in the samples of pre-emulsions and emulsions stabilized with nMPs placed in the alternating magnetic field for different concentrations of silicone oil (SO) to castor oil: (a) 5%, (b) 10% and (c) 15%. (d) A summary of the values of temperature elevations after 30 s of measurements for pre-emulsions (P) and emulsions (E) with different magnetic particles to silicone oil mass ratios. The intensity of magnetic field was 16.2 kA/m.

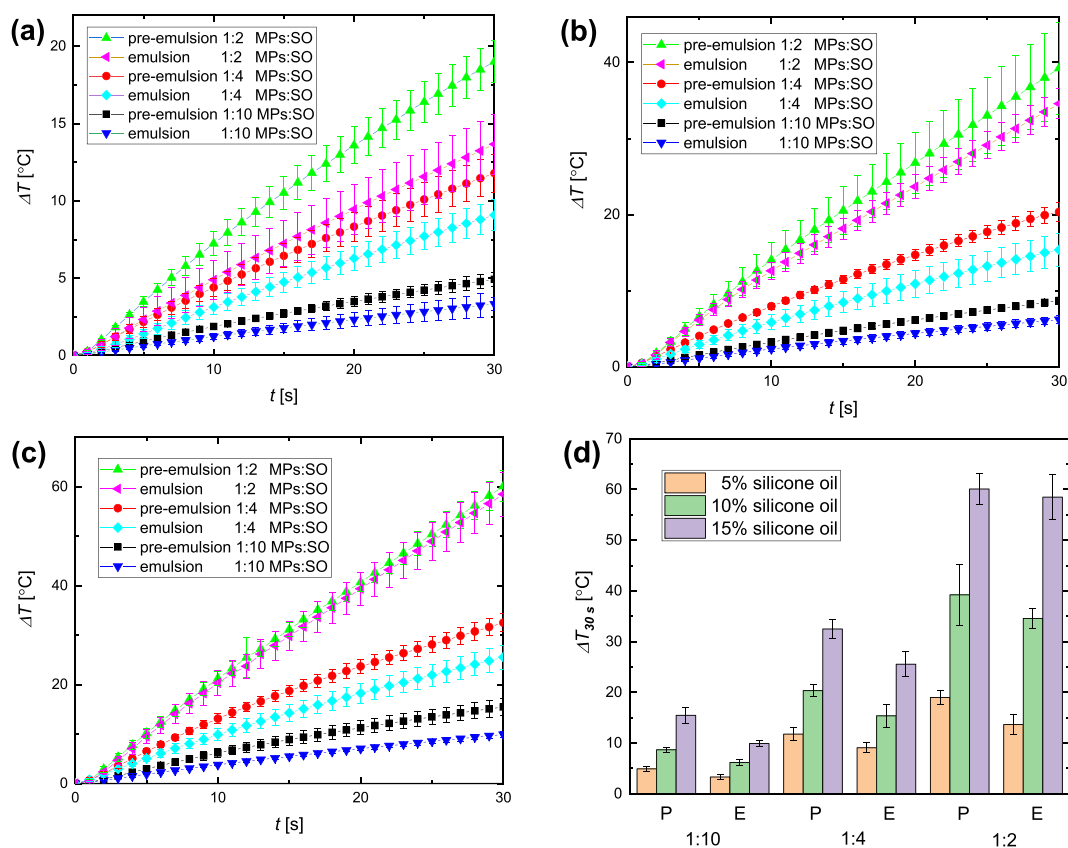


Fig. 6. Temperature increase vs. time recorded in the samples of pre-emulsions and emulsions stabilized with μ MPs placed in the alternating magnetic field for different concentrations of silicone oil (SO) to castor oil: (a) 5%, (b) 10% and (c) 15%. (d) A summary of the values of temperature elevations after 30 s of measurements for pre-emulsions (P) and emulsions (E) with different magnetic particles to silicone oil mass ratios. The intensity of magnetic field was 16.2 kA/m.

The results in Fig. 6 show the same dependence on the concentration of magnetite particles used in the experiments as in Fig. 5. Also, the differences between pre-emulsions and emulsions are clear for bigger

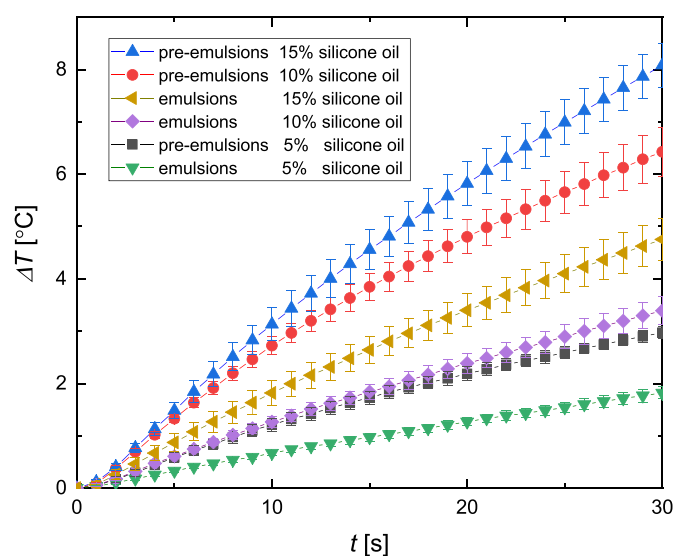


Fig. 7. Temperature increase vs. time recorded in the samples of pre-emulsions and emulsions stabilized with functionalized nanoparticles OA-MPs placed in the alternating magnetic field for different concentrations of silicone oil (SO) to castor oil. Magnetic nanoparticles – silicone oil mass ratio was constant (1:4) and the intensity of magnetic field was 16.2 kA/m.

magnetite particles. It must be noted here, that, due to the size of particles, the Brown relaxation does not dominate anymore, so this difference should not be explained with the potential inhibition of Brown relaxations. The heating efficiency for systems stabilized with μ MPs is, however, much better. It is reflected in significantly higher temperature increase when comparing the results for the same concentrations of silicone oils and particles in Figs. 5 and 6. The reason is additional magnetic energy loss in large particles due to the magnetic hysteresis. For the same magnetic field intensity, magnetic energy loss is higher for the mechanism of hysteresis (see, Eq. (3)). Hysteresis can occur also in case of our smaller particles (nMPs) because of polydispersity, but it is not dominating, so it does not help in better heating performance so much.

In general, results that one can find in the literature on parameters responsible for magnetic heating efficiency differs from study to study. It is because the obtaining results depends on mutual connections

Table 1

Temperature increase after 30 s in the alternating magnetic field for pre-emulsions and emulsions stabilized with different magnetite particles for magnetic particles – silicone oil mass ratio 1:4. The intensity of magnetic field was 16.2 kA/m.

Particles (for 1:4 MPs:SO, 30 s in AMF)		ΔT for 5% SO [°C]	ΔT for 10% SO [°C]	ΔT for 15% SO [°C]
OA-MPs	Emulsions	2.97 ± 0.10	6.43 ± 0.47	8.08 ± 0.42
	Pre-emulsions	1.82 ± 0.12	3.39 ± 0.27	4.75 ± 0.40
nMPs	Emulsions	6.16 ± 0.74	12.69 ± 0.65	16.66 ± 1.61
	Pre-emulsions	3.80 ± 0.09	9.11 ± 0.89	14.81 ± 1.39
μ MPs	Emulsions	11.79 ± 1.24	20.35 ± 1.20	32.50 ± 1.79
	Pre-emulsions	9.08 ± 0.99	15.38 ± 2.20	25.56 ± 2.42

between properties of magnetic materials and the magnetic field applied. However, we proved that the increasing concentration regardless particle sizes leads to better efficiency of magnetic heating for Pickering emulsions as well as increasing the size of particle. As different mechanisms of heating (i.e. relaxation and hysteresis losses) can contribute to the efficiency of the process at the same time, in the next paragraph we evaluate this contribution.

3.2. The effect of magnetic field intensity on heating rate of Pickering emulsions

As it was stated in **Introduction** section, the magnetic heating efficiency does not only depend on properties of magnetic materials used but also on properties of applied magnetic fields. Fig. 8 presents the dependences of specific absorption rate vs. magnetic field intensity measured in pre-emulsions and emulsions stabilized with different magnetite particles. Specific absorption rate (SAR) is a measure of heating efficiency and is commonly used for comparison between different samples in magnetic heating measurements [34]. The most popular expression for SAR is:

$$SAR = \frac{c_p}{m_{magnetite}} \cdot \frac{dT}{dt} \quad (4)$$

where c_p is here a specific heat calculated for the mixture of magnetite, silicone oil and castor oil, $\frac{dT}{dt}$ is the initial temperature rise rate and $m_{magnetite}$ is a mass of magnetite particles used in given sample. Most of works present the results of SAR in $[W/g_{magnetite}]$. It is not a correct unit for SAR, however we also expressed our results in such values in this study.

The dissipated magnetic power loss under the alternating magnetic field (P) can be expressed as:

$$P = A \cdot H^n \quad (5)$$

where H is an amplitude of the alternating magnetic field intensity, n is a derived parameter and A is a coefficient. Many of authors suggest that the value of n indicates the dominating mechanism of magnetic energy dissipation (i.e. $n = 2$ for Brown and Néel relaxation, $n = 3$ for hysteresis loss), as was reflected also in Eqs. (1) and (3). But, the curves fitted in Fig. 8 do not increase with the power of 2 or 3. It means that our systems are much more complex than simple magnetic fluids and because of additional mechanisms influencing the process of magnetic heating such as interactions between particles, basic assumptions can be compromised [35]. A supporting influence of interactions may be reflected in higher values of n both for **nMPs** and **μMPs**.

In Fig. 8, the differences in magnetic heating of pre-emulsions and emulsions are the more significant, the higher amplitude of magnetic field is used. For low values of H , both for droplets with stable particle shell around them and for pre-emulsions, the functions increased in the same way. This observation relates to **nMPs** and **μMPs**, however, for **nMPs** the differences in temperature increase rate seem to be the less significant. At the same time, according to the Eq. (3), the higher intensity of the alternating magnetic field causes the higher contribution of hysteresis mechanism comparing to relaxation [36]. What is interesting, the heating of pre-emulsions stabilized with **OA-MPs** is significantly higher even for very low values of the magnetic field intensity. It can stem from the fact, that for this nanoparticles the effect of Brown relaxation was not restrained in non-completely stable emulsions, while

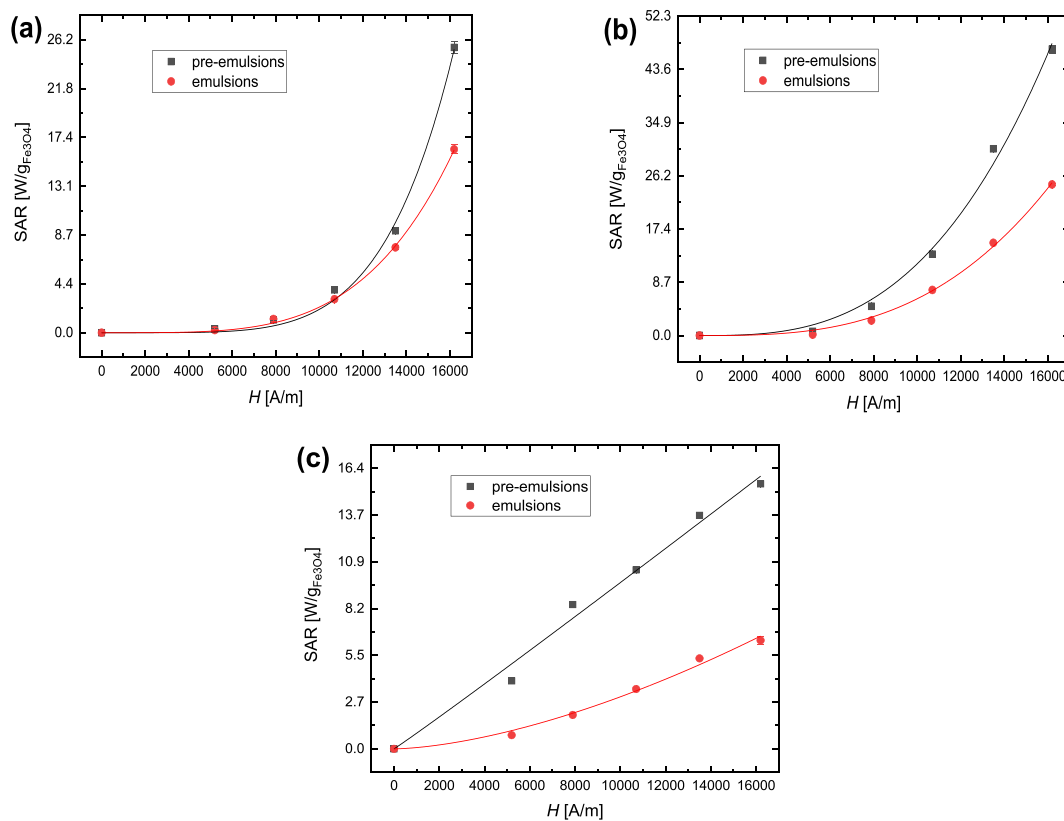


Fig. 8. Specific absorption rate (SAR) vs. alternating magnetic field intensity for different magnetite particles used to stabilize emulsions systems: (a) **nMPs**, (b) **μMPs** and (c) **OA-MPs**. The concentration of silicone oil in relation to castor oil was 10% w/w and magnetite particles to silicone oil mass ratio was 1:4 in each samples. The values for measurement points were fitted to the function like in Eq. (5).

after the stabilization in the electric field, the oscillations of particles were inhibited.

4. Discussion

Our paper aimed to show the influence of the solidity of particle shell on magnetic heating in the system with particle-stabilized droplets. As it was shown above, this difference occurred regardless the particle sizes, concentrations and magnetic field (although, for low intensities it was merely observed, see Fig. 8). This lack of dependence of mechanism on this key difference is depicted in Fig. 9, where specific absorption rates were plotted for three types of magnetic particles.

We already showed that the temperature elevation in our samples was higher when bigger magnetite particles were used. At the same time, the way the temperature increased for emulsions and pre-emulsions seems to be similar. It can mean that both for stable and merely stable emulsions this dependence is fulfilled. However, our systems are much more complicated than traditional magnetic fluids. Also, the obtained results differ from those from other papers. The SAR values for pre-emulsions ranged from 15 W/g to 40 W/g for the maximum settings of our setup (16.2 kA/m). We find comparing pre-emulsions rather than emulsions with the literature more reasonable since they are more similar to two-phase systems such as ferrofluids. In works on ferrofluids, scientists have obtained really diverse SAR values, ranged from 120 to 750 W/g [37–40], sometimes only 20 W/g [41] or, on the contrary, even 2000–3000 W/g [42,43]. It must be emphasized here that results are strongly dependent on parameters used in the study, mostly magnetite particle size, magnetic field intensity, and a carrier liquid. For other magnetic material, for instance, in case of magnetosomes used as magnetic material, maximum reported SAR values were about 500 W/g [44,45]. Also, SAR values, although usually presented, are calculated using different formulas.

Some authors have suggested that for samples where particle-particle interactions are negligible, SAR values (expressed in $W/g_{magnetite}$ units) increase linearly with the concentration of magnetic material used in given dispersion [46]. For our emulsion systems there was no significant dependence of SAR on mass concentration of magnetite. However, after averaging the results, the SAR values were significantly higher for pre-emulsions than for emulsions after electro-coalescence as is presented in Fig. 9. What is interesting, the most significant difference is for droplets coated by OA-MPs what seems to correspond very

well with the observed difference between magnetization for pre-emulsions and emulsions (see, Fig. 3a).

Describing the heating efficiency of particles attached to the droplets interface brings new aspects to be taken into account. At the droplet surface, particles are in different spatial arrangement comparing to the particles dispersed in the fluid. We can term these structures as hollow clusters. When clusters consisted of small magnetic particles dispersed in a liquid were studied under the AC magnetic field, the heating efficiency was better for single particles than for clusters [33,47]. The same is for our results in Fig. 5–7. If we assume that in case of emulsions after the additional stabilization in the electric field droplets are densely covered by particles, their affinity to clusters is better that is reflected in worse heating performance for emulsions comparing to pre-emulsions stabilized with each kind of magnetic particles. Our droplets covered by particles can be somehow compared to the systems described in works of Taketomi et al. [48,49]. In that studies, particles were entrapped in the micellar structures and interactions between particles was found to be responsible for a decrease in a residual magnetization of samples. Such interactions should be stronger for bigger particles, but, as it was already stated in our paper, interactions do not always facilitate a generation of heat [50].

As was shown in work of Hu et al. [51], mechanisms in the alternating magnetic field that occur for small particles (Brown and Néel relaxations) can be used not only to induce a temperature rise but also to accelerate the microstructural evolution on the droplet interfaces because of stress developing in the thin shells. In our experiments, we used radio-frequency magnetic field (356 kHz) to induce heating in the magnetite-stabilized emulsions. However, also lower (or even extremely lower) frequencies can be used i.e. to alter the permeability of colloidal capsules shell when consisting magnetic particles [52].

A number of studies provides insight into the properties and structure of magnetic Pickering emulsions. Some of these emulsions were formed with sufficient stability by using ultrasonic homogenization [53–56]. In our experiments, we showed that for O/O emulsions stabilized with magnetite particles, the ultrasonic homogenization is not sufficient for fabricating completely stable emulsions. Although, even partial coverage of particles may, under certain conditions, lead to kinematic stability of droplets [57,58], the difference in coverage influences also heating efficiency what is important when it comes to potential applications. What is more, for dense particle layer constituting a shell around the droplet, the inside of droplet can be heated to the higher temperature and this temperature can remain increased longer. The thermal expansion is there more severe and it could cause loosening the shell and enable a release from the inside. Such concept could be utilized in theranostic applications – parallel imaging, heating and drug release by using the same carriers. It would be for particles that are not soft particles. For soft particles mixed with the magnetic ones, the rigid shell can be formed [21]. For droplets where magnetic particles are entrapped inside and subsequently placed in the alternating magnetic field [12], heating up the droplet from the inside could also change the thermal expansion of a droplet. But, Brown relaxation cannot be inhibited because the oscillating movement of particles inside a droplet is not hindered as it can be for the particles residing the oil-oil interface. Heating efficiency measured macroscopically could be different comparing to the situation when the magnetic particle shell is around the droplet and it can be significant especially for small particles where relaxation phenomena dominate in the process of magnetic heating.

When it comes to potential application in medicine, the important issue seems to be the size of objects used as heating agents. On the one hand, the small particles can be easily transferred through the arteries in a body and form more stable colloids [31]. But, also relatively large magnetic particles could be used because of better heating performance and, what is more interesting in this context, difficulties with washing them away the tumor comparing to smaller magnetic particles [35]. Also bigger objects, like droplets covered by magnetic particles with evidenced heating performance are therefore worth being studied.

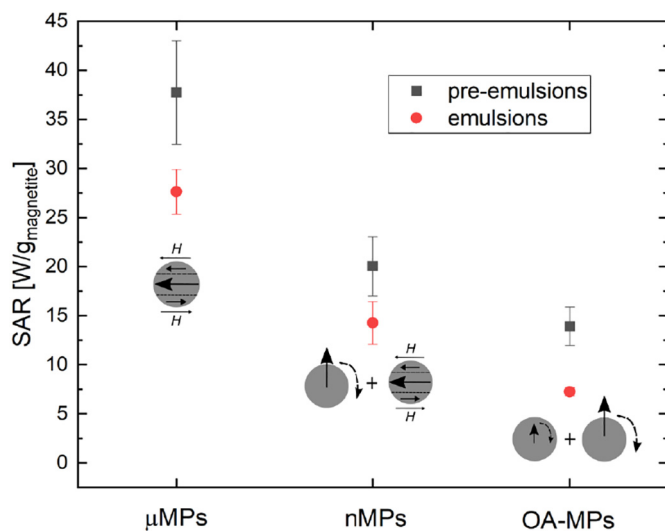


Fig. 9. Specific absorption rate values (Eq. (4)) averaged for different mass concentrations of magnetite (0.5–6.1% depending upon the sample) for different types of particles. The intensity of magnetic field was 16.2 kA/m.

Emulsion droplets could be used also e.g. to enhance ultrasound imaging. Additionally, such droplets could be used in double modalities by coupling at the same time heating and imaging (theranostics) [59]. Considering the potential application for systems consisting of magnetic particles must be linked to the discussion on their toxicity. In general, many studies have shown toxic effects in cells linked to the exposition to nanomaterials, like DNA damage or oxidative stress with its long-term consequences [60]. The main reason responsible for them is the generation of free radicals. When the damage of cancer cells is the aim of therapy, the toxicity of particles is desirable. However, magnetic particles used as heating agents should not be additionally toxic, among others, because hyperthermia is an adjunctive therapy for other medical procedures, namely radio-, and chemotherapy. Experimental studies showed that magnetic nanoparticles generate greater toxicity for living cells when they are not coated by a biocompatible layer [61]. Also, oleic acid is used as a surfactant for the coating of magnetic particles to achieve their biocompatibility [62]. The problem with the toxicity of particles could be more serious for a large amount of magnetic material used in therapy. Intravenous administration of therapeutic substances is the primary way to introduce them into a body [63]. However, it was found that only a small amount of provided substances was captured in destined tissues [64]. That is why the significant amounts of magnetic material must be applied to ensure their high enough concentration in tissues. It could bear the risk of side effects for the whole human body. The studies on mice on magnetic hyperthermia using ferrofluids show that an excess of magnetic material accumulates in a liver, spleen and, what is important in regards to our work, no differences in accumulation of particles were detected comparing experiments without and with magnetic heating [65].

5. Conclusions

In this study, we reported the differences in heating efficiency between emulsions with droplets barely and successfully covered by magnetite particles placed in AC magnetic field. The temperature elevation recorded in Pickering emulsions stabilized under the electric field was lower than for coarse emulsions prepared only during quick ultrasonic homogenization. These results were observed for a wide range of inner phase concentrations and for magnetite particles of different sizes (tens of nanometers, hundreds of nanometers and micrometers). The proposed explanation is that a dense particle shell around droplets interfered the heat transfer in such system, i.e. the inside of droplet enclosed by particles owing to a heating in nano- and microscale remained the high-temperature zone, but the heat cannot transfer into the continuous phase of emulsion where the temperature sensor was placed. It can bring some implications when it comes to potential magnetic hyperthermia therapy using magnetic Pickering droplets. As we can see, the stable droplets, despite of their potential in drug delivery via intravenous therapies, exhibit worse heating performance comparing to colloidal systems more similar to magnetic fluids.

Author contribution

AJ and RB developed a concept of experiments and designed them. RB performed the calorimetric experiments, as well as analyzed and presented the data. KP prepared magnetic particles functionalized with oleic acid. MR performed magnetic measurements of samples. RB wrote the first version of the manuscript. All authors contributed to the finalization of the manuscript.

Declaration of competing interest

The authors declare that they have no known competing financial interests or personal relationships that could have appeared to influence the work reported in this paper.

Acknowledgments

The authors would like to acknowledge Polish National Science Centre for support through the project no. 2019/35/N/ST5/00402 (PRELUDIUM) and Slovak Academy of Sciences and Ministry of Education in the framework of project VEGA 2/0011/20, and Slovak Research and Development Agency under the Contract No. APVV-18-0160.

References

- [1] D. Gonzalez Ortiz, C. Pochat-Bohatier, J. Cambedouzo, M. Bechelany, P. Miele, Current trends in Pickering emulsions: particle morphology and applications, *Engineering* 6 (2020) 468–482.
- [2] C.L.G. Harman, M.A. Patel, S. Guldin, G.-L. Davies, Recent developments in Pickering emulsions for biomedical applications, *Curr. Opin. Colloid Interface Sci.* 39 (2019) 173–189.
- [3] L.E. Low, S.P. Siva, Y.K. Ho, E.S. Chan, B.T. Tey, Recent advances of characterization techniques for the formation, physical properties and stability of Pickering emulsion, *Adv. Colloid Interf. Sci.* 277 (2020), 102117.
- [4] B. Brugger, W. Richtering, Magnetic, Thermosensitive microgels as stimuli-responsive emulsifiers allowing for remote control of Separability and stability of oil in water-emulsions, *Adv. Mater.* 19 (19) (2007) 2973–2978.
- [5] H. Yang, H. Zhang, J. Peng, Y. Zhang, G. Du, Y. Fang, Smart magnetic ionic liquid-based Pickering emulsions stabilized by amphiphilic Fe₃O₄ nanoparticles: highly efficient extraction systems for water purification, *J. Colloid Interface Sci.* 485 (2017) 213–222.
- [6] H. Wang, K.-Y. Lin, B. Jing, G. Krylova, G.E. Sigmon, P. McGinn, Y. Zhu, C. Na, Removal of oil droplets from contaminated water using magnetic carbon nanotubes, *Water Res.* 47 (12) (2013) 4198–4205.
- [7] J.-H. Park, A.M. Derfus, E. Segal, K.S. Vecchio, S.N. Bhatia, M.J. Sailor, Local heating of discrete droplets using magnetic porous silicon-based photonic crystals, *J. Am. Chem. Soc.* 128 (24) (2006) 7938–7946.
- [8] M. Okochi, H. Tsuchiya, F. Kumazawa, M. Shikida, H. Honda, Droplet-based gene expression analysis using a device with magnetic force-based-droplet-handling system, *J. Biosci. Bioeng.* 109 (2) (2010) 193–197.
- [9] Z. Li, P. Wang, L. Tong, L. Zhang, Local heating of individual droplets using photothermal effects of gold nanorods, 2012 Asia Communications and Photonics Conference (ACP) 2012, pp. 1–3.
- [10] A. Kaiser, T. Liu, W. Richtering, A.M. Schmidt, Magnetic capsules and Pickering emulsions stabilized by Core–Shell particles, *Langmuir* 25 (13) (2009) 7335–7341.
- [11] B.B. Lahiri, S. Ranoo, J. Philip, Effect of orientational ordering of magnetic nanoemulsions immobilized in agar gel on magnetic hyperthermia, *J. Magn. Magn. Mater.* 451 (2018) 254–268.
- [12] B.B. Lahiri, S. Ranoo, A.W. Zaibudeen, J. Philip, Magnetic hyperthermia in magnetic nanoemulsions: effects of polydispersity, particle concentration and medium viscosity, *J. Magn. Magn. Mater.* 441 (2017) 310–327.
- [13] A.P. Guimarães, A.P. Guimarães, Principles of Nanomagnetism, Springer, 2009.
- [14] Q.A. Pankhurst, J. Connolly, S.K. Jones, J. Dobson, Applications of magnetic nanoparticles in biomedicine, *J. Phys. D: Appl. Phys.* 36 (13) (2003) R167–R181.
- [15] R.E. Rosensweig, Heating magnetic fluid with alternating magnetic field, *J. Magn. Magn. Mater.* 252 (2002) 370–374.
- [16] J. Estelrich, E. Escribano, J. Queralt, M.A. Busquets, Iron oxide nanoparticles for magnetically-guided and magnetically-responsive drug delivery, *Int. J. Mol. Sci.* 16 (4) (2015) 8070–8101.
- [17] R. Hiergeist, W. Andrä, N. Buske, R. Hergt, I. Hilger, U. Richter, W. Kaiser, Application of magnetite ferrofluids for hyperthermia, *J. Magn. Magn. Mater.* 201 (1) (1999) 420–422.
- [18] M. Kachniarz, R. Szweczyk, Study on the Rayleigh hysteresis model and its applicability in modeling magnetic hysteresis phenomenon in ferromagnetic materials, *Acta Phys. Pol. A* 131 (5) (2017).
- [19] A. Skumiel, K. Kaczmarek, D. Flak, M. Rajnak, I. Antal, H. Brząkała, The influence of magnetic nanoparticle concentration with dextran polymers in agar gel on heating efficiency in magnetic hyperthermia, *J. Mol. Liq.* 304 (2020), 112734.
- [20] J.C. Bear, P.S. Patrick, A. Casson, P. Southern, F.-Y. Lin, M.J. Powell, Q.A. Pankhurst, T. Kalber, M. Lythgoe, I.P. Parkin, A.G. Mayes, Magnetic hyperthermia controlled drug release in the GI tract: solving the problem of detection, *Sci. Rep.* 6 (1) (2016), 34271.
- [21] R. Bielas, D. Surdeko, K. Kaczmarek, A. Józefczak, The potential of magnetic heating for fabricating Pickering-emulsion-based capsules, *Colloids Surf. B: Biointerfaces* 192 (2020), 111070.
- [22] Y. Chevalier, M.-A. Bolzinger, Emulsions stabilized with solid nanoparticles: Pickering emulsions, *Colloids Surf. A Physicochem. Eng. Asp.* 439 (2013) 23–34.
- [23] B.P. Binks, A.T. Tyowua, Oil-in-oil emulsions stabilised solely by solid particles, *Soft Matter* 12 (3) (2016) 876–887.
- [24] S.J. Kemp, R.M. Ferguson, A.P. Khandhar, K.M. Krishnan, Monodisperse magnetite nanoparticles with nearly ideal saturation magnetization, *RSC Adv.* 6 (81) (2016) 77452–77464.
- [25] Z. Rozynek, R. Bielas, A. Józefczak, Efficient formation of oil-in-oil Pickering emulsions with narrow size distributions by using electric fields, *Soft Matter* 14 (24) (2018) 5140–5149.
- [26] R. Bielas, Z. Rozynek, T. Hornowski, A. Józefczak, Ultrasound control of oil-in-oil Pickering emulsions preparation, *J. Phys. D: Appl. Phys.* 53 (8) (2019), 085301.

- [27] A. Mikkelsen, K. Khobai, F.K. Eriksen, K.J. Måløy, Z. Rozynek, Particle-covered drops in electric fields: drop deformation and surface particle organization, *Soft Matter* 14 (26) (2018) 5442–5451.
- [28] M. Rajnak, V.I. Petrenko, M.V. Avdeev, O.I. Ivankov, A. Feoktystov, B. Dolnik, J. Kurimsky, P. Kopcansky, M. Timko, Direct observation of electric field induced pattern formation and particle aggregation in ferrofluids, *Appl. Phys. Lett.* 107 (7) (2015), 073108.
- [29] M. Osaci, M. Cacciola, The influence of the magnetic nanoparticles coating from colloidal system on the magnetic relaxation time, *Beilstein Archives* 2019 (2019) 154.
- [30] Q. Ding, D. Liu, D. Guo, F. Yang, X. Pang, R. Che, N. Zhou, J. Xie, J. Sun, Z. Huang, N. Gu, Shape-controlled fabrication of magnetite silver hybrid nanoparticles with high performance magnetic hyperthermia, *Biomaterials* 124 (2017) 35–46.
- [31] A.E. Deatsch, B.A. Evans, Heating efficiency in magnetic nanoparticle hyperthermia, *J. Magn. Magn. Mater.* 354 (2014) 163–172.
- [32] C. Haase, U. Nowak, Role of dipole-dipole interactions for hyperthermia heating of magnetic nanoparticle ensembles, *Phys. Rev. B* 85 (4) (2012), 045435.
- [33] K. Kaczmarek, R. Mrówczyński, T. Hornowski, R. Bielas, A. Józefczak, The effect of tissue-mimicking phantom compressibility on magnetic hyperthermia, *Nanomaterials* 9 (5) (2019) 803.
- [34] E.A. Périgo, G. Hemery, O. Sandre, D. Ortega, E. Garaio, F. Plazaola, F.J. Teran, Fundamentals and advances in magnetic hyperthermia, *Appl. Phys. Rev.* 2 (4) (2015), 041302.
- [35] A.Y. Zubarev, L.Y. Iskakova, A.P. Safronov, R.V. Krekhno, D.K. Kuznetsov, I.V. Beketov, Positive feedback of interparticle interaction on magnetic hyperthermia, *J. Magn. Magn. Mater.* 489 (2019), 165402.
- [36] A. Józefczak, B. Leszczyński, A. Skumiel, T. Hornowski, A comparison between acoustic properties and heat effects in biogenic (magnetosomes) and abiotic magnetite nanoparticle suspensions, *J. Magn. Magn. Mater.* 407 (2016) 92–100.
- [37] M.S.A. Darwish, Effect of carriers on heating efficiency of oleic acid-stabilized magnetite nanoparticles, *J. Mol. Liq.* 231 (2017) 80–85.
- [38] A. Skumiel, T. Hornowski, A. Józefczak, Heating characteristics of transformer oil-based magnetic fluids of different magnetic particle concentrations, *Int. J. Thermophys.* 32 (4) (2011) 876–885.
- [39] J. Mohapatra, F. Zeng, K. Elkins, M. Xing, M. Ghimire, S. Yoon, S.R. Mishra, J.P. Liu, Size-dependent magnetic and inductive heating properties of Fe₃O₄ nanoparticles: scaling laws across the superparamagnetic size, *Phys. Chem. Chem. Phys.* 20 (18) (2018) 12879–12887.
- [40] P.I.P. Soares, C.A.T. Laia, A. Carvalho, L.C.J. Pereira, J.T. Coutinho, I.M.M. Ferreira, C.M.M. Novo, J.P. Borges, Iron oxide nanoparticles stabilized with a bilayer of oleic acid for magnetic hyperthermia and MRI applications, *Appl. Surf. Sci.* 383 (2016) 240–247.
- [41] B.B. Lahiri, S. Rano, T. Muthukumar, J. Philip, S. Singh, A. Biswas, A. Das, Magnetic hyperthermia in water based ferrofluids: effects of initial susceptibility and size polydispersity on heating efficiency, *AIP Conference Proceedings* 1942 (1) (2018), 040019.
- [42] S. Tong, C.A. Quinto, L. Zhang, P. Mohindra, G. Bao, Size-dependent heating of magnetic iron oxide nanoparticles, *ACS Nano* 11 (7) (2017) 6808–6816.
- [43] O.L. Lanier, O.I. Korotych, A.G. Monsalve, D. Wable, S. Savliwala, N.W.F. Grooms, C. Nacea, O.R. Tuitt, J. Dobson, Evaluation of magnetic nanoparticles for magnetic fluid hyperthermia, *Int. J. Hyperth.* 36 (1) (2019) 686–700.
- [44] M. Molcan, H. Gojzewski, A. Skumiel, S. Dutz, J. Kovac, M. Kubovcikova, P. Kopcansky, L. Vekas, M. Timko, Energy losses in mechanically modified bacterial magnetosomes, *J. Phys. D: Appl. Phys.* 49 (36) (2016), 365002.
- [45] N.A. Usov, E.M. Gubanova, Application of magnetosomes in magnetic hyperthermia, *Nanomaterials* 10 (7) (2020) 1320.
- [46] M. Etheridge, J.C. Bischof, Optimizing magnetic nanoparticle based thermal therapies within the physical limits of heating, *Ann. Biomed. Eng.* 41 (1) (2013) 78–88.
- [47] R. Fu, Y. Yan, C. Roberts, Z. Liu, Y. Chen, The role of dipole interactions in hyperthermia heating colloidal clusters of densely-packed superparamagnetic nanoparticles, *Sci. Rep.* 8 (1) (2018) 4704.
- [48] S. Taketomi, R.V. Drew, R.D. Shull, Anomalous magnetic aftereffect of a frozen magnetic fluid, *IEEE Trans. Magn.* 40 (4) (2004) 3039–3041.
- [49] S. Taketomi, R.V. Drew, R.D. Shull, Peculiar magnetic aftereffect of highly diluted frozen magnetic fluids, *J. Magn. Magn. Mater.* 307 (1) (2006) 77–84.
- [50] G. Salas, S. Veintemillas-Verdaguer, M.d.P. Morales, Relationship between physico-chemical properties of magnetic fluids and their heating capacity, *Int. J. Hyperth.* 29 (8) (2013) 768–776.
- [51] S.-H. Hu, C.-H. Tsai, C.-F. Liao, D.-M. Liu, S.-Y. Chen, Controlled rupture of magnetic polyelectrolyte microcapsules for drug delivery, *Langmuir* 24 (20) (2008) 11811–11818.
- [52] D. Luo, R.N. Poston, D.J. Gould, G.B. Sukhorukov, Magnetically targetable microcapsules display subtle changes in permeability and drug release in response to a biologically compatible low frequency alternating magnetic field, *Mater. Sci. Eng. C* 94 (2019) 647–655.
- [53] J.A. Flores, A.A. Jahnke, A. Pavia-Sanders, Z. Cheng, K.L. Wooley, Magnetically-active Pickering emulsions stabilized by hybrid inorganic/organic networks, *Soft Matter* 12 (46) (2016) 9342–9354.
- [54] A. Józefczak, R. Wlazło, Ultrasonic studies of emulsion stability in the presence of magnetic nanoparticles, *Advances in Condensed Matter Physics* 2015 (2015), 398219.
- [55] L.E. Low, B.T. Tey, B.H. Ong, E.S. Chan, S.Y. Tang, Palm olein-in-water Pickering emulsion stabilized by Fe₃O₄-cellulose nanocrystal nanocomposites and their responses to pH, *Carbohydr. Polym.* 155 (2017) 391–399.
- [56] L.E. Low, B.H. Ong, B.T. Tey, S.Y. Tang, Factors affecting the stability and physical properties of Pickering emulsions stabilized by Fe₃O₄@CNC Nanocomposites, *Progress in Drug Discovery & Biomedical Science* 3 (1) (2020).
- [57] F. Gautier, M. Destribats, R. Perrier-Cornet, J.-F. Dechézelles, J. Giermanska, V. Héroguez, S. Ravaine, F. Leal-Calderon, V. Schmitt, Pickering emulsions with stimutable particles: from highly- to weakly-covered interfaces, *Phys. Chem. Chem. Phys.* 9 (48) (2007) 6455–6462.
- [58] T.S. Horozov, B.P. Binks, Particle-stabilized emulsions: a bilayer or a bridging monolayer? *Angew. Chem. Int. Ed.* 45 (5) (2006) 773–776.
- [59] A. de Leon, P. Wei, F. Bordera, D. Wegierak, M. McMillen, D. Yan, C. Hemmingsen, M.C. Kolios, E.B. Pentzer, A.A. Exner, Pickering bubbles as dual-modality ultrasound and Photoacoustic contrast agents, *ACS Appl. Mater. Interfaces* 12 (2020) 22308–22317.
- [60] A. Erofeev, P. Gorelkin, A. Garanina, A. Alova, M. Efreanova, N. Vorobyeva, C. Edwards, Y. Korchev, A. Majouga, Novel method for rapid toxicity screening of magnetic nanoparticles, *Sci. Rep.* 8 (1) (2018) 7462.
- [61] M. Mahmoudi, A. Simchi, M. Imani, M.A. Shokrgozar, A.S. Milani, U.O. Häfeli, P. Stroeve, A new approach for the in vitro identification of the cytotoxicity of superparamagnetic iron oxide nanoparticles, *Colloids Surf. B: Biointerfaces* 75 (1) (2010) 300–309.
- [62] M. Mahdavi, M.B. Ahmad, M.J. Haron, F. Namvar, B. Nadi, M.Z.A. Rahman, J. Amin, Synthesis, surface modification and characterisation of biocompatible magnetic iron oxide nanoparticles for biomedical applications, *Molecules* 18 (7) (2013) 7533–7548.
- [63] T. Kubiak, Nanoparticles as radiosensitizers in photon and hadron radiotherapy, *Acta Bio-Optica et Informatica Medica. Inżynieria Biomedyczna* 23 (1) (2017).
- [64] S.-J. Seo, J.-K. Jeon, E.-J. Jeong, W.-S. Chang, G.-H. Choi, J.-K. Kim, Enhancement of tumor regression by coulomb nanoradiator effect in proton treatment of iron-oxide nanoparticle-loaded orthotopic rat glioma model: implication of novel particle induced radiation therapy, *Journal of Cancer Therapy* 4 (11) (2013) 25.
- [65] M. Kettering, H. Richter, F. Wiekhorst, S. Bremer-Streck, L. Trahms, W.A. Kaiser, I. Hilger, Minimal-invasive magnetic heating of tumors does not alter intra-tumoral nanoparticle accumulation, allowing for repeated therapy sessions: an in vivo study in mice, *Nanotechnology* 22 (50) (2011), 505102.

[Publication IV]

The effect of particle shell on cooling rates in oil-in-oil magnetic
Pickering emulsions

R. Bielas, A. Józefczak

Materials, 2020, 13(21): 4783.

Article

The Effect of Particle Shell on Cooling Rates in Oil-in-Oil Magnetic Pickering Emulsions

Rafał Bielas * and Arkadiusz Józefczak *

Chair of Acoustics, Faculty of Physics, Adam Mickiewicz University in Poznań, Uniwersytetu Poznańskiego 2, 61-614 Poznań, Poland

* Correspondence: rafal.bielas@amu.edu.pl (R.B.); aras@amu.edu.pl (A.J.)

Received: 9 October 2020; Accepted: 23 October 2020; Published: 26 October 2020

Abstract: Pickering emulsions (particle-stabilized emulsions) are usually considered because of their unique properties compared to surfactant-stabilized emulsions including better stability against emulsion aging. However, the interesting feature of particle-stabilized emulsions could be revealed during their magnetic heating. When magnetic particles constitute a shell around droplets and the sample is placed in an alternating magnetic field, a temperature increase appears due to energy dissipation from magnetic relaxation and hysteresis within magnetic particles. We hypothesize that the solidity of the magnetic particle shell around droplets can influence the process of heat transfer from inside the droplet to the surrounding medium. In this way, particle-stabilized emulsions can be considered as materials with changeable heat transfer. We investigated macroscopically heating and cooling of oil-in-oil magnetic Pickering emulsions with merely packed particle layers and these with a stable particle shell. The change in stability of the shell was obtained here by using the coalescence of droplets under the electric field. The results from calorimetric measurements show that the presence of a stable particle shell caused a slower temperature decrease in samples, especially for lower intensities of the magnetic field. The retarded heat transfer from magnetic Pickering droplets can be utilized in further potential applications where delayed heat transfer is desirable.

Keywords: Pickering emulsion; particle-stabilized emulsion; magnetic heating; magnetic field; coalescence; calorimetric measurements

1. Introduction

Emulsions are ubiquitous systems utilized in a very broad range of industrial branches, in medicine, and in our daily life. In the last decades, emulsions stabilized with surfactants have been gradually replaced by Pickering emulsions, i.e., emulsions stabilized with particles rather than surface-active chemicals. Such systems are indicated as more eco-friendly promising materials for food processing [1,2], industrial applications such as oil recovery [3,4] or protection of wood [5], and formulation of new pharmaceuticals [6,7]. The unique properties of particles used as stabilizers open new opportunities for practical use, such as a controlled release of cargo encapsulated in droplets under external stimuli. In this context, magnetic Pickering emulsions are often invoked. The shell around emulsion droplets consisting of materials susceptible to the magnetic field can result in the controlled positioning of droplets [8]. The alternating magnetic field can induce relaxation processes (namely Néel and Brown) or magnetic hysteresis in magnetic particles that lead to losses of magnetic energy [9]. This energy dissipation is converted into heat, which is a well-known fact utilized, among others, in magnetic hyperthermia therapies [10,11] and magnetically-induced catalysis to perform reactions such as CO₂ methanation [12]. This fact also makes the heating generated in magnetic Pickering emulsions the potential object of interest.

In Pickering emulsions, particles adsorb to the droplet surface due to capillary forces. The solid particle shell formed in such a way prevents coalescence of the droplets and Oswald ripening [13]. However, when magnetic particles are used as stabilizers, their presence alters not only the stability of emulsion droplets. During the application of the AC magnetic field, every particle is a source of heat. The fact that they reside in the interface between the droplet and surrounding medium results in heating both the inside of the droplet and the layer around the droplet. The heat transfer from the droplet inside might be somehow retarded, especially for the high-temperature increase, because of solidity of the shell. This can influence the therapeutic effect when Pickering droplets would be used in magnetic hyperthermia, but it can also open new applications of this material, that is, the material having a heat transfer latency.

It is well-known that particles can enhance the properties of liquids serving as coolants e.g., in transformers. Additionally, magnetic particles were used to enrich cooling transformer oils because they may improve thermal conductivity [14], so the elements of the transformer can be better protected against over-heating. In the case of Pickering droplets capsulated in a solid magnetic particle shell, the situation can be opposite as the heat transfer through the emulsion with droplets coated by magnetic particles and immersed in surrounding liquid is hindered. Potentially, the heat entrapped within the droplet could be transported and released under external stimuli in the destined place. To prove the existence of the aforementioned phenomenon, the comparison between emulsion systems in two different stages, i.e., one with droplets poorly coated with magnetite particles and another with a reinforced particle shell, was performed. The use of a two-step approach to fabricating Pickering emulsions by using ultrasound homogenization and an electric field [15] gives us the unique opportunity to test droplets with varying degrees of coverage by solid particles. As we will show, this difference also influenced also the process of heat transfer that is reflected in different cooling rates.

To investigate the process of cooling in a quantitative way the so-called Newton's law can be used [16]. In the case of our study, the temporal temperature measured in the emulsion system after the alternating magnetic field is turned off can be expressed as [17]:

$$T(t) = T_{sur} + (T_0 - T_{sur})exp\left(-\frac{t}{\tau}\right), \quad (1)$$

where T_{sur} refers to the temperature of the medium surrounding the sample, T_0 is the temperature at the beginning of the cooling process and τ is a derived parameter, the cooling time constant that can be considered as a measure of cooling rate. Another approach is also possible. Usually, to evaluate the heating performance of a given medium, non-adiabatic setups are used. This is because the measurements using adiabatic systems are time-consuming, expensive, and hard to construct. However, the measurements under non-adiabatic conditions can be still be considered as reliable. They are very common but, some reports suggest the strong need of including quantified non-adiabatic losses into the calculation of the final results [18]. Under the non-adiabatic conditions of calorimetric measurements commonly represented in scientific papers, the loss of provided external energy from the sample to the environment starts when the temperature of the sample exceeds the temperature of the surrounding medium. This loss is due to three main mechanisms, i.e., thermal conduction, convection, and radiation. Because the effect of those mechanisms is dependent on the temperature gradient inside the sample to varying degrees, the non-linear relation between the temperature T and power loss can be expressed as [18,19]:

$$c_p \cdot \frac{dT(t)}{dt} = P + L\Delta T + B\Delta T^2 + C\Delta T^3 + R\Delta T^4 \quad (2)$$

where c_p is the specific heat of the sample, P is the power provided in the process of heating, and the parameters L , B , C , and R are coefficients in a fourth-order polynomial. The order of the polynomial is motivated by the mechanism of thermal radiation that depends on the fourth power of temperature difference and certainly occurs. According to [18,19], for small differences between the temperature of the surrounding medium and the temperature of the sample, it should be possible to simplify the abovementioned expression to the linear relation.

In this work, we performed the calorimetric measurements under non-adiabatic conditions on two types of magnetic emulsion systems: the first system formed by using ultrasonic homogenization with poor particle coating around the droplets and the second system formed by ultrasonic homogenization and subsequent electro-coalescence that resulted in much better coverage of the droplets. The measurements provided evidence showing that a difference in the solidity of magnetic particle shells around emulsion droplets influenced not only heating but also cooling rates.

2. Materials and Methods

2.1. Particles and Oils

Three types of magnetic particles (MPs) were utilized in our experiments as stabilizers in magnetite-stabilized emulsions: magnetic microparticles with declared sizes of $<5 \mu\text{m}$ (μMPs) purchased from Sigma-Aldrich, magnetic nanoparticles with sizes of 50–100 nm (nMPs) purchased from Sigma-Aldrich and magnetic nanoparticles with sizes of 10 nm (OA-MPs) synthesized in the process of co-precipitation and additionally functionalized with oleic acid as a surfactant as described in [20]. We prepared oil-in-oil emulsions where castor oil (MERLIN, MA 220-1) was the continuous phase and silicone oil (Rhodorsil oils 47 V 50) was the dispersed phase. The basic characteristics of the materials used are presented in Table 1.

Table 1. List of physical parameters of materials used in the experiments. The values were given for room temperature. If not otherwise stated, the values were taken from data sheets.

	Castor Oil	Silicone Oil	Magnetite Particles
Dynamic viscosity [mPa·s]	700	50	-
Thermal conductivity [W/m·K]	0.18	0.15	5.0 [21]
Specific heat [J/kg·K]	1800	1460	950 (OA-MPs, calculated ¹) 650 (pristine MPs, [22]) 63.67 (OA-MPs, measured, [20])
Magnetization saturation [emu/g]	-	-	89.46 (nMPs, measured, [20]) 85.06 (μMPs , measured, [20])

¹ In the case of magnetic particles functionalized with oleic acid (OA-MPs), we assumed that the oleic coating accounts for 20% of the mass of magnetic material. The weighted value of specific heat was calculated as in [22].

2.2. Ultrasound and the Electric Field in the Formation of Magnetic Pre-emulsions and Emulsions

The process of formation of the colloidal systems tested in this experiment was done based on a two-step procedure involving ultrasonic homogenization and coalescence in an electric field first developed in [15]. Briefly, an ultrasonic homogenizer (Sonoplus HD 300, Bandelin, Berlin, Germany, working frequency of 18 kHz) was used for the sonication of samples with a fixed concentration of substrates, i.e., 10% *w/w* of silicone oil and 2.3% *w/w* of magnetite particles. The sonication time was 60 s or 120 s for systems with non-functionalized particles and particles with oleic acid coating, respectively. The acoustic intensity was estimated as 17 W/cm². As shown in our previous articles [15,23], for oil-in-oil emulsions ultrasonic homogenization resulted in the formation of small droplets barely coated by particles that we consistently called the pre-emulsion. An electric field was utilized to stabilize these droplets via consecutive events of coalescence. As a result, after 20 min under the electric field of 200–600 V/mm the coverage of droplets by particles increased significantly to the level that prevented their further coalescence. The results from SEM (scanning electron microscopy imaging) for particles used as stabilizers are presented in Figure 1. The examples of stable Pickering droplets taken by optical microscopy were also included as inset pictures.

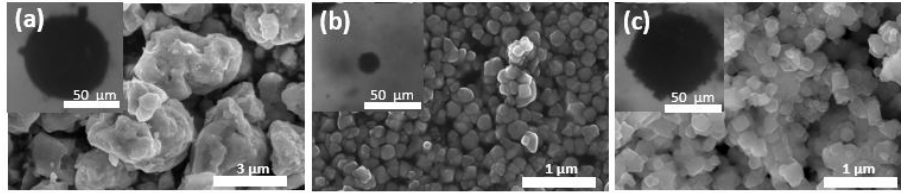


Figure 1. Scanning electron microscopy data for (a) OA-MPs, (b) nMPs, and (c) μ MPs. The inset images present examples of emulsion droplets coated by these particles after stabilization in an electric field.

The process of Pickering emulsion formation under the electric field is governed by the so-called limited coalescence regime [15]. The final droplet size depends on the size of particles and their concentration in relation to the dispersed phase. As we mentioned above, the concentrations of both silicone oil and particles were fixed. This means that the size of fully covered Pickering droplets should be related to the size of magnetic particles used as stabilizers. This is not fulfilled in the case of emulsions with small particles functionalized with oleic acid (OA-MPs), which is caused by the presence of a surfactant layer.

2.3. Idea of the Experiment

The heat generation under the AC magnetic field is due to the relaxation and hysteresis losses occurring in magnetic particles and is influenced by several factors such as particle size, intensity of the magnetic field used, viscosity of the hosting medium. In our previous work [20], we showed that also a specific arrangement of particles at the oil-oil interfaces may change the heating performance of emulsions. This change in our experiments is caused by electro-coalescence of emulsion droplets. As the total surface of the dispersed phase decreases when droplets merge, the coverage of droplets increases. This difference can also change the heat transfer after magnetic heating. The postulated differences between pre-emulsions and emulsions that influence the process of heat transfer are illustrated in Figure 2. They may lead to the differences in results from calorimetric measurements when not only the temperature increased but also the cooling down is studied.

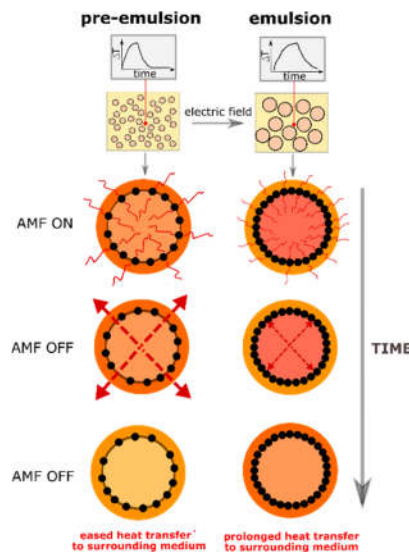


Figure 2. A schematic illustration of the idea of experiments. Different colors relate to different temperatures within the magnetic particle shell and outside this. When the alternating magnetic field (AMF) is on, the red lines represent heat generated by particle excitation both toward inside and outside the droplet. When the AMF is switched off, the red arrows represent heat transfer from the particle shell to the surrounding medium. For a solid particle shell, the heat transfer might be retarded, and in the emulsion the higher temperature is maintained longer.

In Figure 2, when the AC magnetic field (AMF) is on, the temperature around the droplets is different for the emulsion system with non-solid and more solid particle shells around droplets [20]. In both cases, the heat generated in magnetic particles is transferred into the droplet inside and from the droplet's surface, as shown schematically with red lines of various lengths. After turning off the magnetic field, the macroscopic temperature in the medium decreases, but in different way due to the varying difficulty of heat transfer from the inside of droplets to the surrounding medium for the droplets in pre-emulsions and emulsions. This hypothesis is explained in the next paragraphs.

2.4. Calorimetric Measurements under an AC Magnetic Field

To evaluate the heating and cooling rates when magnetic emulsion systems were exposed to the alternating magnetic field, a compact induction heating system (EASYHEAT, Ambrell Co., Rochester, NY, USA) was used. The sample cell, filled with either pre-emulsion or emulsion, was placed inside the container with distilled water. The temperature of the water was maintained at 20 °C using an external thermostat. This allowed us to provide constant experimental conditions for all of the measurements regardless of the room temperature. The induction coil was immersed in water, and the sample cell was located in the middle of the coil. The temperature change during magnetic heating was measured by a temperature sensor system (FLUOROTEMP, Photon Control, Burnaby, BC, Canada) equipped with an optic fiber probe (FTP-NY2,) and placed centrally in the cuvette. A single measurement lasted 600 s. The scheme of the setup for calorimetric measurements is presented in Figure 3.

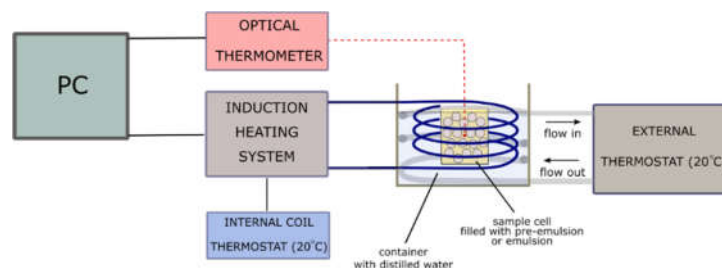


Figure 3. The scheme of the experimental setup for calorimetric measurements of magnetite-stabilized emulsions under an AC magnetic field. The measurement cell filled with either pre-emulsion or emulsion was placed in the induction coil. The induction coil was immersed in the thermostated container with distilled water where the temperature of 20 °C was maintained by an external thermostat. Additionally, the induction was water-cooled to efficiently diminish the effect of heating of the coil.

3. Results

3.1. Temperature Increase and Decrease in Pre-Emulsions and Stable Emulsions under an AC Magnetic Field

In our experiments, we were able to regulate the dynamics of magnetic heating and to investigate its influence on the process of subsequent cooling. The dynamics were affected by the type of magnetic particles and the intensity of the magnetic field, i.e., the size of particles influences the heating efficiency owing to the increasing effect of hysteresis losses on the overall heat generation. The increased temperature elevation when bigger particles were stabilizers occurred both for merely stable and stable emulsion systems. To show the results to be independent of the dynamics of heating, we conducted another experiment (scenario A) where the time of heating was 30 s. There were no limits in maximum temperature. The different dynamics of heating are in turn clear when comparing the time in which the final temperature was reached. In this experimental scenario (scenario B), the final temperature realizable in the sample was fixed at 25 °C. Above this temperature, the heating system turned off automatically.

The comparison between the two scenarios is presented in Figure 4. The one type of magnetic particles—OA-MPs, nanoparticles coated by oleic acid—was chosen as a stabilizer.

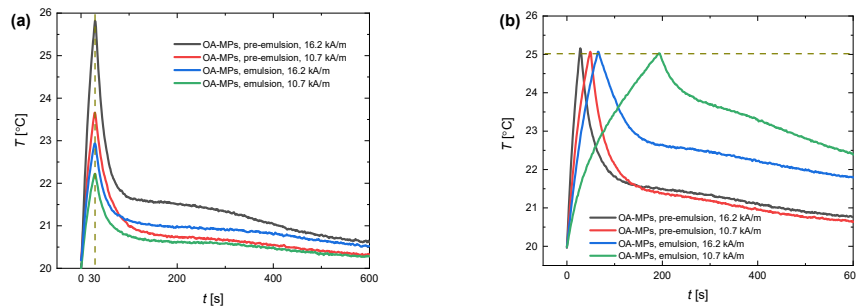


Figure 4. The temperature versus time for measurements under the AC magnetic field of the amplitude of 10.7 and 16.2 kA/m for pre-emulsions and stable emulsions stabilized with OA-MPs for the situation (a) when the induction heating system was turned off automatically after 30 s and (b) when the induction heating system was turned off automatically when the temperature was above 25 °C. The curves represent the process of heating and the subsequent cooling down process due to the constant temperature in the thermostated container (20 °C) after turning off the magnetic field. The mass concentration of silicone oil in relation to castor oil and the concentration of magnetite were the same for each of samples (10% and 2.3%, respectively). The results had uncertainty values of 1–5% that were not presented in the graph for better clarity.

As one can see, the temperature evolution in time differed for various magnetic field intensity values and the level of particle shell solidity (pre-emulsions vs. emulsions). In Figure 4a, the highest temperature increase after 30 s of heating was obtained for pre-emulsions under the magnetic field with an intensity of 16.2 kA/m. The fact that pre-emulsions exhibit better heating performance than emulsions was observed and discussed in our previous work [20]. For particles with a small magnetic core such as OA-MPs, the potential reason can be the inhibition of Brown relaxation when residing at the droplet interface. A lower intensity of the magnetic field (10.7 kA/m) led to a significantly smaller temperature increase. When the temperature was limited, the most dynamic temperature increase was achieved for pre-emulsions heated under the AC magnetic field with an intensity of 16.2 kA/m. For lower magnetic field intensity, the temperature elevation was significantly slower.

Interestingly, the temperature in samples decreased not always with the same dynamics, despite the same temperature being maintained in the thermostated container where the induction coil with samples was immersed (20 °C) and the same temperature was reached in the samples (25 °C). From Figure 4 it is clear that the chosen scenario not only influenced the temperature increase but also the way the sample is cooled down. In the next paragraph, we will take a closer look at only the process of cooling for systems stabilized with different magnetic particles.

3.2. Cooling Process for Constant Time of Magnetic Heating

In the first experimental scenario (scenario A), the magnetic field was switched off after 30 s. Figure 5 presents the temporal evolution of the temperature after the AC magnetic field was off (panel I) and the temperature change rate (dT/dt) plotted as a function of the temperature change between the maximum temperature T_{MAX} reached during the heating process and the temperature observed for the time after magnetic heating. The analysis of the cooling rate was performed not only qualitatively but also quantitatively. In our case, the use of Newton's law (see Equation (1)) for fitting the experimental results of temperature decrease was not satisfactory. The coefficient of determination, R^2 was in the order of 0.5–0.6, which is clear evidence of a poor agreement between Newton's equation and the way our system cools down. This is why we utilized the analysis proposed in works of Wildeboer and Lahiri and their co-workers [18,19] based on the Equation (2) to analytically describe the differences in cooling rates between samples.

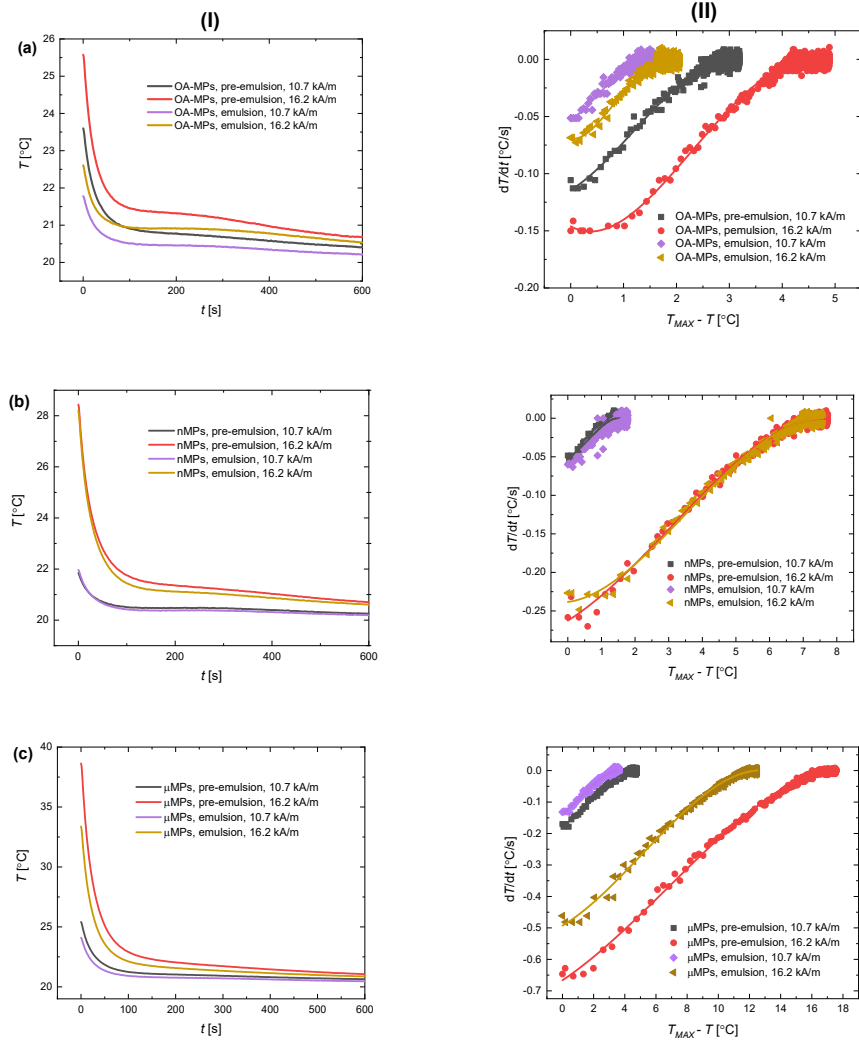


Figure 5. (I) The temperature versus time during cooling down after heating and (II) the temperature change rate versus temperature difference after magnetic heating for pre- and emulsions stabilized with (a) OA-MPs, (b) nMPs, and (c) μ MPs particles for measurements under the AC magnetic field of an amplitude of 10.7 and 16.2 kA/m. The experimental points representing dT/dt (recorded every second) were fitted to polynomial from Equation (2) whose trending lines were added. The mass concentration of silicone oil in relation to castor oil and the concentration of magnetite were the same for each of samples (10% and 2.3%, respectively), and the operating time of the AC magnetic field was 30 s. The results had uncertainty values of 1–5% that were not presented in the graph for better clarity.

The results from Figure 5 show the differences in the cooling dynamics when various particles and intensities of the magnetic field were used. The absolute temperature difference after 600 s of measurement is most significant for the systems stabilized with μ MPs and higher magnetic field intensity. The temperature change during cooling down is simply dependent on the heating efficiency of a given sample. For samples where the temperature increased more during magnetic heating, the temperature maintains at a higher level after the AC magnetic field is off. That is why the curves representing pre-emulsions with μ MPs (Figure 5c) and higher magnetic field intensities are in general higher than others. At the same time, there are also subtle differences between pre-emulsions and emulsions for each sample, i.e., the temperature after dynamic decrease maintains higher values for pre-emulsions than for emulsions. This is the other evidence of the difference in heating efficiency resulting from the change in particle coverage of the droplets.

The results from Figure 5 (panel II) reflect the cooling dynamics and show that is highest just after the magnetic field is turned off. The temperature decreases, so the derivative dT/dt is negative, and we obtained the lowest values of dT/dt for temperatures nearest the maximum temperature recorded in the sample, i.e., the smallest values of $T_{MAX} - T$. The experimental points were successfully fitted to Equation 2 ($R^2 = 0.99$), which indicates that thermal conduction, convection, and radiation occurred together during the process of cooling our systems for a wide range of temperature increase. As we mentioned, fitting the curves showing temperature decrease vs. time to Equation (1) was not satisfactory, which possibly indicates the strong influence of convection and radiation on the process of cooling in our experiments [24]. Although the differences in the temperature between the surrounding medium (20 °C) and the sample did not exceed a few degrees Celsius, in the case of our emulsion systems, the linear approximation of the results did not bring a desired agreement.

3.3. Cooling Process for Constant Maximum Temperature

Much more interesting to understand is how the presence of a stable particle shell around the droplets in Pickering emulsions influences the way heat is transferred is the situation when the samples reach the same fixed temperature (25 °C) in each measurement, as is the case for the experimental scenario B. In this case, the potential differences in cooling between samples cannot be caused simply by the different temperature increase during magnetic heating. The results of the temperature evolution in time after the AC magnetic field was off (panel I) and the calculated values of dT/dt as a function of the temperature change (panel II) are presented in Figure 6.

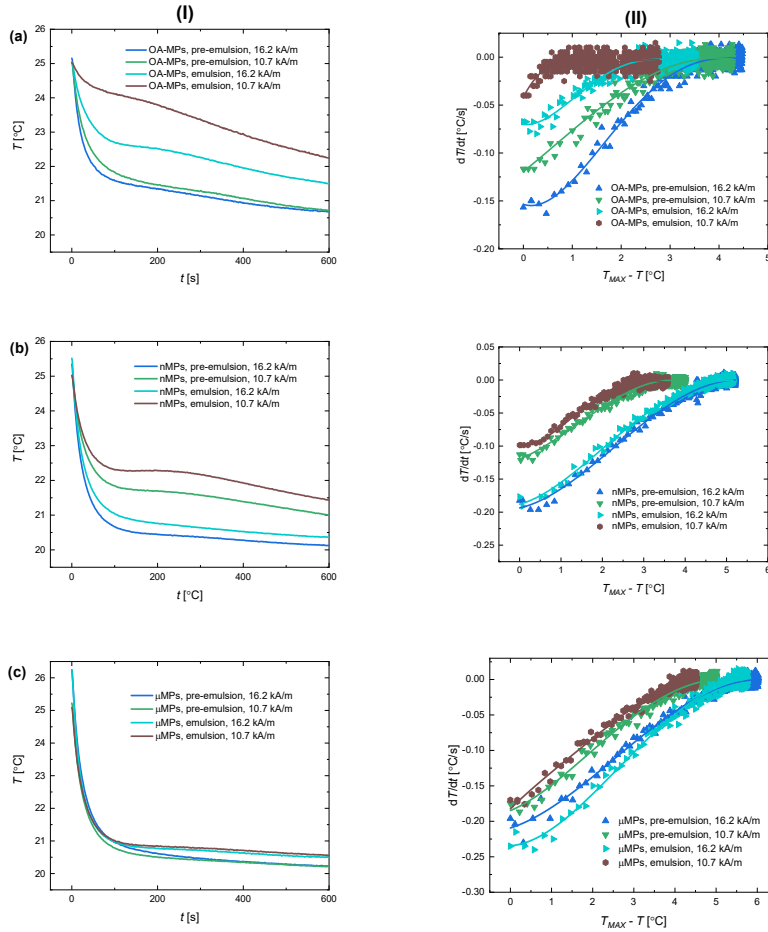


Figure 6. (I) The temperature versus time during cooling down after heating and (II) the temperature change rate versus temperature difference after magnetic heating for pre- and emulsions stabilized with (a) OA-MPs, (b) nMPs, and (c) μ MPs particles for measurements under the AC magnetic field of an amplitude of 10.7 and 16.2 kA/m. The experimental points representing dT/dt (recorded every second) were fitted to polynomial from Equation (2) whose trending lines were added. The mass concentration of silicone oil in relation to castor oil and the concentration of magnetite were the same for each of samples (10% and 2.3%, respectively) and the time when the AC magnetic field was turned on was when the temperature in the sample exceeded 25 °C. The results had uncertainty values of 1–5% that were not presented in the graph for better clarity.

Figure 6 shows the reversion in temperature decrease (panel I) for intensities of the magnetic field compared to Figure 5. The samples placed in the magnetic field of lower intensity (10.7 kA/m) needed significantly more time to reach the temperature of 25 °C than samples heated in the AC magnetic field of higher intensity. This difference influenced the way the samples cooled down. As presented, this process is much slower for lower intensities, especially when OA-MPs and nMPs were stabilizers.

One can also see that the process of cooling was evidently less dynamic for emulsions compared to pre-emulsions regardless of the particles used as stabilizers and the intensity of the AC magnetic field. Our explanation is that the heat transfer is indeed retarded for emulsions where droplets are coated by a complete particle shell that influences the temperature measured in the whole sample. The effect of particle coating seems to be less significant for μ MPs (Figure 6c), which can be explained by a much higher heating dynamics and the subsequent effective process of transferring heat from the particle shell into the surrounding medium. The abovementioned differences are also reflected in the results of the temperature change rate versus temperature difference (Figure 6, panel II). It is

significant that the temperature change rate takes lower values for pre-emulsions than for emulsions. The dynamics of how these values of the experimental points change are also different for various samples.

4. Discussion

As we presented above, the process of cooling after magnetic heating in emulsions strongly depended on the factors affecting the heating, i.e., the magnitude of the magnetic field applied, the size of particles, and the time of application of the magnetic field. Therefore, it is possible to adjust parameters such as particle size so that the energy can be stored inside the Pickering droplets for a while. The measured temperature decrease in systems with droplets with stable particle coating can be, under certain conditions, slower compared to a situation where droplets are coated by particles to a less extent. Then, the energy transfer is sustained. From the results (Figure 6), for this purpose it would be better to use the particles with lower heating efficiency.

When the magnetic field is turned off, particles are no longer the sources of heat. Nonetheless, the maximum temperature measured for scenario A exceeded the limit of 25 °C, especially for emulsions stabilized with μ MPs (see, the temperature for 0 s in Figure 6c, panel I). This could stem from the fact that energy is entrapped inside the droplet for a while and heat transfer is halted to some extent. It is worth noting that we did not observe this effect in ferrofluids, although the sources of heat and the experimental equipment were the same. For magnetic particles suspended in either castor or silicone oil, the temperature did not exceed that limit, which can be somehow more evidence for the ‘energy capsulation’ occurring in armored droplets. Potentially, the heat entrapped within the droplet could be transported and released under external stimuli in the destined place.

In our paper, we considered macroscopic consequences of nano- and micro-heating from magnetic particles. Nevertheless, the local temperature increase should be high enough to cause a significant temperature increase in the surrounding medium. Additionally, although recent reports suggested that it is not certain [25,26], our results confirm that the particles influence the heating and cooling processes when assessing them in micro- and/or nano-scale.

5. Conclusions

In this work, we evaluated the process of cooling in emulsion systems stabilized with magnetic particles. The way our samples cooled down depended strongly on the intensity of the AC magnetic field used for heating, on the size of magnetic particles and also on the solidity of the particle shell around Pickering droplets. The emulsions with droplets coated to a higher extent by magnetic particles have already been reported to exhibit weaker heating performance [20]. However, as shown in this work, they also cooled down slower compared to emulsions with poorly coated droplets. It was especially clear when the comparison between different samples was performed for the same maximum temperature. The results can be the evidence that emulsions with stable magnetic Pickering droplets are good candidates as materials with sustained heat transfer. This could be another application of oil-in-oil emulsions that have numerous advantages but are still understudied [27].

Author Contributions: A.J. and R.B. initiated the project and designed the experiments. R.B. performed the experiments, analyzed the data, and wrote the first version of the manuscript. The authors discussed together the final version of the manuscript. All authors have read and agreed to the published version of the manuscript.

Funding: This work was supported by the grant, 2019/35/N/ST5/00402 (PRELUDIUM) of the Polish National Science Centre.

Acknowledgments: The authors wish to thank Katarína Paulovičová (IEP SAS, Kosice, Slovakia) for the preparation of magnetic particles coated by oleic acid and Tomasz Hornowski (AMU, Poznań, Poland) for the valuable discussion.

Conflicts of Interest: The authors declare no conflict of interest.

References

1. Feng, X.; Sun, Y.; Yang, Y.; Zhou, X.; Cen, K.; Yu, C.; Xu, T.; Tang, X. Zein nanoparticle stabilized Pickering emulsion enriched with cinnamon oil and its effects on pound cakes. *LWT* **2020**, *122*, 109025.
2. Skelhon, T.S.; Grossiord, N.; Morgan, A.R.; Bon, S.A. Quiescent water-in-oil Pickering emulsions as a route toward healthier fruit juice infused chocolate confectionary. *J. Mater. Chem.* **2012**, *22*, 19289–19295.
3. AfzaliTabar, M.; Alaei, M.; Bazmi, M.; Khojasteh, R.R.; Koolivand-Salooki, M.; Motiee, F.; Rashidi, A. Facile and economical preparation method of nanoporous graphene/silica nanohybrid and evaluation of its Pickering emulsion properties for Chemical Enhanced oil Recovery (C-EOR). *Fuel* **2017**, *206*, 453–466.
4. Lee, J.; Babadagli, T. Optimal design of pickering emulsions for heavy-oil recovery improvement. *J. Dispers. Sci. Tech.* **2019**, 1–15, doi.org/10.1080/01932691.2019.1650754.
5. Jiang, J.; Cao, J.; Wang, W.; Shen, H. Preparation of a synergistically stabilized oil-in-water paraffin Pickering emulsion for potential application in wood treatment. *Holzforschung* **2018**, *72*, 489–497.
6. Marto, J.; Ascenso, A.; Gonçalves, L.M.; Gouveia, L.F.; Manteigas, P.; Pinto, P.; Oliveira, E.; Almeida, A.J.; Ribeiro, H.M. Melatonin-based pickering emulsion for skin's photoprotection. *Drug Deliv.* **2016**, *23*, 1594–1607.
7. Deschamps, F.; Harris, K.R.; Moine, L.; Li, W.; Tselikas, L.; Isoardo, T.; Lewandowski, R.J.; Paci, A.; Huang, N.; de Baere, T. Pickering-emulsion for liver trans-arterial chemo-embolization with oxaliplatin. *Cardiovasc. Interv. Radiol.* **2018**, *41*, 781–788.
8. Low, L.E.; Tan, L.T.-H.; Goh, B.-H.; Tey, B.T.; Ong, B.H.; Tang, S.Y. Magnetic cellulose nanocrystal stabilized Pickering emulsions for enhanced bioactive release and human colon cancer therapy. *Int. J. Biol. Macromol.* **2019**, *127*, 76–84.
9. Rosensweig, R.E. Heating magnetic fluid with alternating magnetic field. *J. Magn. Magn. Mater.* **2002**, *252*, 370–374.
10. Kaczmarek, K.; Hornowski, T.; Antal, I.; Rajnak, M.; Timko, M.; Józefczak, A. Sono-magnetic heating in tumor phantom. *J. Magn. Magn. Mater.* **2020**, *500*, 166396.
11. Skumiel, A.; Kaczmarek, K.; Flak, D.; Rajnak, M.; Antal, I.; Brząkała, H. The influence of magnetic nanoparticle concentration with dextran polymers in agar gel on heating efficiency in magnetic hyperthermia. *J. Mol. Liq.* **2020**, *304*, 112734.
12. Martínez-Prieto, L.M.; Marbaix, J.; Asensio, J.M.; Cerezo-Navarrete, C.; Fazzini, P.-F.; Soulantica, K.; Chaudret, B.; Corma, A. Ultrastable Magnetic Nanoparticles Encapsulated in Carbon for Magnetically Induced Catalysis. *ACS Appl. Nano Mater.* **2020**, *3*, 7076–7087.
13. Binks, B.P.; Tyowua, A.T. Oil-in-oil emulsions stabilised solely by solid particles. *Soft Matter* **2016**, *12*, 876–887.
14. Rajnak, M.; Timko, M.; Kopcansky, P.; Paulovicova, K.; Kuchta, J.; Franko, M.; Kurimsky, J.; Dolnik, B.; Cimbala, R. Transformer oil-based magnetic nanofluid with high dielectric losses tested for cooling of a model transformer. *IEEE Trans. Dielectr. Electr. Insul.* **2019**, *26*, 1343–1349.
15. Rozynek, Z.; Bielas, R.; Józefczak, A. Efficient formation of oil-in-oil Pickering emulsions with narrow size distributions by using electric fields. *Soft Matter* **2018**, *14*, 5140–5149.
16. Davidzon, M.I. Newton's law of cooling and its interpretation. *Int. J. Heat Mass Transf.* **2012**, *55*, 5397–5402.
17. Luo, S.; Schiffbauer, J.; Luo, T. Effect of cooling on droplet size in supersaturation-induced emulsions. *Phys. Chem. Chem. Phys.* **2017**, *19*, 29855–29861.
18. Wildeboer, R.; Southern, P.; Pankhurst, Q. On the reliable measurement of specific absorption rates and intrinsic loss parameters in magnetic hyperthermia materials. *J. Phys. D: Appl. Phys.* **2014**, *47*, 495003.
19. Lahiri, B.; Ranoo, S.; Philip, J. Uncertainties in the estimation of specific absorption rate during radiofrequency alternating magnetic field induced non-adiabatic heating of ferrofluids. *J. Phys. D: Appl. Phys.* **2017**, *50*, 455005.
20. Bielas, R.; Hornowski, T.; Paulovičová, K.; Rajňák, M.; Józefczak, A. The effect of magnetic particles covering the droplets on the heating rate of Pickering emulsions in the AC magnetic field. *J. Mol. Liq.* **2020**, *320*, 114388.
21. Grosu, Y.; Faik, A.; Ortega-Fernández, I.; D'Aguanno, B. Natural Magnetite for thermal energy storage: Excellent thermophysical properties, reversible latent heat transition and controlled thermal conductivity. *Sol. Energy Mater. Sol. Cells* **2017**, *161*, 170–176.
22. Vinogradov, A.N. Physicochemical and Acoustic Properties of Water-Based Magnetic Colloid. *Coll. J.* **2004**, *66*, 29–37.

23. Bielas, R.; Rozynek, Z.; Hornowski, T.; Józefczak, A. Ultrasound control of oil-in-oil Pickering emulsions preparation. *J. Phys. D Appl. Phys.* **2020**, *53*, 085301.
24. Teran, F.J.; Casado, C.; Mikuszeit, N.; Salas, G.; Bollero, A.; Morales, M.P.; Camarero, J.; Miranda, R. Accurate determination of the specific absorption rate in superparamagnetic nanoparticles under non-adiabatic conditions. *Appl. Phys. Lett.* **2012**, *101*, 062413.
25. Chiu-Lam, A.; Rinaldi, C. Nanoscale Thermal Phenomena in the Vicinity of Magnetic Nanoparticles in Alternating Magnetic Fields. *Adv. Funct. Mater.* **2016**, *26*, 3933–3941.
26. Faure, S.; Mille, N.; Kale, S.; Asensio, J.M.; Marbaix, J.; Farger, P.; Stoian, D.; van Beek, W.; Fazzini, P.-F.; Soulantica, K.; et al. Internal Temperature Measurements by X-ray Diffraction on Magnetic Nanoparticles Heated by a High-Frequency Magnetic Field. *J. Phys. Chem. C* **2020**, *124*, 22259–22265.
27. Zia, A.; Pentzer, E.; Thickett, S.; Kempe, K. Advances and Opportunities of Oil-in-Oil Emulsions. *ACS Appl. Mater. Inter.* **2020**, *12*, 38845–38861.

Publisher’s Note: MDPI stays neutral with regard to jurisdictional claims in published maps and institutional affiliations.



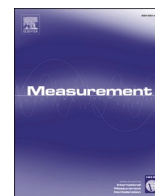
© 2020 by the authors. Licensee MDPI, Basel, Switzerland. This article is an open access article distributed under the terms and conditions of the Creative Commons Attribution (CC BY) license (<http://creativecommons.org/licenses/by/4.0/>).

[Publication V]

Monitoring of Pickering emulsion stability during magnetic heating
using ultrasound measurements

R. Bielas, B. Jameel, A. Józefczak

Measurement, 2021, 178: 109431.



Monitoring of Pickering emulsion stability during magnetic heating using ultrasound measurements

Rafał Bielas, Bassam Jameel, Arkadiusz Józefczak^{*}

Chair of Acoustics, Faculty of Physics, Adam Mickiewicz University in Poznań, Uniwersytetu Poznańskiego 2, 61-614 Poznań, Poland

ARTICLE INFO

Keywords:

Magnetic heating
Alternating magnetic field
Magnetic fluid
Pickering emulsion
Ultrasound
Ultrasound velocity

ABSTRACT

Magnetic heating of colloidal systems is becoming a more and more common route for inducing temperature rise, especially in applications where very local temperature elevation is desired. Although the calorimetric properties of magnetic colloids are extensively investigated, the influence of the alternating magnetic field on their structure has rarely been reported. Meanwhile, potential permanent structural changes such as the formation of agglomerates can affect the stability of magnetic dispersions or magnetic Pickering emulsions. In the present work, we propose to use ultrasound as a technique to determine if such changes occur during magnetic heating. Oil-in-oil emulsions with magnetite particle shells around the droplets and oil-based magnetic fluids were exposed to alternating magnetic fields, and the changes in ultrasonic attenuation and the speed of ultrasound were determined. Finally, changes in acoustic properties were investigated in dispersions of magnetic and polystyrene particles after heating to the melting temperature of the soft particles.

1. Introduction

The generation of heat in colloidal systems under alternating current (AC) magnetic fields has emerged as a research topic of interest in recent decades. Different materials have been suggested for use in magnetic heating, including magnetic fluids, i.e., dispersions of magnetic particles in oils or water, and magnetic emulsions, although the latter has been remarkably less investigated. At present, the heating efficiency of magnetic fluids is of particular oncological interest because it is an essential factor in the magnetic hyperthermia procedure [1,2]. Emulsions whose droplets contain magnetic particles have also been reported in this context [3–5]. Despite interest in magnetic fluids and emulsions, there remain key uncertainties in the behavior of magnetic Pickering emulsions that can be investigated.

In Pickering emulsions, particles attach to the droplet interface through capillary forces [6,7]. The particle and liquid phases of the emulsion can be matched such that their properties allow wetting of the particles by both phases, resulting in exquisite stability [8]. It is believed that, in contrast to the surfactants widely used in emulsion stabilization, the attachment of particles can be irreversible as long as a contact angle is not close to the limiting value [9]. The free-energy change associated with the transfer of a particle from the continuous phase to the liquid-liquid interface depends on the size of the particle, the three-phase

contact angle, and the interfacial tension; it reaches its maximum value for a particle wetted to an intermediate extent by both phases [10]. The presence of magnetic particles at the droplet interface offers new opportunities such as droplet positioning [11], control of the emulsion stability under an external static magnetic field, and/or magnetic heating [11–13]; further, it allows the relatively straightforward re-use of particles through the application of external magnetic fields [14]. Biocompatible magnetic cellulose particles were shown to be efficient in targeting drug release and magnetic hyperthermia therapy for colon cancer [15], and magnetic particles adsorbed to double Pickering droplets can serve as microreactors with controllable motion [16].

Regardless of whether the magnetic particles are dispersed in a liquid medium or are attached to the droplet interface, under an AC magnetic field, they act as sources of heat due to the dissipation of magnetic energy into Néel and Brown relaxation processes, or into the magnetic hysteresis when particle size exceeds the limit for of single-domain particles [17]. Brown relaxation can be inhibited when particle movement is locked, e.g., in a very viscous medium or gel network. For this reason, testing magnetic heating in tissue-mimicking media is important [18]. As we have shown in our previous works [19,20], the attachment to the droplet interface can influence the heating performance of magnetic particles, i.e., heating and cooling efficiency were lower for droplets with dense particle shells. The temperature increase under an

^{*} Corresponding author.

E-mail address: aras@amu.edu.pl (A. Józefczak).

AC magnetic field also varied with magnetic material concentrations and magnetic field intensity. Although a temperature rise of 5–8 °C above the temperature of a human body is sufficient for hyperthermia therapy [21], significantly higher temperatures are needed for applications such as inducing thermal ablation of tissues. For adequately high concentration of magnetic particles on droplet interfaces, it is possible to utilize the temperature elevation above the glass transition temperature of soft polystyrene or polyethylene particles allowing sintering to occur. AC magnetic fields have been used to solidify particle shells around droplets, thus fabricating colloidal capsules from Pickering-emulsions precursors [22].

During the process of magnetic heating, various calorimetric measurement methods are used, the most popular of which is optical thermometry [23]. To monitor the temperature in tissues during medical procedures, more sophisticated techniques have been developed such as magnetic resonance imaging [24], magnetomotive optical coherence elastography [25], and methods combining magnetomotive and ultrasound imaging [26]. However, a substantial question remains as to whether the application of the alternating magnetic field induces only temperature elevation or if it is accompanied by the possible changes in the structure of the magnetic colloids, especially with regard to magnetic Pickering emulsions. This potential unintended consequence of magnetic heating seemed not to be of scientific interest until now. The generally efficient and robust approach for evaluating samples using optical microscopy imaging must be considered deprecated here due to the non-transparent nature of most magnetic colloids, i.e., the frequently used iron oxide (magnetite or maghemite) particles are black-colored, significantly limiting the possibility of direct optical evaluation. The solution may be the use of ultrasound techniques.

The main advantage of using low-intensity ultrasonic waves is their ability to penetrate a tested system without damaging its structure, and they are used in numerous industrial applications such as the identification of defects in materials [27,28] or measurement of their thickness [29,30]. Colloidal systems, including magnetic fluids [31], are also frequently characterized by ultrasound since tested samples do not need to be prepared in a particular, refined way as with methods based on light scattering, neutron scattering, and others in which the samples have to be diluted before the measurements [32]. Specific acoustic parameters such as the attenuation coefficient and speed of ultrasound (i.e., sound velocity) provide information about the properties of the medium.

When a tested medium is homogenous, the ultrasonic waves propagate with the speed dependent on compressibility and density. Viscosity, in turn, mainly controls the absorption of ultrasonic waves by the medium according to well-known Stokes-Kirchhoff formula [33]. These parameters decrease with decreasing temperature. The presence of inhomogeneities (scatterers) in a medium, e.g., the emulsion droplets or particles, or both (as in the case of Pickering emulsions), alters the average properties of the medium and causes the discontinuities in properties across phase boundaries. These contrasts in properties such as compressibility, thermal properties, and density [34] contribute to additional attenuation of ultrasonic waves. The cyclic pulsation of particles and droplets due to differences in compression and expansion, in response to propagating acoustic waves, can cause the additional sound radiation that dissipates the energy of the propagating ultrasound. On the other hand, the temperature change caused by local heating and cooling of scattering objects as ultrasound propagates through the sample can be different due to different thermal conductivities and expansion coefficients. This leads to cyclic heat flow. Finally, so-called visco-inertial effects can occur when particle/droplet motion relative to the continuous phase is induced. The different types of colloidal systems feature different responses, e.g., in emulsions without particle shells the effect of differences in thermal properties is the most significant [35]. These responses have been described by theories that consider the abovementioned relationships and allow the calculation of attenuation coefficients and the speed of ultrasound in emulsions, dispersions,

and capsulated emulsions, as a function of frequency, particle size, and particle concentration [36–38].

Despite great interest in the characterization of colloidal systems by ultrasound, to the best of our knowledge, there have been no results concerning the monitoring of structural changes during magnetic heating. Only a few studies have shown the possibility of using ultrasonic spectroscopy to describe the properties of non-magnetic Pickering emulsions [39,40]. In our past work, we show that ultrasound can be used to assess the long-term stability of magnetic oil/water Pickering emulsions formed using magnetic fluids [41]. Ultrasound was also used in studies of structural changes in magnetic fluids under DC magnetic fields [42,43]. However, it has not been used to show structural changes after dynamic processes, of which heating under the AC magnetic field is one example. In this paper, we use the measurements of the speed of ultrasound and ultrasonic attenuation coefficient as tools for monitoring changes in the properties of Pickering emulsions exposed to magnetic heating. We compare the results for magnetic Pickering emulsions with those for magnetic dispersions and magnetite-soft particle dispersions, in which particles are partially sintered due to high-temperature heating.

2. Materials and methods

2.1. Characterization of oils and particles

In this experimental work, we mainly prepared the emulsions of oil-in-oil, stabilized with magnetite particles, with various mass ratios between magnetic particles and silicone oil. Castor oil (MA 220-1, MERLIN, Spain) was used as a continuous phase in which silicone oil (Rhodosil Oils 47V 50, VWR Chemicals, USA) were dispersed. The emulsions were stabilized by magnetic nanoparticles in the powder form (Sigma-Aldrich Co., USA) without any coating. To show the comparison between magnetic fluids and magnetic Pickering emulsions, we performed experiments on dispersions of magnetite particles in castor oil using the above-mentioned substrates. Dispersions of both magnetite and soft particles in castor oil were also prepared. For this, polystyrene particles (Dynoseeds, TS10 6317, Microbeads AS, Norway) were used. The scanning electron microscopy (SEM) images and calculated particle size distributions for solid particles are shown in Fig. 1. For magnetic particles, a magnetization curve is also presented.

2.2. Preparation of the samples

Magnetic Pickering emulsions were efficiently prepared by applying ultrasound and electric fields, as was described in our prior work [44]. In short, magnetite-emulsions were prepared by adding magnetic particles, silicone oil, and castor oil into a quartz cuvette (17.5 mm × 20 mm × 32 mm) and mixing them via an ultrasonic homogenizer (Sonoplus HD 300, Bandelin, Berlin, Germany). The sample cell was sonicated for three minutes with an ultrasonic probe (KE 76) with a diameter of 12 mm. The acoustic intensity was ~ 17 W cm⁻² and the working frequency was 18 kHz. In previous work [44], we showed that a short ultrasonic homogenization alone did not result in the fabrication of stable Pickering droplets. For this reason, we used a DC electric field to ensure the efficient formation of dense particle shells around the oil droplets.

The system of emulsion preparation under an electric field consisted of the power supply (DF 1730SL, NDN Co., Warsaw, Poland), signal generator (RSDG 800, Siglent Technologies Co., Cohran Rd Solon, OH, USA), and high voltage amplifier (UltraVolt 1AA12-P4, Advanced Energy Inc., Fort Collins, CO, USA), which were connected to two copper electrodes placed inside the cuvette. The Pickering emulsions, stabilized with particles, were achieved after 20 min. The fabrication process was monitored using a CMOS camera (UI-3590CP-C-HQ, IDS). Fig. 2 presents the appearance of the magnetic Pickering emulsion after preparation using ultrasound and an electric field.

Fig. 2 shows that optical monitoring, especially the evaluation of

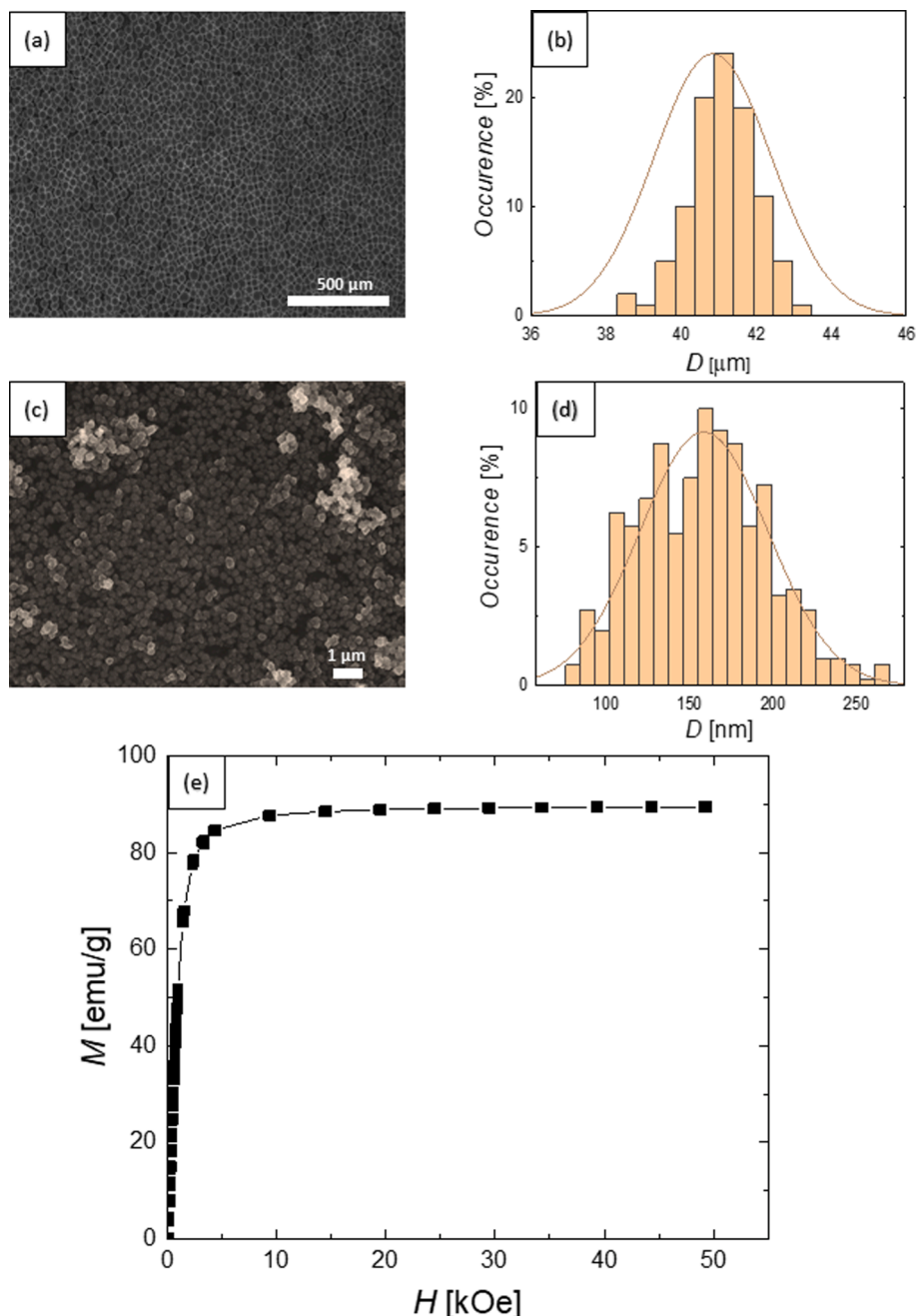


Fig. 1. Characterization of particles used as stabilizers: (a) scanning electron microscopy (SEM) images and (b) calculated particle size distribution for polystyrene (PS) microparticles; (c) SEM images and (d) calculated particle size distribution for magnetite nanoparticles; (e) magnetization curve from vibrating sample magnetometer (VSM) measurements [19].

particles forming shells around the droplets, cannot be accurate without dilution. After dilution, agglomerates of particles and droplets are visible. However, under the higher magnification (Fig. 2d), it is clear that these agglomerates consist of Pickering droplets coated by particles with evaluated mean sizes of roughly 7–11 μm. It must be stressed that the dilution of the system can create a false image of the actual magnetic emulsion structure. The situation is similar during, for instance, electron microscopy imaging. To obtain SEM or transmission electron microscopy (TEM) images with good quality, multiple dilutions of the sample must be performed.

The samples of dispersions of magnetite particles in castor oil and dispersions of mixed magnetic and soft particles in castor oil were prepared in the same quartz glass cuvette by ultrasonic homogenization for three minutes.

2.3. Experimental setup

In our experiments, we used an alternating magnetic field (AMF) heating system and ultrasonic system combined to monitor changes in acoustic parameters of magnetic colloids after magnetic heating. The schematic illustration of the system is presented in Fig. 3.

To make the temperature inside the sample equivalent to the room temperature for all of the experiments, a thermostated bath (PolyScience Co., Niles, IL, USA) was used. The sample magnetic colloid was placed in the induction coil of the heating system (EASYHEAT, Ambrell Co., Rochester, NY, USA), which has an alternating magnetic field intensity of 16.2 kA m^{-1} and frequency of 360 kHz. The magnetic field produced an increase in the temperature of the sample. The change in temperature was measured by a sensor with an FTP-NY2 optical fiber probe and 1-

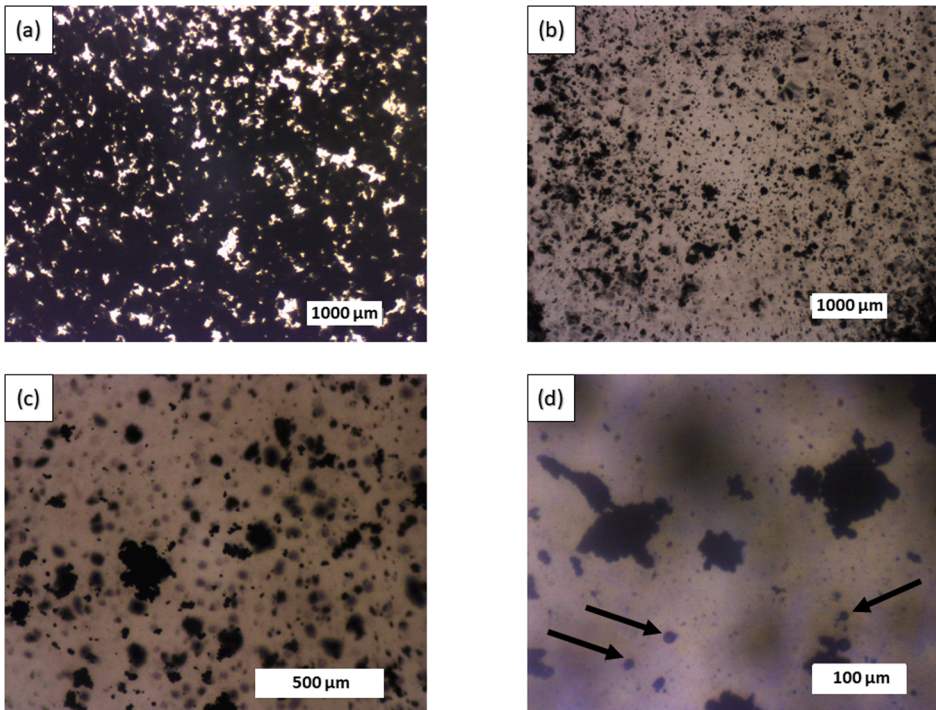


Fig. 2. Optical microscopy image for the emulsions (10% silicone oil, 1:2 magnetite : silicone oil mass ratio) after 20 min of an electric field applied with an intensity of 600 V mm^{-1} : (a) the images without sample dilution, (b) the images after a dilution of the sample in castor oil with original and (c) higher magnification. The images with extreme magnification (d) show single Pickering droplets (arrows). All images were taken using quartz cuvette smaller than for other measurements ($30 \text{ mm} \times 18 \text{ mm} \times 1.3 \text{ mm}$).

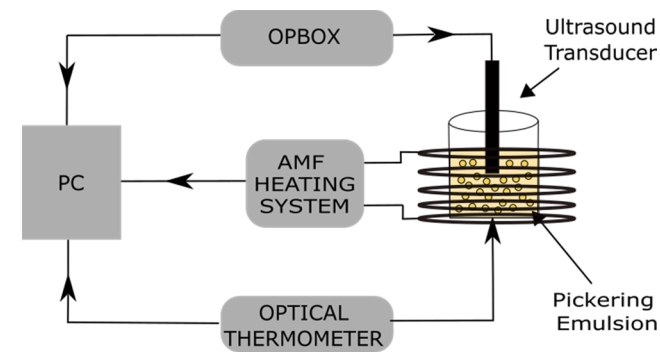


Fig. 3. A scheme of the experimental setup for following the magnetic heating of Pickering emulsions. A sample cell with the emulsion after electro-coalescence was placed in the magnetic coil of the alternating magnetic field (AMF) system. An ultrasonic measurement system with a transducer connected to OPBOX device and an optical thermometer followed the changes in the colloidal system.

second resolution (FLUOROTEMP, Photon Control, Burnaby, BC, Canada). Both magnetic heating system and temperature sensor were driven by PC software. To obtain the change of temperature as a function of time for each experiment, the starting temperature was subtracted from the temperature measured in a given moment. The heating system turned off automatically when the maximum temperature was exceeded.

The ultrasonic system consisted of a single piezoelectric transducer (OPTEL Co., Wrocław, Poland) with a centre frequency of 2.5 MHz and a diameter of 13 mm driven by an ultrasonic testing device OPBOX 2.1 (OPTEL Co., Wrocław, Poland) connected to a PC. A unipolar spike pulse (with an amplitude of 360 V, fall time 20 ns, and pulse repetition frequency 0.9 kHz) was used to generate the ultrasound. The system presented in Fig. 3 was operated in pulse-echo mode, i.e., the ultrasonic wave was generated by the transducer and after traveling through the sample cell and subsequent reflection by its bottom was detected again by the transducer and recorded with a sampling frequency 100 MHz. To prevent the influence of the heating of the transducer's metal chassis

when exposed to the AC magnetic field, the ultrasonic signal was recorded before the AC magnetic field was turned on, and then the transducer was placed away of the sample cell and induction coil. A constant distance of 10 mm between the bottom of the sample cell and the transducer was maintained when measuring, which means that the acoustic path was 20 mm.

During the experiments, we investigated how acoustic parameters differ during the process of magnetic heating and cooling. The software recorded at every second the amplitude of the acoustic signal after traveling through the sample and its travel time (time of flight). Therefore, two acoustic parameters, i.e., the change in the attenuation coefficient ($\Delta\alpha$) and change in the speed of ultrasound (Δc) were determined in relation to the value recorded before the start of heating and cooling. The probable reflection loss did not affect the results as the associated error was constant for each experiment, and its influence was subtracted. The change in the attenuation coefficient was calculated using the formula:

$$\Delta\alpha = \frac{20}{2d} \log_{10} \frac{A_0}{A_n} \quad (1)$$

where $2d = 20 \text{ mm}$ relates to the acoustic path for a signal, A_0 is an amplitude of ultrasonic signal observed before the process of magnetic heating for starting temperature, and A_n is the amplitude of the ultrasonic signal after magnetic heating, recorded every second.

The change in speed of ultrasound was calculated based on the following expression:

$$\Delta c = c_0 - c_n \quad (2)$$

where c_0 and c_n can be expressed as: $2d/t_0$ and $2d/t_n$, respectively. The times t_0 and t_n refer to the time it takes for the acoustic signal to come back to the transducer after traveling through the sample, (measured before the process of magnetic heating, for the starting temperature) and the time measured every second after the initiation of magnetic heating.

Each experiment was repeated at least three times and the mean values of changes in temperature, attenuation coefficient, and speed of ultrasound along with standard deviation values (error bars) are presented in the sections to follow. Fig. 4 presents example pulses before and after magnetic heating, showing how changes in attenuation

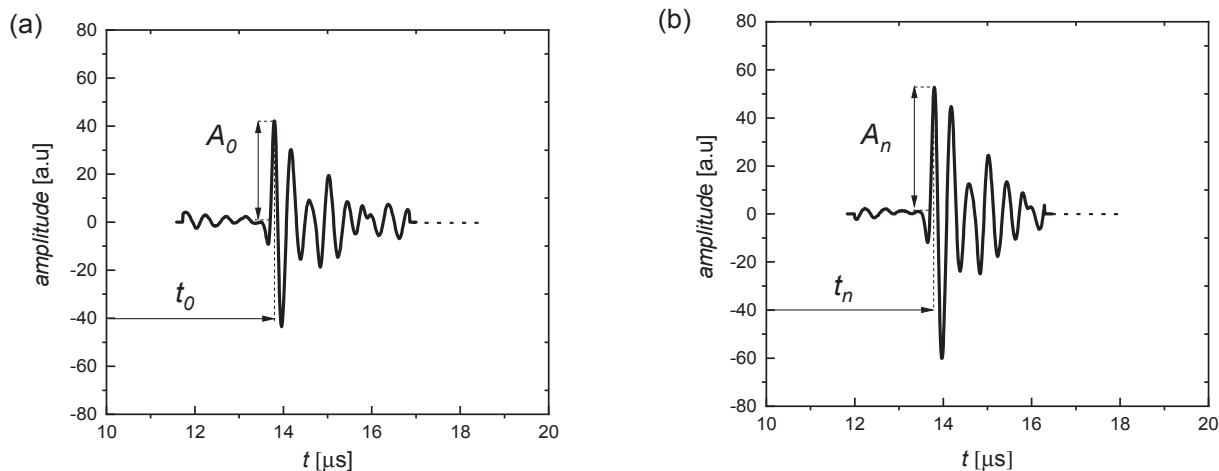


Fig. 4. The example ultrasound signals recorded (a) before magnetic heating and (b) during the cooling process after magnetic heating for magnetic dispersions. The values of amplitudes and time of flight are indicated.

coefficient and the speed of ultrasound were calculated using measured ultrasonic signals after their return to the transducer.

It should be noted that our ultrasonic transducer emitted signals with small amplitudes and high frequencies that combined with high viscosity of a medium precluded the possibility of acoustic cavitation. This

means that our measurements were non-destructive.

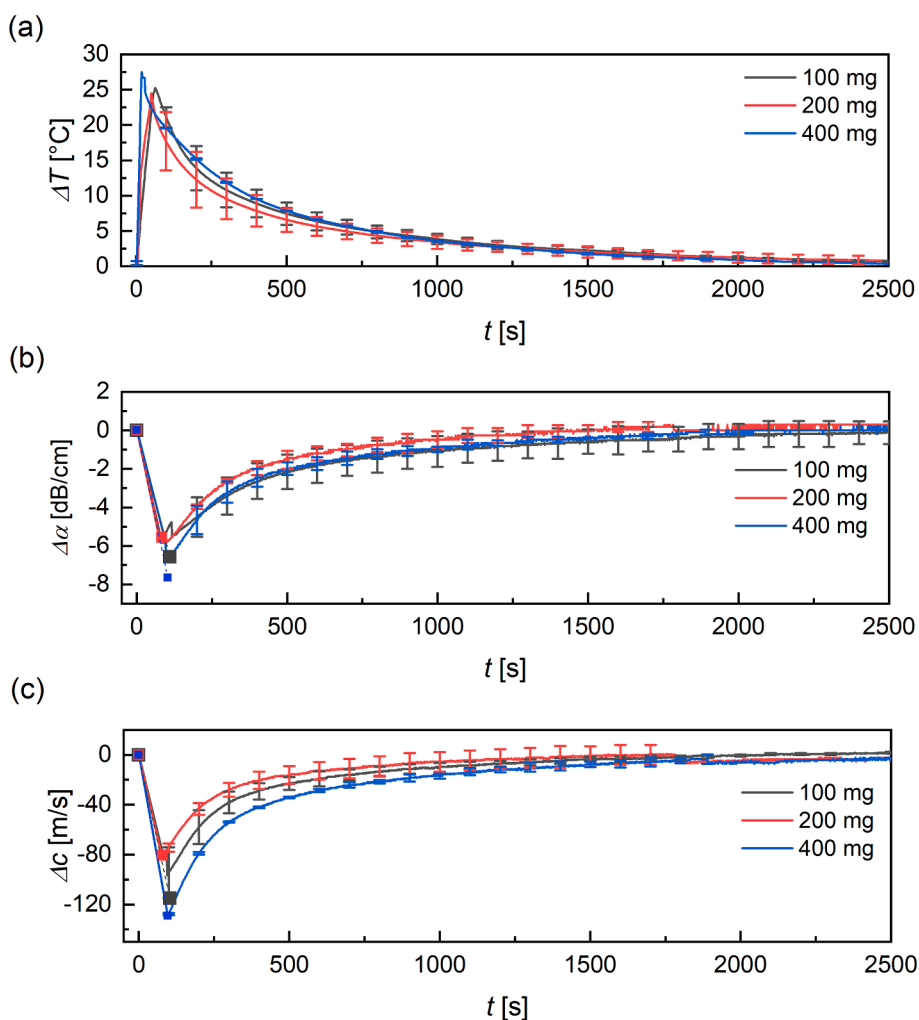


Fig. 5. (a) The temperature change for a magnetite dispersion in castor oil exposed to an AC magnetic field. (b) The change in ultrasonic attenuation coefficient and (c) speed of ultrasound observed after an magnetic field was turned off. Samples differed in the mass of dispersed magnetic particles.

3. Results and discussion

3.1. Calorimetric and ultrasonic measurements of castor oil-based magnetic fluids

We first investigated the potential changes in ultrasonic properties of magnetic fluids occurring due to heating by an alternating magnetic field and subsequent cooling back to the starting temperature. Fig. 5 presents changes in temperature, ultrasonic attenuation, and speed of ultrasound during magnetic heating and subsequent cooling for different concentrations of magnetite particles. For all samples, the magnetic field was turned off after the temperature in the sample exceeded 45 °C. Fig. 6 shows the results for the same mass of magnetic particles, but for different heating durations, i.e., the magnetic field was turned off after the temperature in the sample exceeded 25, 35, and 45 °C, respectively.

Over time, the results of temperature evolution show different heating rates for different amounts of magnetic particles (Fig. 5). The most dynamic heating was for the highest concentration of magnetite. Due to the gradient between the room temperature and the current temperature of the sample, the temperature started decreasing after the AC magnetic field is turned off. In the beginning, the cooling process was fast, but then it slowed down. Such slight changes in the temperature for the latter phase of cooling did not influence acoustic properties.

Because of the high temperature that can be induced in a metal chassis of the transducer when exposed to the AC magnetic field, the values of acoustic parameters during heating were somehow reconstructed (dotted lines in Fig. 5–Fig. 8). To reduce heating of transducer chassis, we removed the transducer from the sample cell during the

times when the AC magnetic field was on. The transducer was immersed in the sample cell again after the AC magnetic field was turned off. Owing to high intensities of magnetic fields, the high temperature increase induced in the metal chassis of the transducer could certainly affect the temperature rise observed in the tested sample. Thus, ultrasound was not used to follow the whole process of heating, but measurements were performed for starting and maximum temperature, and for the whole process of cooling down. Ultrasonic attenuation coefficient and speed of ultrasound measured in this way differed significantly from the starting values due to significant temperature change, and this was clear for both for different concentrations of particles (Fig. 5) and different temperatures when magnetic heating was turned off (Fig. 6). In Fig. 5, one can observe that for a higher concentration of magnetite particles the temperature reached the limiting value (45 °C) faster than for samples with lower concentration. Ultrasound data also provided this distinction, e.g., the difference in attenuation coefficient was around 1.6 dB/cm and in the speed of ultrasound was around 50 m/s between samples with 400 mg and 100 mg of magnetite particles (Fig. 5b,c). The effect of heating on acoustic parameters was evident for the constant magnetite concentration experiment. For instance, the maximum difference in attenuation coefficient between samples heated to 25 °C and 45 °C was around 4 dB/cm (Fig. 6b) and in the speed of ultrasound was around 110 m/s (Fig. 6c). The ultrasound technique was therefore sensitive to changes in the temperature of the sample. From a theoretical point of view, both attenuation coefficient and speed of ultrasound are dependent on the temperature because of the relation between temperature, viscosity, and density, which explains the differences between samples in Fig. 6. When the impact of temperature change on properties

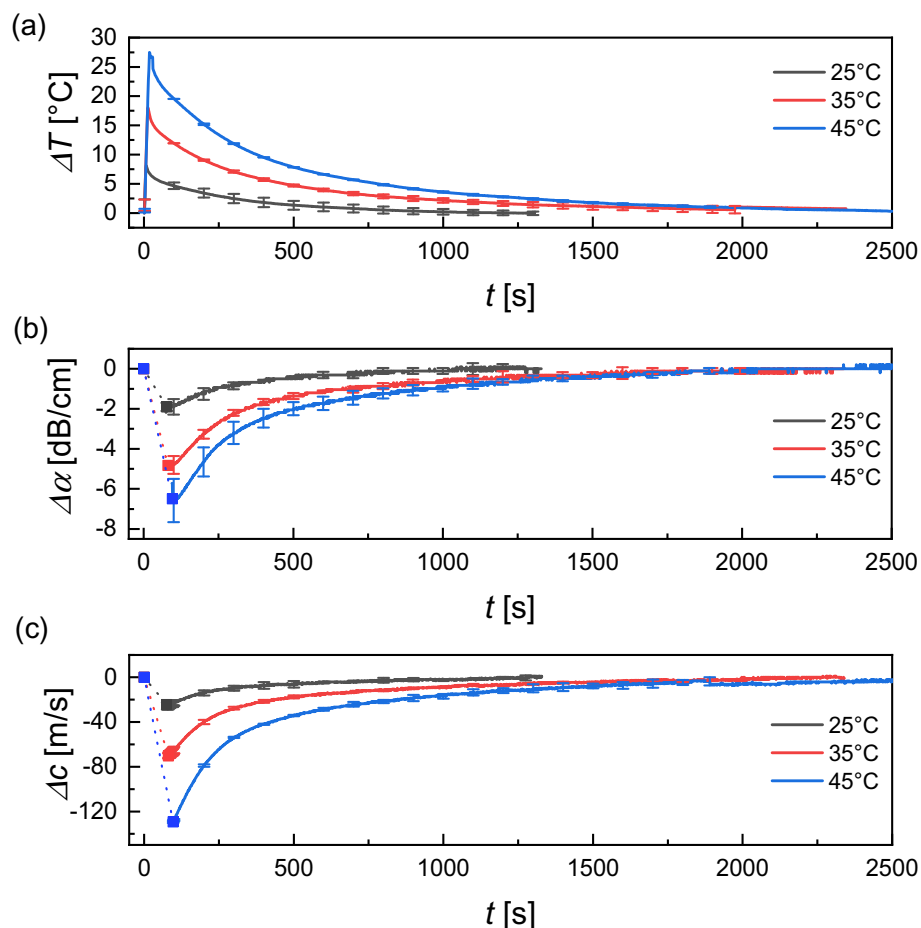


Fig. 6. (a) The temperature change for a magnetite dispersion in castor oil exposed to an AC magnetic field. (b) The change of ultrasonic attenuation coefficient and (c) speed of ultrasound observed after a magnetic field was turned off. The mass of magnetic particles was 400 mg, but the duration of application of the AC magnetic field was different.

of magnetic fluids has been investigated in the literature, the attenuation coefficient decreased as the viscosity of the carrier fluid increased at higher temperatures [31]. Others have shown similar dependence [45], but additionally, the measured change in acoustic properties during the process of non-magnetic heating of the magnetic fluid was higher than expected based on the decrease of viscosity and density. The formation of structures of magnetic particles in magnetic fluids under the influence of static magnetic fields was indicated as a possible explanation.

Interestingly, for our study the amount of magnetic particles did not affect the dependence of the acoustic properties of the magnetic fluid on the temperature, such as the limiting temperature, i.e., the curves corresponding to different magnetic particle concentrations in Fig. 5 are close each other, especially for the attenuation data. Although, the absolute values of attenuation coefficient and speed of ultrasound surely varied from sample to sample because of the presence of additional scatterers, the relative coefficient did not necessarily vary.

While the temperature of the sample returned to the starting temperature, the acoustic parameters presented in Figs. 5 and 6 returned to these measured before magnetic heating. This indicates that no permanent changes occurred in the structure of the castor oil-based magnetic fluid as a consequence of magnetic heating. This would generally be challenging to demonstrate using optical microscopy because of the limitations for optically opaque systems and by other techniques such as TEM, SEM, or dynamic light scattering (DLS) because of sample preparation. Our experiments demonstrate the sensitivity of ultrasonic waves for monitoring the two-phase system, especially for constant concentrations of magnetite particles with different final magnetic heating temperatures. The results for the three-phase systems (Pickering emulsions) are presented in the next section.

3.2. Calorimetric and ultrasonic measurements of magnetic Pickering emulsions

As the main goal of the study was to investigate the potential changes in acoustic properties of magnetic Pickering droplets when exposed to AC magnetic fields, after the preparation of an emulsion using ultrasound and electric fields, we performed the same experiment as for magnetite particles dispersed in castor oil. The temporal evolution of the temperature and ultrasonic parameters during and after magnetic heating for different amounts of magnetic particles used as stabilizers is presented in Fig. 7. Fig. 8 shows the results for different temperatures when the magnetic field was turned off.

As one can see, the results from Figs. 7 and 8 are comparable to those obtained for magnetic fluids. Most importantly, the acoustic parameters returned to their value measured before magnetic heating along with cooling, which indicates the absence of permanent structural changes occurring under the AC magnetic field. In emulsions, coalescence of droplets can occur under the magnetic field, analogically to electro-coalescence. However, the change in droplet size would influence the acoustic parameters [35], and at the end of measurements, the values would not be close to those at the beginning of the experiment.

For Pickering emulsions, the lack of differences for samples with various amounts of particles (Fig. 7) is more apparent than for magnetic dispersions. When looking at changes in the speed of ultrasound change, the data corresponding to different amounts of magnetite particles in the emulsion samples overlapped especially well. However, when the samples with the same amount of magnetic material were heated up to different temperatures (Fig. 8), the changes in attenuation coefficient and speed of ultrasound exhibited differences for 25 °C and 45 °C around

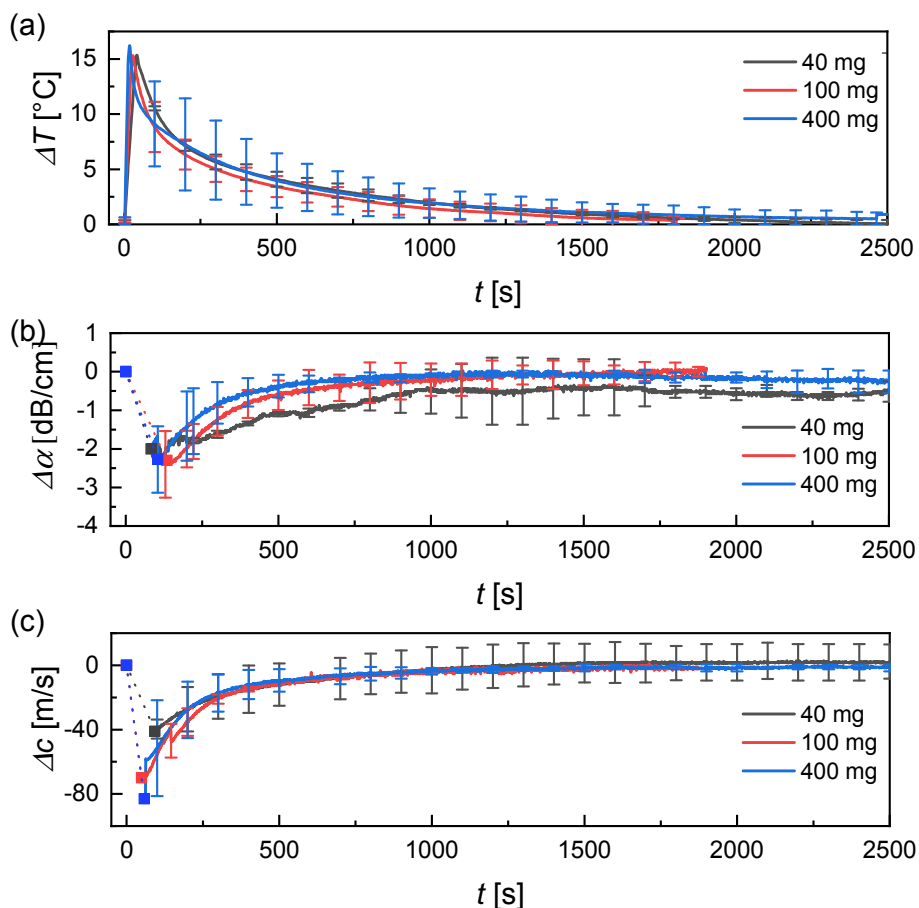


Fig. 7. (a) The temperature change for magnetite-stabilized emulsions exposed to an AC magnetic field. (b) The change of ultrasonic attenuation coefficient and (c) speed of ultrasound observed after magnetic field was turned off. Samples differed in the mass of dispersed magnetic particles.

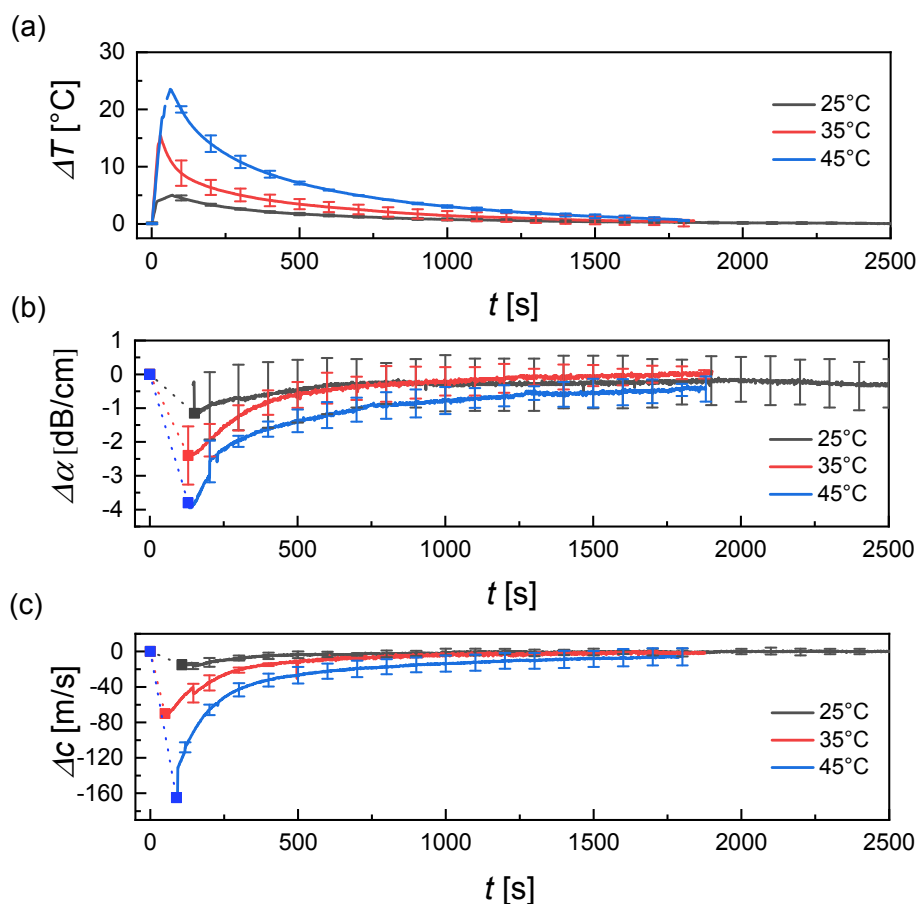


Fig. 8. (a) The temperature change for magnetite-stabilized emulsions exposed to AC magnetic field. (b) The change of ultrasonic attenuation coefficient and (c) speed of ultrasound observed after magnetic field was turned off. The mass of magnetic particles was 100 mg, but the duration of application of the AC magnetic field was different.

3 dB/cm and 140 m/s, respectively. We should note that the amount of silicone oil was the same for each experiment (1:10). The presence of additional phases (inner phase, silicone oil) led to more significant deviations in the speed of ultrasound compared to magnetic fluids; the change in attenuation coefficient between starting temperature and maximum temperature was however smaller for emulsions than for dispersions.

Different concentrations of magnetite were used to form magnetic fluids and stabilize silicone oil droplets, and this affected the heating rate, i.e., the same temperature was achieved faster when more magnetic particles were in the samples. However, the presence of the third phase did not influence the structures of the colloidal systems and the change in structures under the magnetic field. Despite the fact that, for higher concentrations of magnetic particles, there are undoubtedly stronger dipole–dipole interactions, the “relaxation of particles” when the magnetic field was turned off was not reflected in ultrasonic measurements. This observation supports the efficiency of our method of using ultrasound and electric fields to form stable Pickering emulsions. Even after applying the AC magnetic field and exposing it to higher temperatures, the emulsion was still as stable as when formed, according to the acoustic measurements.

3.3. The changes in properties of sintered soft particles dispersed in castor oil

The above results provided evidence that the AC magnetic field did not cause permanent structural changes in magnetic fluids and magnetic Pickering emulsions as their ultrasonic properties did not change after

magnetic heating and cooling to the starting temperature. To show that ultrasound is sensitive to such structural changes when they do occur, we exposed the mixture of magnetic and polystyrene particles dispersed in castor oil to magnetic heating. The appearance of such dispersion is presented in Fig. 9.

Because of the high content of magnetite particles in the dispersion and the long duration of magnetic field application, the temperature in the sample was high enough to induce sintering of soft particles. After cooling down, this resulted in changes in polystyrene particle size that are evident when comparing particle size in Figs. 1c and 9c. The AC magnetic heating also caused the formation of bigger structures consisting of both magnetite and polystyrene, as shown in Fig. 9d. The changes in the structure were permanent in this case, as shown by ultrasound measurements: in Fig. 10, the change of attenuation coefficient and speed of ultrasound before and after magnetic heating of magnetite-polystyrene dispersion is presented. The sample was consecutively cooled down, so both values are for the same temperature.

The ultrasound technique was efficient to show the change in structure caused by high temperature. The fusion of polystyrene particles and the formation of larger structures presented in Fig. 9 can be considered a kind of coalescence; it influenced the size distribution of scatterers in the medium, which led to a change in acoustic parameters after the sample had cooled down. The difference in attenuation coefficient is twice that of the magnetic emulsions and magnetic fluids after cooling down. The difference in speed of ultrasound is much smaller, but still more evident than for other colloids investigated in this work.

In this work, we analyzed the ultrasonic signals in the time domain to the investigate acoustic properties of magnetic colloids over time.

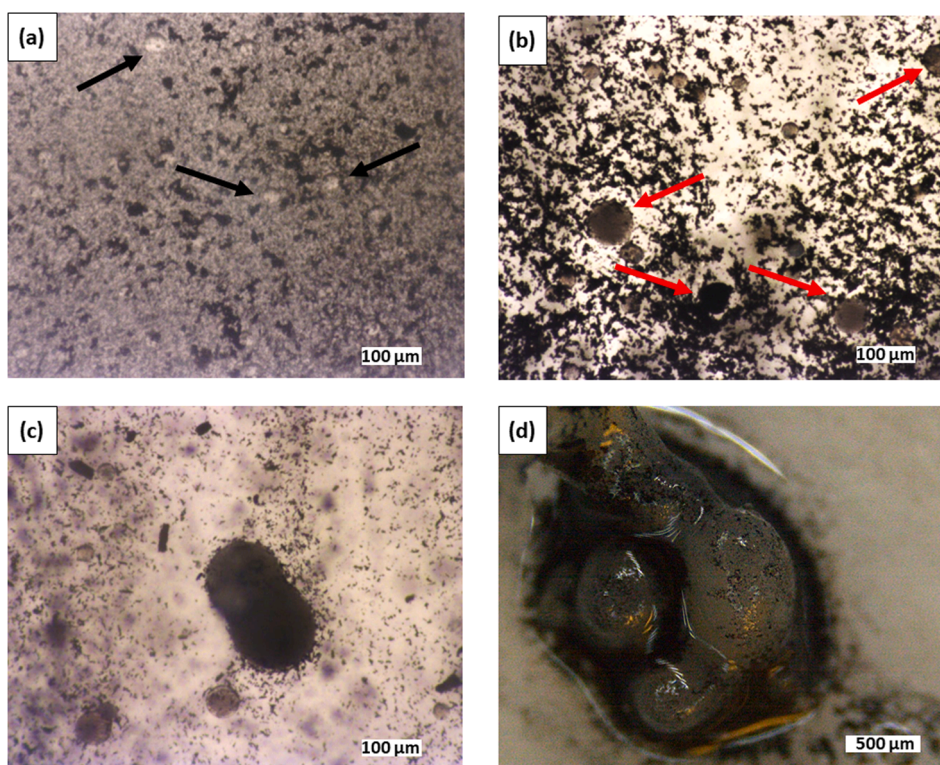


Fig. 9. Optical microscopy image of polystyrene-magnetite dispersions in castor oil: (a) before magnetic heating, (b) after 2 min of magnetic heating with $H = 16.2$ kA/m. The arrows indicate polystyrene particles. (c) An example of partially fused polystyrene particles and (d) is massive magnetite-polystyrene agglomerate formed under extremely high temperatures. All images were taken after the dilution of the system.

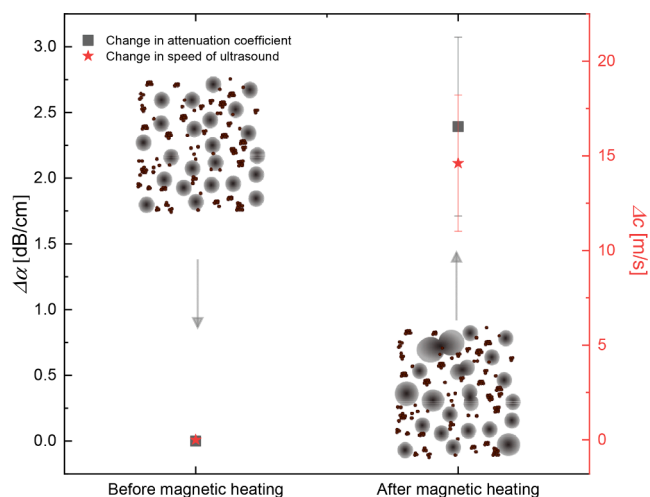


Fig. 10. The change in attenuation coefficient (black) and speed of ultrasound (red) for polystyrene-magnetite dispersions in castor oil (a) before magnetic heating and (b) after 2 min of magnetic heating with $H = 16.2$ kA·m⁻¹ and subsequent cooling to the room temperature. The samples consisted of 3500 mg of castor oil, 350 mg of polystyrene particles and 250 mg of magnetite particles. The schematic macroscopic appearance of colloidal systems before and after heating is also presented.

However, it is possible to use frequency analysis as a supplementary method of monitoring colloidal systems [46]. When the ultrasonic transducers generate the signals with a large enough broad-band frequency range, not only signal amplitude and time of flight carry information (see Fig. 4), but also the frequency, i.e., the frequency-dependent attenuation coefficient can be also affected by changes in the tested medium as well as the speed of ultrasound. It could be especially

interesting for the comparison of the colloidal system's properties in two stages, e.g., before and after sintering as in Fig. 10. In the case of ultrasonic pulses used to plot Fig. 10, frequency analysis did not reveal significant changes either in the attenuation coefficient or speed of ultrasound (see, Supplementary Materials, Fig. S1). Nonetheless, such analysis combined with theoretical descriptions such as Epstein-Carhart-Allegra-Hawley's (ECAH) theory can allow determination of the size distribution of particles or droplets [47] when ultrasonic signals are broad-band. This procedure is, however, complicated by the need for exact parameters of the medium such as thermal expansion coefficient or speed of ultrasound in each of the substrates.

Some groups have reported using ultrasound measurements of the speed of ultrasound and the change in compressibility of a whole magnetic fluid to determine the formation of larger structures such as clusters [48]. Assuming that the change in compressibility can be evidence of structural change of the emulsion, Preetz et al. showed that absolute values of speed of sound increased when the rigid shells around emulsion droplets were formed in the process of encapsulation [49]. Similarly, the efficient fabrication of capsules from Pickering droplets due to magnetic heating could be indicated by the difference in acoustic parameters since our results showed the suitability of the ultrasound technique for showing changes occurring under the AC magnetic field.

Ultrasound is here shown as a tool to reveal structural changes during the dynamic process of magnetic heating. However, ultrasound is more and more often used to follow temperature changes [50] due to the correlation between ultrasound velocity and temperature of the medium, although rarely for magnetic heating [51]. Ultrasound has potential to follow temperature deviations under magnetic heating. Fig. 11 presents the change in the speed of ultrasound in the function of temperature in the sample for pure oils, magnetic fluids, and magnetic emulsions. The results for magnetic fluids and emulsions were obtained in the experiment of magnetic heating.

There was no significant difference between pure oils and magnetic colloidal systems regarding the dependence of the speed of ultrasound

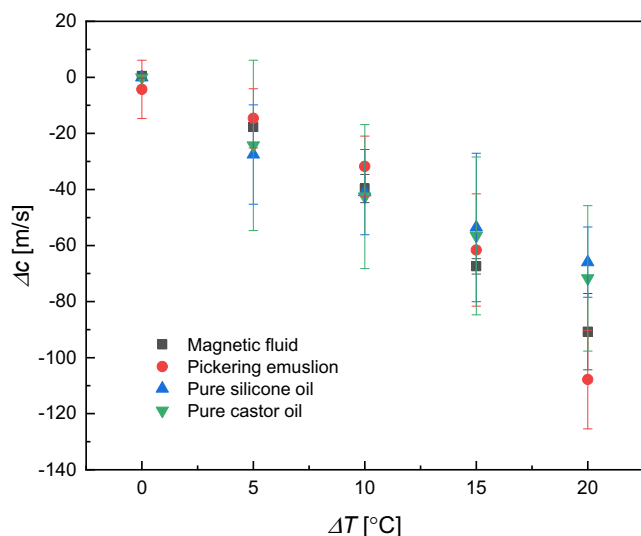


Fig. 11. The change in speed of ultrasound *versus* temperature increase in the sample. For magnetic fluids and emulsions, the same mass of magnetite particles was used (100 mg). The change in speed of sound is the difference between the value obtained for room temperature and that obtained for temperature measured inside the sample. For pure oils, the temperature increase was induced by a thermostated bath.

on the temperature. However, the addition of magnetic particles (and silicone droplets for Pickering emulsions) seemed to be more important for more significant temperature deviations. A linear dependence of the change of speed of ultrasound *versus* a change of temperature is well-documented for pure oils and magnetic fluids [50,52]. It could be useful for monitoring the temperature in the samples during magnetic heating along with following the potential structural changes.

The difference in ultrasonic attenuation between magnetic suspensions and emulsions indicates that the latter can be more useful for ultrasonic hyperthermia applications, i.e., when the absorption of acoustic energy is transformed into heat. The presence of solid magnetic particles at the droplet interface could be useful for simultaneously enhancing acoustic contrast in ultrasonic imaging in what is a potential dual theranostic application.

4. Conclusion

In this paper, we propose simple ultrasonic measurements for evaluating potential changes in the structure of magnetic colloids exposed to AC magnetic fields. The results were different for emulsions stabilised solely with magnetite nanoparticles and dispersions of mixed magnetic and soft particles. The changes of ultrasonic parameters were correlated with temperature changes. The heating and cooling rate depended on the concentrations of magnetic particles and magnetic heating time; irrespective of these, the ultrasonic parameters returned to the starting values along with the temperature. We also showed the efficiency of using ultrasonic measurements to monitor magnetite-soft particle dispersions in which particles are partially sintered under high temperatures. In comparison to results obtained after cooling down magnetic fluids and magnetic Pickering emulsions, a difference in acoustic parameters after magnetic heating and subsequent cooling was revealed. This demonstrates that ultrasound was sensitive to the structural changes such as the change in the size of soft particles due to their fusion or the formation of larger structures consisting of sintered polystyrene and magnetite particles, as we showed by microscopy imaging.

The presented results from ultrasonic measurements show that AC magnetic fields can be used for heating colloidal systems in applications where the stability during and after heating must be maintained. It is particularly important for magnetic Pickering emulsions that are

candidates for heating carriers in thermal therapies or facilitated catalysis.

CRediT authorship contribution statement

Rafał Bielas: Investigation, Formal analysis, Visualization, Conceptualization, Writing - original draft. **Bassam Jameel:** Investigation, Visualization, Writing - original draft. **Arkadiusz Józefczak:** Conceptualization, Methodology, Supervision.

Declaration of Competing Interest

There is no conflict of interest to declare.

Acknowledgements

The authors would like to acknowledge Polish National Science Centre for support through the projects no. 2019/35/N/ST5/00402 (PRELUDIUM) and no. 2019/35/O/ST3/00503 (PRELUDIUM BIS). They also wish to thank Yaroslav Harkavyy (AMU, Poznań) to take microscopy images of sintered agglomerates and Prof. Tomasz Hornowski (AMU, Poznań) for valuable discussions.

Appendix A. Supplementary material

Supplementary data to this article can be found online at <https://doi.org/10.1016/j.measurement.2021.109431>.

References

- [1] P. Das, M. Colombo, D. Prosperi, Recent advances in magnetic fluid hyperthermia for cancer therapy, *Colloids Surf. Biointerfaces* 174 (2019) 42–55.
- [2] A. Bhardwaj, K. Parekh, N. Jain, In vitro hyperthermic effect of magnetic fluid on cervical and breast cancer cells, *Sci. Rep.* 10 (1) (2020) 1–13.
- [3] B. Lahiri, S. Ranoo, J. Philip, Effect of orientational ordering of magnetic nanoemulsions immobilized in agar gel on magnetic hyperthermia, *J. Magn. Magn. Mater.* 451 (2018) 254–268.
- [4] B. Lahiri, S. Ranoo, A. Zaibudeen, J. Philip, Magnetic hyperthermia in magnetic nanoemulsions: Effects of polydispersity, particle concentration and medium viscosity, *J. Magn. Magn. Mater.* 441 (2017) 310–327.
- [5] S. Ranoo, B.B. Lahiri, M. Nandy, J. Philip, Enhanced magnetic heating efficiency at acidic pH for magnetic nanoemulsions stabilized with a weak polyelectrolyte, *J. Colloid Interface Sci.* 579 (2020) 582–597.
- [6] R. Aveyard, B.P. Binks, J.H. Clint, Emulsions stabilised solely by colloidal particles, *Adv. Colloid Interface Sci.* 100 (2003) 503–546.
- [7] L.E. Low, S.P. Siva, Y.K. Ho, E.S. Chan, B.T. Tey, Recent advances of characterization techniques for the formation, physical properties and stability of Pickering emulsion, *Adv. Colloid Interface Sci.* 277 (2020), 102117.
- [8] Z. Rozynek, R. Castberg, A. Kalicka, P. Jankowski, P. Garstecki, Electric field manipulation of particles in leaky dielectric liquids, *Arch. Mech.* 67 (5) (2015) 385–399.
- [9] M. Destribats, S. Gineste, E. Laurichesse, H. Tanner, F. Leal-Calderon, V. Heroguez, V. Schmitt, Pickering Emulsions: What Are the Main Parameters Determining the Emulsion Type and Interfacial Properties? *Langmuir* 30 (31) (2014) 9313–9326.
- [10] S. Arditty, C.P. Whitby, B.P. Binks, V. Schmitt, F. Leal-Calderon, Some general features of limited coalescence in solid-stabilized emulsions, *Eur. Phys. J. E* 11 (3) (2003) 273–281.
- [11] T.A. Prileszky, E.M. Furst, Magnetite nanoparticles program the assembly, response, and reconfiguration of structured emulsions, *Soft Matter* 15 (7) (2019) 1529–1538.
- [12] M. Jalili Darbandi Sofla, S. Norouzi-Apourvari, M. Schaffie, The effect of magnetic field on stability of conventional and pickering water-in-crude oil emulsions stabilized with fumed silica and iron oxide nanoparticles, *J. Mol. Liquids* 314 (2020) 113629.
- [13] H. Yang, S. Wang, W. Zhang, J. Wu, S. Yang, D. Yu, X. Wu, Y. Sun, J. Wang, Rapid demulsification of pickering emulsions triggered by controllable magnetic field, *Sci. Rep.* 10 (1) (2020) 16565.
- [14] L.E. Low, B.T. Tey, B.H. Ong, S.Y. Tang, Unravelling pH-responsive behaviour of Fe₃O₄@CNCs-stabilized Pickering emulsions under the influence of magnetic field, *Polymer* 141 (2018) 93–101.
- [15] L.E. Low, L.T.-H. Tan, B.-H. Goh, B.T. Tey, B.H. Ong, S.Y. Tang, Magnetic cellulose nanocrystal stabilized Pickering emulsions for enhanced bioactive release and human colon cancer therapy, *Int. J. Biol. Macromol.* 127 (2019) 76–84.
- [16] C.A. Zentner, A. Concellón, T.M. Swager, Controlled movement of complex double emulsions via interfacially confined magnetic nanoparticles, *ACS Cent. Sci.* 6 (8) (2020) 1460–1466.

- [17] D.L. Huber, Synthesis, Properties, and Applications of Iron Nanoparticles, *Small* 1 (5) (2005) 482–501.
- [18] K. Kaczmarek, R. Mrówczyński, T. Hornowski, R. Bielas, A. Józefczak, The effect of tissue-mimicking phantom compressibility on magnetic hyperthermia, *Nanomaterials* 9, (5) (2019) 803.
- [19] R. Bielas, T. Hornowski, K. Paulovičová, M. Rajňák, A. Józefczak, The effect of magnetic particles covering the droplets on the heating rate of Pickering emulsions in the AC magnetic field, *J. Mol. Liq.* 320 (2020), 114388.
- [20] R. Bielas, A. Józefczak, The Effect of Particle Shell on Cooling Rates in Oil-in-Oil Magnetic Pickering Emulsions, *Materials* 13, (21) (2020) 4783.
- [21] H. Kok, A. Kotte, J. Crezee, Planning, optimisation and evaluation of hyperthermia treatments, *Int. J. Hyperth.* 33 (6) (2017) 593–607.
- [22] R. Bielas, D. Surdeko, K. Kaczmarek, A. Józefczak, The potential of magnetic heating for fabricating Pickering-emulsion-based capsules, *Colloids Surf. B: Biointerfaces* 2020, 111070.
- [23] L. Steinmetz, C. Kirsch, C. Geers, A. Fink, M. Bonmarin, Investigating a Lock-In Thermal Imaging Setup for the Detection and Characterization of Magnetic Nanoparticles, *Nanomaterials* 10 (2020) 1665.
- [24] S. Curto, P. Faridi, T.B. Shrestha, M. Pyle, L. Maurmann, D. Troyer, S.H. Bossmann, P. Prakash, An integrated platform for small-animal hyperthermia investigations under ultra-high-field MRI guidance, *Int. J. Hyperth.* 34 (4) (2018) 341–351.
- [25] P.-C. Huang, E.J. Chaney, R.R. Iyer, D.R. Spillman, B. Odintsov, N.A. Sobh, S. A. Boppart, Interstitial magnetic radiotherapy dosimetry based on shear wave magnetomotive optical coherence elastography, *Biomed. Opt. Express* 10 (2) (2019) 539–551.
- [26] Y. Hadadian, J.H. Uliana, A.A.O. Carneiro, T.Z. Pavan, A Novel Theranostic Platform: Integration of Magnetomotive and Thermal Ultrasound Imaging with Magnetic Hyperthermia, *IEEE Trans. Biomed. Eng.* (2020) 1.
- [27] L. Bai, A. Velichko, B.W. Drinkwater, Ultrasonic defect characterisation—Use of amplitude, phase, and frequency information, *J. Acoust. Soc. Am.* 143 (1) (2018) 349–360.
- [28] M. Toozandehjani, K.A. Matori, F. Ostovan, F. Mustapha, N.I. Zahari, A. Oskoueian, On the correlation between microstructural evolution and ultrasonic properties: a review, *J. Mater. Sci.* 50 (7) (2015) 2643–2665.
- [29] S. Cong, T. Gang, Ultrasonic thickness measurement for aluminum alloy irregular surface parts based on spectral analysis, *Trans. Nonferrous Metals Soc. China* 22 (2012) s323–s328.
- [30] Y.-M. Cheong, K.-M. Kim, D.-J. Kim, High-temperature ultrasonic thickness monitoring for pipe thinning in a flow-accelerated corrosion proof test facility, *Nucl. Eng. Technol.* 49 (7) (2017) 1463–1471.
- [31] M.A. Bramantya, M. Motozawa, T. Sawada, Ultrasonic propagation velocity in magnetic and magnetorheological fluids due to an external magnetic field, *J. Phys.: Condens. Matter* 22, (32) (2010), 324102.
- [32] A.A. Lizunova, A.A. Loshkarev, Y.M. Tokunov, V.V. Ivanov, Comparison of the results of measurements of the sizes of nanoparticles in stable colloidal solutions by the methods of acoustic spectroscopy, dynamic light scattering, and transmission electron microscopy, *Meas. Tech.* 59 (11) (2017) 1151–1155.
- [33] A.S. Dukhin, P.J. Goetz, Characterization of liquids, nano-and microparticulates, and porous bodies using ultrasound, Elsevier, 2010.
- [34] R. Challis, M. Povey, M. Mather, A. Holmes, Ultrasound techniques for characterizing colloidal dispersions, *Rep. Prog. Phys.* 68 (7) (2005) 1541.
- [35] R. Bielas, Z. Rozynek, T. Hornowski, A. Józefczak, Ultrasound control of oil-in-oil Pickering emulsions preparation, *J. Phys. D Appl. Phys.* 53 (8) (2019), 085301.
- [36] P.S. Epstein, R.R. Carhart, The absorption of sound in suspensions and emulsions. I. Water fog in air, *J. Acoust. Soc. Am.* 25 (3) (1953) 553–565.
- [37] J. Allegra, S. Hawley, Attenuation of sound in suspensions and emulsions: Theory and experiments, *J. Acoust. Soc. Am.* 51 (5B) (1972) 1545–1564.
- [38] L. Anson, R. Chivers, Ultrasonic scattering from spherical shells including viscous and thermal effects, *J. Acoust. Soc. Am.* 93 (4) (1993) 1687–1699.
- [39] D. Venkataramani, J.E. Smay, C.P. Aichele, Transient stability of surfactant and solid stabilized water-in-oil emulsions, *Colloids Surf., A* 490 (2016) 84–90.
- [40] Nguyen Thao Tran, Ultrasound Scattering Studies on Pickering Emulsion, *Proc. Symp. Ultrasonic Electron.* 2016 (2016) 37.
- [41] A. Józefczak, R. Wlazło, Ultrasonic studies of emulsion stability in the presence of magnetic nanoparticles, *Adv. Condens. Matter Phys.* 2015 (2015).
- [42] J. Kúdelčík, P. Bury, P. Kopčanský, M. Timko, Structure of nanoparticles in transformer oil-based magnetic fluids, anisotropy of acoustic attenuation, *J. Magn. Mater.* 388 (2015) 28–34.
- [43] Z. Rozynek, A. Józefczak, K.D. Knudsen, A. Skumiel, T. Hornowski, J.O. Fossum, M. Timko, P. Kopčanský, M. Koneracká, Structuring from nanoparticles in oil-based ferrofluids, *Eur. Phys. J. E* 34 (3) (2011) 28.
- [44] Z. Rozynek, R. Bielas, A. Józefczak, Efficient formation of oil-in-oil Pickering emulsions with narrow size distributions by using electric fields, *Soft Matter* 14 (24) (2018) 5140–5149.
- [45] P. Regulska, A. Skumiel, A. Józefczak, Acoustic and magnetic properties dependence of restructuring different magnetic fluids subjected to external magnetic field, *Arch. Acoust.* 31 (4 (S)) (2014) 153-158.
- [46] J. Bauer-Marschallinger, T. Berer, H. Grun, H. Roitner, B. Reitingner, P. Burgholzer, Broadband high-frequency measurement of ultrasonic attenuation of tissues and liquids, *IEEE Trans. Ultrason., Ferroelectr., Freq. Control* 59 (12) (2012) 2631–2645.
- [47] A. Richter, T. Voigt, S. Ripperger, Ultrasonic attenuation spectroscopy of emulsions with droplet sizes greater than 10 μm , *J. Colloid Interface Sci.* 315 (2) (2007) 482–492.
- [48] A. Józefczak, A. Skumiel, Ultrasonic investigation of magnetic nanoparticles suspension with PEG biocompatible coating, *J. Magn. Mater.* 323 (11) (2011) 1509–1516.
- [49] C. Preetz, A. Hauser, G. Hause, A. Kramer, K. Mäder, Application of atomic force microscopy and ultrasonic resonator technology on nanoscale: Distinction of nanoemulsions from nanocapsules, *Eur. J. Pharm. Sci.* 39 (1) (2010) 141–151.
- [50] P.A. Oliveira, R.M.B. Silva, G.C. Morais, A.V. Alvarenga, R.P.B.C. Félix, Speed of sound as a function of temperature for ultrasonic propagation in soybean oil, *J. Phys. Conf. Ser.* 733 (2016), 012040.
- [51] A. Skumiel, T. Hornowski, A. Józefczak, M. Koralewski, B. Leszczyński, Uses and limitation of different thermometers for measuring heating efficiency of magnetic fluids, *Appl. Therm. Eng.* 100 (2016) 1308–1318.
- [52] Š. Hardoň, J. Kúdelčík, M. Rajňák, In Study of structural arrangement in ferrofluid at various temperatures by acoustic spectroscopy, in: *AIP Conference Proceedings*, 2018; AIP Publishing LLC: p 020016.

Electronic Supplementary Materials for:

**Monitoring of Pickering emulsion stability during magnetic heating
using ultrasound measurements**

Rafał Bielas, Bassam Jameel, Arkadiusz Józefczak*

Chair of Acoustics, Faculty of Physics, Adam Mickiewicz University in Poznań,
Uniwersytetu Poznańskiego 2, 61-614 Poznań, Poland

e-mail: aras@amu.edu.pl

1. The analysis of ultrasonic signals in frequency domain

When an ultrasonic signal is received on the transducer after propagation through the medium, its time waveform, i.e. the amplitude *versus* time graph, is recorded. It provides the information on the change of the amplitude of ultrasonic pulse and the time in which pulse travelled in the sample cell. This leads to the determination of attenuation coefficient and speed of ultrasound (ultrasound velocity) as was presented in **Fig. 4**. However, it is possible to express the recorded signal also in the frequency domain using analysis based on Fourier transformation.

Let us assume that the ultrasonic signal in the time domain is $p(t)$ and its Fourier transform calculated *via* Fast Fourier Transform (FFT) algorithm is expressed as $F(f)$. As the results of Fourier transformation are within the set of complex numbers, it is possible to obtain the module ($|F(f)|$) and the argument (φ) of $F(f)$ to find the amplitude spectrum and the phase spectrum of the signal $p(t)$ respectively. To calculate the attenuation coefficient, $\alpha(f)$, and the speed of ultrasound, $c(f)$, one can use the following formula [1, 2]:

$$\alpha(f) = \frac{20}{2d} \log_{10} \frac{|F_2(f)|}{|F_1(f)|}, \quad (\text{S1.1})$$

$$c(f) = \frac{2\pi f \cdot 2d}{2\pi f n - \varphi_1 - \varphi_2}. \quad (\text{S1.2})$$

In the equations, $2d$ relates to the acoustic path of signal and n is an integer associated with the ambiguity of the phase shift. The indices (1) and (2) denote the spectra obtained for tested medium and pure water, respectively. By using the so-called reference method [2], the calculation of absolute value of attenuation coefficient and speed of ultrasound was possible without obtaining data for different positions of the ultrasonic transducer. Instead of this, we used the pulse recorded in distilled water as the reference signal, $p_2(t)$ with its FFT expressed as $F_2(f)$ for the same distance between the transducer and reflecting surface (for the comparison, see **Section 2.3**).

It is worth noting that **Eq. S1** is similar to **Eq. 1** while the expression for the speed of ultrasound (**Eq. 2**) is much less complicated compared to **Eq. S2**. The calculation of phase velocity in the frequency domain demands determining not only the time of flight over the given distance but also the phase shift between two signals what is generally challenging due to ambiguity of phase expressed in radians.

2. The ultrasonic parameters in function of frequency for sintered soft particles dispersed in magnetic fluid

Using the pulses recorded in the dispersion of soft polystyrene particles (Dynoseeds, TS10 6317, Microbeads AS, Norway, $\sim 40 \mu\text{m}$ in size) and magnetic particles (Sigma-Aldrich Co., USA, $\sim 150 \text{ nm}$ in size) in castor oil (see, **Fig. 10**), the frequency analysis resulted in the attenuation coefficient and phase velocity spectra presented in **Fig. S1**. In comparison to the data presented in time domain (**Fig. 10**), we had to use here the reference method to determine ultrasonic spectra. Hence, two different curves are corresponding to the situation before and after magnetic heating. Both of them were obtained by taking a pulse observed in the dispersion ($p_1(t)$) and pure water ($p_2(t)$) into the **Eqs. S1-S2**.

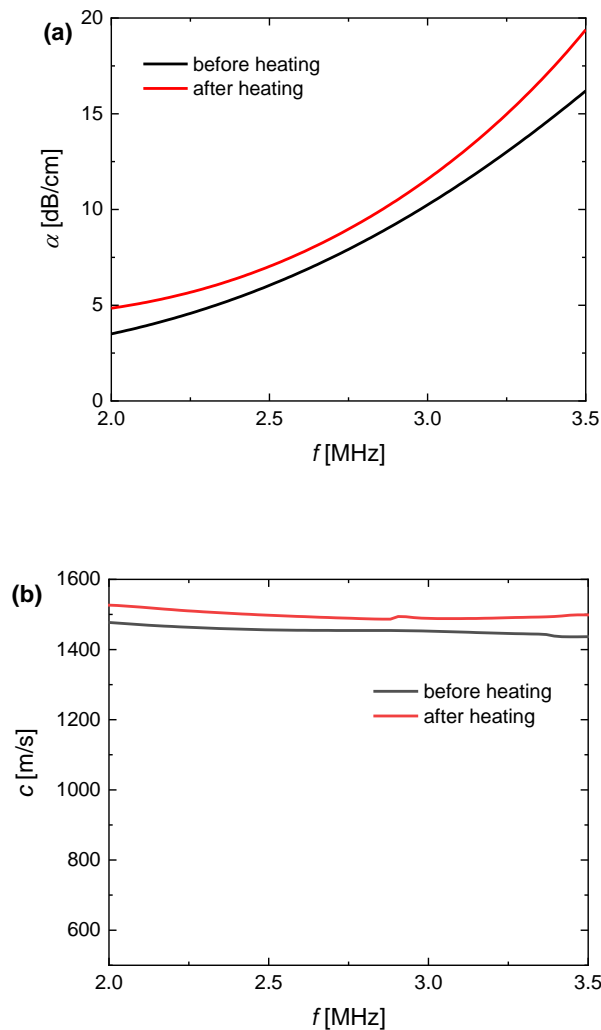


Fig. S1 The attenuation coefficient (a) and phase velocity (b) in the function of frequency for the signals recorded before and after magnetic heating of the dispersion of magnetic particles, polystyrene particles and castor oil. The time of application of the alternating magnetic field ($16.2 \text{ kA}\cdot\text{m}^{-1}$) was 2 minutes. The sample was cooled back to the room temperature, thus both measurements were performed in the same temperature.

As one can see, both attenuation coefficient and phase velocity of ultrasound expressed in the function of frequency was different before and after magnetic heating, similarly to the results in **Fig. 10**. However, the frequency range for the results presented above is narrow. It is due to the transducer we used for this experiment that did not generate wide-band frequency signals. The analysis in frequency domain can be supplementary in the monitoring of dynamic processes in colloidal systems. For wide-band transducers it is possible to observe characteristic maxima and minima in the spectra that can lead to e.g. the determination of the size of scatterers [3].

References:

1. Peters, F.; Petit, L., A broad band spectroscopy method for ultrasound wave velocity and attenuation measurement in dispersive media. *Ultrasonics* **2003**, *41*, (5), 357-363.
2. Hornowski, T.; Józefczak, A.; Skumiel, A.; Łabowski, M., Effect of Poly (Ethylene Glycol) Coating on the Acoustic Properties of Biocompatible Magnetic Fluid. *International Journal of Thermophysics* **2010**, *31*, (1), 70-76.
3. Józefczak, A.; Hornowski, T.; Anita, K.; Molčan, M.; Leszczyński, B.; Timko, M., The Effect of Sonication on Acoustic Properties of Biogenic Ferroparticle Suspension. *Archives of Acoustics* **2016**, *41*, (1), 161–168.

[Publication VI]

The potential of magnetic heating for fabricating
Pickering-emulsions-based capsules

R. Bielas, D. Surdeko, K. Kaczmarek, A. Józefczak

Colloids and Surfaces B: Biointerfaces, 2020, 192: 111070.



The potential of magnetic heating for fabricating Pickering-emulsion-based capsules

Rafał Bielas^a, Dawid Surdeko^{a,b}, Katarzyna Kaczmarek^a, Arkadiusz Józefczak^{a,*}

^a Department of Acoustics, Faculty of Physics, Adam Mickiewicz University in Poznań, Uniwersytetu Poznańskiego 2, 61-614 Poznań, Poland

^b Faculty of Science and Technology, University of Twente, P.O. BOX 217, 7500 AE Enschede, The Netherlands

ARTICLE INFO

Keywords:

Magnetic heating
Pickering emulsions
Colloidal capsules
Specific absorption rate
Magnetic particles
Alternating magnetic field

ABSTRACT

Pickering emulsions (particle-stabilized emulsions) have been widely explored due to their potential applications, one of which is using them as precursors for the formation of colloidal capsules that could be utilized in, among others, the pharmacy and food industries. Here, we present a novel approach to fabricating such colloidal capsules by using heating in the alternating magnetic field. When exposed to the alternating magnetic field, magnetic particles, owing to the hysteresis and/or relaxation losses, become sources of nano- and micro-heating that can significantly increase the temperature of the colloidal system. This temperature rise was evaluated in oil-in-oil Pickering emulsions stabilized by both magnetite and polystyrene particles. When a sample reached high enough temperature, particle fusion caused by glass transition of polystyrene was observed on surfaces of colloidal droplets. Oil droplets covered with shells of fused polystyrene particles were proved to be less susceptible to external stress, which can be evidence of the successful formation of capsules from Pickering emulsion droplets as templates.

1. Introduction

Colloidal capsules have become the emerging class of structures due to their applications, mainly in the pharmaceutical industry [1], where they may provide great possibilities for controlled release of encapsulated species [2,3]. There are several routes for fabricating colloidal capsules from particle-stabilized emulsions (Pickering emulsions), including the use of polyelectrolyte complexation on the particle layers [4], gel trapping [5], polymerization [6] or sintering [7]. The last one leads to the formation of the capsule shell, as particles on the droplet surfaces are fused under high temperature. An important factor here is the glass transition temperature (T_g). Above this value particles can fuse without being completely melted [8]. Other factors, such as time of sintering and particle concentration, should also be taken into account [9]. In this paper, we propose the potential new technique of production of colloidal capsules from oil-in-oil Pickering emulsions by using magnetic particles in the alternating magnetic field.

Magnetic nano- and microparticles have long been known as heating agents. When immersed in a medium, the heat from these sources is then dissipated into their immediate surroundings [10]. The generation of thermal energy by particles placed in the alternating magnetic field is based on energy dissipation owing to three main mechanisms: hysteresis, Néel, and Brownian relaxation, and induction

of eddy currents. The last one is, in principle, negligible for small objects such as nano- or microparticles of very low electrical conductivity [11]. Energy dissipation due to hysteresis losses occurs for magnetic particles of sizes above the critical value [12]. Magnetic energy is dissipated into heat by movement of the magnetic domain walls, and heat losses are proportional to the third power of the magnetic field's amplitude [13]. Energy dissipation is also related to two independent relaxation mechanisms: Brown and Néel. In Brownian relaxation rotation of a spontaneous magnetization vector causes rotation of the whole particle. This rotation is being resisted by the surrounding medium due to its viscosity and therefore relaxation occurs. In this mechanism relaxation time τ_B depends on the hydrodynamic volume of a magnetic particle V_h , shear viscosity of the medium η , and temperature T :

$$\tau_B = \frac{3\eta V_h}{k_B T} \quad (1)$$

In Néel mechanism relaxation time τ_N can be expressed as:

$$\tau_N = \tau_0 \exp\left(\frac{KV}{k_B T}\right) \quad (2)$$

where $\tau_0 \approx 10^{-9}$ s and KV refers to the energy barrier that the magnetic moment must overcome to reverse its direction within the particle. The most typical situation is when both relaxation mechanisms and

* Corresponding author.

E-mail address: aras@amu.edu.pl (A. Józefczak).

hysteresis losses arise at the same time. However, the size of the particles determines the dominating mechanism [12,13].

Magnetic heating has been commonly associated with the application in magnetic particles-mediated hyperthermia that is a promising modality to help cancer treatment [14]. However, this temperature rise can also be used in other applications. For instance, magnetic heating can help in fragmentation of cancer cells and destroying them directly [15]. Temperature elevation may also enable reversible emulsion destabilization, as in the work of Kaiser et al., where polystyrene-magnetite particles were used to stabilize emulsions [16]. Using the oscillating magnetic field to affect the organization of so-called endoskeletal droplets was also recently demonstrated [17]. Nano-heating, i.e. a phenomenon allowing for heat to be delivered up to 100 nm away from magnetic nanoparticle surface, were used in chemical procedures like in flow reactors [18,19] or catalysis [20,21]. In the latter case, induction heating by nanoparticles is currently a subject of increasing scientific interest [22].

Various types of particles, e.g. silver [23], gold [24], silica [25], polystyrene [26] or clay [27] can be utilized for fabrication of colloidal capsules. Magnetic particles were also used for that purpose [28,29]. These attempts are of great importance, since the external magnetic field is believed to be one of the methods to trigger a cargo release from capsules [30]. In the literature, one can find some examples of the use of different particles together to stabilize emulsions [16,31] and to form colloidosomes [32]. In our work, we used polystyrene microparticles along with magnetite particles that acted as heat sources. We primarily investigated how the presence of magnetic material affects the temperature rise in particle-stabilized emulsions (Pickering emulsions) placed in the alternating magnetic field. Then, we performed experiments for single droplets with a polystyrene-magnetite coating exposing them to the magnetic field which resulted in a temperature elevation. As we will show, magnetic field-induced heating can provide a new potential method of fabricating colloidal capsules from Pickering droplets. It is a novel contribution to the investigation of heating effect in particle-stabilized emulsions. What is also important, there is a lack of reports on usage of oil-in-oil emulsions for production of colloidal capsules [33].

2. Materials and Methods

2.1. Materials

To form oil-in-oil Pickering emulsions we used silicone oil (Rhodorsil oils 47 V 50, a viscosity of 50 mPa·s) for the dispersed phase and castor oil (MERLIN, MA 220-1, a viscosity of 700 mPa·s) for the continuous phase. As stabilizers we used polystyrene particles (PSPs, Dynoseeds, TS10 6317, Microbeads AS) with average size $\sim 10 \mu\text{m}$ and two types of magnetite particles in the form of powder (MPs, Sigma-Aldrich Co.): smaller (nMPs, 50-100 nm in size, density of around $4800\text{-}5100 \text{ kg}\cdot\text{m}^{-3}$) and bigger (μMPs , $< 5 \mu\text{m}$ in size, a density of about $4800\text{-}5100 \text{ kg}\cdot\text{m}^{-3}$). Polystyrene particles underwent a surface modification according to the method described in [34]. Briefly, PSPs were dispersed in the solution of acrylate polymer (PFC 502AFA, FluoroPEL™, Cytonix as modifier) and methoxy-nonafluorobutane (7100 Engineered Fluid, 3M™ Novec™ as solvent). After the evaporation of the solvent, the PSPs were thoroughly washed and dried. After this procedure, their affinity to the continuous phase of the emulsion was increased that facilitated the stability of the particles at the interface.

2.2. Preparation of magnetite-polystyrene Pickering emulsions

Pickering emulsions were prepared according to the method described in detail in one of our previous works [35]. Briefly, the mixture of particles and oils was homogenized for 30 seconds using ultrasonic device (Sonoplus HD 300, Bandelin, acoustic intensity estimated as $17 \text{ W}\cdot\text{cm}^{-2}$, working frequency of 18 kHz) resulting in formation of a non-

stable emulsion. The main mechanism involved in emulsification using ultrasound is ultrasonic cavitation. The implosion of cavitation bubbles occurs in the presence of high energy ultrasonic waves and causes dispersion of the inner phase. In our case, the acoustic power was high enough to produce what we call “pre-emulsion”, i.e. small silicone droplets but barely covered by particles. In the electric field, due to consecutive events of electrocoalescence, droplets formed during ultrasonication would get gradually covered with particles, up to the point of complete surface coverage. The electric field was supplied to the copper electrodes placed on the sides of a glass cuvette (30 mm x 18 mm x 1.3 mm) by DC-to-DC high voltage amplifier (UltraVolt 1AA12-P4, Advanced Energy Co.). We followed the process of preparation of Pickering emulsions using a CMOS camera (UI-3590CP-C-HQ, IDS) mounted on a high-magnification zoom lens system (MVL12 \times 3Z, Thorlabs), a light source and a computer for collecting images and recording videos. In each experiment, for each sample, we used the same amount of the polystyrene particles, silicone oil and castor oil (silicone oil to castor oil mass ratio 1:10, polystyrene particles to silicone oil mass ratio: 1:4). However, samples differed in the amount of magnetic particles used - from 1:8 to 1:1 polystyrene-magnetite mass ratios.

2.3. Calorimetric measurements in magnetic field

Calorimetric measurements were performed using a compact induction heating system (EASYHEAT, Ambrell Co.) as a source of the alternating magnetic field. The frequency of the field was 356 kHz and the intensity was 16.2 kA/m. The temperature in the emulsion sample was measured using a temperature sensor system (FLUOTEMP, Photon Control Inc.) with an optic fiber temperature probe (model FTP-NY2) and a pyrometer (VT02, Fluke Co.). During experiments, the fiber was placed centrally in the sample. The sample cell was the same as the one used for experiments in the electric field. Induction coil was cooled efficiently by an external system, therefore the temperature rise from the coil was found to be negligible (measured as $\sim 0.12 \text{ }^\circ\text{C}$). A single measurement lasted 120 seconds. The scheme of the experiment is presented in Fig. 1.

3. Results and Discussion

3.1. Magnetic heating measurements

In the first experimental step, we prepared Pickering emulsions stabilized with magnetite and polystyrene particles used together, as it was described in section 2.2. The optical microscopy measurements were performed to characterize the appearance of emulsions after ultrasonic homogenization and subsequent stabilization in the electric field. The results are presented in Fig. 2.

As one can see, there is no significant aggregation in the emulsion and the droplets were covered sufficiently by both polystyrene and magnetite particles (in size of micrometers) as it is evidenced by dark and bright particles in Fig. 2b. Because of a difference in wettability, magnetic particles (MPs) were more attached to the droplet interface than polystyrene particles (PSPs). However, the distribution of particles suggested that there was a potential for a fusion of polystyrene under exposure to a high enough local temperature. In the experiment, the concentration of silicone oil droplets (10% w/w) was low enough to ensure direct optical observation without any dilution. Speaking of which, we found the possibility of direct observation most significant for our concept of Pickering emulsions formation in the electric field [29]. After formation in the electric field, particles at the droplet interface formed such a dense layer that ensured the stability against further coalescence events.

In order to show the efficiency of heating induced by magnetic particles in an external magnetic field, we investigated such low-concentrated Pickering emulsions (10% silicone oil to castor oil mass ratio) stabilized with both polystyrene and magnetite particles, and compared

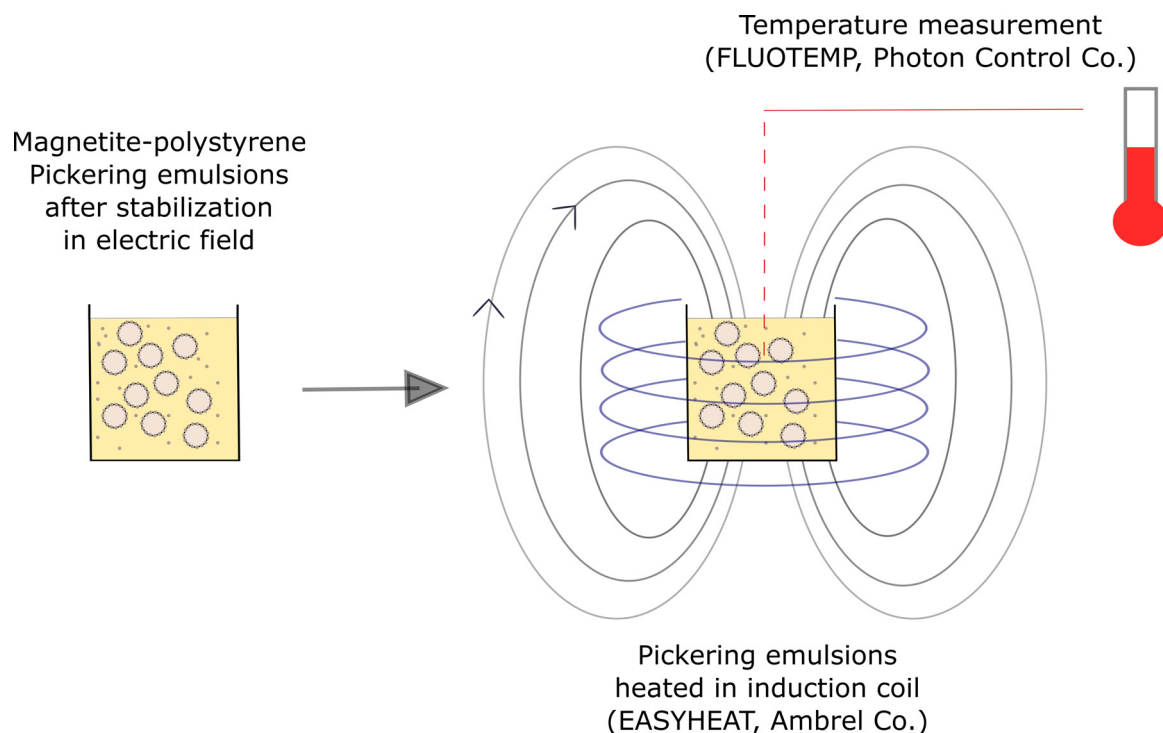


Fig. 1. A schematic illustration of the magnetic heating measurements.

them with corresponding pre-emulsions (i.e. systems where silicone oil droplets were not completely covered by **PSPs** and **MPs**) exposed to the same conditions. The results are presented in Fig. 3.

The increase of temperature was more dynamic and the final temperature increase was higher for the emulsions stabilized by magnetic microparticles (Fig. 3b,d). It is in clear accordance with theoretical predictions. The relaxation mechanisms responsible for the generation of heat for small magnetite particles are hindered for sufficiently large particles because the Brown and Néel relaxation times are dependent on particle dimensions. For bigger particles, μ **MPs**, relaxation times are very long and the only hysteresis loss can contribute to the generation of heat since particle sizes are above a critical value of the single-domain particles [36]. In Fig. 3, it is also clearly seen that the temperature increase is determined by the amount of the magnetic material in the sample (expressed as a mass ratio to the **PSPs**).

The efficiency of heating is often characterized by the specific absorption rate (SAR), expressed as initial temperature rise $\frac{dT}{dt}$ multiplied the specific heat c_p of a sample:

$$SAR = c_p \left(\frac{dT}{dt} \right)_{t=0} \quad (3)$$

We determined this parameter for emulsions stabilized with **PSPs** and different **MPs** by fitting the experimental curves from Fig. 3 to the Box-Lucas equation [37,38]:

$$\Delta T(t) = T_{max} \cdot (1 - \exp(-\frac{t}{\tau})) \quad (4)$$

The parameters T_{max} and τ were derived from the fitting. Therefore, the initial increase of the temperature during heating can be expressed as a derivative: $(\frac{dT}{dt})_{t=0} = \frac{T_{max}}{\tau}$.

We also compared this data with results obtained for pre-emulsions, i.e. emulsions that would only go through the process of ultrasonic homogenization, but not the stabilization in the electric field. The results are presented in Fig. 4.

The tendency observed in Fig. 4 corresponds very well to the temperature elevations. The most effective heating occurred for the emulsions stabilized with the highest concentration of the magnetite

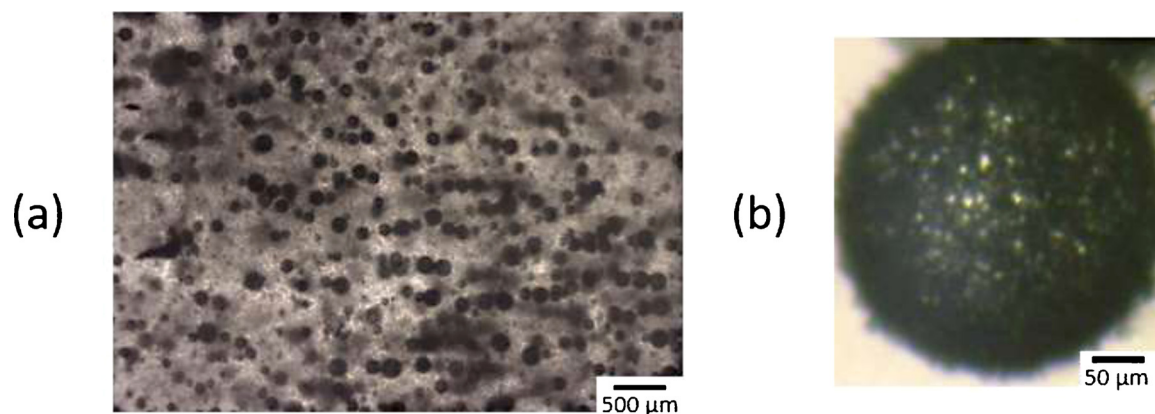


Fig. 2. (a) Optical microscope image of a Pickering emulsion after ultrasonic homogenization and subsequent stabilization in the electric field for 20 minutes. The silicone oil - castor oil mass ratio was 1:10, polystyrene particles - silicone oil mass ratio was 1:4 and magnetite particles (< 5 μ m in size) to polystyrene particles mass ratio was 1:8. (b) A single, non-sintered Pickering droplet extracted from the overall picture.

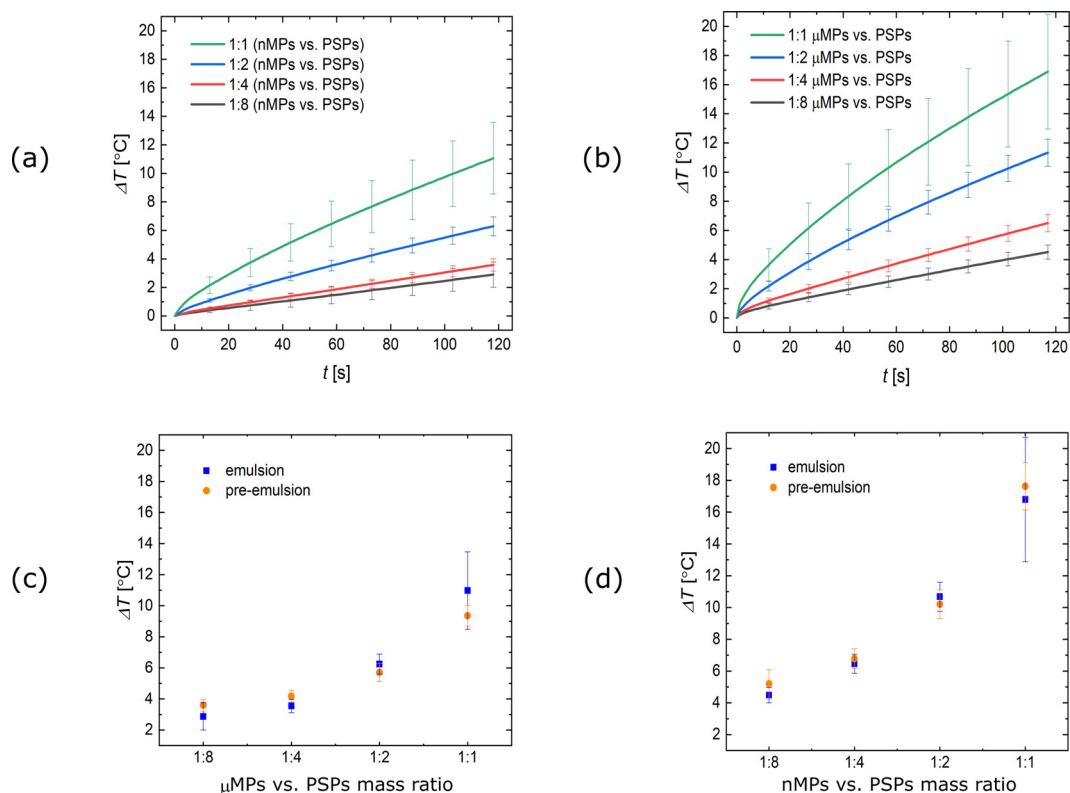


Fig. 3. Temperature increase within 120 seconds under the alternating magnetic field for Pickering emulsions with (a) magnetic nanoparticles, **nMPs**, and (b) magnetic microparticles, **μMPs** . Total temperature rise in 120 s of magnetic heating for (c) magnetic nanoparticles, **nMPs** and (d) magnetic microparticles, **μMPs** .

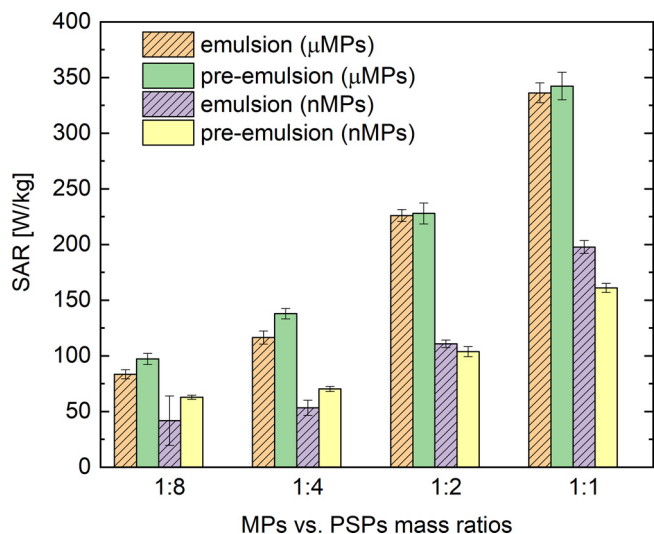


Fig. 4. Specific absorption rate for emulsions and pre-emulsions stabilized with magnetic particles of different sizes (micrometers vs. nanometers) and with different mass ratios.

microparticles, **μMPs** . Again, it is due to an evident hysteresis loss that is exhibited significantly only for bigger magnetic particles. Interestingly, especially when **μMPs** were used, heating efficiency was higher for the pre-emulsions than for the emulsions. It can mean that the influence of attachment of magnetic particles to the droplet interface and their location simultaneously in both of liquids is reflected in our SAR results. There are some explanations for this. In pre-emulsions, there are no dense particle layers around the droplets and not all of the particles are placed on the oil-oil interface. In case of small magnetic particles, **nMPs**, rotation of a whole particle is not suppressed by the attachment

to the oil-oil interface, which allows the Brownian mechanism to have a greater impact on the system. For stable Pickering droplets, the particles are packed at the interface so densely, that the particle rotation is difficult due to friction between adjacent particles. For bigger particles, those relaxation mechanisms do not occur.

The differences in heating efficiency between a pre-emulsion and a stabilized emulsion can arise from contrast in thermal properties between the inner and the outer phase of the emulsion and the interactions between stabilizing particles. In literature, the efficiency of magnetic heating is reported to be dependent on the size of particles. However, so far scientists have focused on nanoparticles. It was shown that heating efficiency exhibits an explicit maximum that strongly depends on experimental conditions [39,40]. The bigger particles, micrometer in size, have in turn not been reported in magnetic heating applications. Our results seem to indicate there is a difference in heat generation by a single magnetic particle compared to a particle cluster. Sufficiently large agglomerates cool down slower than the surface of a single particle [41]. The closely packed particles attached to the droplet surface – as in case of particle shell around oil droplets – could be considered as a kind of such hollow sphere particle agglomerate. For particle layer, the magnetic interactions between particles can influence the heat generation as it is for clusters [42].

The temperature rise in samples of magnetic particles dispersed in castor oil was also recorded. The magnetite concentration in these samples was 0.6 % w/w.

The mass concentration of particles in each of the measured samples was the same, hence a difference in temperature rise in Fig. 5 should be linked to the difference in the mechanisms involved in the process of magnetic heating. As for emulsions stabilized by particles, bigger particles (**μMPs**) were more efficient as sources of heat in magnetite suspension. It was due to energy losses from magnetic hysteresis. In parallel, the temperature rise observed for suspensions was higher than for the emulsions, regardless of the size of the particles used.

The obtained results indicate there is a high potential of efficient

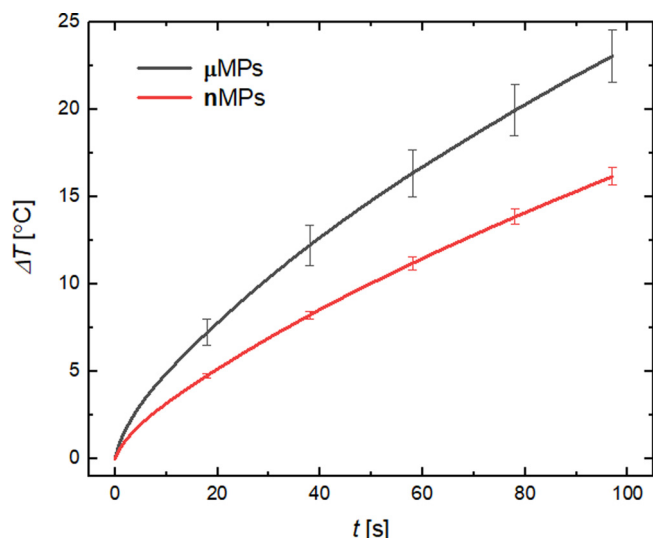


Fig. 5. Temperature rise in time of magnetic heating for different-size magnetic particles suspended in castor oil.

heating when **MPs** are used as mediators. The longer the exposure to the alternating magnetic field and/or the concentration of **MPs**, the higher the observed temperature increase. This rise is significant and occurs not only for the emulsions but also for the suspensions. This fact is of importance for colloidal capsule formation that will be described in the next section.

3.2. Formation of Pickering-emulsion-based capsules

In the previous paragraph, we showed that under alternating magnetic field magnetite particles acted as a good heat source in both Pickering emulsions and suspensions. This insight could be applied to the formation of Pickering-emulsion-based colloidal capsules if a sufficiently high sample temperature can be achieved.

A conceptual scheme of colloidal capsules formation using the magnetic field is presented in Fig. 6. In the first case (Fig. 6a), emulsion droplets prepared as described in section 2.2. were placed in the alternating magnetic field in a glass cuvette. The observed temperature increase was high enough to facilitate sintering of polystyrene particles attached to the droplets of the emulsion and enable formation of colloidal capsules. In the second case (Fig. 6b), a single silicone oil droplet with a polystyrene particle shell was formed in castor oil under the electric field using a mechanical pipette. At first, the particles were located inside the silicone oil droplet. Due to the presence of electrohydrodynamic flows, the particles were moved to the droplet's surface and got attached to the interface [43]. After a few minutes in the electric field, all particles were brought to the droplet's surface and formed a dense layer. This way we obtained Pickering droplet as those presented in our emulsions.

The findings from paragraph 3.1. show clearly the efficiency of heating when oil-in-oil Pickering emulsions were exposed to the external magnetic field. It was also proved that this efficiency depended strongly on the amount of the magnetic material used. In case of particles used in this work, the obtained local temperature can exceed the required temperature of glass transition of polystyrene as it is shown in Supplementary Materials, Fig. S1. It presents mixtures of polystyrene and magnetite particles in the form of a powder sprinkled onto the slide (Fig. S1a). After 2 minutes in the alternating magnetic field (parameters exactly the same as for other experiments) the transition into the glass was clearly visible (see inset pictures in Fig. S1c). In addition, rough pyrometer measurements (Fig. S1b) indicate that the temperature in the mixture of powders was high enough for **PSPs** to be sintered. It is worth pointing out that pyrometer measurements are sensitive only to

the temperature of particle surface. Inside the mixture of powders, the temperature observed would be even higher.

In section 3.1. we showed that the temperature rise is a function of **MPs** concentration in a given emulsion system. Thus, high concentration of **MPs** in the emulsion is able to induce a sufficiently high-temperature rise for sintering **PSPs** to occur. Fig. 7. presents the appearance of a dense emulsion (1:2 silicone oil to castor oil mass ratio) after stabilization in the electric field and following magnetic heating. In Fig. 7c the corresponding temperature measured in this sample is depicted.

As one can see, the temperature increase in such a dense emulsion (50% mass concentration of silicone oil, 7.5% mass concentration of magnetite particles) was very dynamic and a high final rise was achieved. For long heat treatment it was possible to reach the temperature of **PSPs** allowing for their fusion. In this case, it is possible to form numerous capsules at the same time. Because of small dimensions of such droplets and capsules, there are no facile routes to prove evidently that a robust shell around the droplet was formed and, as a result, a capsule was formed. However, in the future, non-direct methods can be proposed to cope with this, e.g. an ultrasound technique [44].

Various types of colloidal particles, including magnetic, may be used for formation of Pickering emulsions [45,46]. Here, we studied those stabilized with magnetite particles due to their potential as templates for fabrication of colloidal capsules in a magnetic field. Induced heat generation is their defining feature. Other groups have also used magnetic particles in this context, for instance to laden bubbles [47]. In addition, preparation of capsules containing magnetic materials is of great importance for magnetic hyperthermia applications [48] and magnetic resonance imaging [49]. An important feature of such droplets and capsules is that they can be administered to a specified region in the patient's body using static magnets. Then an alternating magnetic field may be applied to induce heat generation and cargo release, if thermally responsive soft particles were used in addition to the magnetic particles [50,51].

Now we show a potential of formation of a single colloidal capsule in a magnetite suspension in castor oil. In this case, the capsule does not contain any magnetic particles on its surface. The experiment was performed based on the scheme presented in Fig. 6b. A colloidal capsule obtained this way differs from a non-sintered particle-covered droplet in susceptibility to external stress. Because a particle-covered droplet is less rigid than a capsule, a surface deformation should be observed. In Fig. 8, we present results from the experiment where droplets and subsequently formed capsules were subjected to the electric field of increasing intensity (from 0 V·mm⁻¹ to 195 V·mm⁻¹). The pictures were recorded using the system described in section 2.1. As **μMPs** provided a higher temperature rise in the emulsion system, we used them in this experiment as well.

The quantitative evaluation based on the pictures was also performed. The deformation was calculated using the equation:

$$D = \frac{x_l - x_p}{x_l + x_p} \quad (5)$$

where x_l and x_p are the dimensions of droplets in the longitudinal and parallel direction to the electric field. The magnitude of D is determined by the dielectric constants of the droplet, particles and the continuous phase as well as surface tension [52,53]. We can observe how the deformation evolved as electric field intensity was changed. The values are presented as the inset table in Fig. 8c.

The results indicate clearly that after heating treatment in the alternating magnetic field droplet shell became rigid. Electric field stress did not cause an increase of deformation D as it was in the case of a droplet before heating. This is evidence that our approach to sintering works properly. We performed these experiments using polyethylene microparticles (27-32 μm in size) as well. Also, in this case, we managed to induce a change in the appearance of the particle shell during the heating in an alternating magnetic field. The results are presented in Fig. 9. Because of the difference in glass transition temperature, **PSPs**

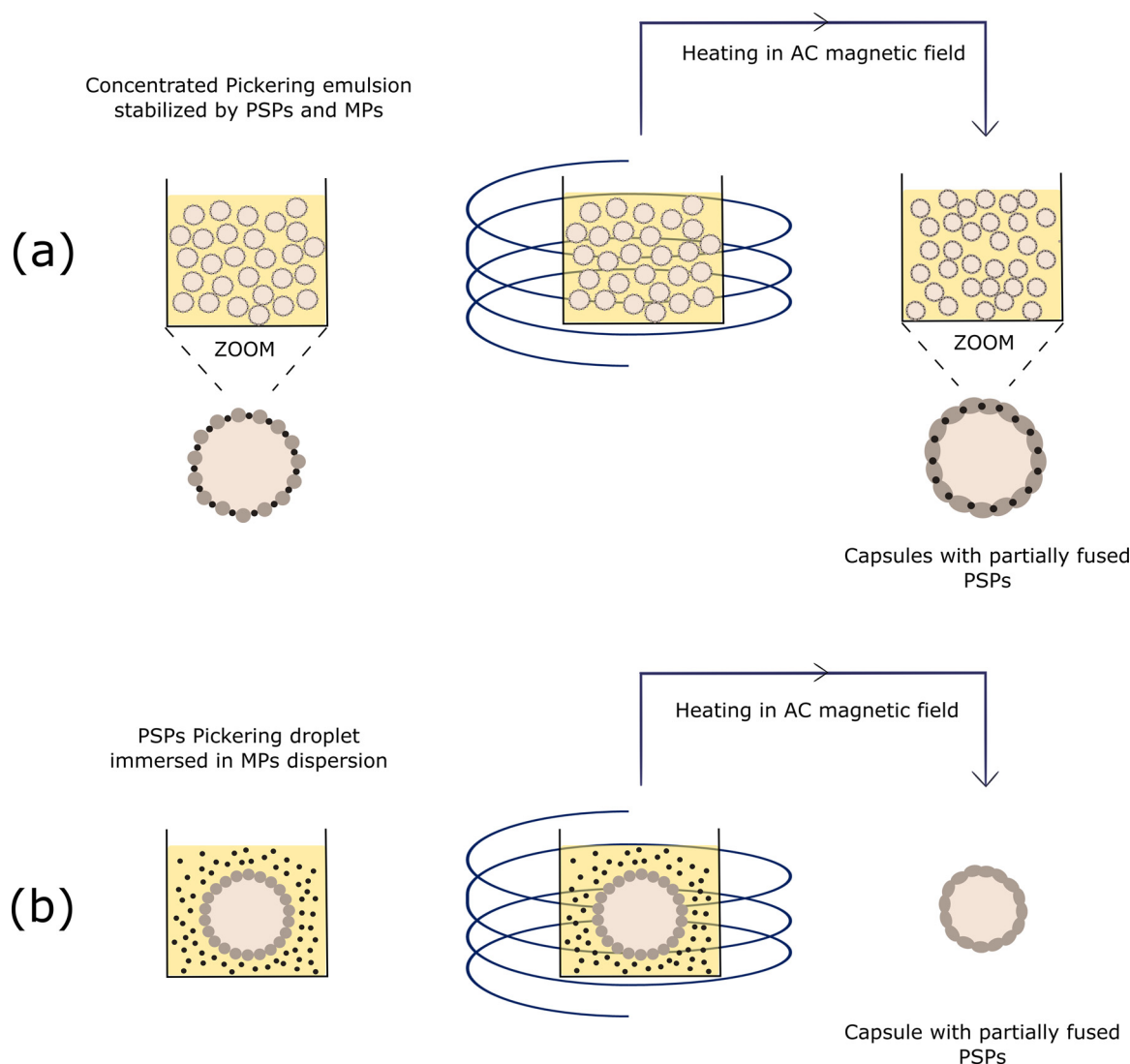


Fig. 6. The concept of fabricating colloidal capsules in the alternating magnetic field.

were detached from the surface, whilst PE particles formed characteristic patches.

Other example of using polyethylene particles is presented in Supplementary Materials, Fig. S2. In this picture, one can see patches of some sort on the droplet's surface formed during the heating process. Based on that observation we think that fabrication of not only colloidosomes but also patchy colloidosomes may be possible, especially when a combination of particles differing in thermal properties (namely, glass transition temperature T_g) is used. Using the presented method of capsule formation, it is possible to achieve results comparable to heating by using other methods, e.g. in a microwave device (Fig. S3). However, by changing parameters such as concentration of magnetite particles in the process of capsule formation, one can achieve greater control compared to heating in a microwave device while making the procedure easier.

In our experiments, the temperature rise induced by the magnetic particles exposed to an alternating magnetic field and immersed in a carrier liquid was accompanied by convection flows observed in the sample cell. These flows could be utilized e.g. to break agglomerates of droplets in emulsions, analogically to breaking droplet chains by strong electrohydrodynamic flows (as it was described in [35]). In the presence of a higher temperature-controlled destabilization of the emulsion systems is possible [16]. In addition, particles [54] and molecules [55] were reported to be more efficient emulsifiers under those

conditions. Magnetic particles could be used as agents for providing temperature elevation in these systems.

3.3. Discussion

In the presented study, the sources of heating were magnetite nano- and microparticles. As indicated in section 3.1., the temperature elevation measured in a system depended on a concentration and a size of magnetic particles. Higher temperatures obtained in emulsions with μ MPS compared to those with nMPS can be explained by microparticles being multi-domain and thus hysteretic loss being an additional mechanism of heat generation. In our calorimetric measurements, we only changed the concentration and the size of particles with magnetic properties, i.e. the amount of dispersed phase (silicone oil) and polystyrene particles (PSPs) remained the same for all tested samples. However, the change in the concentration of silicone oil and PSPs could affect the magnetic heating indirectly by changing heat capacity of the sample and, in general, the mechanism of heat transfer through it. For investigating the influence of different concentrations and sizes of magnetite particles on the heating efficiency of emulsions, calorimetric measurements were carried out for constant parameters of magnetic field. The increase of the intensity of the alternating magnetic field would facilitate the heating efficiency of emulsions and shorten the time when the temperature of the sample exceeds the temperature of

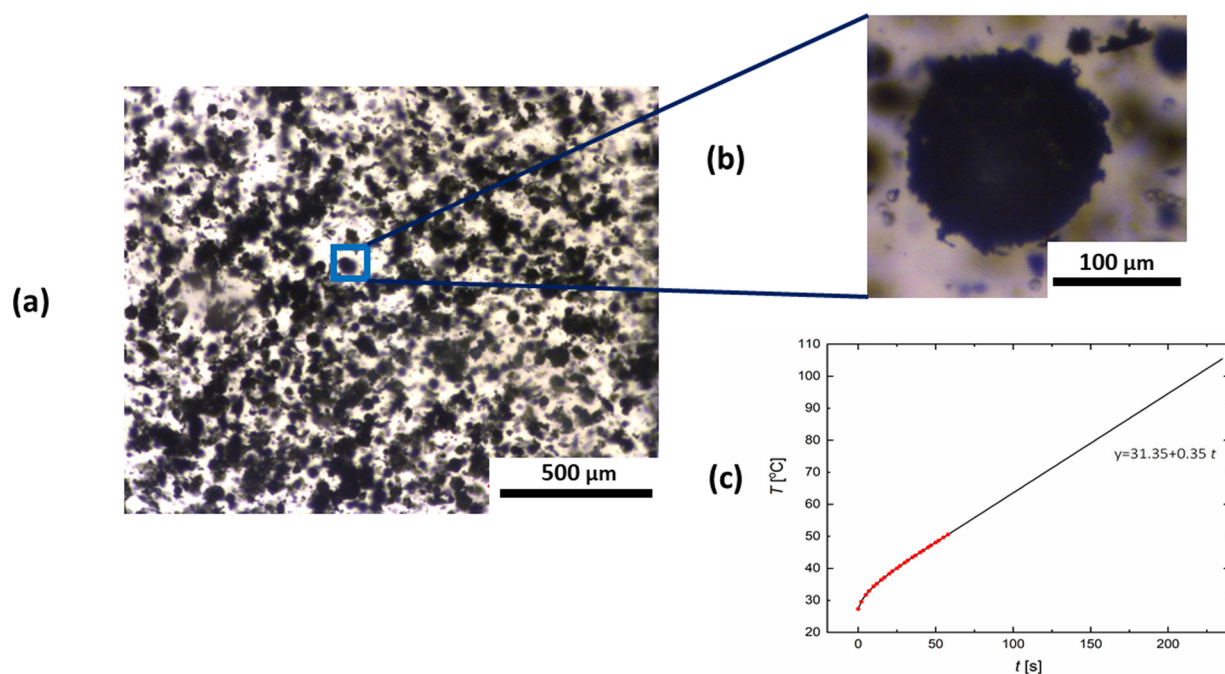


Fig. 7. (a) Appearance of a concentrated emulsion (1:2 silicone oil to castor oil mass ratio) after exposure to heating in the alternating magnetic field (suspension of colloidal capsules). (b) An extracted single Pickering droplet after magnetic heating. (c) Temperature rise recorded in the emulsion sample for mass concentration of magnetic particles equal to 7.5% w/w.

glass transitions.

PSPs undergo glass transition in the temperature above 100 °C [56]. The temperature of glass transition (T_g) varies for different soft particles. For instance, polyethylene particles (the results presented in Fig. S2) are believed to undergo glass transition in lower temperatures, i.e. 70-80 °C [57]. The process of capsule formation can therefore be optimized by using different particles with lower T_g and better efficiency of heat transferring, i.e. with lower heat capacity. Also, different concentrations and sizes of soft particles can have an impact on the

effective process of rigid shell formation around droplets.

The influence of changing the frequency of the magnetic field on the heating efficiency in magnetic hyperthermia has been documented in the literature. For instance, for magnetic fluid with magnetite nanoparticles coated by a dextran layer Skumiel et al. indicated a significant dependency of heating efficiency on frequency [58]. At the same time, the Brown relaxation is strongly dependent on the viscosity of the medium in which magnetic particles are immersed (see Eq. 1). The high viscosity limits the ability of particles to rotate in samples under the

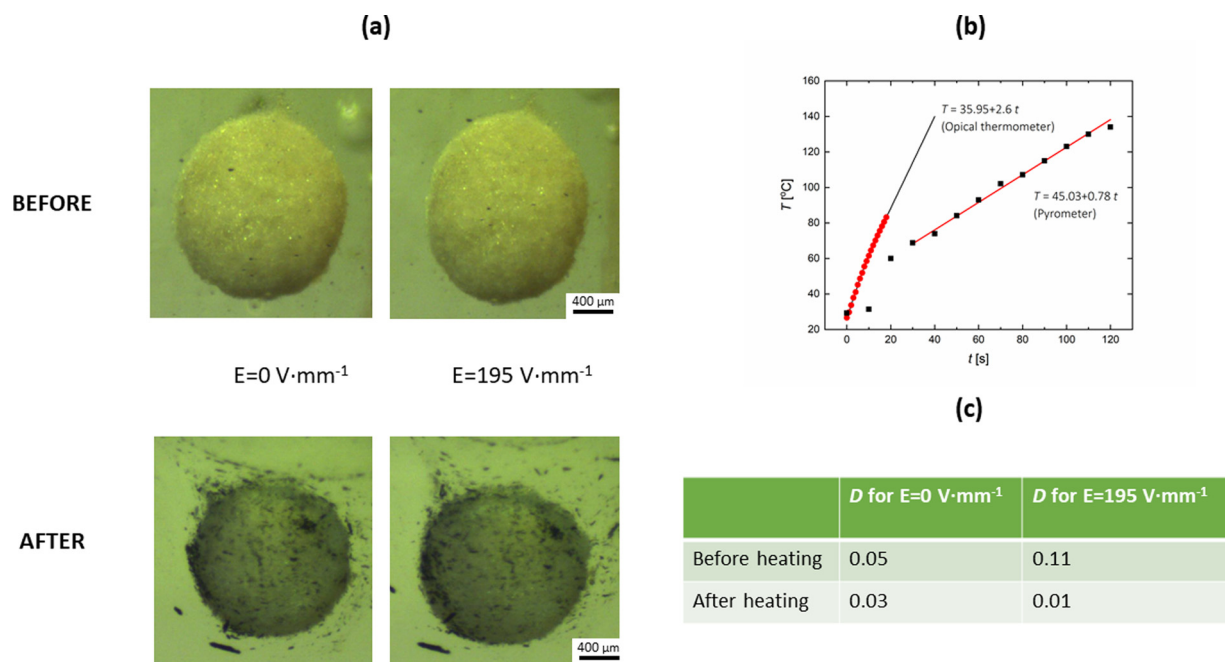


Fig. 8. (a) Pickering droplets before and after alternating magnetic-field induced heating for ~40 seconds. Pictures are taken using an optical microscope (section 2.1.). (b) Temperature rise recorded by an optical thermometer and a pyrometer in a suspension of μ MPPs in castor oil during the fabrication of the capsule (c) Deformations D calculated before and after magnetic heating treatment (Eq. 5).

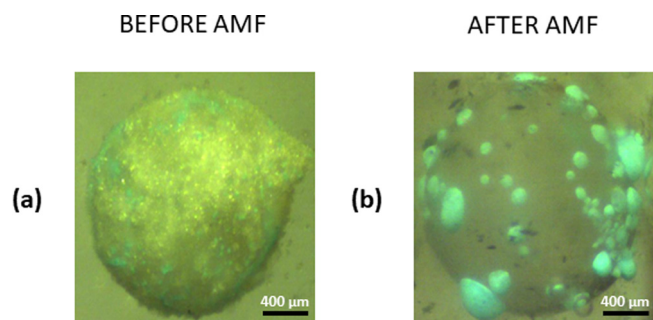


Fig. 9. Pickering droplets covered by both polystyrene (PSPs) and polyethylene particles (PEPs) (a) before and (b) after the application of the alternating magnetic field (AMF). Pictures are taken using an optical microscope (section 2.1.).

alternating magnetic field [46,59]. Thus, using emulsions with different outer phase i.e. oil-in-water emulsions, would increase the heating effect of a sample and speed up the process of capsule formation from emulsions as templates. A subtle point was that particles resided at the same time in the outer and inner phase of emulsion with different dynamic viscosity (700 mPa·s vs. 50 mPa·s respectively). In the case of fabricating capsules from polystyrene-covered droplets immersed in MPs dispersion, the situation is much simpler, i.e. the change of viscosity of carrier liquids to those of lower viscosity should facilitate the process of heating because of the increased influence of Brown relaxation mechanism.

We conducted the appropriate and indispensable experiments to evaluate calorimetric properties of Pickering emulsions with droplets covered by soft particles (PSPs) and magnetic particles as well as to investigate the potential of capsule formation from Pickering droplets precursors. As indicated above, the process can also be optimized by changing parameters connected to the alternating magnetic field and emulsions. Our concept to use the heat generated under an alternating magnetic field to increase the temperature of Pickering emulsions and to fabricate sintered shells around droplets can be widely utilized in the future as it is not limited to oil-in-oil emulsion systems. The other types of particles, including those of biological origin, can be explored as well. Our approach to the formation of Pickering emulsions takes advantage of limited coalescence that results in a facile control of the size of droplets. With the use of smaller particles for the stabilization of emulsion precursors, fabrication of much smaller capsules (micrometer in size) will be also possible, further extending the applicability of our method.

4. Conclusions

In this study, the formation of capsules by using magnetic heating was proposed as a novel potential application of alternating magnetic fields. Oil-in-oil Pickering emulsions stabilized by both magnetite and polystyrene colloidal particles were exposed to the alternating magnetic field. As a result, we observed a temperature rise in the emulsion system that can be utilized to form colloidal capsules either from corresponding single Pickering droplet precursors or from bulk Pickering emulsions.

The results of the calorimetric measurements indicated that the efficiency of the heating depended on the size and the concentration of magnetite particles used to co-stabilize emulsions. This efficiency was also shown by the specific absorption rate (SAR) calculations that delivered almost 1.5 times higher values for bigger magnetite particles.

We showed two different but complementary approaches to capsule fabrication. We managed to form droplets with partially fused PSPs from stable emulsion droplets. Sufficient temperature increase was observed for highly concentrated Pickering emulsion. Formation of a single droplet covered by non-magnetic particles and further placing it

into magnetite suspension was also proved to work as intended.

5. Author Contribution

AJ designed the original idea of using an alternating magnetic field to form colloidal capsules. RB designed the experiments. RB and DS performed them. RB analyzed and presented the data. KK participated in data presentation and description. RB wrote the first version of the manuscript. All authors contributed to the finalization of the manuscript.

Conflict of Interests

here is no conflict of interest to declare.

Acknowledgments

The authors would like to acknowledge the support of the Polish National Science Centre by the grants: 2015/17/B/ST7/03566 (OPUS), 2015/19/B/ST3/03055 (OPUS) and 2017/27/N/ST7/00201 (PRELUDIUM). Authors also wish to thank Dr. Tomasz Kubiak (HCSUAS, Gniezno, Poland) for fruitful discussions.

Appendix A. Supplementary data

Supplementary material related to this article can be found, in the online version, at doi:<https://doi.org/10.1016/j.colsurfb.2020.111070>.

References

- [1] Z. Rozynek, A. Józefczak, Patchy colloidosomes—an emerging class of structures, *Eur. Phys. J. Spec. Top.* 225 (4) (2016) 741–756.
- [2] T. Squillaro, A. Cimini, G. Peluso, A. Giordano, M.A.B. Melone, Nano-delivery systems for encapsulation of dietary polyphenols: An experimental approach for neurodegenerative diseases and brain tumors, *Biochem. Pharm.* 154 (2018) 303–317.
- [3] Q. Sun, Z. Zhao, E.A.H. Hall, A.F. Routh, Metal Coated Colloidosomes as Carriers for an Antibiotic, *Front. Chem.* 6 (2018) 196.
- [4] G. Kaufman, S. Nejati, R. Sarfati, R. Boltvanskiy, M. Loewenberg, E.R. Dufresne, C.O. Osuji, Soft microcapsules with highly plastic shells formed by interfacial polyelectrolyte–nanoparticle complexation, *Soft Matter* 11 (2015) 7478–7482.
- [5] O.J. Cayre, P.F. Noble, V.N. Paunov, Fabrication of novel colloidosome microcapsules with gelled aqueous cores, *J. Mater. Chem.* 14 (2004) 3351–3355.
- [6] N.N. Shahidan, R. Liu, S. Thaiboonrod, C. Alexander, K.M. Shakesheff, B.R. Saunders, Hollow Colloidosomes Prepared Using Accelerated Solvent Evaporation, *Langmuir* 29 (2013) 13676–13685.
- [7] M.F. Hsu, M.G. Nikolaidis, A.D. Dinsmore, A.R. Bausch, V.D. Gordon, X. Chen, J.W. Hutchinson, D.A. Weitz, M. Marquez, Self-assembled Shells Composed of Colloidal Particles: Fabrication and Characterization, *Langmuir* 21 (2005) 2963–2970.
- [8] S. Laib, A.F. Routh, Fabrication of colloidosomes at low temperature for the encapsulation of thermally sensitive compounds, *J. Colloid Interface, Sci.* 317 (1) (2008) 121–129.
- [9] H.N. Yow, A.F. Routh, Release Profiles of Encapsulated Actives from Colloidosomes Sintered for Various Durations, *Langmuir* 25 (1) (2009) 159–166.
- [10] S. Dutz, R. Hergt, Magnetic particle hyperthermia—a promising tumour therapy? *Nanotechnology* 25 (2014) 452001.
- [11] R. Hergt, S. Dutz, R. Müller, M. Zeisberger, Magnetic particle hyperthermia: nanoparticle magnetism and materials development for cancer therapy, *J. Phys., Condens. Matter* 18 (38) (2006) S2919–S2934.
- [12] Q. Li, C.W. Kartikowati, S. Horie, T. Ogi, T. Iwaki, K. Okuyama, Correlation between particle size/domain structure and magnetic properties of highly crystalline Fe₃O₄ nanoparticles, *Sci. Rep.* 7 (2017) 9894.
- [13] A. Józefczak, B. Leszczyński, A. Skumiel, T. Hornowski, A comparison between acoustic properties and heat effects in biogenic (magnetosomes) and abiotic magnetite nanoparticle suspensions, *J. Magn. Magn. Mater.* 407 (2016) 92–100.
- [14] O.L. Gobbo, K. Sjaastad, M.W. Radomski, Y. Volkov, A. Prina-Mello, Magnetic nanoparticles in cancer theranostics, *Theranostics* 5 (11) (2015) 1249.
- [15] S. Moise, J.M. Byrne, A.J. El Haj, N.D. Telling, The potential of magnetic hyperthermia for triggering the differentiation of cancer cells, *Nanoscale* 10 (44) (2018) 20519–20525.
- [16] A. Kaiser, T. Liu, W. Richtering, A.M. Schmidt, Magnetic capsules and pickering emulsions stabilized by core-shell particles, *Langmuir* 25 (13) (2009) 7335–7341.
- [17] T.A. Prileszky, E.M. Furst, Magnetite nanoparticles program the assembly, response, and reconfiguration of structured emulsions, *Soft Matter* 15 (7) (2019) 1529–1538.
- [18] S. Ceylan, C. Friese, C. Lammel, K. Mazac, A. Kirschning, Inductive Heating for

- Organic Synthesis by Using Functionalized Magnetic Nanoparticles Inside Microreactors, *Angew. Chem. Int. Ed.* 47 (46) (2008) 8950–8953.
- [19] S. Ceylan, L. Coutable, J. Wegner, A. Kirschning, Inductive Heating with Magnetic Materials inside Flow Reactors, *Chem. Eur. J.* 17 (6) (2011) 1884–1893.
- [20] A. Meffre, B. Mehdaoui, V. Connord, J. Carrey, P.F. Fazzini, S. Lachaize, M. Respaud, B. Chaudret, Complex Nano-objects Displaying Both Magnetic and Catalytic Properties: A Proof of Concept for Magnetically Induced Heterogeneous Catalysis, *Nano Lett.* 15 (5) (2015) 3241–3248.
- [21] J.M. Asensio, A.B. Miguel, P.-F. Fazzini, P.W.N.M. van Leeuwen, B. Chaudret, Hydrodeoxygenation Using Magnetic Induction: High-Temperature Heterogeneous Catalysis in Solution, *Angew. Chem. Int. Ed.* 58 (33) (2019) 11306–11310.
- [22] W. Wang, G. Tuci, C. Duong-Viet, Y. Liu, A. Rossin, L. Luconi, J.-M. Nhut, L. Nguyen-Dinh, C. Pham-Huu, G. Giambastiani, Induction Heating: An Enabling Technology for the Heat Management in Catalytic Processes, *ACS Catal.* (2019) 7921–7935.
- [23] Q. Sun, H. Gao, G.B. Sukhorukov, A.F. Routh, Silver-Coated Colloidosomes as Carriers for an Anticancer Drug, *ACS Appl. Mater. Interfaces* 9 (38) (2017) 32599–32606.
- [24] Q. Sun, Y. Du, E.A.H. Hall, D. Luo, G.B. Sukhorukov, A.F. Routh, A fabrication method of gold coated colloidosomes and their application as targeted drug carriers, *Soft Matter* 14 (14) (2018) 2594–2603.
- [25] H. Jiang, L. Hong, Y. Li, T. Ngai, All-Silica Submicrometer Colloidosomes for Cargo Protection and Tunable Release, *Angew. Chem. Int. Ed.* 57 (36) (2018) 11662–11666.
- [26] D. Yin, L. Bai, Y. Jia, J. Liu, Q. Zhang, Microencapsulation through thermally sintering Pickering emulsion-based colloidosomes, *Soft Matter* 13 (20) (2017) 3720–3725.
- [27] G. Mallikarjunachari, T. Nallamilli, P. Ravindran, M.G. Basavaraj, Nanoindentation of clay colloidosomes, *Colloids Surf, A Physicochem. Eng. Asp.* 550 (2018) 167–175.
- [28] L. Zhang, F. Zhang, Y.-S. Wang, Y.-L. Sun, W.-F. Dong, J.-F. Song, Q.-S. Huo, H.-B. Sun, Magnetic colloidosomes fabricated by Fe₃O₄-SiO₂ hetero-nanorods, *Soft Matter* 7 (16) (2011) 7375–7381.
- [29] J.S. Sander, A.R. Studart, Nanoparticle-Filled Complex Colloidosomes for Tunable Cargo Release, *Langmuir* 29 (49) (2013) 15168–15173.
- [30] D.G. Shchukin, E. Shchukina, Capsules with external navigation and triggered release, *Curr. Opin. Pharmacol.* 18 (2014) 42–46.
- [31] Y. Qu, R. Huang, W. Qi, Q. Qu, R. Su, Z. He, Structural Insight into Stabilization of Pickering Emulsions with Fe₃O₄@SiO₂ Nanoparticles for Enzyme Catalysis in Organic Media, *Part. Part. Syst. Char.* 34 (7) (2017) 1700117.
- [32] T. Bollhorst, S. Shahabi, K. Wörz, C. Petters, R. Dringen, M. Maas, K. Rezwan, Bifunctional Submicron Colloidosomes Coassembled from Fluorescent and Superparamagnetic Nanoparticles, *Angew. Chem. Int. Ed.* 127 (1) (2015) 120–125.
- [33] A.M. Bago Rodriguez, B.P. Binks, Capsules from Pickering emulsion templates, *Curr. Opin. Colloid Interface Sci.* 44 (2019) 107–129.
- [34] Z. Rozynek, M. Kaczmarek-Klinowska, A. Magdziarz, Assembly and Rearrangement of Particles Confined at a Surface of a Droplet, and Intruder Motion in Electro-Shaken Particle Films, *Materials* 9 (8) (2016) 679.
- [35] Z. Rozynek, R. Bielas, A. Józefczak, Efficient formation of oil-in-oil Pickering emulsions with narrow size distributions by using electric fields, *Soft Matter* 14 (24) (2018) 5140–5149.
- [36] J. Estelrich, E. Escribano, J. Queralt, M.A. Busquets, Iron Oxide Nanoparticles for Magnetically-Guided and Magnetically-Responsive Drug Delivery, *Int. J. Mol. Sci.* 16 (4) (2015) 8070–8101.
- [37] U.M. Engelmann, J. Seifert, B. Mues, S. Roitsch, C. Ménager, A.M. Schmidt, I. Slabu, Heating efficiency of magnetic nanoparticles decreases with gradual immobilization in hydrogels, *J. Magn. Magn. Mater.* 471 (2019) 486–494.
- [38] R.R. Wildeboer, P. Southern, Q.A. Pankhurst, On the reliable measurement of specific absorption rates and intrinsic loss parameters in magnetic hyperthermia materials, *J. Phys. D Appl. Phys.* 47 (49) (2014) 495003.
- [39] J. Mohapatra, F. Zeng, K. Elkins, M. Xing, M. Ghimire, S. Yoon, S.R. Mishra, J.P. Liu, Size-dependent magnetic and inductive heating properties of Fe₃O₄ nanoparticles: scaling laws across the superparamagnetic size, *Phys. Chem. Chem. Phys.* 20 (18) (2018) 12879–12887.
- [40] S. Tong, C.A. Quinto, L. Zhang, P. Mohindra, G. Bao, Size-Dependent Heating of Magnetic Iron Oxide Nanoparticles, *ACS Nano* 11 (7) (2017) 6808–6816.
- [41] D. Sakellari, K. Brintakis, A. Kostopoulou, E. Myrovali, K. Simeonidis, A. Lappas, M. Angelakeris, Ferrimagnetic nanocrystal assemblies as versatile magnetic particle hyperthermia mediators, *Mater. Sci. Eng. C* 58 (2016) 187–193.
- [42] R. Fu, Y. Yan, C. Roberts, Z. Liu, Y. Chen, The role of dipole interactions in hyperthermia heating colloidal clusters of densely-packed superparamagnetic nanoparticles, *Sci. Rep.* 8 (1) (2018) 4704.
- [43] Z. Rozynek, K. Khobaib, A. Mikkelsen, Opening and Closing of Particle Shells on Droplets via Electric Fields and Its Applications, *ACS Appl. Mater. Interfaces* 11 (25) (2019) 22840–22850.
- [44] R. Bielas, Z. Rozynek, T. Hornowski, A. Józefczak, Ultrasound control of oil-in-oil Pickering emulsions preparation, *J. Phys. D Appl. Phys.* 53 (2019) 085301.
- [45] A. Józefczak, R. Wlazło, Ultrasonic studies of emulsion stability in the presence of magnetic nanoparticles, *Adv. Cond. Matter Phys.* 2015 (2015) 1–9.
- [46] B.B. Lahiri, S. Ranoo, A.W. Zaibudeen, J. Philip, Magnetic hyperthermia in magnetic nanoemulsions: Effects of polydispersity, particle concentration and medium viscosity, *J. Magn. Magn. Mater.* 441 (2017) 310–327.
- [47] J.A. Rodrigues, E. Rio, J. Bobroff, D. Langevin, W. Drenckhan, Generation and manipulation of bubbles and foams stabilised by magnetic nanoparticles, *Colloids Surf, A Physicochem. Eng. Asp.* 384 (1) (2011) 408–416.
- [48] T. Miyazaki, A. Miyaoka, E. Ishida, Z. Li, M. Kawashita, M. Hiraoka, Preparation of ferromagnetic microcapsules for hyperthermia using water/oil emulsion as a reaction field, *Mater. Sci. Eng. C* 32 (4) (2012) 692–696.
- [49] O.A. Inozemtseva, S.V. German, N.A. Navolokin, A.B. Bucharskaya, G.N. Maslyakova, D.A. Gorin, Chapter 6 - Encapsulated Magnetite Nanoparticles: Preparation and Application as Multifunctional Tool for Drug Delivery Systems, in: D.P. Nikolelis, G.-P. Nikoleli (Eds.), *Nanotechnology and Biosensors*, Elsevier, 2018, pp. 175–192.
- [50] J.F. Liu, B. Jang, D. Issadore, A. Tsourkas, Use of magnetic fields and nanoparticles to trigger drug release and improve tumor targeting, *Wiley Interdiscip. Rev. Nanomed. Nanobiotechnol.* 11 (2019) e1571.
- [51] K. Katagiri, M. Nakamura, K. Koumoto, Magneto-responsive Smart Capsules Formed with Polyelectrolytes, Lipid Bilayers and Magnetic Nanoparticles, *ACS Appl. Mater. Interfaces* 2 (3) (2010) 768–773.
- [52] Z. Rozynek, R. Castberg, A. Kalicka, P. Jankowski, P. Garstecki, Electric field manipulation of particles in leaky dielectric liquids, *Arch. Mech.* 67 (5) (2015) 385–399.
- [53] A. Mikkelsen, Z. Rozynek, K. Khobaib, P. Dommersnes, J.O. Fossum, Transient deformation dynamics of particle laden droplets in electric field, *Colloids Surf, A Physicochem. Eng. Asp.* 532 (2017) 252–256.
- [54] F. Liu, C.-H. Tang, Soy glycinin as food-grade Pickering stabilizers: Part. I. Structural characteristics, emulsifying properties and adsorption/arrangement at interface, *Food Hydrocoll.* 60 (2016) 606–619.
- [55] W. Peng, X. Kong, Y. Chen, C. Zhang, Y. Yang, Y. Hua, Effects of heat treatment on the emulsifying properties of pea proteins, *Food Hydrocoll.* 52 (2016) 301–310.
- [56] J. Rieger, The glass transition temperature of polystyrene, *J. Therm. Anal. Calorim.* 46 (3) (1996) 965–972.
- [57] C.E. Wilkes, J.W. Summers, C.A. Daniels, M.T. Berard, *PVC Handbook*, Hanser Munich, 2005.
- [58] A. Skumiel, A. Józefczak, M. Timko, P. Kopčanský, F. Herchl, M. Koneracká, N. Tomašovičová, Heating Effect in Biocompatible Magnetic Fluid, *Inter. J. Thermophys.* 28 (5) (2007) 1461–1469.
- [59] K. Kaczmarek, R. Mrówczyński, T. Hornowski, R. Bielas, A. Józefczak, The Effect of Tissue-Mimicking Phantom Compressibility on Magnetic Hyperthermia, *Nanomaterials* 9 (5) (2019) 803.

Supplementary Materials for:

The potential of magnetic heating for fabricating Pickering-emulsion-based capsules

Rafał Bielas¹, Dawid Surdeko^{1,2}, Katarzyna Kaczmarek¹ and Arkadiusz Józefczak^{1,*}

¹Department of Acoustics, Faculty of Physics, Adam Mickiewicz University in Poznań,
Uniwersytetu Poznańskiego 2, 61-614 Poznań, Poland

²Faculty of Science and Technology, University of Twente, P.O. BOX 217, 7500 AE Enschede,
The Netherlands

*e-mail: aras@amu.edu.pl

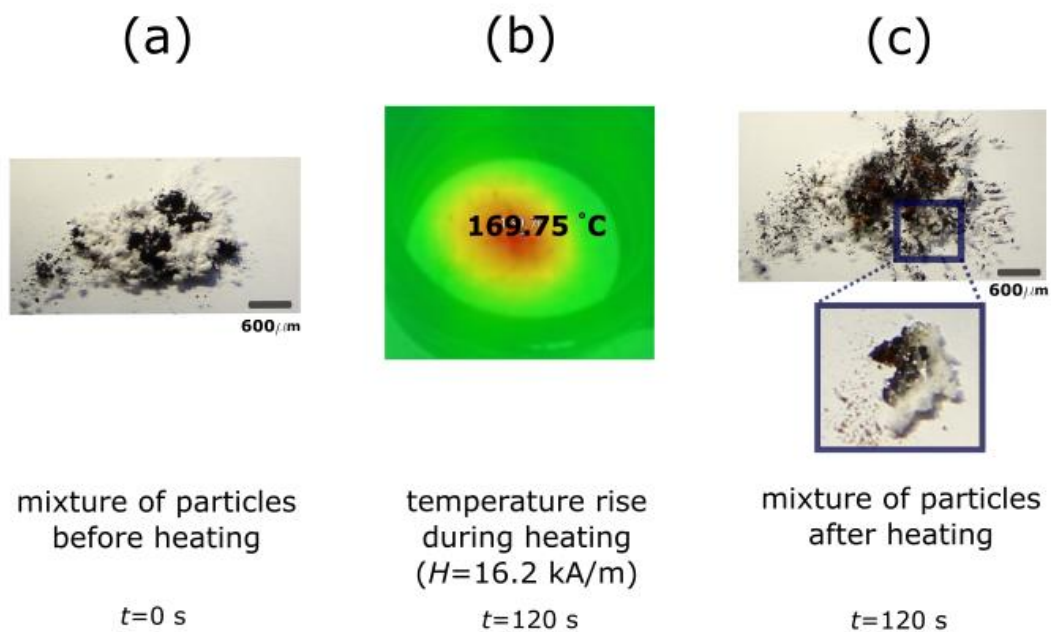


Fig. S1. (a) The mixture of particle powders sprinkled onto the glass slide before the magnetic field was turned on. (b) The temperature rise measured in the mixture of particles during the magnetic heating by the pyrometer. (c) The effect of magnetic heating on the glass transition of polystyrene particles when mixed with magnetic particle powder. The insets present fragment of sintered polystyrene particles after zoom in. The scale bars are 600 μm .

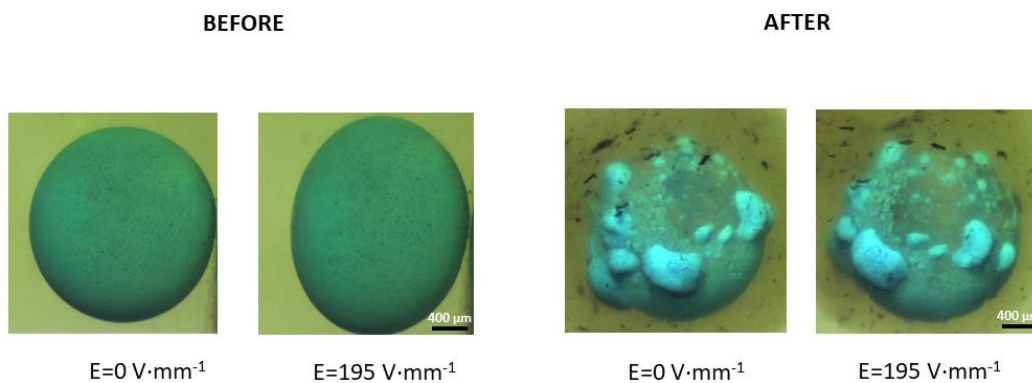


Fig. S2 Examples of magnetic heating for silicone oil droplet covered by other colloidal particles. Silicone oil droplet was fully covered by PE particles. After heating the particles were partially fused, as evidenced by lack of deformation under the electric stress. Pictures were taken using an optical microscope (see section 2.1. in the paper). Polyethylene particles (27-32 μm) were purchased from Cospheric Co. Polystyrene particles ($\sim 10 \mu\text{m}$) were purchased from Microbeeds Co.

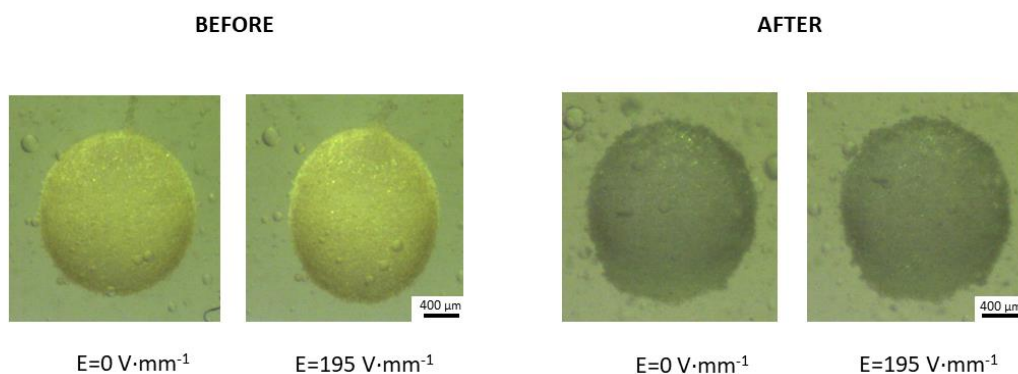


Fig. S3 Pickering droplets before and after heating in a microwave device. Silicone oil droplets are covered by polystyrene particles ($\sim 10 \mu\text{m}$) purchased from Microbeeds Co.

Appendix I: List of other publications

1. A. Józefczak, K. Kaczmarek, **R. Bielas**, Magnetic mediators in ultrasound theranostics, submitted to *Theranostics* (2021).
2. K. Kaczmarek, **R. Bielas**, M. Siluk, T. Hornowski, A. Józefczak, Comparison of magnetic and non-magnetic nanoparticles as sonosensitizers in ultrasonic hyperthermia, *Acta Physica Polonica A*, 2020, 137(5). DOI: : 10.12693/APhysPolA.137.653.
3. **R. Bielas**, A. Bochińska, A. Józefczak, The influence of initial temperature on ultrasonic hyperthermia measurements, *Applied Acoustics*, 2020, 164, 107259.
DOI: 10.1016/j.apacoust.2020.107259
4. K. Kaczmarek, R. Mrówczyński, T. Hornowski, **R. Bielas**, A. Józefczak, Effect of tissue-mimicking phantom compressibility on magnetic hyperthermia, *Nanomaterials*, 2019, 9(5), 803.
DOI: 10.3390/nano9050803.
5. K. Kaczmarek, T. Hornowski, **R. Bielas**, D. Żak, M. Timko, A. Józefczak, *Dependence of Ultrasonic and Magnetic Hyperthermia on The Concentration of Magnetic Nanoparticles*, *Acta Physica Polonica A*, 2018, 133(3), 716-718. DOI: 10.12693/APhysPolA.133.716
6. **R. Bielas**, *Wpływ materiałów dźwiękoaktywujących na hipertermię ultradźwiękową*, in: *Studium badawcze młodych akustyków 2017*. ISBN 978-83-908774-5-7 (in Polish).

Appendix II: List of significant conference presentations

1. 47th Winter School on Wave and Quantum Acoustics, Szczyrk, 26.02 - 1.03.2018, **oral presentation:** *Monitoring of Pickering emulsion formation by optical microscopy and ultrasounds*
2. NanoTech Poland International Conference & Exhibition, Poznań, 6 - 9.06.2018, **oral presentation:** *Formation and characterization of oil-in-oil Pickering emulsions*
3. Polish-German Structured Conference on Acoustics jointed with 65. Open Seminar on Acoustics, Ustka, 11-14.09.2018, **oral presentation:** *Ultrasonic studies on Pickering emulsion formation process*
4. 20th Small Triangle Meeting on Theoretical Physics, Humene (Slovakia), 8-10.10.2018, **oral presentation:** *Pickering emulsion - how to make and characterize it using ultrasound and electric field?*
5. Juelich Soft Matter Days, Juelich (Germany), 20-23.11.2019, **poster:** *Efficient formation of oil-in-oil Pickering emulsions by using electric fields*
6. 48th Winter School on Wave and Quantum Acoustics, Szczyrk, 25-28.02.2019, **oral presentation:** *The influence of various sonosensitizers on ultrasonic heating*
7. XVI Akustyka w Audiologii i Foniatrii, Poznań, 17-18.05.2019, **invited lecture** (in Polish): *Możliwości wykorzystania kapsułek koloidalnych na bazie emulsji Pickeringa w nowoczesnych terapiach medycznych*
8. Czech-Slovak Conference on Magnetism, Košice (Slovakia), 3-7.06.2019, **poster:** *Comparison between magnetic and non-magnetic nanoparticles as sonosensitizers in ultrasonic hyperthermia.*
9. 14th School on Acousto-Optics and Applications, Toruń, 24-27.06.2019, **oral presentation.:** *Acoustical and optical control of Pickering emulsions formation in electric field*
10. 66th Open Seminar on Acoustics, Boszkowo-Poznań, 17-20.09.2019, **oral presentation.:** *The use of ultrasonic homogenization, electrocoalescence and magnetic field in formation of colloidal capsules*
11. 21st Small Triangle Meeting on Theoretical Physics, Spisska Nova Ves (Slovakia), 6-9.10.2019, **oral presentation:** *Magnetic heating of particle-stabilized emulsions and its applications*
12. 49th Winter School on Wave and Quantum Acoustics, Szczyrk, 24-27.02.2020, **oral presentation.:** *Particle-stabilized emulsions – acoustical properties and applications*
13. e-Forum Acusticum 2020, Lyon (France) 7-11.12.2020, **oral presentation:** *Ultrasonic study on emulsions stabilized with particles of different origins*

Appendix III: List of awards and distinctions

1. Acoustical Society of America International Student Grant (ASA-CIRE) for young acousticians (2019)
2. European Acoustics Association Young Scientist Conference Attendance grant (2019) for the conference e-Forum Acusticum 2020, Lyon, France
3. Polish Acoustical Society (PTA) scholarship for young scientists for the attendance in Open Seminar of Acoustics, Ustka, 2018
4. Invited lecture on the conference: XVI Konferencja z cyklu: Akustyka w Audiologii i Foniatrii, Poznań, 2019
5. Rector Scholarship for the best Ph.D. students at Adam Mickiewicz University in Poznań (2018, 2020)

Appendix IV: Other scientific activities

- Member of the organizing committee of the 66th Open Seminar of Acoustics (Boszkowo-Poznań, 2019)
- Member of the Polish Acoustical Society (PTA)
- Member of the European Acoustics Association (EAA)
- Student member of the Acoustical Society of America (ASA)

Oświadczenie

Ja, niżej podpisany, Rafał Bielas, doktorant Wydziału Fizyki Uniwersytetu im. Adama Mickiewicza w Poznaniu oświadczam, że przedkładaną rozprawę doktorską pt.:

Pickering emulsions formed using ultrasound and electric fields – their characteristics and applications

napisałem samodzielnie. Oznacza to, że przy pisaniu pracy, poza niezbędnymi konsultacjami, nie korzystałem z pomocy innych osób, a w szczególności nie zlecałem opracowania rozprawy lub jej istotnych części innym osobom, ani nie odpisywałem tej rozprawy lub jej istotnych części od innych osób.

Równocześnie wyrażam zgodę na to, że w sytuacji gdyby powyższe oświadczenie okazało się nieprawdziwe, decyzja o nadaniu mi stopnia naukowego doktora zostanie cofnięta.

Rafał Bielas

Rafał Bielas